



HAL
open science

New Challenge in Octupolar Architecturs for Nonlinear Optic (NLO)

Mehmet Menaf Ayhan

► **To cite this version:**

Mehmet Menaf Ayhan. New Challenge in Octupolar Architecturs for Nonlinear Optic (NLO). Other. Ecole normale supérieure de lyon - ENS LYON; Gebze Institute of Technology (Kocaeli, Turquie), 2012. English. NNT: 2012ENSL0736 . tel-00741371

HAL Id: tel-00741371

<https://theses.hal.science/tel-00741371>

Submitted on 12 Oct 2012

HAL is a multi-disciplinary open access archive for the deposit and dissemination of scientific research documents, whether they are published or not. The documents may come from teaching and research institutions in France or abroad, or from public or private research centers.

L'archive ouverte pluridisciplinaire **HAL**, est destinée au dépôt et à la diffusion de documents scientifiques de niveau recherche, publiés ou non, émanant des établissements d'enseignement et de recherche français ou étrangers, des laboratoires publics ou privés.

THÈSE

en vue de l'obtention du grade de

Docteur de l'École Normale Supérieure de Lyon - Université de Lyon

Discipline: Chimie

**Laboratoire Chimie pour l'optique
École Doctorale Université de Lyon**

présentée et soutenue publiquement le 10 Septembre 2012
par **Mehmet Menaf AYHAN**

New Challenge in Octupolar Architectures for Non Linear Optic (NLO)

Directeur de thèse : Madame Chantal ANDRAUD

Co- directeur de thèse : Madame Ayşe Gül GÜREK

Après l'avis de : Monsieur Ahmet GÜL
Monsieur Ulvi AVCIATA

Devant la Commission d'Examen formée de :

Madame Chantal ANDRAUD	Directeur de thèse
Madame Ayşe GÜL GÜREK	Co-directeur de thèse
Monsieur Ahmet GÜL	Rapporteur
Monsieur Ulvi AVCIATA	Rapporteur
Monsieur Vefa AHSEN	Examineur
Monsieur Yann BRETONNIERE	Examineur

SUMMARY

THE TITLE of THESIS: New Challenge in Octupolar Architectures for Non Linear Optic (NLO)

AUTHOR: Mehmet Menaf AYHAN

The design of nonlinear optical (NLO) molecules has become a focus of current research in telecommunications, information technologies and optical data storage. Donor-acceptor substituted dipolar molecules have been the most investigated NLO chromophores. Dipolar molecules, however, have several limitations such as low optical transparency, low thermal stability and their strong tendency to adopt anti-parallel packing in the solid state.

Recently, a new class of materials based on octupolar symmetries, which lack permanent dipole moments, has been proposed for NLO applications. At a structural level, it can be shown that the basic template for 3D *octupolar* molecules comes to a cube with alternating charges at the corners such as donor and acceptor substituent. Despite all the various structures reported, it is worth noting that no molecules actually representing the “real” octupolar cube have been obtained so far.

In this thesis, we showed that the real octupolar cube can be demonstrated by lanthanide III complexes based on ABAB type phthalocyanine featuring alternating electron donor and electron acceptor groups. These structures are characterized by UV-NIR, X-Ray and exhibit highest quadratic hyperpolarizability ever reported for an octupolar molecule.

Moreover, this work was extended to nonoctupolar lanthanide homoleptic double-decker complexes based on AB_3 , A_4 , B_4 , T_4 type phthalocyanines. It was observed that these molecules present a quite large quadratic hyperpolarizability too, but smaller than the one obtained for the $Ln(ABAB)_2$ series, as expected.

SOMMAIRE

LE TITRE DE LA THÈSE: Nouveau challenge dans la conception d'architecture moléculaire pour l'optique non-linéaire (ONL).

AUTEUR: Mehmet Menaf AYHAN

La conception de molécules pour l'optique non linéaires (ONL) est devenue un centre de recherche de pointe pour les télécommunications, les technologies de l'information et le stockage de données optiques. Les molécules dipolaires substituées par des groupes donneur-accepteur ont été les chromophores les plus étudiés pour l'ONL. Cependant les molécules dipolaires diverses limitations telles que leur transparence optique, leur faible stabilité thermique et leur tendance à adopter un alignement antiparallèle à l'état solide.

Récemment, une nouvelle classe de matériaux est apparue basé sur des symétries octupolaire qui ne possède pas de dipôle permanent, pour les applications ONL. Au niveau structural, la structure générique idéale pour des molécules tridimensionnelles avec une distribution de charges octupolaire est un cube avec des charges opposées alternées à chaque angle. À ce jour, aucune molécule représentant le cube vrai (déformé) avec huit charges alternées aux sommets et délocalisation des charges complètes entre les plans supérieurs et inférieurs n'a été décrite.

Dans le cadre de cette thèse, des complexes de lanthanides III à partir de phthalocyanines de type ABAB présentant en alternance des groupes donneurs et accepteurs d'électrons ont été synthétisés représentant le premier réel octupole. Ces structures ont été caractérisé par UV-NIR, X-Ray et présentent les plus élevés hyperpolarisabilité quadratique jamais enregistré pour des molécules octupolaires.

En outre, ce travail a été étendu à divers type de double-decker de lanthanides homoleptiques non-octupolaire basé sur des phthalocyanines AB₃, A₄, B₄, T₄. Il a été observé que ces complexes présentent aussi des mesures d'hyperpolarisabilité quadratique élevés, mais inférieure a celles trouvé pour la série de complexes Ln (ABAB)₂ octupolaire, comme prévu.

ACKNOWLEDGMENTS

On the occasion of the completion of the thesis, it is my pleasant duty to express my gratitude for all those whose support and encouragement made my task much easier.

I have no words to thank, admire and appreciate the people behind this thesis Prof. Dr. Ayşe Gül GÜREK and Dr. Chantal ANDRAUD, my research supervisors, whose invaluable suggestions and incessant encouragement helped me to understand subject better.

I take immense pleasure to offer my special thanks to Prof. Dr. Vefa AHSEN, Ass. Prof. Dr. Catherine HIREL and Dr. Yann BRETONNIERE for their helps and encouragements.

I would like to thank the other members of my committee, Prof. Dr. Ulvi AVCIATA and Prof. Dr. Ahmet GÜL.

I wish to thank Prof. Dr. Joseph ZYSS, Prof. Dr. Isabelle Ledoux-Rak, and Anu SINGH from ENS-Cachan, for all NLO measurements.

I wish to thank the members of Chemistry department at GIT and ENS-Lyon for their supports and friendly environments.

I wish to express my thanks to my colleagues for their most friendly cooperation and support in the needy hours.

I express my profound thanks to the French Embassy in Ankara for having given me an opportunity to carry out my doctoral work by PHD co-tutelle fellowship.

I cannot express my gratitude in mere words to my parents for their affectionate encouragement and support throughout.

TABLE OF CONTENTS

SUMMARY	<u>1</u>
ÖZET	2
ACKNOWLEDGMENTS	3
TABLE OF CONTENTS	4
ABBREVIATIONS	10
LIST OF FIGURES	11
LIST OF TABLES	16
1. INTRODUCTION	17
2. BIBLIOGRAPHIC DATA	20
2.1. Definition of Nonlinear Optic	21
2.2. Origin of Nonlinear Optic	21
2.3. Definition of Second-Order Nonlinear Optic	23
2.4. Materials for Second-Order Nonlinear Optic	26
2.4.1. Inorganic Materials	27
2.4.2. Organic Materials	27
2.4.3. Metal-Based Materials	28
2.5. Phthalocyanine and Related Materials	29
2.5.1. Synthesis of Phthalocyanines	33
2.5.2. The reaction mechanism of phthalocyanine	34
2.5.3. Nomenclature of phthalocyanines	35
2.5.4. Applications of phthalocyanine	35
2.5.4.1. Nonlinear optics	36
2.6. Materials design for second-order nonlinear optic	38
2.6.1 Push-Pull Systems	38
2.6.1.1. Organic Push-Pull Systems	39

2.6.1.2.	Metal-Based Push-Pull Systems	43
2.6.1.3.	Phthalocyanine and related materials Push-Pull systems	47
2.6.2.	Octupolar Systems	51
2.6.2.1.	Definition of octupolar system	53
2.6.2.2.	Two dimensional (2D) octupolar materials	55
2.6.2.2.1.	Two dimensional (2D) octupolar organic materials	56
2.6.2.2.2.	Two dimensional (2D) octupolar metal-based materials	58
2.6.2.2.3.	Two dimensional (2D) octupolar Phthalocyanine materials	63
2.6.2.3.	Three dimensional (3D) octupolar materials	64
2.6.2.3.1.	Three dimensional (3D) octupolar organic materials	65
2.6.2.3.2.	Three dimensional (3D) octupolar metal-based materials	68
2.6.2.3.3.	Three dimensional (3D) octupolar phthalocyanine materials	70
2.7.	Experimental determination methods of first hyperpolarizability (β)	72
2.7.1.	Kurtz Powder	72
2.7.2.	Electric field-induced second harmonic generation (EFISH)	72
2.7.3.	Hyper-Rayleigh Scattering (HRS)	73
2.8.	Objective of the Thesis	76
3.	RESULT AND DISCUSSION	80
3.1	Analyzes of octupolar bis(phthalocyaninato) Ln(III) double-decker complexes (Ln(ABAB) ₂ (Lu, Dy, Eu, Y, Nd))	81
3.1.1.	Synthesis of crosswise ABAB phthalocyanine	81
3.1.2.	Synthesis of octupolar bis(phthalocyaninato) Ln(III) double-decker	

complexes $(Ln(ABAB)_2 (Lu, Dy, Eu, Y, Nd))$	86
3.1.3. UV-NIR measurements of neutral Form of octupolar bis(phthalocyaninato) $Ln(III)$ double-decker complexes $(Ln(ABAB)_2 (Lu, Dy, Eu, Y, Nd))$	89
3.1.4. Single crystal X-RAY measurements of octupolar bis(phthalocyaninato) $Ln(III)$ double-decker complexes $(Ln(ABAB)_2 (Lu, Dy, Eu, Y, Nd))$	96
3.1.5. Hyper-Rayleigh Scattering (HRS) Measurements of Neutral Form of octupolar bis(phthalocyaninato) $Ln(III)$ double-decker complexes $(Ln(ABAB)_2 (Lu, Dy, Eu, Y, Nd))$	98
3.1.6. Analyzes of oxidized and reduced form of octupolar bis(phthalocyaninato) $Ln(III)$ double-decker complexes $(Ln(ABAB)_2 (Lu, Dy, Eu, Y, Nd))$	102
3.1.6.1 UV-NIR measurements of oxidized and reduced form of octupolar bis(phthalocyaninato) $Ln(III)$ double-decker complexes $(Ln(ABAB)_2 (Lu, Dy, Eu, Y, Nd))$	103
3.1.6.2 Hyper-Rayleigh Scattering (HRS) measurements of oxidized and reduced form of octupolar bis(phthalocyaninato) $Ln(III)$ double-decker complexes $(Ln(ABAB)_2 (Lu, Dy, Eu, Y, Nd))$	106
3.2. Analyzes of nonoctupolar bis(phthalocyaninato) $Ln(III)$ double-decker complexes $Ln(AB3)_2 (12-15)$, $Ln(A4)_2 (16-18)$, $Ln(B4)_2 (19-23)$, $Ln(T4)_2 (24-26)$	111
3.2.1. Synthesis of nonoctupolar bis(phthalocyaninato) $Ln(III)$ double-decker complexes $Ln(AB3)_2 (12-15)$, $Ln(A4)_2 (16-18)$, $Ln(B4)_2 (19-23)$, $Ln(T4)_2 (24-26)$	111
3.2.2. UV-NIR measurements of nonoctupolar bis(phthalocyaninato) $Ln(III)$ double-decker complexes $Ln(AB3)_2 (12-15)$, $Ln(A4)_2 (16-18)$, $Ln(B4)_2 (19-23)$, $Ln(T4)_2 (24-26)$	113
3.2.3. Hyper-Rayleigh Scattering (HRS) measurements of nonoctupolar bis(phthalocyaninato) $Ln(III)$ double-decker complexes	

(Ln(AB3) ₂ (12-15), Ln(A4) ₂ (16-18), Ln(B4) ₂ (19-23), Ln(T4) ₂ (24-26))	121
3.2.3.1. Hyperpolarizability of oxidized form nonoctupolar Ln(Pc) ₂ (Ln(AB3) ₂ (12-14), Ln(A4) ₂ (16-18), Ln(B4) ₂ (19-21), Ln(T4) ₂ (24-26))	124
3.2.3.2. Hyperpolarizability of reduced form nonoctupolar Ln(Pc) ₂ (Ln(AB3) ₂ (12-14), Ln(A4) ₂ (16-18), Ln(B4) ₂ (19-21), Ln(T4) ₂ (24-26))	127
4. EXPERIMENTAL PART	129
4.1. General Remarks	131
4.2. Syntheses	131
4.2.1. 1,2-dicyano-4-(hexylthio)benzene (1)	132
4.2.2. 4,5-Bis(hexylthio)-1,2-dicyanobenzene (2)	133
4.2.3. 4,5-Bis(hexylthio)-1,3-diiminoisindolin (3)	134
4.2.4. 1,3,3-Trichloroisindolenine (4)	134
4.2.5. 2,3,16,17-tetra(hexylthio)phthalocyanine (5) and 2,3,9,10,16,17 hexa(hexylthio)phthalocyanine (6)	135
4.2.6. General method for the synthesis of ABAB and AB3 homoleptic bis(phthalocyaninato) lanthanide(III) complexes ((Ln(ABAB) ₂) (7-11), (Ln(AB3) ₂) (12-15))	137
4.2.6.1. ABAB Bis(phthalocyaninato) europium(III) complex (Eu(ABAB) ₂)(7)	138
4.2.6.2. ABAB Bis(phthalocyaninato) dysprosium(III) complex (Dy(ABAB) ₂)(8)	138
4.2.6.3. ABAB Bis(phthalocyaninato) lutetium(III) complex (Lu(ABAB) ₂) (9)	138
4.2.6.4. ABAB Bis(phthalocyaninato) yttrium(III) complex (Y(ABAB) ₂) (10)	139
4.2.6.5. ABAB Bis(phthalocyaninato) neodymium(III) complex (Nd(ABAB) ₂) (11)	139

4.2.6.6.	AB ₃ Bis(phthalocyaninato) europium(III) complex (Eu(AB ₃) ₂)(12)	139
4.2.6.7.	AB ₃ Bis(phthalocyaninato) dysprosium(III) complex (Dy(AB ₃) ₂)(13)	140
4.2.6.8.	AB ₃ Bis(phthalocyaninato) lutetium(III) complex (Lu(AB ₃) ₂)(14)	140
4.2.6.9.	AB ₃ Bis(phthalocyaninato) yttrium(III) complex (Y (AB ₃) ₂)(15)	140
4.2.7.	General method for the synthesis of homoleptic bis(phthalocyaninato) lanthanide(III) complexes ((Ln(A ₄) ₂) (16- 18), (Ln(B ₄) ₂) (19-23), (Ln(T ₄) ₂) (24-26))	141
4.2.7.1.	The unsubstituted (A ₄) bis(phthalocyaninato) europium(III) complex (Eu(A ₄) ₂) (16)	141
4.2.7.2.	The unsubstituted (A ₄) bis(phthalocyaninato) dysprosium(III) complex (Dy(A ₄) ₂) (17)	125
4.2.7.3.	The unsubstituted (A ₄) bis(phthalocyaninato) lutetium(III) complex (Lu(A ₄) ₂) (18)	142
4.2.7.4.	The octahexylthia substituted (B ₄) bis(phthalocyaninato) europium(III) complex (Eu(B ₄) ₂) (19)	143
4.2.7.5.	The octahexylthia substituted (B ₄) bis(phthalocyaninato) dysprosium(III) complex (Dy(B ₄) ₂) (20)	143
4.2.7.6.	The octahexylthia substituted (B ₄) bis(phthalocyaninato) lutetium(III) complex (Lu(B ₄) ₂) (21)	128
4.2.7.7.	The octahexylthia substituted (B ₄) bis(phthalocyaninato) yttrium(III) complex (Y(B ₄) ₂) (22)	144
4.2.7.8.	The octahexylthia substituted (B ₄) bis(phthalocyaninato) neodymium(III) complex (Nd(B ₄) ₂) (23)	144
4.2.7.9.	The tetrahexylthia substituted (T ₄) bis(phthalocyaninato) europium(III) complex (Eu(T ₄) ₂) (24)	145
4.2.7.10.	The tetrahexylthia substituted (T ₄) bis(phthalocyaninato) dysprosium(III) complex (Dy(B ₄) ₂) (25)	145
4.2.7.11.	The tetrahexylthia substituted (T ₄) bis(phthalocyaninato)	

lutetium(III) complex (Lu(T ₄) ₂) (26)	146
5. GENERAL CONCLUSION	147
REFERENCES	151
ANNEX1	168
ANNEX2	179
ANNEX3	187
ANNEX4	191
CV	204
List and number of the molecules described in the manuscript	205

ABBREVIATIONS

DBU	1.8-diazabicyclo[5.4.0] undec-7-ene
DCM	Dichloromethan
DMF	Dimethylformamide
DHB	Dihydroxy benzoic acid
DMSO	Dimethylsulfoxide
EFISH	Electric-field-induced second-harmonic generation
EPR	Electron Paramagnetic Resonance
Esu	ElectroStatic Unit of charge
H ₂ Pc	Metal free phthalocyanine
HRS	Hyper-Rayleigh scattering
ICT	Intra molecular charge transfer
Ln	Lanthanide
MPc	Metallophthalocyanine
MPF	Multi-photon fluorescence
NLO	Nonlinear Optic
NMR	Nuclear Magnetic Resonance
Pc	Phthalocyanine
TEA	triethyl amin
UV-NIR	Ultra-Violet near Infrared

LIST OF FIGURES

Figures	Page
2.1. Induced polarisation as a function of time. (a) Linear and representation as a function of applied field	6
2.2. Induced polarisation as a function of time. (b) nonlinear and representation as a function of applied field.	7
2.3. The process of second-harmonic generation	8
2.4. Plots of the electric field of (a) an applied electromagnetic wave and (b) the induced dipole from a molecule with a centre of inversion	8
2.5. Plots of the electric field of (a) an applied electromagnetic wave and (b) the induced dipole in a second-order NLO material	9
2.6. The first phthalocyanines synthesis	14
2.7. Various methods for preparing free phthalocyanine	15
2.8. Various methods for preparing metallo phthalocyanine	16
2.9. Proposition of a reaction mechanism for a MPc	17
2.10. Nomenclature of Phthalocyanine Analogues	18
2.11. Structure of different type of Pcs a) porphyrin b) subPcc) double decker Pcs	20
2.12. Charge transfer in metallophthalocyanines	21
2.13. a -The prototypical dipolar D- π -A <i>p</i> -nitroaniline molecule, b - Dipolar charge distribution in prototypical dipolar systems	22
2.14. Typical push-pull type benchmarks	23
2.15. The second order optical nonlinearity in a donor or acceptor substituted benzene.	24
2.16. Values of β for para, meta and ortho nitroaniline	24
2.17. Selected ferrocenyl complexes	28
2.18. Selected ferrocenyl and ruthenocenyl complexes	29
2.19. Selected Ruthenium(II) amine complexes	29
2.20. Stilbazole and Bis(stilbazole) metal complexes	30

2.21. Donor and/or bridge role of the metal centre in Schiff base complexes on passing from unsubstituted to D/A substituted.	31
2.22. Structures of tetra substituted push-pull phthalocynines	32
2.23. Structure of extended π -conjugation length push-pull phthalocynines	33
2.24. Structures of 11a and 11b push-pull phthalocynines	34
2.25. Structures of 12a-c push-pull porphyrines	35
2.26. Structures of 13a push-pull porphyrine	35
2.27. Structures of phthalocyanine-triazolehemiporphyrzine dimers	36
2.28. Cubic octupolar archetype template.	38
2.29. Schematic representation of 2D-octupolar symmetries	39
2.30. The structures of 2D octupolar a- TATB, b- triazine, c-boroxine molecules	40
2.31. The structures of 1,3,5-trisubstituted benzenederivaties	41
2.32. The structures of 1,3,5-trimethoxybenzene derivatives	41
2.33. The structures of 1,3,5-trinitrobenzene derivatives	42
2.34. The structures of tris(bipyridine) complexes	43
2.35. The structures of 1,3,5-substituted with $Ru^{II}\sigma$ -acetylide complexes	44
2.36. The structure of 1,3,5-substituted with $Fe^{II}\sigma$ -acetylide complexe	45
2.37 The structure of tris(dipicolinato)lanthanide(III) series complexes	45
2.38. The variation of the quadratic hyperpolarizability with ionic radius (a) and f orbital filling (b)	46
2.39. Structures of octupolar 1,3,5-trisubstituted benzene -triazine molecules and their Second-Order NLO Properties	47
2.40. Structures of subphthalocyanines and Second-Order NLO Properties	48
2.41. Various strategies for engineering of octupolar 3D molecules	49
2.42. The structures of octupolar molecules of D_{2d} symmetry derived from an orthogonalized biphenyl core.	50
2.43. Schematic representation of general octupolar distribution and pCP template	51
2.44. The (4,7,12,15)tetra-substitution pattern for [2.2]p-cyclophane(pCp) as a point-charge template for an octupole	52

2.45. The structures of 3D octupolar bipyridine metal complexes	53
2.46. Octupolar aryl trisphthalocyanine phosphonium salt	54
2.47. 3D octupolar Pc based compounds and their Second-Order NLO Properties	55
2.48. Schematic representation of HRS process in bulk liquid	57
2.49. Benchmark materials for HRS experiment	59
2.50. Schematic representation of general octupolar distribution and pCP template	60
2.51. (a) Schematic representation of a molecule with square geometry (b) A cubic octupole template (c) A disordered cubic octupole template	61
2.52. Sandwiches phthalocyanines and porphyrins as a octupole template	61
2.53. The structures of crosswise ABAB type free Pc and octupolar double decker lanthanides bis(phthalocyanines)	62
2.54. The structures of non-octupolar AB ₃ , A ₄ , B ₄ , T ₄ type double decker lanthanide homoleptic bis(phthalocyanines)	63
3.1. (a) Schematic of a molecule with square geometry (b) A cubic octupole template (c) A disordered cubic octupole template	65
3.2. The statistical condensation approach for synthesize ABAB type pc	66
3.3. The statistical condensation approach for steric hinderance Pc	66
3.4. The first regioselective approach for crosswise-Pc	67
3.5. The regioselective approach for crosswise-Pc	68
3.6. Synthetic route of crosswise ABAB type Pc by regioselective approach.	69
3.7. Synthesis of bis(phthalocyaninato) Y(III) double-decker complexes	71
3.8. The synthesize approach for octupolar Ln(Pc) ₂	72
3.9. Absorption spectra of free phthalocyanine (i) and metallo phthalocyanine (ii) and Electronic transitions accounting for B and Q bands of phthalocyanines	73
3.10. UV-Vis Spectrum of ABAB (5) type free phthalocyanines	74
3.11. UV-NIR spectrum of a neutral Ln(Pc) ₂ bisphthalocyanine and scmatic representation of the MO levels	75
3.12. UV-NIR spectrum of Lu(ABAB) ₂ Bis-phthalocyanine (1 x 10 ⁻⁵ M) in	

CHCl ₃	76
3.13. The UV-NIR spectrum of neutral Ln(Eu, Dy, Lu, Y, Nd)(Pc(ABAB) ₂) in CHCl ₃ (1x10 ⁻⁵ M)	77
3.14. Plot of the interplane distances vs lanthanide ionic radius	78
3.15. Crystallographic structure of Lu(ABAB) ₂ (9)	79
3.16. The interplane distance (d _{N4-N4}) of Ln(ABAB) (Lu, Eu, Dy, Nd, Y)	80
3.17. The interplane distance (d _{N4-N4}) of Ln(ABAB) ₂ vs lanthanide contraction	80
3.18. The twist angles φ _T of Ln(ABAB) ₂ (Lu, Eu, Dy, Y, Nd)	81
3.19. Plot of the hyperpolarisability β vs Ln(ABAB) ₂ (a) and f-orbital filling (b)	85
3.20. The UV-NIR spectrum of neutral Ln (Eu, Dy, Lu, Y, Nd)(ABAB) ₂ in CHCl ₃ (1x10 ⁻⁵ M) (b) Plot of the interplane distances vs lanthanide ionic radius	85
3.21. Neutral, oxidized, and reduced forms of Ln(Pc) ₂	87
3.22. UV-NIR spectrum of Lu(ABAB) ₂ Bis-phthalocyanine (1 x 10 ⁻⁵ M) in CHCl ₃ + Br ₂ (oxidized)	85
3.23. UV-NIR spectrum of reduced form of Lu(ABAB) ₂ Bis-phthalocyanine (1 x 10 ⁻⁵ M) in (1/10 -THF/CHCl ₃ + 3 mg NaBH ₄)	87
3.24. Plot of the hyperpolarisability coefficient β vs oxidized form of Ln(ABAB) ₂	91
3.25. UV-NIR spectra of Eu(ABAB) ₂ bis(Phthalocyanine) (7) (1 x 10 ⁻⁵ M)	92
3.26. Plot of the hyperpolarisability coefficient β vs reduced form of Ln(ABAB) ₂	94
3.27. UV-NIR spectrum of Eu(ABAB) ₂ Bis(Phthalocyanine) (7) (1 x 10 ⁻⁵ M)	96
3.28. Tetramerization Solid-state approach for homoleptic bis(Pcs)	96
3.29. The method in solution approach cyclic tetramerization for homoleptic bis-Pcs	97
3.30. The synthesis approach for Ln(AB3) ₂	97
3.31. UV-Vis spectra of AB3 (6) type free phthalocyanine	98
3.32. The UV-NIR spectra of neutral Lu(Pc(SC ₆) _{n.0-8}) ₂ in CHCl ₃ (1x10 ⁻⁵ M)	99
3.33. The UV-NIR spectra of neutral Lu(Pc(SC ₆) _{n.0-8}) ₂ in CHCl ₃ (1x10 ⁻⁵ M)	100
3.34. UV-NIR spectra of Lu(Pc) ₂ Bis(phthalocyanine) (1 x 10 ⁻⁵ M) in CHCl ₃ + Br ₂ (oxidized)	102

3.35. UV-NIR spectra of reduced Lu(Pc) ₂ Bis(phthalocyanine) (1 x 10 ⁻⁵ M) in CHCl ₃	104
3.36. Plot of the hyperpolarisability coefficient β vs Lu(Pc) ₂	106
3.37. The UV-NIR spectra of neutral Lu(Pc(SC ₆) _{n:0-8}) ₂ in CHCl ₃ (1x10 ⁻⁵ M)	108
3.38. Plot of the hyperpolarisability coefficient β vs (a) octupolar Lu(ABAB) ₂ (b) nonoctupolar Lu(B4) ₂	110

LIST OF TABLES

Table	Page
2.1. Static hyperpolarizability for a series of conjugated donor–acceptor compounds containing heterocyclic rings	25
2.2. Static hyperpolarizability and decomposition temperature (Td) of a number of thermally stable chromophores with good nonlinearity	27
3.1. UV-NIR spectral data of neutral forms of Ln(Eu, Dy, Lu, Nd, Y)(ABAB) ₂ Bis(phthalocyanine) (1 x 10 ⁻⁵ M)	76
3.2. The second-order NLO data for the octupole Ln(ABAB) ₂ (7-11)	83
3.3. UV-NIR spectra of oxidized forms of Ln(Eu, Dy, Lu, Nd, Y)(ABAB) ₂ Bis-phthalocyanine (1 x 10 ⁻⁵ M)	89
3.4. UV-NIR spectra of reduced forms of Ln(Eu, Dy, Lu, Nd, Y)(ABAB) ₂ Bis-phthalocyanine (1 x 10 ⁻⁵ M)	90
3.5. The second-order NLO data for the octupole Ln(ABAB) ₂ (7-11)	91
3.6. The second-order NLO data for the octupole Ln(ABAB) ₂ (7-11)	93
3.7. UV-NIR spectral data of neutral forms of Ln(AB3) ₂ (12-14), Ln(A4) ₂ (16-18), Ln(B4) ₂ (19-21), Ln(T4) ₂ (24-26) Bis(phthalocyanine) (1 x 10 ⁻⁵ M)	101
3.8. UV-NIR spectra of oxidized forms of Ln(AB3) ₂ (12-14), Ln(A4) ₂ (16-18), Ln(B4) ₂ (19-21), Ln(T4) ₂ (24-26) Bis-phthalocyanine (1 x 10 ⁻⁵ M)	103
3.9. UV-NIR spectra of reduced forms of Ln(AB3) ₂ (12-14), Ln(A4) ₂ (16-18), Ln(B4) ₂ (19-21), Ln(T4) ₂ (24-26) Bis-phthalocyanine (1 x 10 ⁻⁵ M)	105
3.10. The second-order NLO data for the nonoctupole Ln(AB3) ₂ (12-14), Ln(A4) ₂ (16-18), Ln(B4) ₂ (19-21), Ln(T4) ₂ (24-26)	106
3.11. The second-order NLO data for the Ln(AB3) ₂ (12-14), Ln(A4) ₂ (16-18), Ln(B4) ₂ (19-21), Ln(T4) ₂ (24-26)	109
3.12. The second-order NLO data for the nonoctupole Ln(AB3) ₂ (12-14), Ln(A4) ₂ (16-18), Ln(B4) ₂ (19-21), Ln(T4) ₂ (24-26)	111

1. INTRODUCTION

The field of nonlinear optics has attracted lot of interest in the past three decades not only because of the possible numerous applications in telecommunications, optical data storage etc., but also because of the fundamental research connected to issues like charge transfer, conjugation, polarization and crystallization into noncentrosymmetric lattices. In principle nonlinear optics (NLO) deals with the interaction of applied electromagnetic fields in various materials to generate new electromagnetic fields altered in frequency, phase or other physical properties. A variety of systems including inorganic materials, organometallic materials, organic molecules and polymers have been studied for NLO activity. Owing to the combination of chemical tunability and choice of synthetic strategies, organic molecules in particular have received much attention. Second order nonlinear optical response in an organic chromophore is intrinsically based on electronic ‘push-pull’ mechanism operative in a molecule containing a donor linked to an acceptor moiety through a conjugated π -electron bridge.

The drawbacks with these systems are that they are not transparent in the visible region and as the conjugation increases their thermal stability and photostability decreases. Another major problem is the retention of the NLO activity when incorporated into devices. To retain the β in bulk state, they either have to crystallize into a non-centrosymmetric crystal or in a poled polymer the non-centrosymmetric alignment should be retained on removal of the applied electric field. Polar molecules usually tend to crystallize into a centrosymmetric crystal restricting their usage as a NLO device in the crystal form, but these find applications in poled polymers where large dipole moments (μ) play an important role. Currently the need is to develop molecules, which are transparent in the visible region and possessing enhanced hyperpolarizabilities, with SHG activity in the bulk state.

Studies based on group theory and quantum mechanics have helped set conceptual foundations to the domain of non-dipolar molecules for nonlinear optics, which became known as octupolar, and more generally *multipolar* molecules. Octupolar molecules, in which symmetry constraints impose a cancellation of the dipole moment, have an intrinsic hyperpolarisability β , in which all the coefficients β_{ijk} have increased values, often higher than the simple dipolar

systems built on the same motif. At a structural level, it can be shown that the most generic template for 3D octupolar molecules is amenable to a cube with alternating charges at the edges such as accounting for donor and acceptor substituents. And these 3D octupolar cubic molecules are expected show high nonlinearities at molecular as well as crystalline scale. In spite of all the various structures reported, there is no molecules actually representing the “real” cube (even if deformed) with eight alternated charges at the corner and delocalization of the charges between the higher and lower planes have been obtained so far.

The goal of this thesis is to synthesize the “real octupolar cube” with sandwich lanthanide complexes of ABAB phthalocyanines bearing alternated electro-donor groups at the edges. Thus, various double decker bislanthanide phthalocyanine derivatives have been designed as a octupolar real cube. As electron donating groups, we choose thiols (strong electron donor) in order to tune the nonlinear optical properties. Series of octupolar and non-octupolar double decker lanthanide bis(phthalocyanine) derivatives have been synthesized and characterized based on various techniques like $^1\text{H-NMR}$, $^{13}\text{C-NMR}$, Mass, IR, and X-Ray crystallography. Nonlinear optical properties are measured with Hyper-Rayleigh Scattering (HRS) technique in solution.

These PhD works have been achieved within a co-directed co-tutelle framework, and therefore included the complete chain from the synthesis of various double decker bis lanthanide phthalocyanine derivatives until their evaluation of nonlinear optical properties by using HRS technique. This double thematic directs the organization of this thesis, with a bibliographic part summarizing firstly nonlinear optic, its origin, and various types of NLO effects. Detailed description is given for second order effects particularly on second harmonic generation followed by review of second order NLO materials studied especially phthalocyanines so far. Emergence and requirement of octupolar systems over dipolar systems are discussed in detail. And then results are given and discussed. We will then develop our results on a synthetic point of view and then detail the results regarding their NLO properties.

2. BIBLIOGRAPHIC DATA

2.1. Definition of nonlinear optic

Nonlinear optic (NLO) can be defined as a phenomena that occur with interaction of sufficiently intense light in various materials to yield new optical properties such as electromagnetic field altered in phase, frequency and amplitude [1,2]. Currently, a great deal of research is being devoted to both organic and inorganic materials that exhibit nonlinear optical (NLO) effects, particularly second harmonic generation (SHG), which, put simply, causes a doubling in the frequency of incident light.

Nowadays, *nonlinearoptic* has evolved into many different branches, depending on the form of the material used for studying the nonlinear phenomena. The ability to manipulate the frequency, phase, polarisation or path of light has very important technological effects. The growth of research in nonlinearoptics is closely linked to the rapid technologicaladvances that have occurred in related fields, such as ultra-fastphenomena, photonics, computer, optical signal processing devices, optical data storage, dynamic image processing, fiber optics, andopticalcommunications [3-5].

2.2. Origin of nonlinearoptic

When a molecule is subjected to an oscillating external electric field (light), the induced change in molecular dipole moment (polarisation) can be expressed by a power series in the field strength E_j (**Fig. 2.1**) as in eqn. (2.1), where p_i is the electronic polarisation induced along the i the molecular axis, α is the linear polarisability, β the quadratic hyperpolarisability, and γ the cubic hyperpolarisability. α in eqn. (2.1) is a second-rank tensor because it relates all of the components of the polarisation vector to all of the components of the electric field vector, and is responsible for the linear optical behaviour. Analogously, β and γ in eqn. (2.1), which relate the polarisation to the square and the cube of the field strength, are respectively, third-rank and fourth-rank tensors, responsible for second-order and

third-order NLO effects. The even-order tensor, β , vanishes in a centrosymmetric environment.

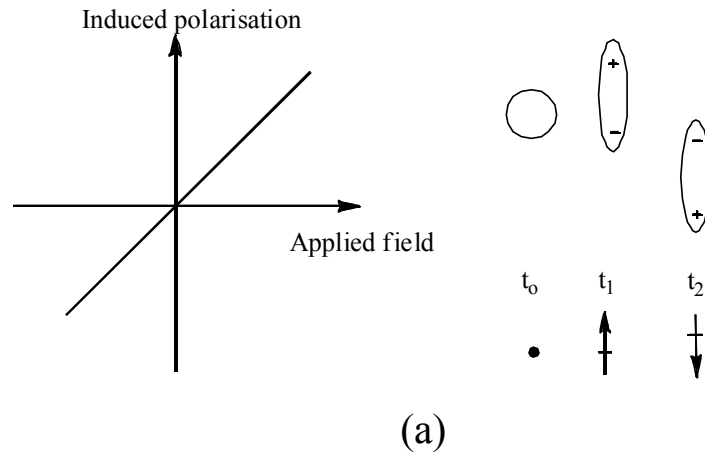


Figure 2.1. Induced polarisation as a function of time. **(a)** Linear and representation as a function of applied field.

$$p_i = \sum_j \alpha_{ij} E_j + \underbrace{\sum_{j \leq k} \beta_{ijk} E_j E_k + \sum_{j \leq k \leq l} \gamma_{ijkl} E_j E_k E_l + \dots}_{\text{Negligible}} \quad \dots (2.1)$$

where,

α_{ij} = Polarisability

β_{ijk} = First hyperpolarisability (second order effects)

γ_{ijkl} = Second hyperpolarisability (third order effects)

and i, j, k, l corresponds to the molecular coordinates.

For small fields the quadratic and cubic terms in eqn. (2.1) can be neglected, so that the induced polarisation is proportional to the strength of the applied field (linear optical behaviour). This equation describes the full picture only if the atomic or molecular potential is classical harmonic potential. However, when a molecule is subjected to very intense field, as a laser light, the material can become so polarized that its polarisability can change and hence the induced polarisation is in nonlinear function of field strength (**Fig. 2.2**) and the second and third terms in eqn. (2.1)

become important, such that nonlinear optical behaviour can be observed. Note that, the ‘nonlinear’ term originates from the nonlinear dependence (quadratic or cubic) of the induced polarisation of the applied field.

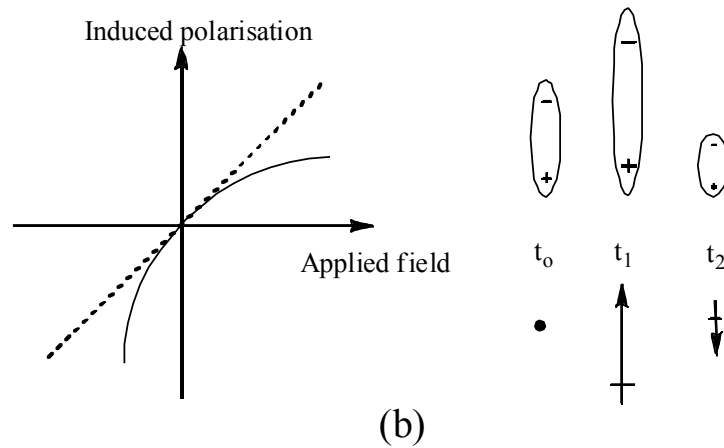


Figure 2.2. Induced polarisation as a function of time. **(b)** nonlinear and representation as a function of applied field.

Since, the second harmonic generation (SHG) is main focus phenomena in this thesis, a detailed discussion about this process is required in order to have a clear picture of the SHG effect discussed in this thesis.

2.3. Definition of second-order nonlinear optic

Second harmonic generation is the main archetypal nonlinear optical process. Second harmonic generation was discovered by Franken *et al.* in 1961 just after the development of intense laser sources [7]. Since then this process has become very important for many applications, such as, frequency doublers, frequency converter, electro-optic modulators and nonlinear optical microscopy [8].

Second-order nonlinear optical effect of molecular materials is associated with first hyperpolarisability (β) also called microscopic quadratic. The process of second-harmonic generation is showed in **Fig. 2.3**. When a laser beam at frequency ω reaches to nonlinear optical material a new beam at frequency 2ω is created. In other words, two photons from the input beam are lost and one photon in the output

beam is created. The efficiency of this process can surpass %50 under proper circumstances [9].

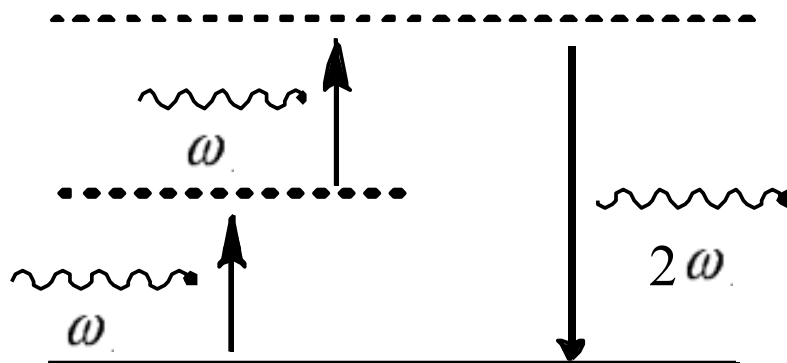


Figure 2.3. The process of second-harmonic generation.

As mentioned earlier, when a medium is exposed to an electromagnetic radiation, oscillating charges in the material will produce the polarization wave and this wave is re-emitted at the same frequency as the incident radiation. But if the electric field is strong enough, the incident polarization is no longer oscillating linearly and the polarization wave is distorted with the applied field as shown in **Fig. 2.4.**

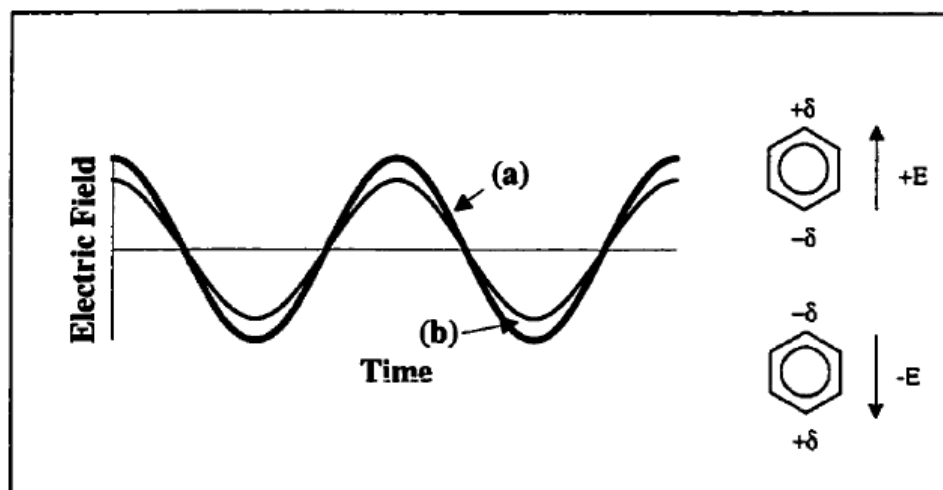


Figure 2.4. Plots of the electric field of (a) an applied electromagnetic wave and (b) the induced dipole from a molecule with a centre of inversion. Adapted from ref. [10]

Fig. 2.4 shows polarization of centrosymmetric molecule such as benzene. In this case the restoring force returning displaced electron density is symmetric, for this reason the magnitude of induced dipole is equal in opposite directions, which

means; they exhibit the first nonlinear term as $+\beta E^2$ and $-\beta E^2$. This contradiction leads to $\beta=0$. Thus the centrosymmetric molecule has zero β value [11].

On the other hand, if the restoring force is dependent upon the direction of charge displacement, then the induced polarization of the atom or molecule will not depend upon the magnitude of applied field anymore, but also upon the direction of the field. **Fig. 2.5** shows the interaction of a strong oscillating electric field with this type of system. The induced polarization wave is distorted because of the nonlinear response.

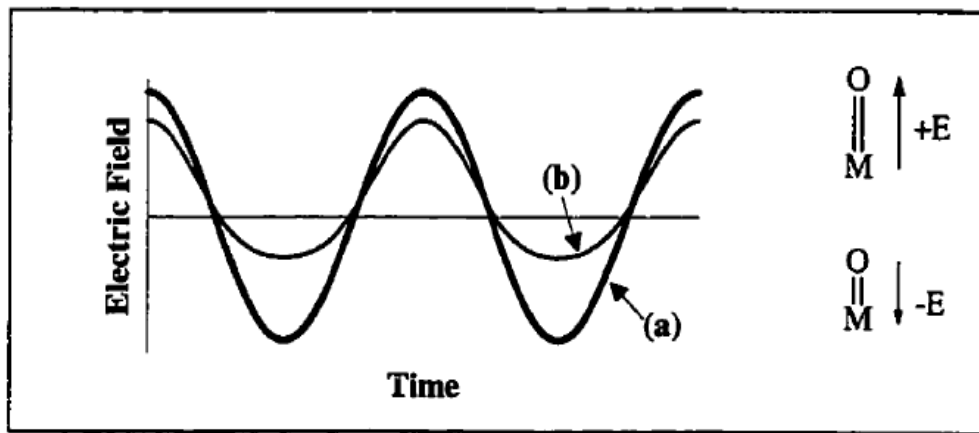


Figure 2.5. Plots of the electric field of (a) an applied electromagnetic wave and (b) the induced dipole in a second-order NLO material. Adapted from ref. [10]

Second-order nonlinear optic effects occur thanks to the nature of this asymmetric polarization wave. Since SHG originates from asymmetry of induced polarization wave, it can say that, only materials, which can produce this asymmetric wave, can produce SHG or any other second-order NLO process [12].

2.4. Materials for second-order nonlinear optic

Nonlinear optical (NLO) materials have significant influence in nonlinear optics and especially on information technology and industrial applications. The target is to make new advance materials exhibiting large NLO response, which also posses all the technological requirements for applications such as wide transparency

range, fast response, high damage threshold but also processability and adaptability [13-16].

Many research efforts have been dedicated to synthesized and designed efficient molecule-based Second-order NLO materials in order to create large first hyperpolarizability (β) values because of their potential applications [17-21]. Design of second-order NLO materials is now quite developed and essential criteria for exhibition of large hyperpolarizabilities have been discovered. The basic rules are as follows:

- ❖ Polarisable material
- ❖ Asymmetric charge distribution
- ❖ A pathway of π -conjugated electrons
- ❖ Asymmetric crystal packing

Moreover, for optical applications, a nonlinear material should possess the subsequent features [22].

- ❖ Wide optical transparency area
- ❖ High laser damage threshold
- ❖ Ability to process into crystals, thin films, etc.
- ❖ Easy of fabrication
- ❖ Nontoxicity and good environmental stability
- ❖ High mechanical strength and thermal stability
- ❖ Fast optical response time.

Since the discovery of NLO effects, several classes of materials have been developed for particular applications. NLO materials can be roughly classified in two different categories as inorganic (crystals, metal based materials) and organic materials. Each category *i.e.* inorganic and organic possesses its own set of benefits and drawbacks as described below [23].

2.4.1. Inorganic materials

The study for effective materials were focused on inorganic materials such as quartz, potassium dihydrogen phosphate (KDP), lithium niobate (LiNbO_3), and its analogues, potassium titanyl phosphate (KTP) and its analogues, since SHG was first observed in single crystal quartz by Franken and co-workers in 1961 [24-28]. Inorganic materials have desirable properties for materials applications, including a large transparency range, good mechanical properties, high optical damage threshold and the fact that they can be grown as large crystals.

The inorganic materials have important drawbacks such as "trade-off" problem between response time and magnitude of optical nonlinearity. Moreover, they have insignificant optical quality because of absorption strongly in the visible region, so reducing many possible applications.

2.4.2. Organic materials

As an alternative to inorganic materials, organic molecules can suppress the limitations identified above and therefore have been of considerable interest for use in nonlinear optics due to their large optical nonlinearities. The NLO effects in organic materials are usually electronic in nature, which leads to fast nonlinear response [29-34]. The architectural flexibility allows for precise molecular design and the determination of structure–property relationships.

The electronic transitions of organic materials improve the NLO efficiencies in the UV–visible region, but also caused decrease of optical transparency. Another drawback of organic materials is that they often have lower thermal and photochemical constancy.

2.4.3. Metal-based materials

The metal-based materials (organometallic and coordination compounds) have arising recent interest achievement in second-order Nonlinear Optic. They offer a large variety of metals that possess the polarizable d electrons and ligands. Therefore these have been suggested: [35- 37]

- a) Metal-based systems can possess metal-to-ligand (MLCT) or ligand-to-metal (LMCT) charge transfer bands in the visible region of the spectrum. These optical absorption bands are usually associated with large second-order activity (although, they can also lead to “transparency“ problems).
- b) Chromophores, such as phthalocyanines and its analogs, containing metal ions are between the most strongly colored materials known. The strength of the optical absorption band (related to its transition dipole moment) is also related with large NLO.
- c) Metal-based compounds have low-energy excited states with excited-state dipole moments considerably different from their respective ground-state dipole moments. Most of these excited states involve transfer of electron density between the central metal and one or more of the associated ligands and have large oscillator strength.
- d) Metal-based compounds also have significant benefits in the range and mix of non-aromatic ligands that can be attached to the metals. These ligands can shift the occupied and unoccupied metal d orbitals that interact with the π -electron orbitals of the conjugated ligand system. This provides a mechanism for fine-tuning and optimizing β or the crystallographic factors that control the bulk susceptibility.

The only predictable drawback is the low energy d-d transitions present in nearly all metal-based compounds, normally observed in the visible light region. This gives rise to what is termed a 'nonlinearity/transparency trade-off'. If a material is to

be used in a frequency doubling then obviously, absorption of the harmonic light that is created will limit the effectiveness of these materials.

As mentioned above, metal based materials have many advantages compared to organic materials for nonlinear applications. First they have large and fast nonlinearities, easy to process and integrate into optical device, tailorability: a fine-tuning of the NLO properties can be achieved by rational modification of the chemical structure.

2.5. Phthalocyanines and related materials

The phthalocyanines were used as materials for Second-Order Nonlinear Optic in this thesis. Therefore, general properties and the different methods available for the preparation of metallated and metal-free phthalocyanines were briefly discussed here.

2.5.1. Synthesis of phthalocyanines

Phthalocyanines belong to the tetrapyrrole macrocycle class, with the structure containing an alternating nitrogen atom-carbon atom ring. Phthalocyanine was discovered accidentally during preparation of *ortho*-cyanobenzamide from phthalamide and acetic anhydride by the British chemists Braun and Tcherniac in 1907 (**Fig. 2.6**) [38].

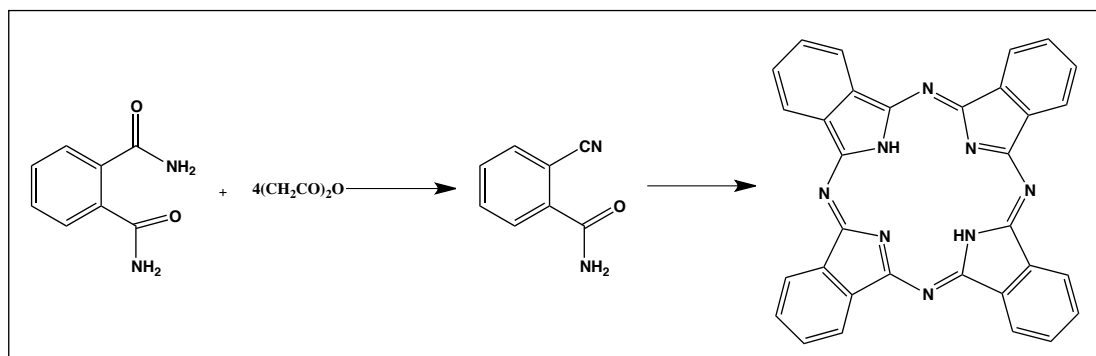


Figure 2.6. The first phthalocyanines synthesis

However, the importance of this material was not recognized until the first patent was granted in 1929 including the synthesis and the properties [39]. Since then, several methods were developed for high yield formation of the metal-free and metallated phthalocyanine.

The precursors that can be used for the synthesis of metal-free phthalocyanines are shown in **Fig. 2.7**. The most common precursor used in the laboratory synthesis are phthalonitrile (1,2-dicyanobenzene), diiminoisoindoline or its substituted derivatives [40]. The metal-free phthalocyanine can be easily obtained by these precursors by heating in high boiling alcohols in the presence of strong organic base (e.g. 1,8-diazabicyclo[5.4.0]undec-7-ene (DBU), 1,5-diazabicyclo[4.3.0]non-5-ene (DBN)) [41-43]

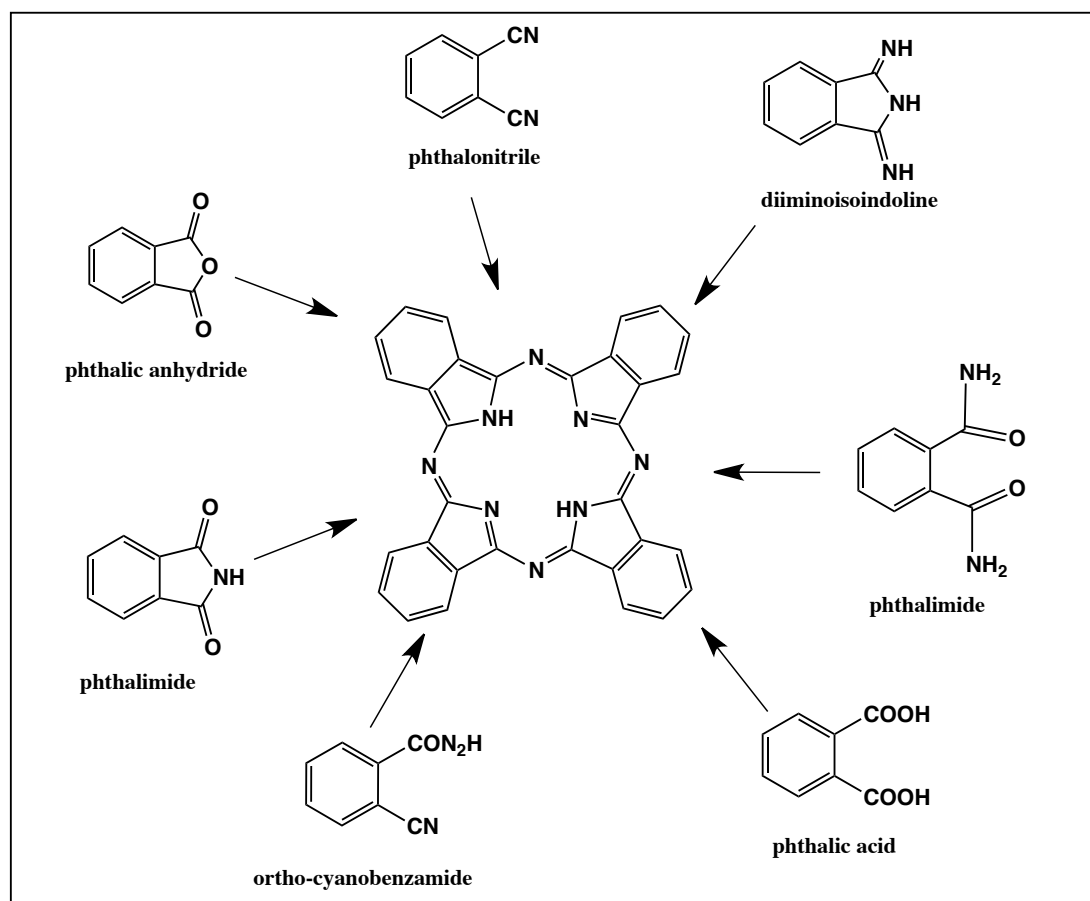


Figure 2.7. Various methods for preparing metal-free phthalocyanine

The synthesis of metal containing phthalocyanine complexes can also be managed in several different ways (**Fig. 2.8**) [44,45]. Most metallophthalocyanines can be obtained from phthalonitrile or diiminoisoindoline in addition of a metal in high-boiling solvents such as DMAE, quinoline or 1-chloronaphthalene [46]. And in case the phthalimide and phthalic acid anhydride, the urea need to be used as a source of nitrogen and a catalyst such as ammonium molybdate in order to obtain metal-containing phthalocyanines.

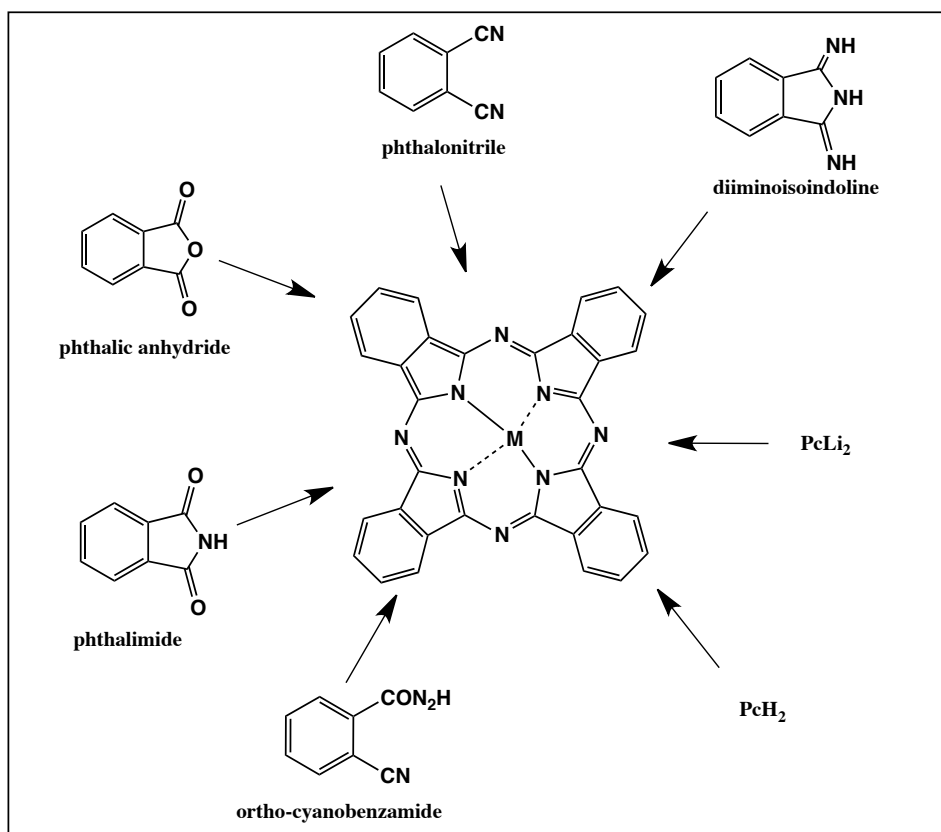


Figure 2.8. Various methods for preparing metallo phthalocyanine

Metal-containing phthalocyanine can also be synthesized by metallation of metal-free phthalocyanines or by the replacement of lithium (Li) from Li₂Pc with suitable metal ions in refluxing solvents like DMF, quinoline or 1- chloronaphthalene [47].

The metallated phthalocyanine complexes have been studied and synthesized over the years, giving rise to compounds with different physical and chemical properties. The lanthanide (III) ions form with phthalocyanines (Pc) complexes of the type Ln(Pc)₂, where the lanthanide ion is sandwiched between two phthalocyanine rings, because the diameter of the trivalent lanthanide ions is too large to make them fit in the cavity of the phthalocyanines. The lanthanide phthalocyanine complexes are only known since the middle 1960's and since then they have been studied widely because of their electrochromic properties [48].

2.5.2. The reaction mechanism of phthalocyanine

It must be noted that the mechanism of formation of phthalocyanine is still not clarified, however some intermediates have been isolated and characterized. Leznoff proposed a mechanism in 1989 and suggested that, in Pc reactions involving organic bases such as DBU and DBN or alkali metalalkoxides in alcohol, the alkoxide can act as nucleophile (Fig. 2.9). Likewise, in metal containing Pc synthesis the counter anion can play the same role as the nucleophile [49-51].

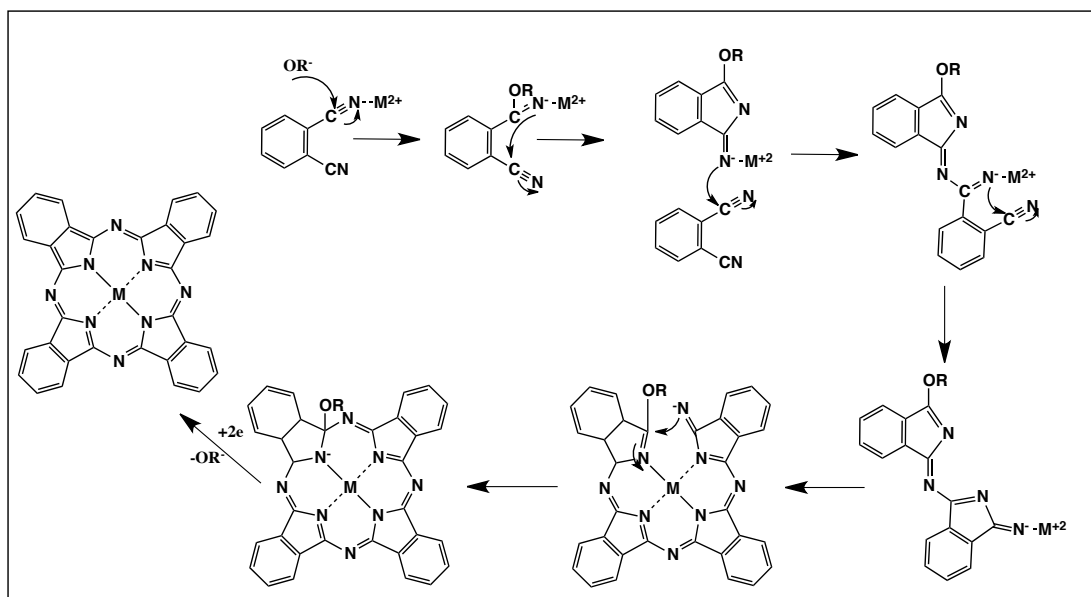


Figure 2.9. Proposition of a reaction mechanism for a MPc.

It is of interest that the cyclotetramerization of phthalonitrile can occur even without the concurrent complexation of a metal ion – at temperature in excess of 200 C within a melt that is in contact with certain metal alloys (e.g. InBi) [52, 53]. It is not clear as to electronic state of the resulting planar metal free macrocycle, which was characterized by single crystal X-ray diffraction.

Finally, it is clear that both the electronic and steric effects of substituents can have a significant influence on the mechanism and outcome of cyclotetramerization reactions.

2.5.2. Nomenclature of phthalocyanines

An unambiguous system for compound nomenclature is required to distinguish the many phthalocyanine derivatives. The phthalocyanines is named with base on the formula $a-(L)_n-n\&p-S-Pc M$ (Fig. 2.10)[54].

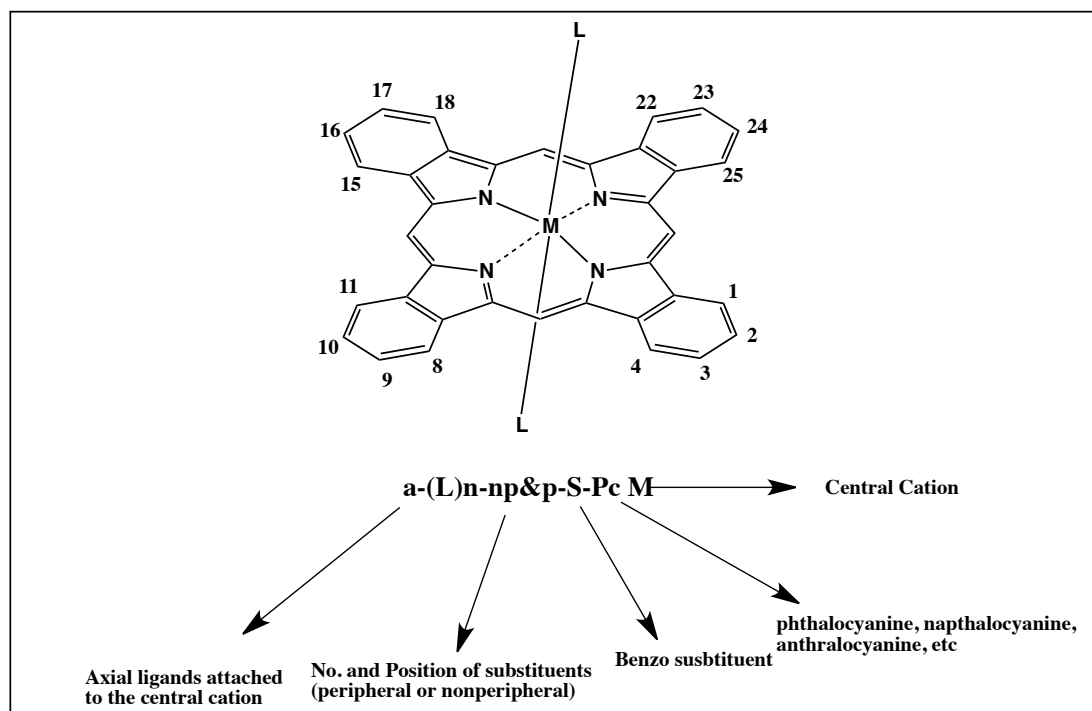


Figure 2.10. Nomenclatures of phthalocyanine analogues

There are sixteen possible sites for macrocycle substitution associated with the four benzo-subunits. The 2,3,9,10,16,17,23,24 carbon atoms are termed the *peripheral* (p) sites and 1,4,8,11,15,18,22,25 carbon atoms are denote the *non-peripheral* (np) sites.

The abbreviation t signifies a peripherally or non-peripherally tetra-substituted Pc, which is usually composed of four isomers. In contrast, there are important materials based on octa(o)-substituted Pcs both with peripheral and with non-peripheral substituents and these are distinguished by the abbreviations op and onp , respectively.

2.5.3. Applications of phthalocyanine

Phthalocyanines are planar macrocyclic aromatic compound, isoelectronic with porphyrins [55-56]. Unsubstituted phthalocyanines and many of substituted ones are highly symmetrical compounds. A great number of unique properties arise from their electronic delocalization, which makes these compounds valuable in different applied fields.

However, the inherent symmetry of the molecule sometimes represents a limitation for many purposes. Thus, the possibility of designing and synthesizing unsymmetrical compounds with substituents located at specific positions will allow fine-tuning of many physical properties, thus enhancing the technological applications of the phthalocyanines.

The phthalocyanines are used traditionally as colorants and as blue and green pigments [55]. Phthalocyanine and its metal-containing derivatives comprise one of the most studied class of functional organic materials.[56–61] The diverse and useful functionality of the phthalocyanine macrocycle originates from its 18π - electron aromatic system which is closely related to that of the naturally occurring porphyrin ring. The additional p-orbital conjugation, afforded by the four benzenoid units and the orbital perturbation caused by the nitrogen atoms at the four meso-positions, have a profound effect on the molecular orbital structure of the porphyrin chromophore. These results in a bathochromic shift of the lowest energy absorption band (the Q-band) in the visible region of the spectrum and a strong enhancement of its intensity (typically $\lambda_{\max} \sim 680$ nm, $\epsilon \sim 200,000$). Their resulting strong color, coupled with renowned chemical and thermal stability, explains the ubiquitous use of phthalocyanines as highly stable blue (or green) pigments and dyes [62–64]. In addition to their long established use as colorants, phthalocyanines are exploited commercially for optical data storage, catalysis, and as photoconductors in Xerography [65-67]. They are also of interest as materials for non-linear optics, liquid crystals, ordered thin films, photodynamic cancer therapy, molecular semiconductors, components of highly conducting charge-transfer salts, and polymers, photovoltaic devices, electrochromic devices, fuel cells, and sensors [68-

87]. The synthesis of phthalocyanine and its substituted derivatives is often driven by the desire to exploit and improve performance in one of these technological or therapeutic arenas.

2.5.4.1. Nonlinear optics

The chemical and physical properties of phthalocyanines provide requirements for NLO materials. Therefore, among metal-based compounds, phthalocyanines and its analogs (double decker Pcs, subphthalocyanines, porphyrine (see Fig. 2.11) have been intensively studied as NLO materials [88-93]. A common application of Pc NLO activity is the eye protection against harm from intense red and IR light [94].

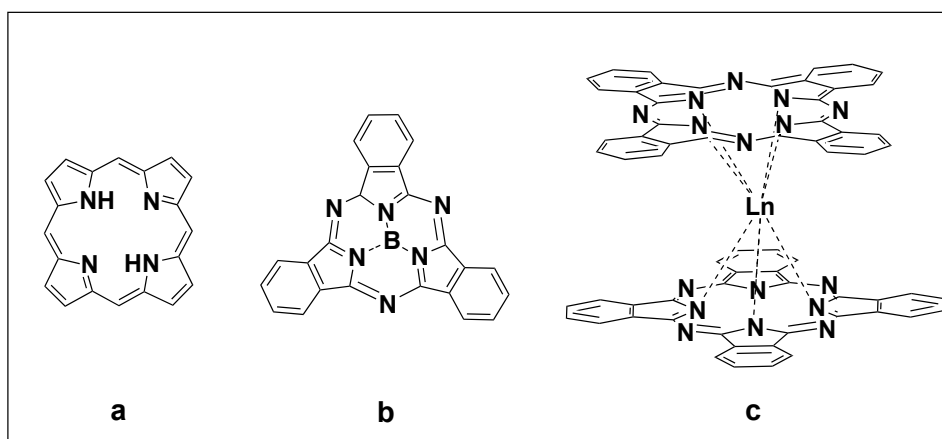


Figure 2.11. Structure of different type of Pcs a) porphyrin b) subPcc) double decker Pcs

The phthalocyanine molecule has a two dimensional π -electron conjugated system (an aromatic system with 18 π -electrons), and a number of adjustments can be made in the macrocycle by incorporating more than 70 different metal atoms [95]. In addition, there are 16 possible sites of substitution on the fused benzene rings, which allow combination of different substituents on the peripheral or non-peripheral positions of the ring.

The metallo phthalocyanines possess a tailoring of electrophysical parameters over a broad range and, finally, allow modulating the electrical and optical behavior of the compounds. Phthalocyanines as organometallics possess metal-to-ligand charge transfer (MLCT), ligand-to-metal charge transfer (LMCT), or intraligand charge transfer (ILCT) which are related to transition dipole moments and low transition energies. Therefore, they can act as donor or acceptor groups of the D- π -A (Push-pull) system, or as polarisable bridge moieties for the design of efficient chromophores.

Fig. 2.12 shows a charge transfer between electron rich ligand to an electron poor metal (LMCT) and metal to ligand (MLCT) [95].

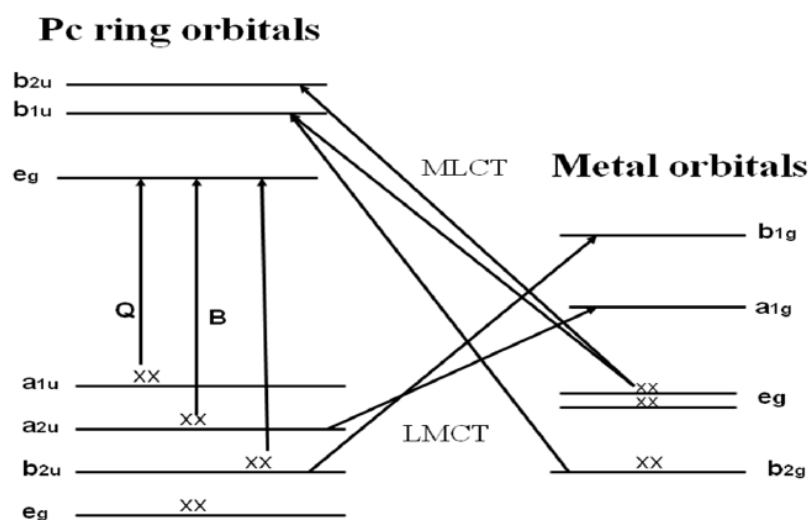


Figure 2.12 Charge transfer in metallophthalocyanines

Typically, phthalocyanines and its analogues (porphyrins, subphthalocyanines) possess highly polarizable delocalized π -electrons, which cause strong nonlinearities. Most NLO studies using Pcs have involved the third-order response (e.g. frequency tripling) since it only requires a highly polarisable π -system, but not an unsymmetrical structure [96].

As mentioned before, planar centrosymmetric materials such as symmetrical phthalocyanines do not exhibit second-order activity. In order to create asymmetry, which is a crucial requirement of second-order NLO, two main approaches have been concerned **a)** peripheral substitution of the phthalocyanine core with donor and

acceptor groups (Push-Pull) and **b**) architectural adjustment of the Pc core to reduce the symmetry for obtaining noncentrosymmetric structures, which presenting octupolarity in the nonlinear response.

2.6. Materials design for second-order nonlinear optic

In order to have high first nonlinear hyperpolarizability β , three kind of methods have been developed **(i)** using different types of conjugation bridge, **(ii)** optimizing the combination of different donors and acceptors, **(iii)** employing multiple charge transfer structures such as octupolar [97-100]. These systems can be categorized in two: **A) Push-Pull systems** and **B) Octupolar systems** and will be explained below.

2.6.1. Push-Pull Systems

The majority of molecular compounds that own large β values contain conjugated π -systems with donor (D) and acceptor (A) moieties. The linear optical properties of such dipolar, polarizable molecules are characterised by low energy and intramolecular charge transfer (ICT) transitions. Over the past decades, much work has been focused towards the optimisation of β values.

Most NLO chromophores are combined of a donor (D) and acceptor (A) groups, which are the molecular units primarily involved in charge redistribution, as well as a bridge as shown in **Fig. 2.13**.

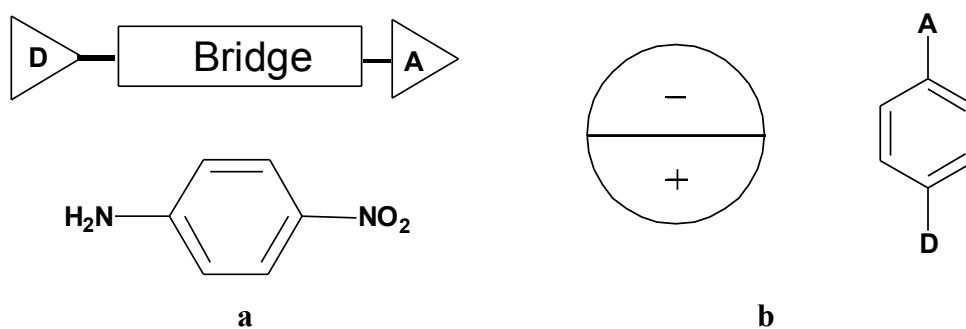


Figure 2.13. a-The prototypical dipolar D- π -A *p*-nitroaniline molecule, b- Dipolar charge distribution in prototypical dipolar systems

The design of chromophores with high second-order nonlinear value has focused chiefly on engineering: (i) the electronic nature of the donor and acceptor groups, and (ii) the conjugation length of the bridge [101-105]. The earlier controls donor-acceptor groups mixing with respect to a specific bridge, while the latter plays a role in modulating donor-acceptor electronic coupling as well as controls the magnitude of the change in dipole moment [106-108].

2.6.1.1. Organic Push-Pull Systems

Inspired by the two-level model and the development of the electric field-induced second harmonic generation (EFISH) technique, a few one-dimensional charge transfer systems such as p-nitroaniline (PNA) and dimethylaminonitrostilbene (DANS) were developed during the 1980s. DANS was considered to be good NLO materials and is still being used as a typical push-pull type benchmark to calculate NLO values of other molecules (**Fig. 2.14**) [109].

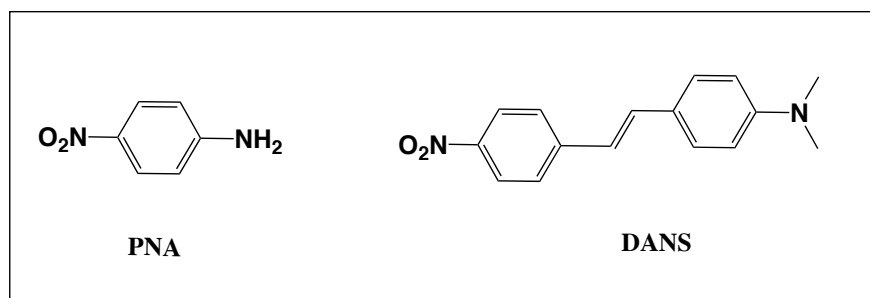


Figure 2.14 Typical push-pull type benchmarks

The PNA molecule has conjugated system, which consists from electron donating amino (NH₂) and electron accepting nitro (NO₂) groups substituted in the para-position. From, these opposite ends of conjugated system results intramolecular charge transfer interactions. Thence, PNA shows much larger first hyperpolarizability than mono substitute benzene because of its asymmetric charge distribution. Benzene doesn't exhibit second-order NLO value because, as explained before, second-order NLO vanish in centrosymmetric media. The second order

optical nonlinearity in a donor or acceptor substituted benzene has been described in **Fig. 2.15** [110].

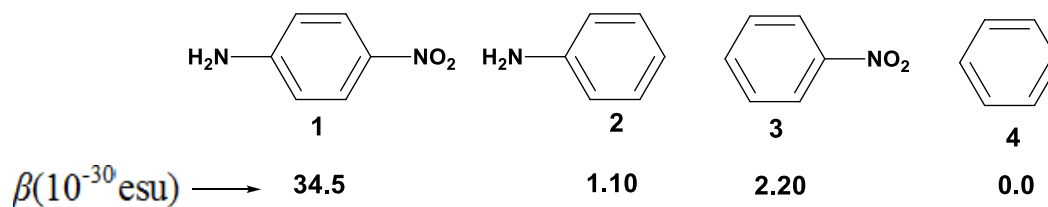


Figure 2.15. The second order optical nonlinearity in a donor or acceptor substituted benzene.

The next step in the modeling process was to consider doubly substituted benzenemolecules with a donor and acceptor group. The para position resulted in the highest β followed by the ortho position with the meta position being the lowest as shown in **Fig. 2.16** [111]. This dependence on position was attributed to intramolecular charge transfer between the donor and acceptor.

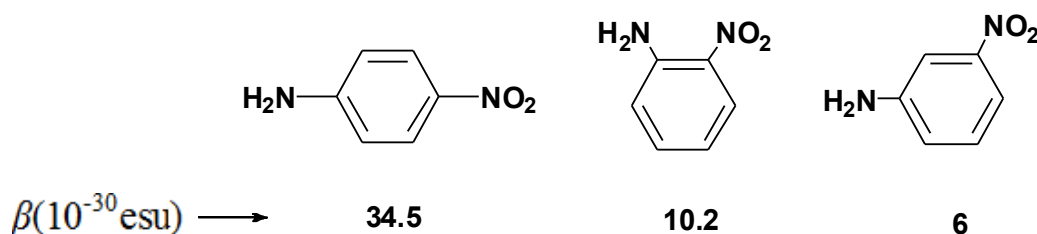
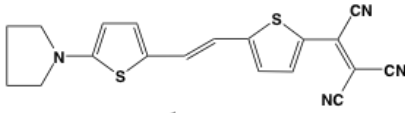
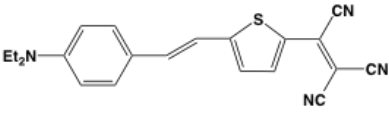
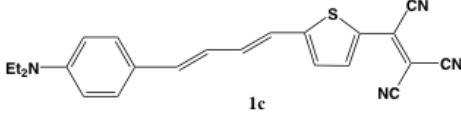
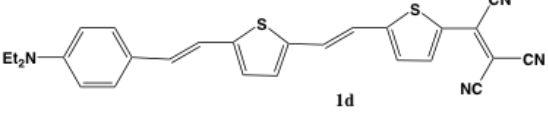


Figure 2.16. Values of β for para, meta and ortho nitroaniline [111]

In the early nineties, Marder and co-workers cemented the way for the expansion of highly advanced NLO chromophores [112,113]. He presented that for a given conjugation bridge there is an ideal combination of donor and acceptor strengths (or ground state polarization) to maximize $\mu\beta$, and that beyond this point, increased donor-acceptor strength (or further ground state polarization) will attenuate $\mu\beta$. More recently, it was shown that the average difference in length between single and double bonds in the molecule, is the related parameter in the optimization of the hyperpolarizability of molecules [114-116].

The high degree of bond length alternation in such molecules is revealing of an inadequate contribution of the charge separated resonance form to the ground state configuration of the molecules and is a direct consequence of the loss of aromatic stabilization in the charge separated form. Thus, many studies were focused on designing molecules with less aromatic character in the ground state. Examples of such optimized molecular structures are shown in **Table 2.1**, together with their hyperpolarizabilities, dipole moments and absorption characteristics.

Table 2.1. Static hyperpolarizability for a series of conjugated donor–acceptor compounds containing heterocyclic rings. Data taken from refs. [117,118]

Compound	$\mu\beta_{(0)}/10^{-48}$ esu
 1a	2564
 1b	3023
 1c	4146
 1d	3469

Materials to be used for electro-optic and frequency doubling applications must not only have good nonlinear values, but also good thermal, chemical stability and low optical loss (high transparency) [118-120].

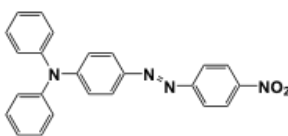
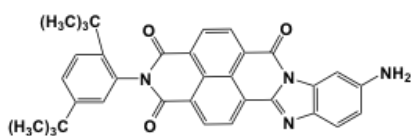
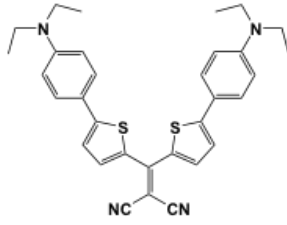
In order to stabilize the nonlinear response during treating and operation, the chromophores need to be chemically stable at all temperatures that the system encounters. Typically, organic molecules for nonlinear optical applications will have to bear extremely high temperatures during fabrication processes (sometimes as high as 300 °C) [121].

As previous studies showed that thermal stabilities of organic materials is extremely challenging without losing the molecules nonlinearity. Improvement of thermal stability of organic chromophores can be succeeded by adding aromatic structures instead of aliphatic ones by along the conjugation path of the molecules. However, as showed above, additional aromatic structure to organic molecules causes to decrease its hyperpolarizability.

Moylan and co-workers avoided this problem by replacing aliphatic dialkylamino donor groups with diarylamino groups, which results in a substantial increase in thermal stability of a broad range of organic chromophores without compromising the nonlinearity of the chromophore [122]. Consequently, those organic compounds possess not only very thermal stability but also high nonlinear response. Some of the investigated organic structures showed thermal stabilities as high as 400 °C.

Other organic push-pull materials with thermal stabilities above 300 °C have been established. For instance, certain naphthalene benzimidazoles display decent nonlinearity and thermal stabilities in excess of 350 °C (**Table 2.2, 3b**). These systems are based on attached ring system that is structurally similar to polyimide, which would make them very soluble in high T_d polyimides [123-125]. Rao *et al.* substituted the most reactive CN group in the tricyanovinyl group with aryl units in tricyanovinylthiophenes in order to increase their chemical and thermal stability (**Table 2.2, 2c**) [126].

Table 2.2. Static hyperpolarizability and decomposition temperature (Td) of a number of thermally stable chromophores with good nonlinearity. Data taken from refs.[120, 125, 126]

Compound	$\mu\beta_{(0)}/10^{-48}$ esu	$T_d/^\circ\text{C}$
 <p>2a</p>	319	393
 <p>2b</p>	199	360
 <p>2c</p>	854	354

2.6.1.2. Metal based Push-Pull systems

As showed in the previous, most second-order NLO metal complexes, as organic NLO chromophores, can be foreseen within a simple molecular scheme constituted by a push-pull system, in which a metal complex selectively replace the donor and/or the acceptor, or the bridge moieties. This is because metal complexes possess intense, low energy metal-to-ligand charge transfer (MLCT), ligand-to metal charge transfer (LMCT), or intraligand charge transfer (ILCT) excitations. Nonlinear optic metal complexes are relatively new and unexplored compare to organic nonlinear optic materials. Metal complexes have good potential as second-order NLO materials. Moreover, in the D- π -A (Push-pull) systems metal complexes are able to act as donor or acceptor groups, or as polarisable bridge [127-130].

Since the Green *et al.* who, reported a powder SHG efficiency 62 times that of

urea for cis-1-ferrocenyl-2-(4-nitrophenyl) ethylene, metal-based molecules were intensely investigated as donor groups, and especially ferrocenyl compounds had special interest among the metal-based complexes for NLO [131,132]. The ferrocenyl compounds can act as a reasonable donor group and their second-order NLO properties are similar with those of related methoxyphenyl organic materials [133,134]. The β values are smaller than expected; correspond to donor strength estimated from binding energy and redox potential. This result indicates that electronic coupling between the metal d-orbitals and the π -network of the substituent is quite poor.

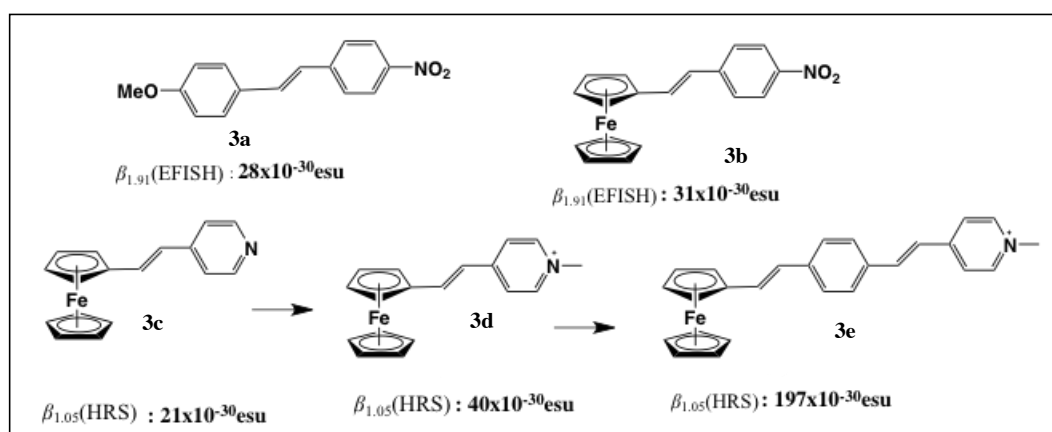


Fig 2.17 Selected ferrocenyl complexes

Some examples of ferrocenyl unit as donor group in push-pull systems derivatives is linked to nitro, pyridine and pyridinium acceptor terminal groups are shown in **Fig. 2.17** [135]. Similarly to organic push-pull systems, an increase of the nonlinearity is observed upon increasing the acceptor strength (e.g. **3d** vs **3c**) and upon conjugated π -linker lengthening (e.g. proceeding from **3d** to **3e**) [136].

One of the advantages of metal complexes over organic compounds is the possibility of tuning NLO response by changing the metal center. For example, the Fe and Ru metal containing compounds have been studied in order to compare NLO properties to each other (**Fig. 2.18**) [137,138]. And because ruthenium has the higher ionization energy compared to iron. The substituting iron with ruthenium in the complex causes a blue shift in the absorption bands and decreases the β values.

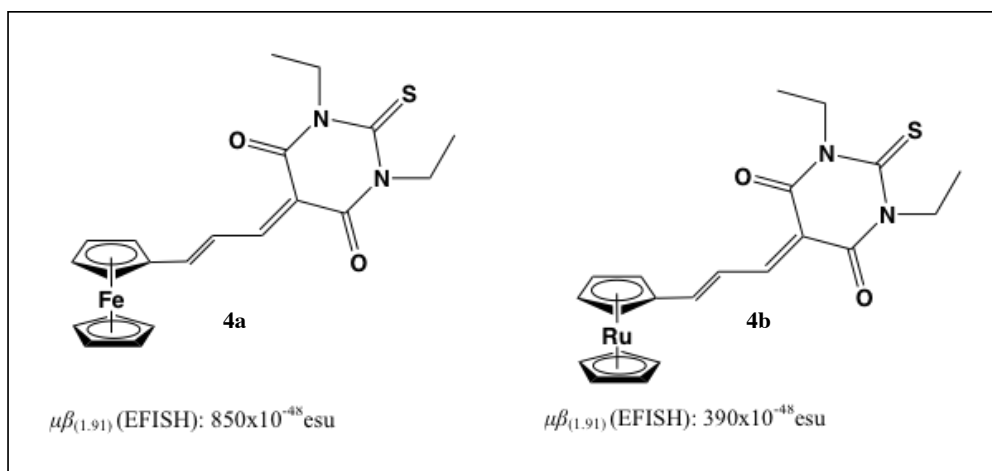


Fig. 2.18 Selected ferrocenyl and ruthenocenyl complexes

Coe and co-workers studied Ruthenium(II) amine complexes, $[\text{Ru}^{\text{II}}(\text{NH}_3)_4\text{L}]^{2+}$ (L =axial ligand) of 4,4-bipyridinium (L) ligands as another interesting class of second-order NLO metal complexes. These complexes show very large β values, even if interfered by resonantly enhanced, which are related with intense excitations between the electron-rich π -donor d^6 Ru^{II} and the acceptor 4,4-bipyridinium ($[\text{d}_\pi(\text{Ru}^{\text{II}}) \rightarrow \pi^*(\text{L})]$ MLCT) (Fig. 2.19) [139].

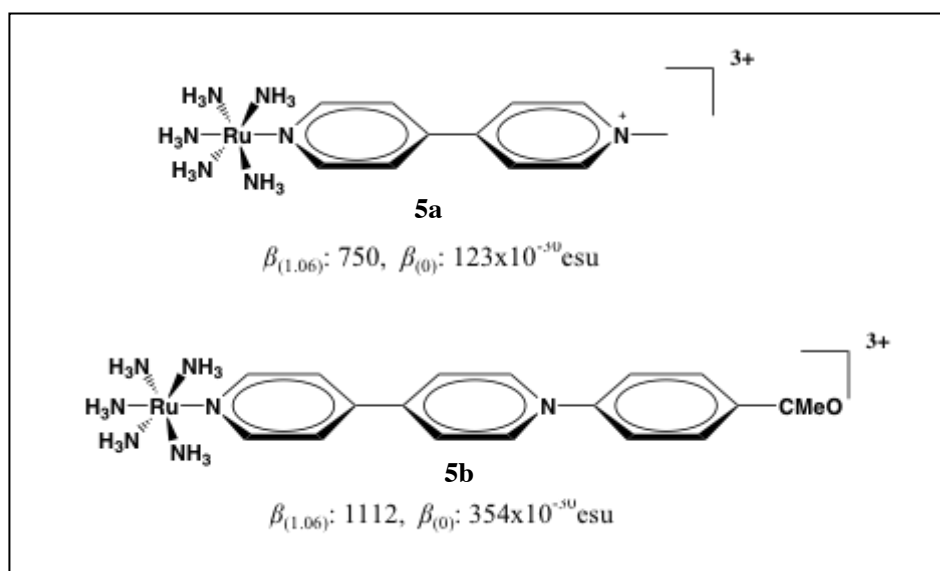


Fig. 2.19. Selected Ruthenium(II) amine complexes

The pyridines and oligopyridines are another important class of NLO Metal complexes, which have noticed recently [140,141]. Especially, the molecular quadratic hyperpolarisabilities of donor-substituted pyridine and stilbazole metal complexes have been investigated intensely [142–145]. Some illustrative examples of donor-substituted stilbazole rhodium(I) and iridium(I) complexes **6a** and **6b** are shown in **Fig. 2.20** [146]. These compounds exhibit strong solvatochromic intraligand charge transfer (ILCT) transitions, which rule the β values. When electron acceptor pyridine ligand coordinate to $[MCl(CO)_2]$, a bathochromic shift of the ILCT occurs, which cause a significant enhancement of the β values. Interestingly, the β values of **6a** and **6b** are similar to that of **6c** ($M.BF_3$). It seems that, acceptor strength of the Lewis acid BF_3 similar with that of stilbazole $[MCl(CO)_2]$.

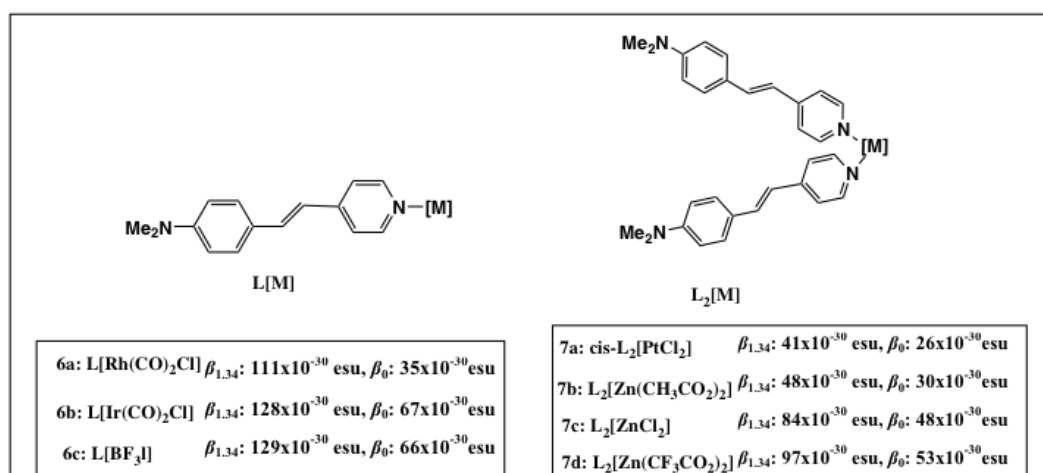


Fig. 2.20 Stilbazole and bis(stilbazole) metal complexes

The bis(salicylaldiminato)metal complexes are first example where metal can act as π -bridging center [147]. And the quadratic hyperpolarisability of these complexes containing different metal ions has been studied over the past ten years. These complexes display enlarged when compared with that of the free ligand. In the case of the metal acting as the donor group, NLO responses negative β , which ruled by MLCT excitations (**Fig. 2.21**) [148,149]. And the value of β is increased by replacing Ni^{II} (d^8) with Co^{II} (d^7) and Cu^{II} (d^9) analogues, due to the involvement of other low-lying MLCT states. However, when the Schiff base ligand is substituted by donor and acceptor substituents such in **8d** (A: NO_2), the situation is different and the β response is now dominated by intraligand charge transfer transitions, with the metal

ion mainly acting as a bridging center (**Fig.2.21**) [150].

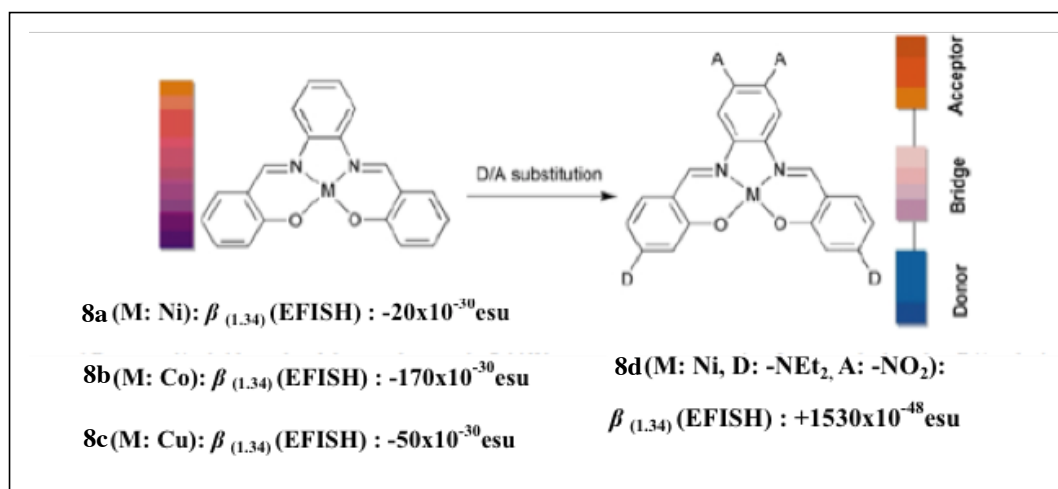


Fig. 2.21 Donor and/or bridge role of the metal centre in Schiff base complexes on passing from unsubstituted to D/A substituted. Adapted from ref. [150]

2.6.1.3. Phthalocyanine and related materials Push-Pull Systems

As mentioned before, only non-centrosymmetric molecules are able to produce second-harmonic generation, so that in principle. In the case of molecules are intrinsically centrosymmetric, as octa or non-substituted phthalocyanines and porphyrins, all the components of the first hyperpolarizability are zero. Therefore, phthalocyanines have to be designed by suitable substituents to obtain good second-order NLO responses. Theoretical calculations developed at the end of the 80's and suggested that push-pull asymmetrically substituted phthalocyanines and porphyrins with appropriately electron donor and acceptor groups possess efficient intramolecular charge transfer, which cause exhibition second-order NLO [151].

This concept is quite useful, because it let us to modulate the NLO response as a function of the peripheral substitution. Tremendous variety of substituents can be attached to the periphery of the phthalocyanine macrocyclic core, by varying the donor-acceptor substitution pattern or even the central metal while keeping the

peripheral groups. However, the synthesis of unsymmetrically substituted push-pull phthalocyanines is a difficult work [151-158].

Probably due to the trouble in the preparation of pure unsymmetrically substituted phthalocyanines and related compounds, few studies on the second-order NLO properties of this kind of compound have been reported. The first researches on the microscopic nonlinear exhibits of unsymmetrically substituted phthalocyanines were reported in 1996 (**Fig. 2.22**) [159,160]. The measurements were consummate by the EFISHG technique, but no sign of relevant β was found [161]. In these studies, both the donor and acceptor functional groups were directly attached to the Pc core [162-165].

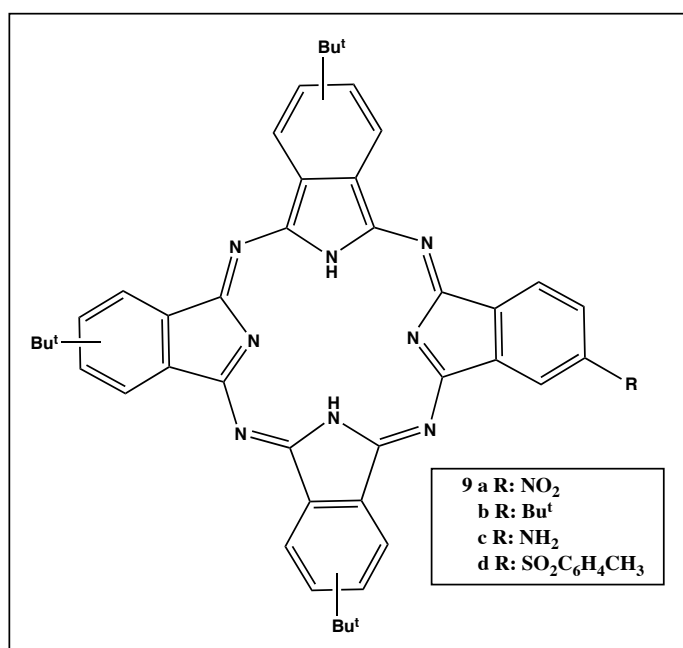


Figure 2.22 Structures of tetra substituted push-pull phthalocyanines

The approach pursued by some authors in order to improve the quadratic hyperpolarizabilities is the extension of the conjugation route. It is well identified that an increase in the number of conjugation units (double or triple bonds) between the donor and acceptor groups in a linear system causes an improvement of the second-order NLO response [166]. For this reason, push-pull phthalocyanines bearing π -delocalized electron acceptor substituents, which induce an extended π -conjugation length, were studied efficiently for second-order NLO [167,168]. Hence, a set of

phthalocyanines **10 a-c** were synthesized for studying the electronic character of the substituents and influence of the position, as well as the role of the central metal atom, on the second-order NLO properties of push-pull phthalocyanines with extended conjugation (**Fig. 2.23**).

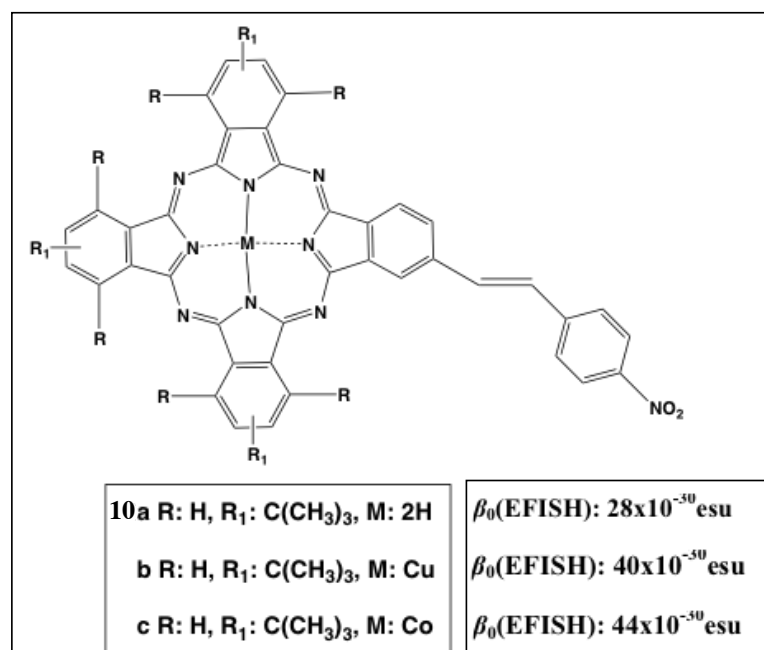


Figure 2.23. Structure of extended π -conjugation length push-pull phthalocyanines

Dipolar $\beta_{\nu}(0)$ component of the β tensor was determined by EFISH experiments [169]. All the values of phthalocyanines **10a-c** are quite significant and much higher than those **9 a-d**, consequently demonstrating the efficiency of the π -electronic extension in enhancing the nonlinear response. Moreover, some interesting structure-activity relationships were concluded from the experimental results. The extension of the conjugation path to the acceptor NO₂ group and metallic ion polarizability definitely increases the second-order NLO hyperpolarizability response.

Likewise, push-pull phthalocyanines bearing exocyclic conjugated nitro groups, such as **11b**, were synthesized and it is also confirm the efficacy of the π -electronic extension approach (**Fig. 2.24**) [170-172].

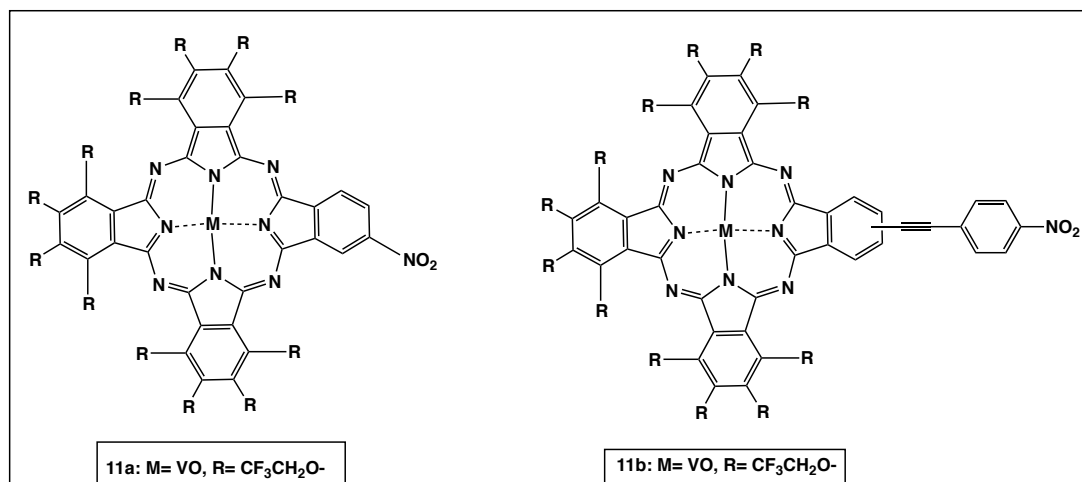


Figure 2.24. Structures of **11a** and **11b** push-pull phthalocyanines

In this study, reported that under the same conditions of thickness and concentration films of **11b** push-pull phthalocyanine derivatives produce larger second-order NLO signals than nitro group is directly attached to the phthalocyanine core **11a**, which may be attributes to the enhancement of the first-order hyperpolarizability (β) in the molecules of phthalocyanine **11b** with extended exocyclic π -conjugation[173].

Alike relationships between the nonlinear response and the π conjugation length between the donor and acceptor end groups have been proven for porphyrin systems [174–177]. The first NLO study of push-pull porphyrins was performed in the beginning of the nineties by Suslick and co-workers [178]. A typical example is 10,20-diphenylporphyrin and its Zn^{II} , Cu^{II} and Ni^{II} complexes **12a-c** bearing an arylethynyl (donor) and nitro-arylethynyl (acceptor) substituent in the 5- and 15-positions, respectively (**Fig. 2.25**). Remarkably high quadratic hypolarisability values have been reported for the Cu^{II} **12a** ($\beta_{1.06}$: 1501×10^{-30} esu) and Zn^{II} **12b** ($\beta_{1.06}$: 4933×10^{-30} esu) complexes, measured by HRS in chloroform with a resonant incident wavelength of 1.06 μm [179].

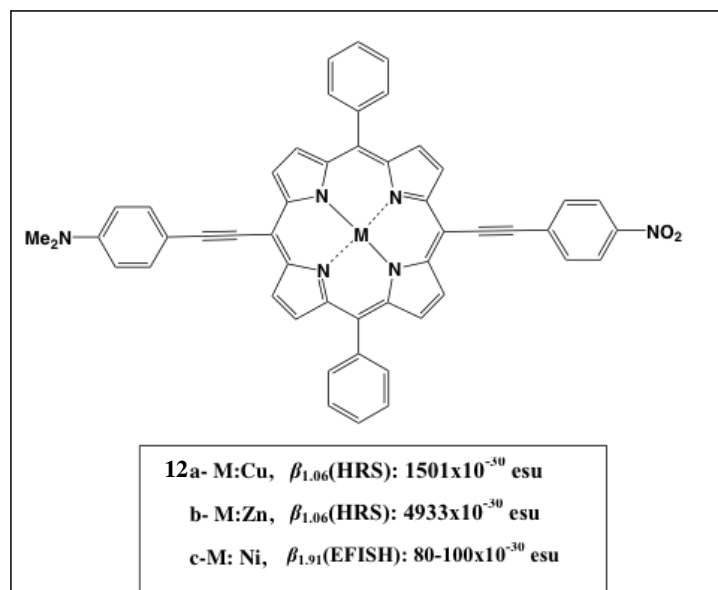


Figure 2.25 Structures of **12a**-cpush-pull porphyrines

The NLO properties of nickel(II) porphyrin chromophores substituted with electron-accepting dicyanoethenyl group **13a** have also been studied by EFISH working at 1.91 μm (**Fig. 2.26**) [180]. This study has exposed a much lower value ($\beta_{1.91}: 124 \times 10^{-30}$ esu), this can be explained by a deviation from coplanarity between the dicyanoethenyl fragment and the plane of the porphyrin, which reduces the electronic coupling across the donor-porphyrin-acceptor.

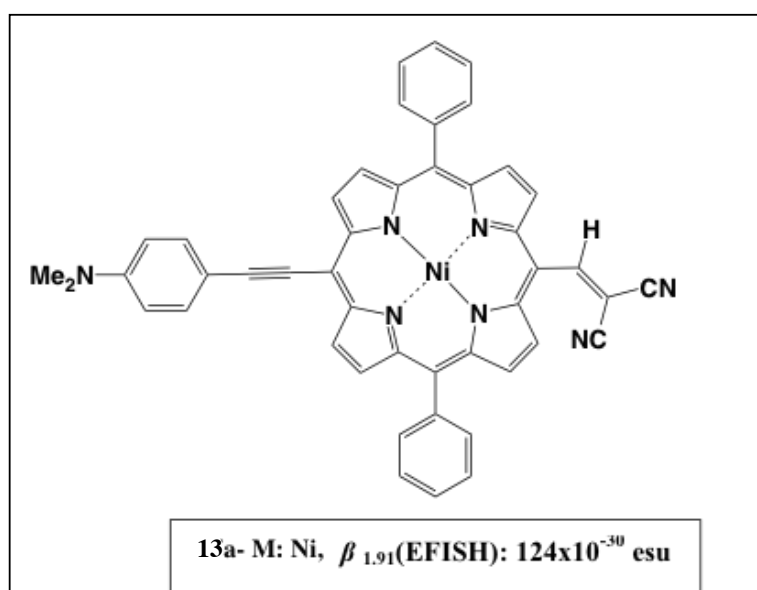


Figure 2.26. Structures of **13a** push-pull porphyrine

As mentioned before, the linear π -conjugated substituents have positively touch the second harmonic generation ability of phthalocyanines, however, the extension of the conjugation with another macrocyclic unit to the Pc core does not increase second-order NLO values. This is the result of the study carried out on phthalocyanine-triazolehemiporphyrzine dimers **14a** (Fig. 2.27)[181]. The existence of the triazolehemiporphyrzine unit seems to interrupt the effective charge transfer between the electron-donor and electron-withdrawing groups.

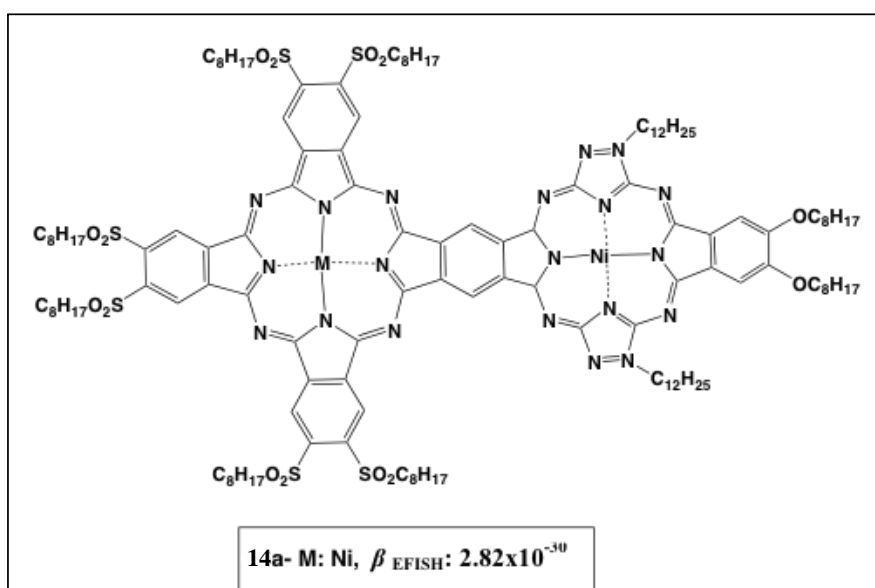


Figure 2.27 Structures of phthalocyanine-triazolehemiporphyrzine dimers

2.6.2. Octupolar Systems

The “D- π -A (Push-pull)” dipolar molecules are most intensively studied as NLO chromophores [182-184]. Optimisation of the structural factors such as the strength of the push and pull group and length has led to high values for the quadratic hyperpolarisabilities β . Significant efforts consequently have been made to built new materials by inserting NLO dipolar push-pull molecules in solid medium in non-centro symmetric arrangements. While these studies have detailed of relationship between the chromophore structure and NLO properties, it has become clear that dipolar molecules have assured limitations and disadvantages such as poor solubility,

aggregation and strong absorption of the second harmonic by the chromophore, thus leading to reduced efficiency-transparency trade off and dipole-dipole interactions, which often cause an antiparallel molecular arrangement and a following cancellation of the nonlinear response at bulk materials [185,186].

In addition to push-pull dipolar molecules, a recently new strategy was introduced for second generation of compounds, which can avoid aforementioned disadvantages. Studies based on group theory and quantum mechanics have assisted set theoretical basics to the field of non-dipolar molecules for nonlinear optics, which became known as octupolar, and more generally multipolar molecules. The concept of octupolar nonlinearities was described in the early 1990 by Zyss and coworkers [187-189].

2.6.2.1. Definition of octupolar system

Since the molecular hyperpolarizability β is a tensor, it turns out from tensorial analysis that it can have two components of order 1 and 3 which is referred to as the dipolar and octupolar irreducible components respectively [190], *i.e*

$$\beta: \beta_{j:1} \oplus \beta_{j:3}$$

The vectorial component (J=1) allows for three independent coefficients while the octupolar component will accommodate seven components, hence making up for the 10 components of a symmetric rank-3 tensor. Thus in addition to dipolar molecules ($\beta_{j=1}$) showing NLO response, from the above analysis it can be deduced that octupolar groups like D_{3h} , T_d *etc.*, should also show NLO response. Molecules that show NLO response due to their octupolar ($\beta_{j=3}$) nature are called octupolar molecules. For a molecule belonging to an octupolar space group (J:3), are nonpolar molecules that have only the octupolar vector contribution of $\beta(J:3)$ and a strict cancellation of all vector-like observables, including the ground- and excited-state dipole moment [191,192].

The advantages of using such nonpolar species for NLO applications include

easier noncentrosymmetric crystallization, no dipolar interaction and improved efficiency-transparency trade-off, which is a crucial parameter to consider while designing NLO devices.

Design of octupolar materials is now quite developed and essential criteria for exhibition of large hyperpolarizabilities have been discovered. The basic rules are as follows [193-197]:

- The β values of the octupoles are assumed to increase as the Charge Transfer energy decreases and with the transition moment's increase
- The β value of octupoles increases gradually with the extent of intramolecular charge transfer (ICT)
- The β value of octupoles increases gradually with increasing the donor-acceptor strength, π orbital energy, and the conjugation length

Appropriately, various derivatives of octupolar molecules were synthesized and their structure-property relationship have been investigated [198-205]. At a structural level, it can be shown that the most general template for octupolar molecules originates to a cube with alternating charges (donor and acceptor groups) at the edges (Fig. 2.28) [190].

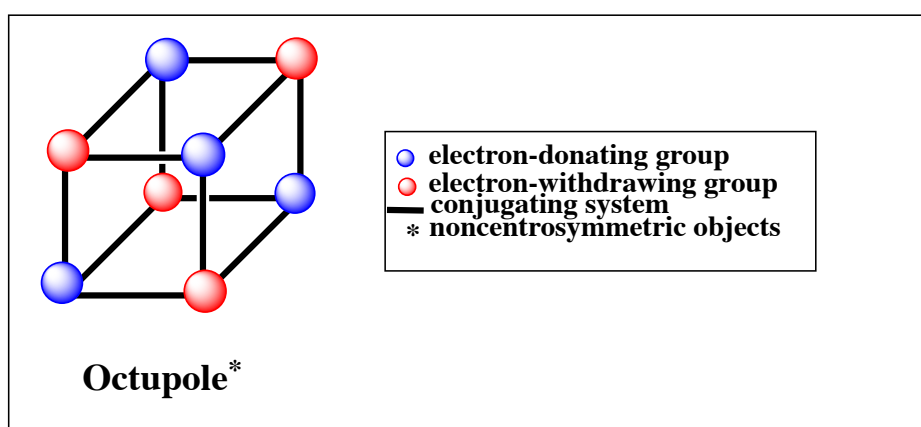


Figure 2.28. Cubic octupolar archetype template.

Basically, purely octupolar symmetries can be derived from this cubic **Td** structure either by projection along a **C₃** axis, giving rise to **D_{3h}** or **D₃** symmetry (TATB route), so called **two-dimensional (2D)** octupolar materials, or by fusion of one type of charge in the barycenter leading to, **Td**, or **D_{2d}** symmetry (“guanidinium route”), so called **three-dimensional (3D)** octupolar materials. Thus, the molecular engineering of octupoles contains of a spatially controlled organization of charge transfers within a molecule so as to reach the preferred symmetry.

2.6.2.2. Two dimensional (2D) octupolar materials

Since the pioneering work of Zyss and coworkers, most studies have been dedicated to molecular optimization of octupolar molecules with a two-dimensional (2D) character of β , leading to enhanced nonlinearities [206,207]. A cubic structure can result in a two-dimensional (2D) octupolar system by projection along a **C₃** axis-giving rise to the **D_{3h}** or **D₃** symmetries (**Fig. 2.29**).

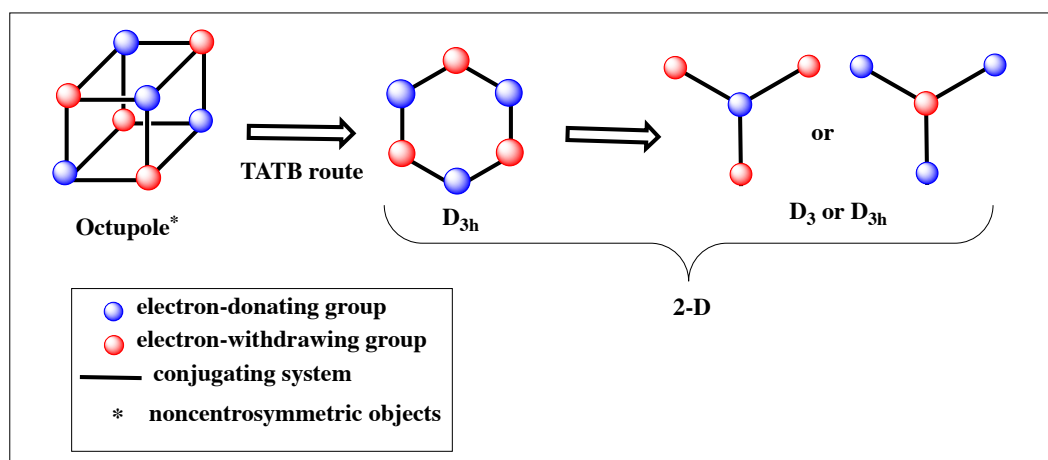


Figure 2.29. Schematic representation of 2D-octupolar symmetries. Adapted from ref. [206]

2.6.2.2.1. Two dimensional (2D) octupolar organic materials

The first example of octupole molecules, namely 1,3,5-triamino-2,4,6-trinitro-benzene (TATB) (**Fig. 2.30**), was described in 1990 by Lehn, Zyss et al [208]. Since then, many 2D octupolar organic molecules with a benzene, triazine, boroxine core that symmetrically hexasubstituted and trisubstituted have been effectively studied [209-211].

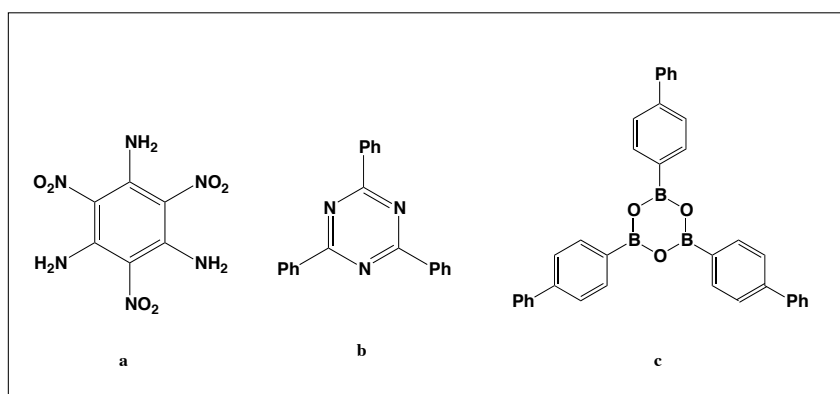


Figure 2.30. The structures of 2D octupolar a- TATB, b- triazine, c-boroxine molecules

The simplest example of two-dimensional octupole material is 1,3,5-trisubstituted benzene [212, 213]. The organic two-dimensional octupole compounds with modest electron donating or -accepting group at the periphery showed very small β values (**1b**, **1c**) (**Fig. 2.31**) [214]. The β value increased substitution with a stronger donor (or acceptor) (**15a**>**15b**; **15e**>**15c**) and longer conjugation length (**16a**>**15a**; **16d**>**15d**). The parallel increase in these values is reliable with the theoretical forecast that the β of the two dimensional octupoles should increase with the extent of ICT [215].

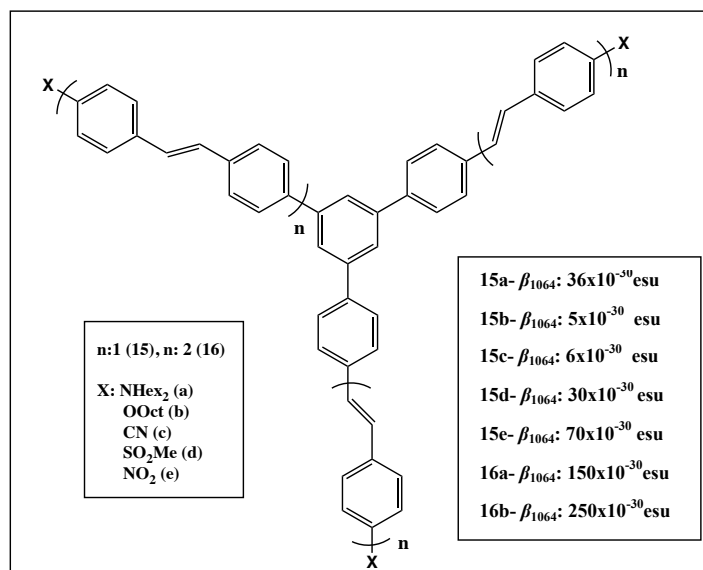


Figure 2.31. The structures of 1,3,5-trisubstituted benzenederivatives

Cho and coworkers studied with 1,3,5-trimethoxybenzene derivatives and had similar conclusions about effect of conjugation length and acceptor strength on β values (Fig. 2.32) [216]. Besides, they showed that β values also increased as the phenyl group in the conjugation bridge was replaced by the thienyl group (**17b** < **18**). This is because the thienyl group has smaller aromatic resonance energy than the phenyl group and thus simplifies the ICT from the donor group to the acceptor group.

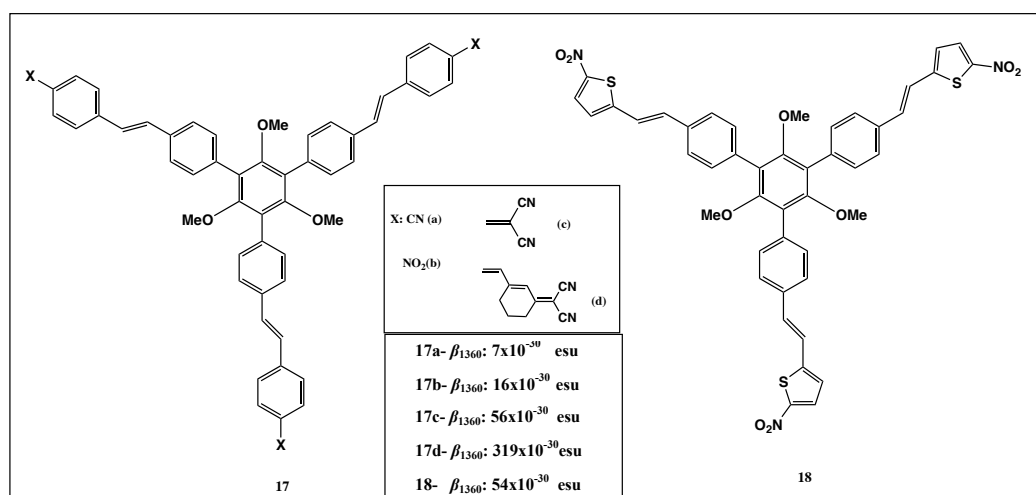


Fig. 2.32 The structures of 1,3,5-trimethoxybenzene derivatives

Moreover, when the triple bond was used as the conjugation bridge instead of double bond, the β value decreases ($19a > 20a$, $19b > 20b$), indicating the poor conjugating capability of triple bond (Fig. 2.33) [217].

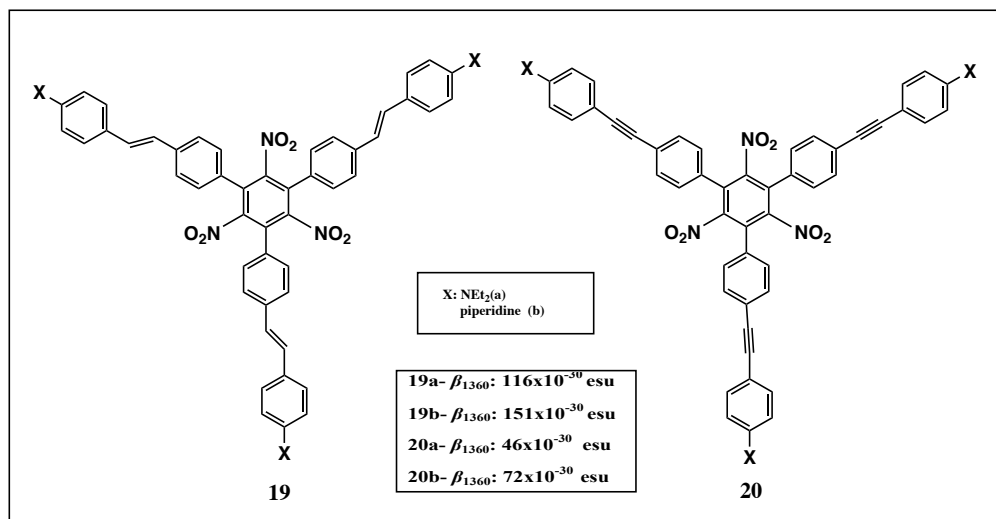


Fig. 2.33 The structures of 1,3,5-trinitrobenzene derivatives

And the β value also increases with the more electron-donating substituent ($19a < 19b$) as expected. Interestingly, the λ_{max} values of **19b** and **20b** are blue shifted and β values increase slightly compared with those of the corresponding dipoles [4-nitro-40-piperidylstilbene and (4-nitro-40-piperidyl)diphenylacetylene], despite a large increase in the molecular weight. The results have been attributed to the steric effect of the NO_2 groups, which interrupt the conjugation between the peripheral donors and central acceptors, reduce the extent of the charge transfer, and decrease the λ_{max} and β .

2.6.2.2.2. Two dimensional (2D) octupolar metal based materials

Metal ions are well appropriate to building two-dimensional (2D) and three dimensional (3D) coordination molecules with 2-fold (D₂) around the metal center. Thanks to this ability, a number of NLO two-dimensional (2D) octupolar metal complexes, mainly based on bipyridine ligands, have been described in the literature [218].

Second-order NLO properties of two-dimensional (2D) octupolar metal complexes were first verified by Zyss et al. for tris(bipyridine) (**21a**) complexes [219]. These complexes possess D_3 symmetry and show intense multidirectional $[d_{\pi}(\text{Ru}^{\text{II}}) \rightarrow \pi^*(\text{bpy or phen})]$ MLCT excitations accountable for their fairly good second-order NLO response. Moreover, very large NLO value was afterward accomplished with substitution of the bipyridine ligands by *p*-dibutylaminostyryl donor groups (**21b**) [219].

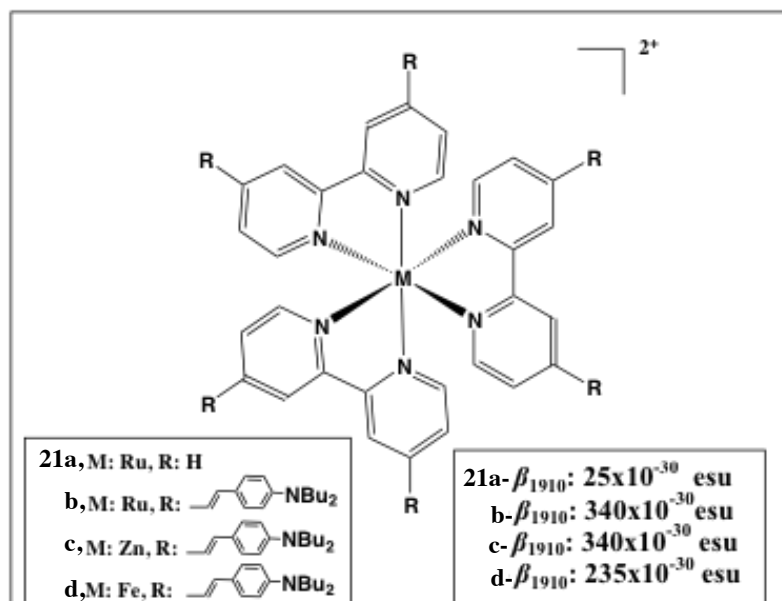


Figure 2.34. The structures of tris(bipyridine) complexes

In these cases the NLO response is connected to very strong, multidirectional MLCT excitations, but the role of the Ru^{II} ion is fundamental in defining the octupolar molecular architecture (**Fig. 2.34**). The change of the central metal ion from $\text{Ru}(\text{II})$ to $\text{Zn}(\text{II})$ in the 2D octahedral complexes does not cause any changes on β (**21b** vs **21c**). On the other hand, the β value for the $\text{Fe}(\text{II})$ complex (**21d**) is much smaller than those for **21b** and **21c**. This result has been credited to the negative contribution of the metal ligand charge transfer transition (MLCT) to the NLO response.

A second class of two-dimensional (2D) octupolar metal-based NLO materials is aromatic rings 1,3,5-substituted with Ru^{II} σ -acetylide complexes (e.g., **Fig. 2.35, 22**) [220]. In this case the 3-fold symmetry axis is determined by the 1,3,5-substituted aromatic ring, while the organometallic moieties act as strong donor groups.

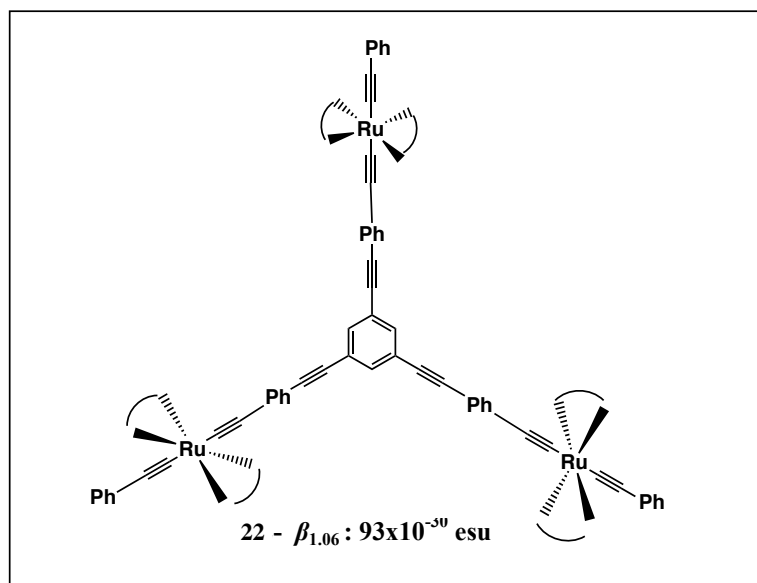


Figure 2.35. The structures of 1,3,5-substituted with Ru^{II} σ -acetylide complexes

Furthermore, recently the octupolar 1,3,5-substituted with Fe^{II} σ -acetylide aromatic complexes, together with related oxidized Fe^{III} species were investigated (**Fig.2.36**) [221]. And as previous case, the lowest MLCT excitations are responsible for the NLO response. In the case of oxidized Fe^{III} species, new absorption bands (related to LMCT transitions at 532 nm) located very close the second harmonic wavelength appear, which might leading to underestimated β values. However, their second-order NLO response seems still related to MLCT excitations. Therefore, it seems that intrinsic NLO activity of the oxidized complexes might be larger than that of the neutral homologues.

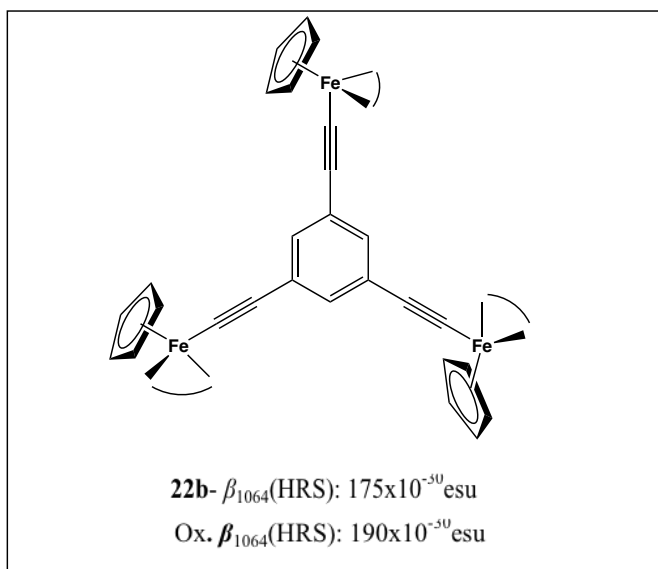


Figure 2.36. The structure of 1,3,5-substituted with Fe^{II} σ -acetylide complex

Among two-dimensional (2D) octupolar metal containing NLO chromophores, studies of lanthanide complexes are strangely very low, even though they have very promising properties for NLO chromophores such as strong Lewis acidity and tailor ability [222]. Moreover, the lanthanide complexes as f-Block elements are particularly well suited for the study of the role of the central metal ion on the NLO properties. Indeed lanthanide(III) ions (lanthanum–lutetium) offer the unique opportunity to design an iso-structural series without any MLCT transition.

Recently, NLO properties of two-dimensional (2D) octupolar tris(dipicolinato)lanthanide(III) series complexes have been studied by Tancrez and *et. al.* (Fig. 2.37)[223].

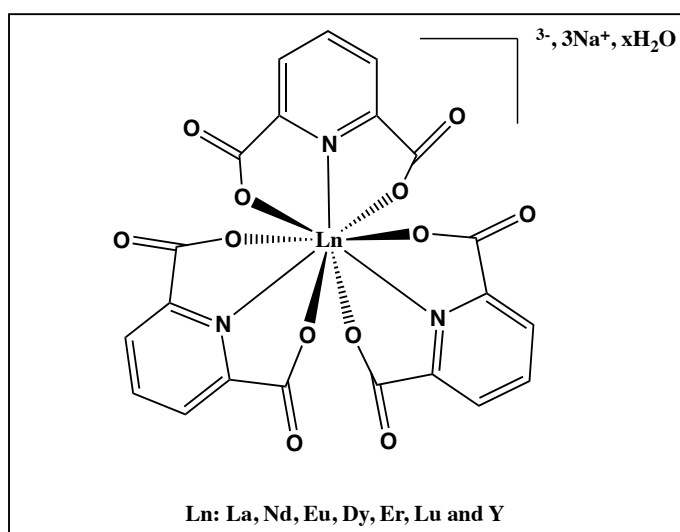
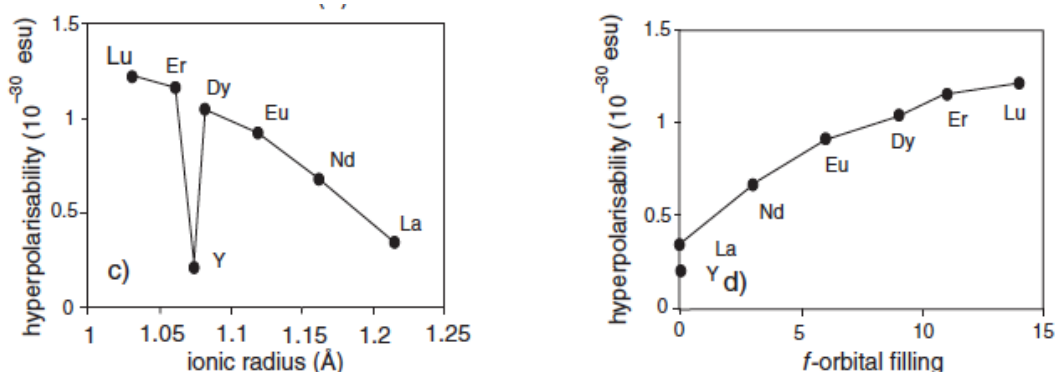


Figure 2.37 The structure of tris(dipicolinato)lanthanide(III) series complexes

These complexes are isostructural and therefore all the complexes show the same UV-visible spectrum. Since the complexes have nonfunctionalised ligand, the NLO activity of these complexes is small as expected.

But more importantly, the NLO activity consistently rises from lanthanum to lutetium complexes along the f-element row. And this result has been credited to the contribution of the lanthanide metals in the NLO activity and called “metal-induced NLO-enhancement” [224].

This effect can be clearly seen by plotting the variations of β with the ionic radius and *f* orbital filling (Fig. 2.38 a). Yttrium has no *f* electron, but is isostructural with other lanthanides. Even though ionic radius of yttrium is between those of dysprosium and erbium, the NLO activity of yttrium is much lower than dysprosium and erbium (Fig. 2.38 b).



a **b**
Figure 2.38. The variation of the quadratic hyperpolarizability with ionic radius (a) and *f* orbital filling (b)

And authors suggested that the metal contribution to the quadratic hyperpolarizability is not due to geometrical considerations like the lanthanide contraction but to its electronic configuration [224].

2.6.2.2.3. Two-dimensional (2D) octupolarphthalocyanine materials

The 1,3,5-trisubstituted benzene material is the most studied building block for achieving for two-dimensional octupolar symmetry and recently, 2,4,6-trisubstituted 1,3,5-triazine molecules have also been shown to be very promising applicants structures for 2D octupolar materials [225]. Thus, a series of pseudo- D_{3h} symmetrical 1,3,5-tris(phthalocyaninyl)benzenes **23a–c** and 2,4,6-tris(phthalocyaninyl)-1,3,5-triazine **23d** were preliminary synthesized and studied their NLO (**Fig. 2.39**) [226].

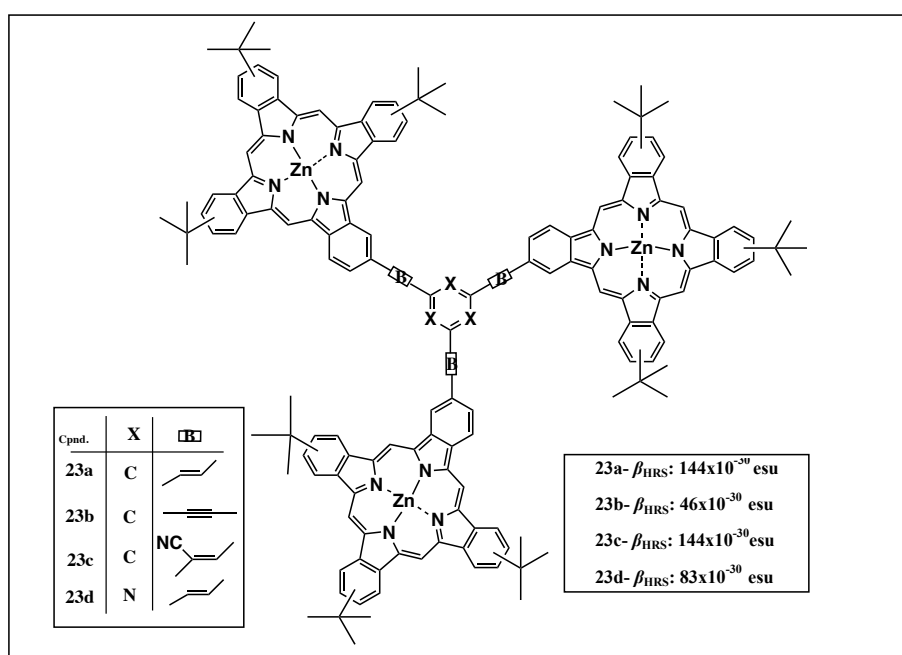


Figure 2.39. Structures of octupolar 1,3,5-trisubstituted benzene -triazine molecules and their Second-Order NLO Properties

Remarkably, because of a strong octupolar effect and an extension of the π -conjugation, these compounds exhibited an enhanced quadratic NLO response with compare to push-pull Pc's with dipolar character as expected. And second order NLO response at the molecular level has been measured by HRS and gavemuch higher results than corresponding nonoctupolar Pc.

Another possible method for the two-dimensional octupolar route is the axial substitution of metallic phthalocyanines. The introduction of a substituent in the axial position breaks the centrosymmetry of the Pc macrocycle and adds to the

molecule an non-negligible octupolar character. It is well-known that the combination of dipolar and octupolar features yields interesting NLO properties. Some examples of axially substituted phthalocyanines have been reported, titanium(IV), gallium(III) and indium(III) derivatives axially substituted by different ligands [227]. Particularly, titanium and gallium phthalocyanines have been measured by EFISH and HRS. Among the formal structural modifications of the phthalocyanine core to reduce the symmetry, the most exciting one is the subphthalocyanine route [228].

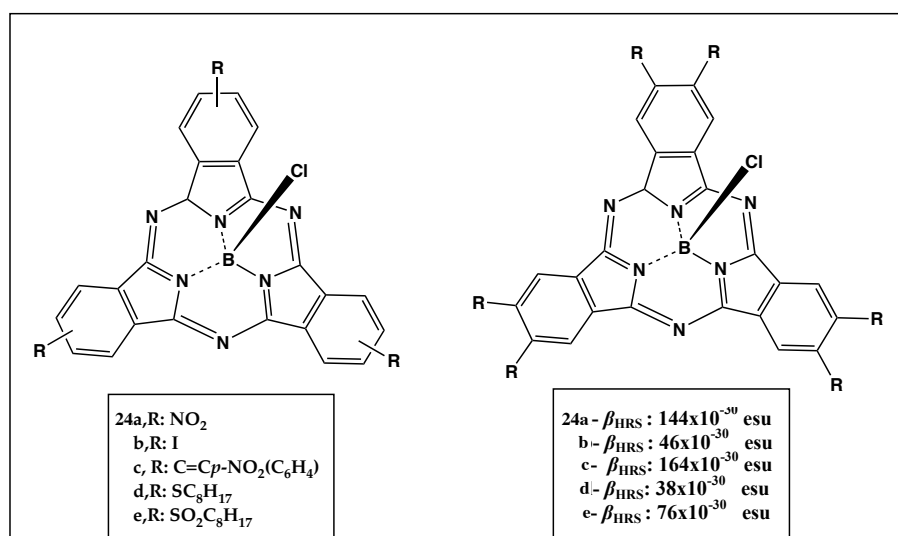


Figure 2.40. Structures of subphthalocyanines and Second-Order NLO Properties

These compounds have shown to be good high-performance second-order molecules and therefore constitute an optimal route to practical NLO applications (Fig. 2.40). Thus, various subphthalocyanines bearing representative electron-donor or acceptor groups were synthesized and their NLO properties were measured employing HRS, EFISH methods [229].

2.6.2.3. Three-dimensional (3D) octupolar materials

Most researches have been dedicated to molecular optimization of octupolar molecules with a two-dimensional (2D) structure of β , leading to improved nonlinearities. In contrast, few three-dimensional (3D) octupolar molecules have been studied, leading to high nonlinearities but at the expense of a fairly reduced

transparency in the visible region. Three-dimensional (3D) simplified structures such as T_d or D_{2d} symmetry like tetrahedral metal complexes or substituted biphenyls were deduced from this basic cubic point charge template by projecting the charges (Fig. 2.41) [230].

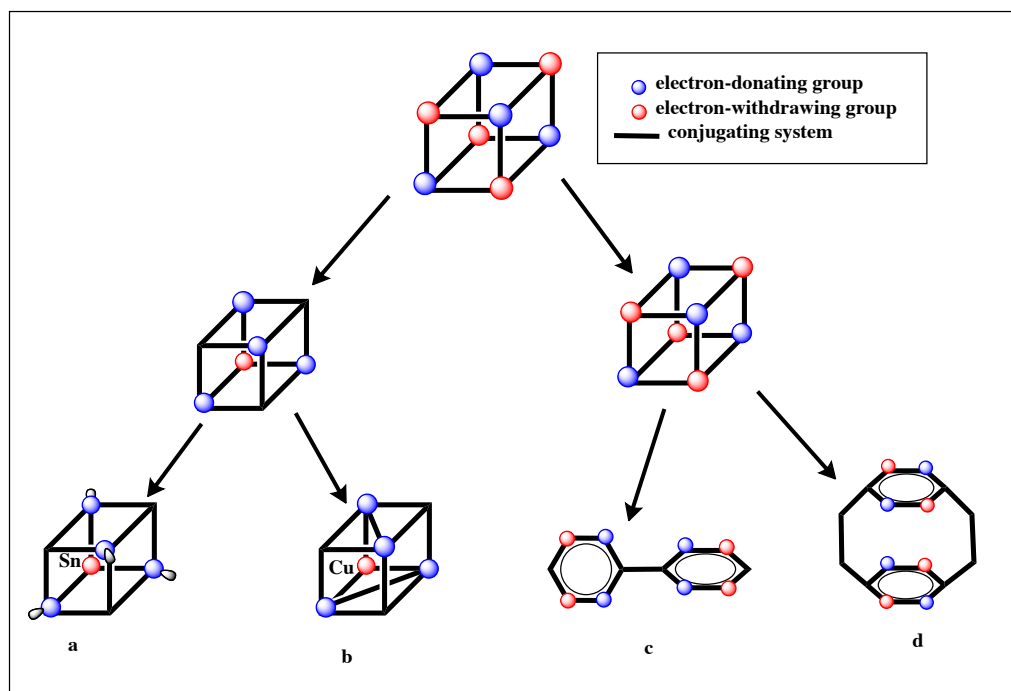


Figure 2.41. Various strategies for engineering of octupolar 3D molecules. Adapted from ref. [230]

2.6.2.3.1. Three-dimensional (3D) organic octupolar materials

The design of 3D organic octupole materials with higher symmetry is a quite challenge for chemists. Tetrahedral structures have been preferred by different groups for the construction three-dimensional organic molecules. Banchard-Desce *et al.* have recently defined some tetra substituted biphenylene chromophores with D_{2d} symmetry (**25a-e**) that combine excellent transparency in the visible region and enhanced first-order hyperpolarizabilities [231].

The molecular design of these 3D organic molecules is based on ortho substitution by donor or acceptor groups brings the two phenylene moieties in an orthogonal conformation (Fig. 2.42).

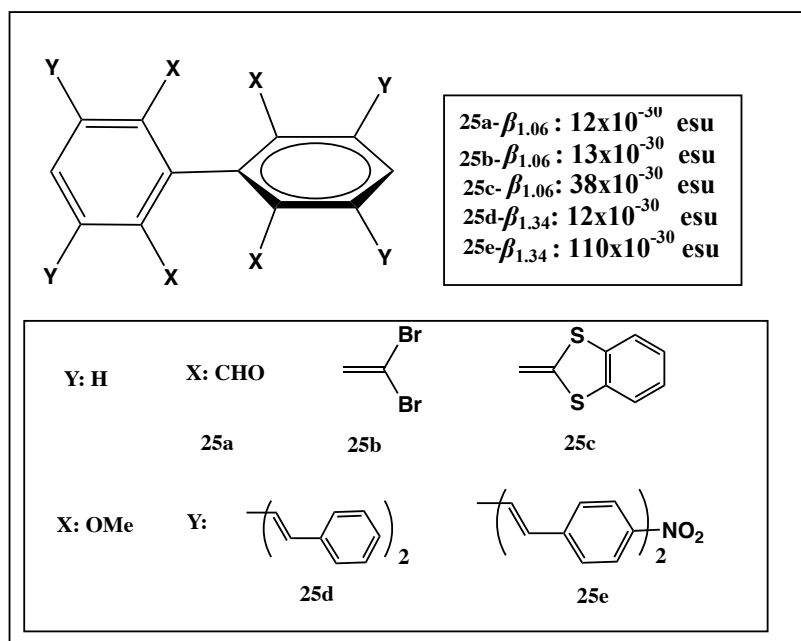


Figure 2.42 The structures of octupolar molecules of D_{2d} symmetry derived from an orthogonalized biphenyl core.

The first generation of octupolar biphenyls (**25a**, **25b**, **25c**) corresponds to molecules bearing electron-withdrawing and/or electron-donating substituents on the four ortho positions of the phenyl rings in order to allow for charge transfer from the substituents to the phenyl rings. In a second step, they have decided to extend the conjugation length of the substituents so as to further optimize the basic molecular structure, which this expansion was proven quite successful in the case of 1D push-pull dipolar chromophores. Thus, they have applied this promising strategy by designing of three dimensional (3D) organic octupolar biphenyls, which provide an interesting approach to improved nonlinearity-transparency trade-off and offer many opportunities for optimization of the octupolar nonlinearities.

As mentioned before, push-pull organic NLO materials use traditional single and double bond alternation of polyene-like conjugated chains, which cause decrease transparency-efficiency tradeoff in some cases. Recently Zyss et al. have proposed and demonstrated an alternative approach for unconventional through-space intramolecular charge transfer provided by the paracyclophane (pCP) moiety [230]. To take full advantage to this approach, on the basis of the substitutional

potential of the pCP at different carbon sites, Bazan et al. successfully extended this approach to octupolar and more generally multipolar pCP based units [227]. They also suggested that by extended two- and three-dimensional dimensionality for p-cyclophane (pCp) bearing octupolar charge distributions, it can be ideally designed a three-dimensional conjugated core based on the (eventually distorted) cubic template, as displayed in **Fig. 2.43**.

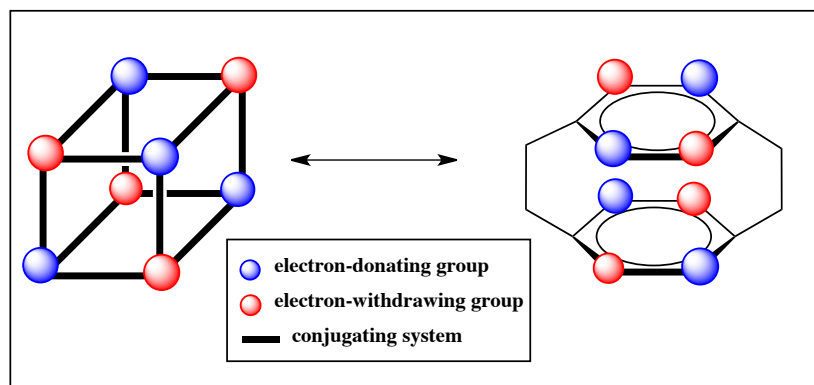


Figure 2.43. Schematic representation of general octupolar distribution and pCP template. Adapted from ref. [232]

The p-cyclophane (pCp) structure has a properly flexible backbone that allows for subsequent functionalization. Substitution at the 4, 7, 12, and 15 positions leads to an extended cubic molecular structure with orthorhombic symmetry features letting for three-dimensional (3D) arrangements, including the boundary case of octupoles, as shown in the **Figure 2.44**.

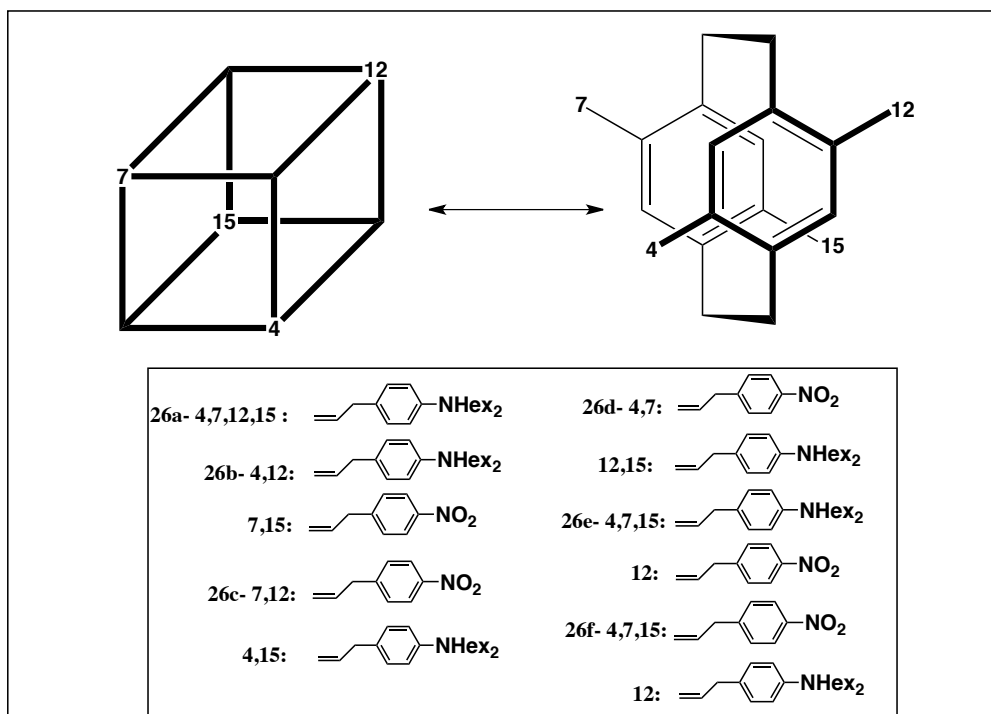


Figure 2.44. The (4,7,12,15)tetra-substitution pattern for [2.2]**p**-cyclophane(pCp) as a point-charge template for an octupole

They have reported a clear experimental evidence of large through-space octupolar and dipolar contributions to the second-order hyperpolarizability β value of various multipolar donor-acceptor groups (**26a-f**) in the form of a distorted cube to highlight the geometric relationships between pCP derivatives[232].

The significant nonzero β value of the is a first approval of the through-space ICT, although it is made of two centrosymmetric subunits. The three-dimensional charge transfer of D_2 symmetric **26a** shows a strong octupolar character as expected. The dipolar contribution ($\beta_{j:1}: 50 \times 10^{-30}$ esu vs $\beta_{j:3}: 130 \times 10^{-30}$ esu) of compound is weak compared to octupolar contribution but it can be increased by variations of the molecular geometry[232]. Moreover, compound **26a**, which paracyclophane core having four N,N-dialkylamino electron donor groups on alternate positions of both benzene rings is known as the closest example for a cubic template molecule so far.

2.6.2.3.2. Threedimensional (3D) octupolar metal based materials

Coordination chemistry can be a useful way and a powerful tool to build up three-dimensional octupolar materials. After the first demonstration of the potential of metal based complexes $[\text{Ru}(\text{bpy})_3]^{2+}$, which has two-dimensional D_3 symmetry

[233]. A variety of 3D octupolar based on metal complexes have been designed and investigated.

Particularly 4,4'-disubstituted 2,2'-bipyridine metal complexes are very good candidates for the construction of 3D-pseudotetrahedral octupolar complexes [234]. The metal plays two important roles that both contribute to NLO activity: **i**) gathering ligands in a prearranged octupolar arrangement, and **ii**) inducing a strong intraligand charge transfer (ILCT) transition as a Lewis acid. Recently, three-dimensional 3D pseudo tetrahedral D_{2d} (Cu^I , Ag^I , Zn^{II}) octupolar metal complexes have been reported describe in detail optical (absorption and emission), and nonlinear optical properties (β) by Bozec et.al. (**Fig. 2.45**) [235].

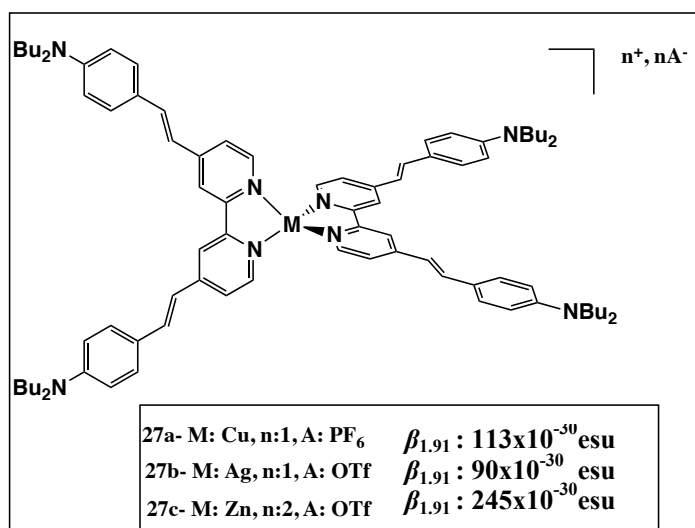


Figure 2.45. The structures of 3D octupolar bipyridine metal complexes

Among 4,4'-disubstituted 2,2'-bipyridine substituted 3D metal complexes, the stronger Lewis acidity of the dicationic zinc(II) ion inducing a larger bathochromic shift of the ILCT transition. And The result of measurements performed at 1906 nm reveal that the β value of the bipyridyl metal complexes decrease with the metal ion in the order, $Zn^{2+} > Cu^+ > Ag^+$ (**27c > 27a > 27b**). The result has been credited the relative Lewis acidity of the metal ion. The Lewis acidity of the central metal ions controls the strength of the ILCT bathochromic shift and, therefore, the stronger Lewis acid persuades a more red-shifted ILCT transition, consequently a larger NLO activity.

2.6.2.3.3. Three dimensional (3D) octupolar phthalocyanines materials

As mentioned before, the first-order hyperpolarizability tensor β could be reduced in a particularly way into dipolar $\beta_{J=1}$ and octupolar $\beta_{J=3}$ contributions and many organic and inorganic NLO chromophores that fulfill the octupolar symmetry requirements were studied. Between these NLO chromophores, phthalocyanines provide additional degrees of freedom to help in the design of efficient three-dimensional nonlinear octupolar molecules. One of the possible approaches to reach Pc-based octupolar constructions is the preparation of the Pc cores into T_d structures by means of attaching to a tetravalent atom such as phosphorus[236].

Thus, the aryl trisphthalocyanine phosphonium salt Pc molecule has been prepared as a first described example for phthalocyanine incorporated within octupolar tetrahedral framework. The molecule exhibited very good second order NLO response compared to the corresponding nonoctupolar Pc, shown in **Fig. 2.46**[237].

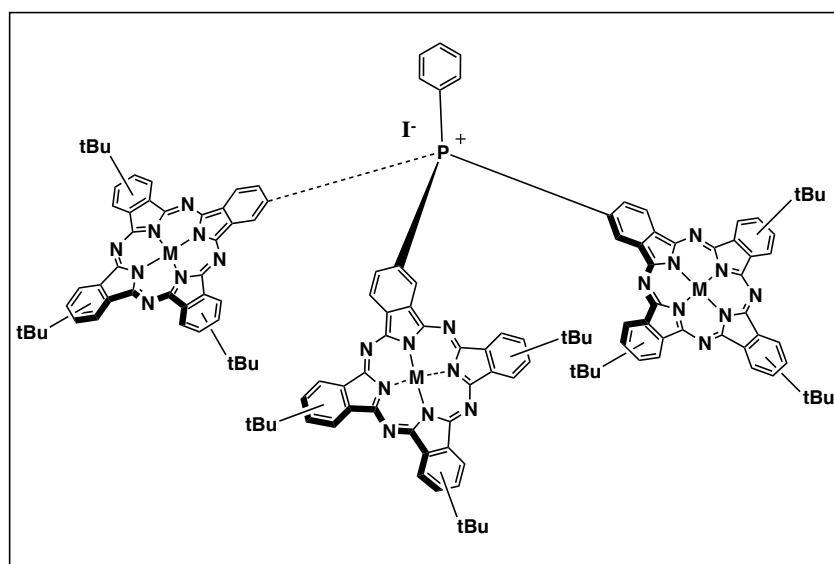


Figure 2.46. Octupolar aryl trisphthalocyanine phosphonium salt

Moreover, two series of 3D octupolar Pc-based compounds presenting a central carbon or silicon atom have been synthesized for NLO study. This design is based on the

original idea to induce the necessary noncentrosymmetry directly and solely by the octupolar symmetry, without any conjugation among the Pc moieties (**Fig. 2.47**).

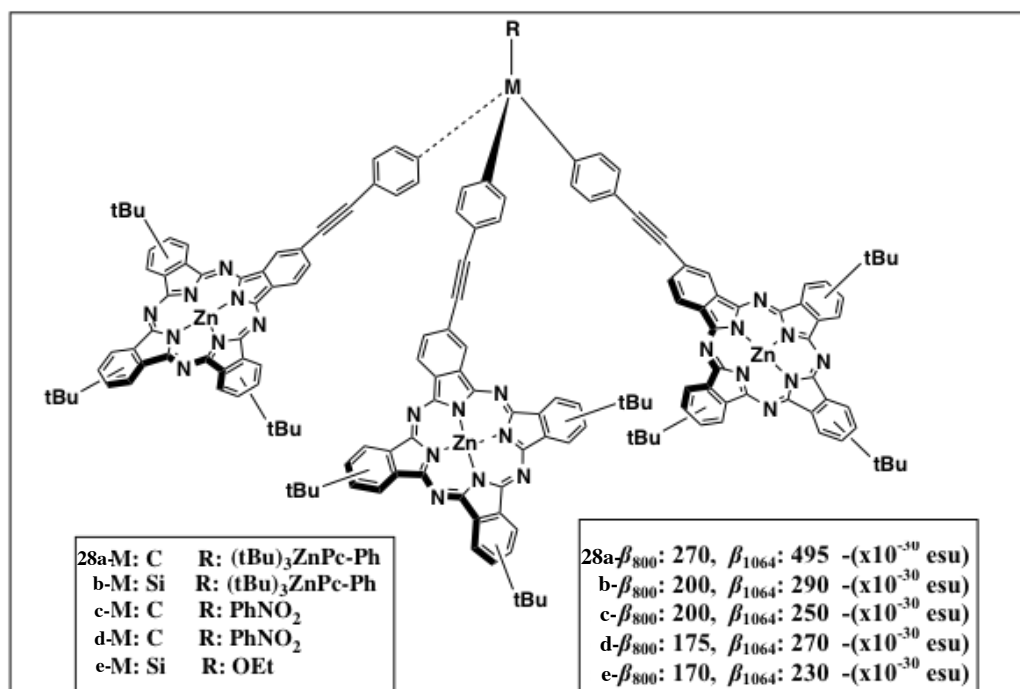


Figure 2.47. 3D octupolar Pc based compounds and their Second-Order NLO Properties

The second-order NLO results convincingly show that these molecules have octupolar fashion (largely **T_d** symmetry for the C-centered compounds **28a**, **28c**, and **28d**, and largely **D_{2d}** symmetry for the Si centered compounds **28b** and **28e**) nondipolar subunits that by themselves are centrosymmetric and, consequence, inactive for second order NLO. The resulting first hyperpolarizability is significant for a chromophore that is not a push-pull structure and compares favorably with both the dipolar and octupolar existing examples in the literature. This shows the intrinsic potential of the octupolar symmetry itself, without relying on cancellation of multipolar charge transfer contributions [238].

2.7. Experimental determination methods of first hyperpolarizability (β)

Second and third nonlinearities are determined by several techniques. The most known techniques are: Electric field-induced second harmonic generation (EFISH), Hyper-Rayleigh scattering (HRS), Kurtz Powder, Third harmonic generation (THG), degenerate four wave mixing (DFWM), optical Kerr gate (OKG) and the Z-scan technique [239]. While EFISH, HRS and Kurtz powder are used to determine second-order NLO activity of molecular materials, THG, DFWM, OKG and Z-scan technique are used to determine third-order NLO activity.

Since, this thesis focus on the Second-order NLO, here we will present a small part for the measurements methods for second-order nonlinear optics.

2.7.1. Kurtz Powder:

The Kurtz powder technique is an efficient method for the determination of second order nonlinear activity of powder materials [240]. In this method a laser is directed into a powdered sample and the emitted light at the second harmonic frequency is collected and compared with reference sample to able to measure of NLO efficiency. This method is crude compare to other method but it is a very good method for the evaluation of a large numbers of powdered materials [241].

2.7.2. Electric field-induced second harmonic generation (EFISH):

In EFISH technique, a strong static electric field is applied to solution of NLO active molecules. The interaction of the electric field with the permanent dipoles of these molecules induces an array in the orientation of the molecules. The limited removal isotropy causes second harmonic generation (SHG) [242]. This technique allows the determination β value from detected second harmonic light intensity for dipolar molecules [243,244]. This method has some disadvantages. First

of all, this method requires a complex apparatus and the molecules must have permanent dipole moment. Also the molecules should not ionize in solution [245].

2.7.3. Hyper-Rayleigh Scattering (HRS):

Hyper-Rayleigh scattering (HRS) is a method for determination the second harmonic scattered light of nonlinear optical chromophores in solution as a function of the concentration. This method requires high peak-power fundamental laser pulses and an efficient collection system of harmonic scattered photons. Because second-order nonlinear effects are vanished in the electric dipole approximation, the efficiency of Hyper-Rayleigh scattering in bulk solution is quite low. This is why this method is discovered in 1965 just after development of megawatt peak power pulsed laser [246,247]. Hyper Rayleigh scattering also is known as Harmonic light Scattering (HLS).

The HRS measures the amount of light incoherently scattered at exactly twice the frequency of an powerful laser beam [248]. Basic HRS process representation is showed in **Figure 2.48**.

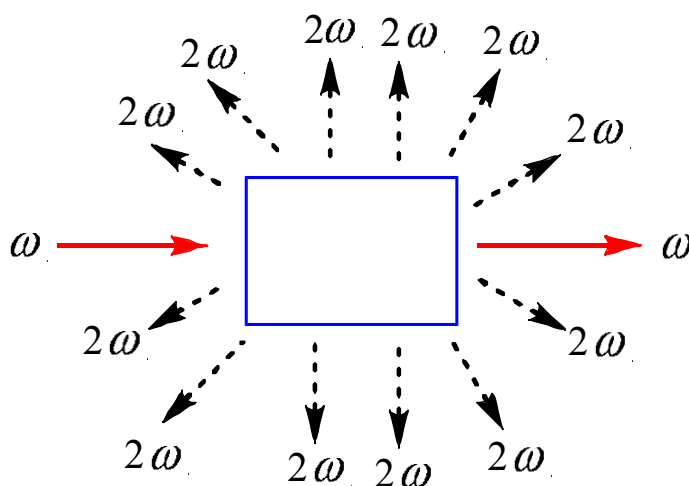


Figure 2.48. Schematic representation of HRS process in bulk liquid.

Hyper-Rayleigh scattering method is an alternative to EFISH method and this method does not require an external applied field unlike EFISH method. Thence, this method let us able to measure molecules that lack a permanent dipole moment but

have an octupolar, ionic chromophores, conductive materials, polymers and proteins, to which the EFISH can't [249-252]. The HRS technique is related with changing in the chromophore concentration and orientation. When intense laser beam at ω frequency is concentrate into NLO material containing solution, local density and orientation changing of the material raise frequency scattering of light from ω to 2ω in all directions. And latter frequency is proportional to total average of β^2 tensor shown on the polarization directions of the incident and scattered light. Thus, β value and several component of β tensor of nonlinear molecules are accessible straightforwardly. HRS experiment uses internal and external reference methods in order to extract reliable first molecular hyperpolarizability data.

In the internal method, the solvent is used as a reference for solute hyperpolarizability measurement [253-255]. This method was used for determining β of molecules by the Hyper-Rayleigh Scattering method until 1997. However, this method was abandoned because it's a few disadvantages, which are;

- Intercepts are small and errors in determining the intercepts are large [256]
- Solvent dependence of β can't be carried out unless calibration is done for each solvent.
- Solvents such as benzene can't be utilized.

As a result of these disadvantages a new method, which called external method, was proposed. The external method uses references materials, which their β^2 value is known precisely [257]. The second harmonic intensity from known reference and the unknown solute are both measured in the same solvent and experimental set up in order to keep G and the intercept constant. Then the ratio of slopes is equal to the ratio of β^2 's. This is described by the following equation:

$$\frac{\text{Slope (reference)}}{\text{Slope (sample)}} = \frac{\beta^2(\text{reference})}{\beta^2(\text{sample})}$$

References materials are chosen according to HRS experiment laser wavelength and shown in **Fig. 2.49** [258,259].

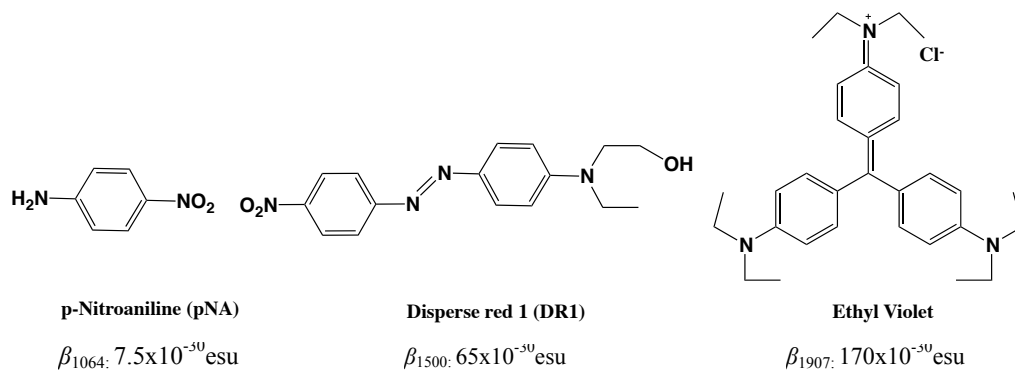


Figure 2.49. Benchmark materials for HRS experiment

2.8. Objective of the thesis

Despite all the various structures reported, it is worth noting that no molecules actually representing the “real” cube (even if deformed) with eight alternated charges at the corner and delocalization of the charges between the higher and lower plans have been obtained so far. To our knowledge the closest examples are the derivative of paracyclophane synthesised by the group of Bazan (See **Fig. 2.50**) [232]. In these compounds there is an electronic “through space” charge delocalisation between the higher cycle and the lower cycle. The described compounds, however, only have four identical functional groups (generally electro-donor) and not eight groups with alternating electro-donor/electro-acceptor. Since, paracyclophane (pCP) derivatives are organic molecules, they have certain limitations and drawbacks as mentioned before.

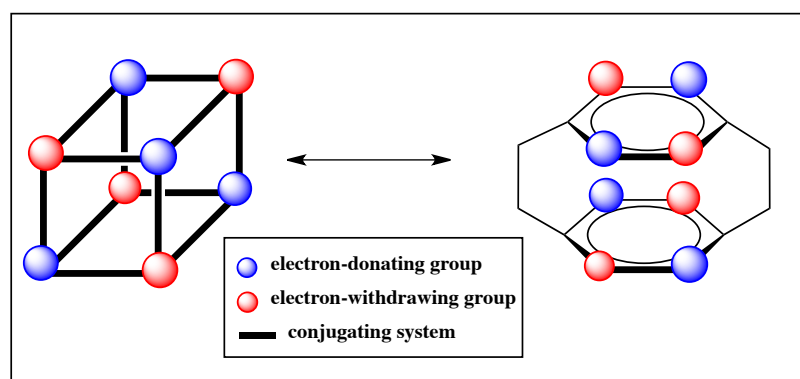


Figure 2.50. Schematic representation of general octupolar distribution and pCP template. Adapted from ref. [233]

Our primary target in this work is to prepare a synthon, which can be used as templates for cubic octupoles, with eight alternated charges at the corner and delocalization of the charges between the higher and lower plans.

This “through space” charge delocalisation between two cycles also exists in the “sandwiches” complexes formed by two units of phthalocyanines or porphyrins

coordinated by various ions, especially lanthanides III. In these compounds, the metal ion is located between the two plans of two macrocycles [260].

The strategy to obtain an octupolar molecule, which represent a real cube and their possible assembly into 3D noncentrosymmetric cubic structures are shown in **Fig. 2.51.b,c**. The square unit represented by a substituted crosswise **ABAB** phthalocyanine (**A**: acceptor; **B**: donor) in **Fig. 2.51.a**.

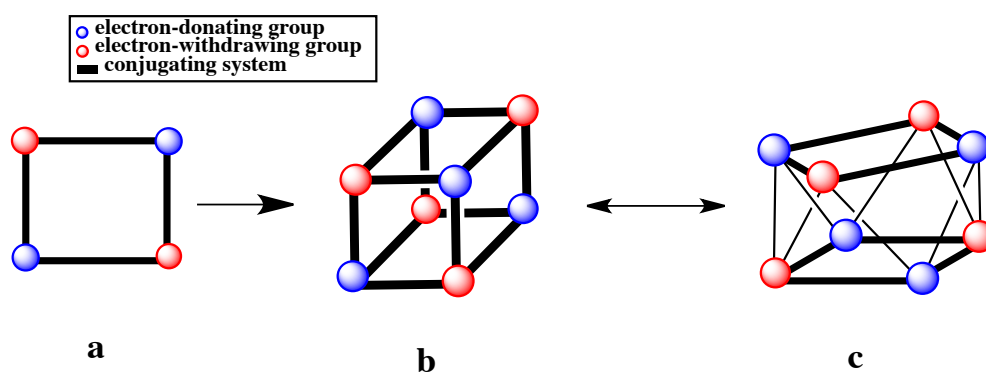


Figure 2.51. (a) Schematic representation of a molecule with square geometry (b) A cubic octupole template (c) A disordered cubic octupole template

So, we predicted that the real octupolar cube can be obtained by designing a bis(phthalocyaninato) Ln(III) double-decker complex of a crosswise ABAB phthalocyanine bearing alternating electron-donor and electron-acceptor groups (see **Fig. 2.52**).

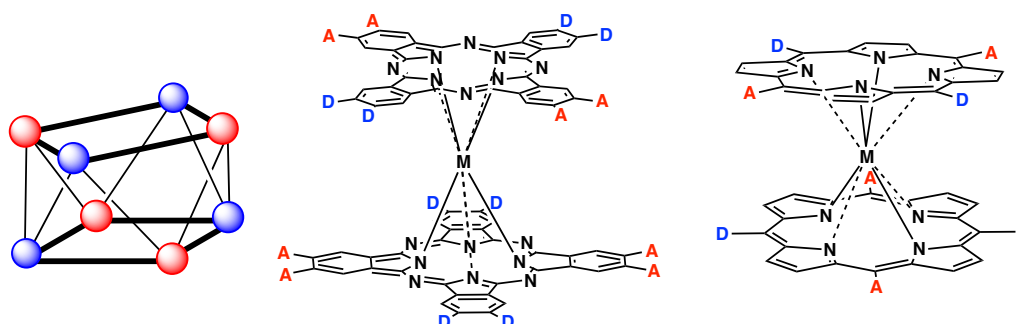


Figure 2.52. Double decker phthalocyanines and porphyrins as an octupole template

Moreover, phthalocyanines and porphyrins offer additional benefits as metal-coordinated complexes for NLO response compare to organic and inorganic materials as mentioned before.

Within the scope of this thesis, ABAB (crosswise) type phthalocyanines (Pcs) bearing electro-donor (-SC₆) and relatively electro-acceptor (-H) groups, and their Lanthanides III (Ln III) complexes were synthesized (see **Fig. 2.53**). Then NLO properties (β) of these compounds were measured by using the HRS techniques.

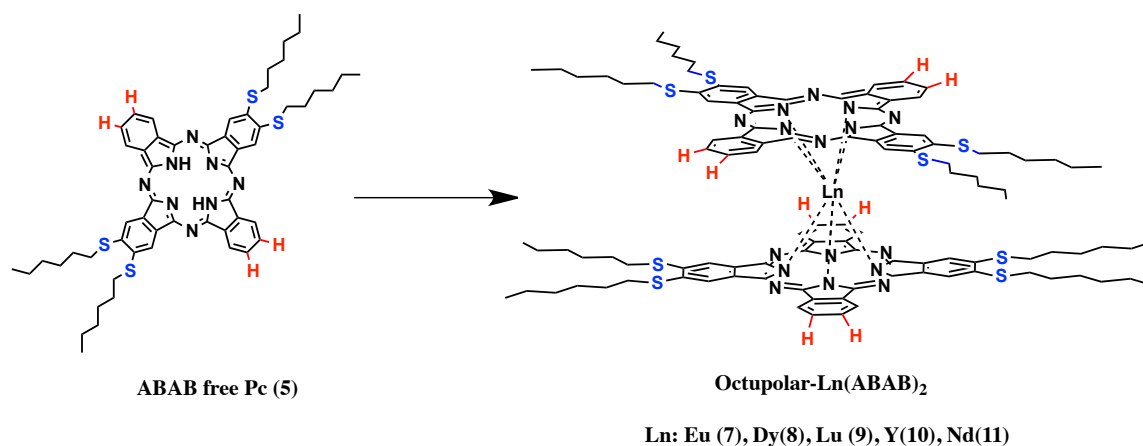


Figure 2.53. The structures of crosswise ABAB type free Pc and octupolar double decker lanthanide bis(phthalocyanines)

In order to understand better the second-order nonlinear properties of octupolar lanthanide phthalocyanine, related non-octupolar double-decker lanthanide bisphthalocyanines complexes were synthesized (See **Fig. 2.54**). Their second-order NLO responses were measured and compared with those of the octupolar bis(phthalocyanines) complexes.

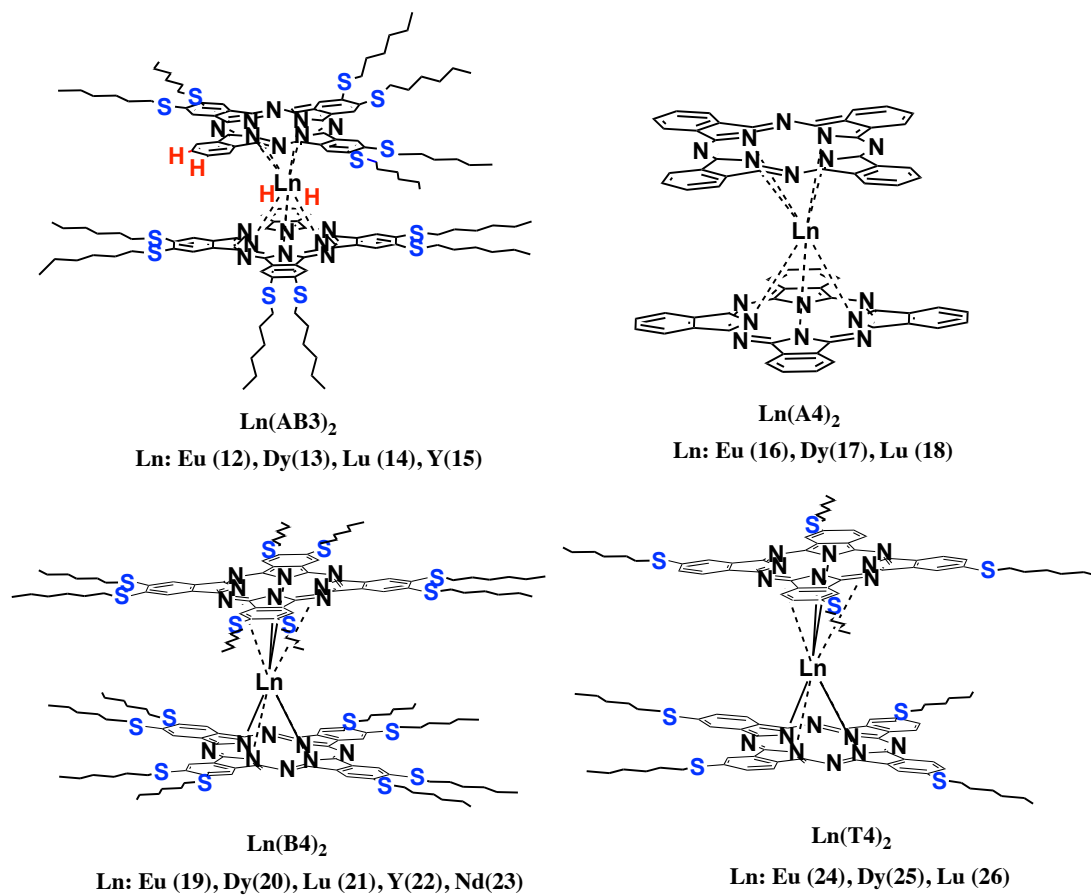


Fig. 2.54 The structures of non-octupolar AB₃, A₄, B₄, T₄ type double decker lanthanide bis(phthalocyanines)

3- RESULTS AND DISCUSSION

3.1. Analyzes of octupolar bis(phthalocyaninato) Ln(III) double-decker complexes (Ln(ABAB)₂ (Lu, Dy, Eu, Y, Nd))

3.1.1. Synthesis of crosswise ABAB phthalocyanine

In order to obtain the real octupolar cube by bis(phthalocyaninato) Ln(III) double-decker complex, we started with the molecular synthesis of the square unit as shown in **Fig. 3.1**. Two methods could be used to obtain crosswise-**ABAB** phthalocyanines:

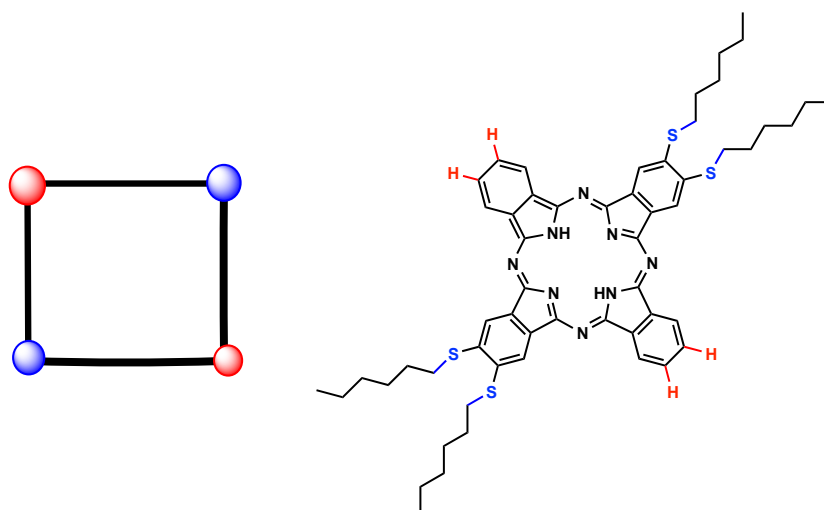


Figure 3.1 The crosswise-ABAB phthalocyanines as a square unit

The first method is the statistical condensation of differently substituted two precursors (A and B), namely, phthalodinitriles or 1,3-diiminoisoindolines [261]. This approach affords a statistical mixture of six phthalocyanines, AAAB, BBBA, AABB, **ABAB**, AAAA, BBBB shown in **Fig. 3.2**. Commonly, the precursors are mixed up in a 1:1 (A/B) ratio, to favor the formation of the unsymmetrical **ABAB** derivative [262,263].

However, the separation of these isomers by chromatographic methods is quite difficult and overall yield of ABAB phthalocyanine (D_{2h} symmetry) is very low [264].

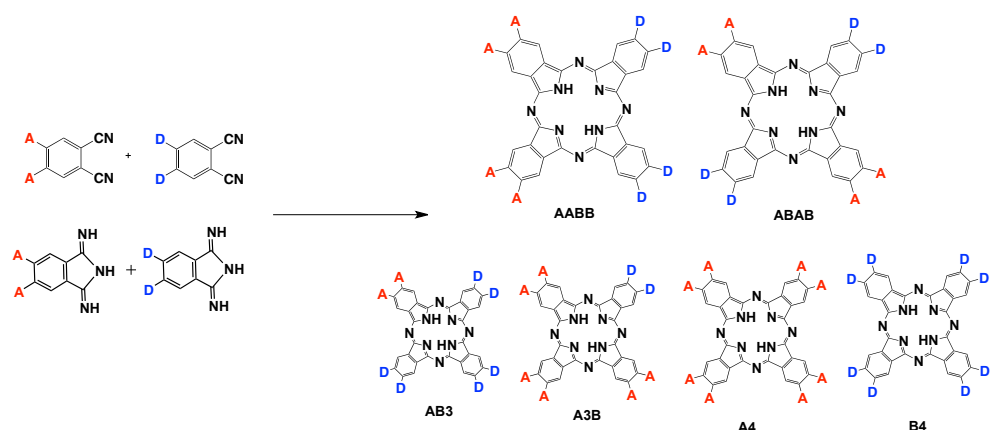


Figure 3.2. The statistical condensation approach for the synthesis of ABAB type pc.

Under conditions of statistical condensation, all six possible isomers are formed except for rare cases in which one of dinitriles is sterically hindered [211]. Attaching large substituents at the non-peripheral positions of phthalodinitrile or diiminoindoline can reduce the number of possible compounds. Steric hinderances in one of the starting dinitrils result in the formation of mixtures of only three isomers, viz., A4, A3B, ABAB, where A is the non-hindered unit [212].

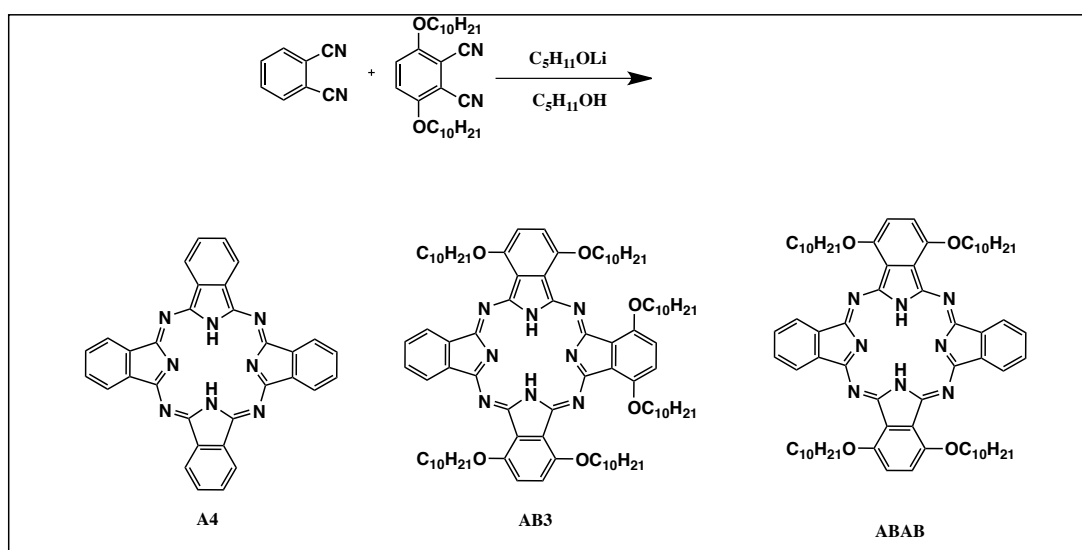


Figure 3.3. The statistical condensation approach for steric hinderance Pc

The first steric hindrance free base crosswise ABAB phthalocyanine was synthesized by Kudrik and et. al [264]. The mixture of A4, A3B and an isomer of the ABAB type phthalocyanine with overall yield 7% were obtained by addition of a 10-fold excess of phthalonitrile to a boiling solution of the 3,4-bis(decyloxy) phthalonitrile (**Fig. 3.3**). The ABAB form is predominant in the mixture of isomers thanks to the steric hindrance, which caused by nonperipheral substitutions. Moreover, the steric hindrance also not allows formations of types of B4, AB3 and AABB [264].

The other procedure is involves the synthesis of the ABAB-type phthalocyanines under mild conditions from equivalent amounts of two different phthalyl derivatives, namely 1,3-diiminoisoindoline and 1,3,3-trichloroisoindolenine, in the presence of a base and a reducing agent. This regioselective method was reported first by Yound and Onyebuagu (**Fig. 3.4**) [265]. They successfully increased the regioselectivity and yield of the synthesis of crosswise ABAB phthalocyanine. And they suggested that this method allow obtaining only ABAB type phthalocyanine [265].

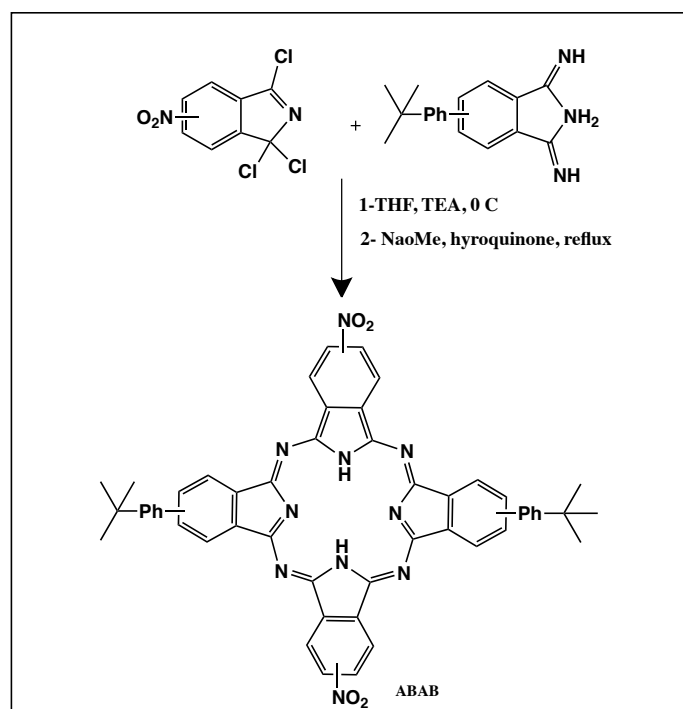


Figure 3.4 The regioselective approach for crosswise-Pc

However, the research of Hanack and *et. al.* showed that the regioselective method also allow to produce AB3 type phthalocyanine and trace amount of B4 type phthalocyanine beside of ABAB type phthalocyanine in contrast to the Yound and Onyebuagu results. The yield of ABAB type phthalocyanine (15.3%) is about 10 times higher than AB3 type phthalocyanine (1.3 %) (**Fig. 3.5**)[266].

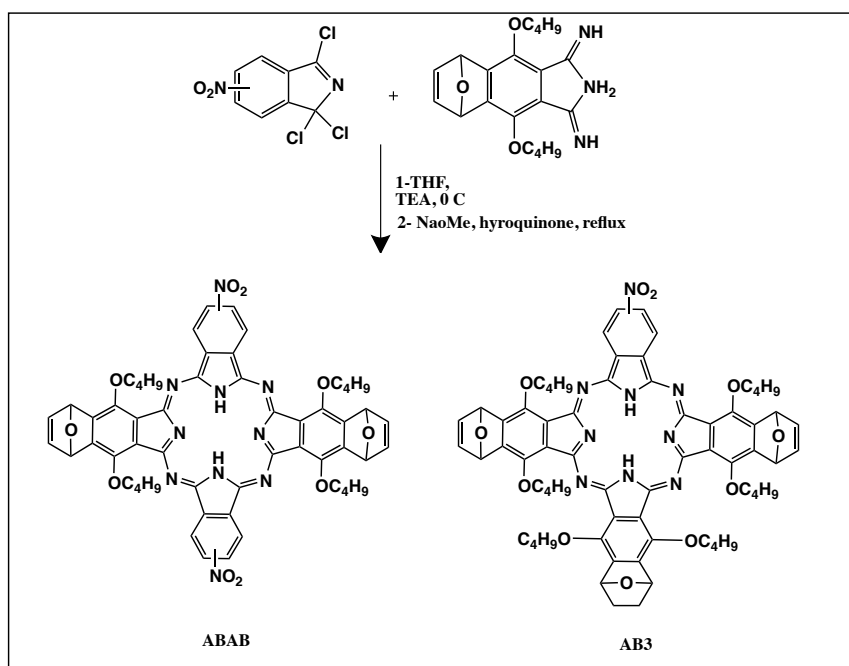


Figure3.5 The regioselective approach for crosswise-Pc

They suggested that the formation of AB3 may have been due to traces of water in the reaction mixture, resulting in partial hydrolyses of trichloroisindoline, which cause a troubled the stoichiometric balance of precursors [266].

The regioselective method clearly has advantages compare to statistical method such as better yield and easy separation. Therefore, we decided to use regioselective approach to synthesis the square unit as shown in **Fig.3.1a**.

The 4,5-bis(hexylthio)diiminoisindoline (yield 95%) is synthesized by treating the corresponding 4,5-bis(hexylthio)phthalonitrile with ammonia and sodium

methoxide in methanol(**Fig. 3.6**)[267]. And 1,3,3-Trichloroisindolenine (yield 80%) is obtained by chlorination of phthalimide with PCl_5 in *o*-dichlorobenzene[268].

The synthesis of the ABAB type Pc was succeeded by a cross-condensation of the 4,5-bis(hexylthio) diiminoisoindoline with an equimolar amount of 1,3,3-trichloro isoindoline. The **ABAB** type phthalocyanine was obtained as the major product (yield 8 %) (**Fig. 3.6**), but significant amounts of 2,3,9,10,16,17-hexa(hexylthio)phthalocyanine (yield 2%) (**AB₃**) and traces amount of 2,3,9,10,16,17,23,24-octa(hexylthio)phthalocyanine the symmetric derivative (**B₄**) were produced, requiring through the purification by chromatography. This result supports to observation of Hanack and *et.al*.

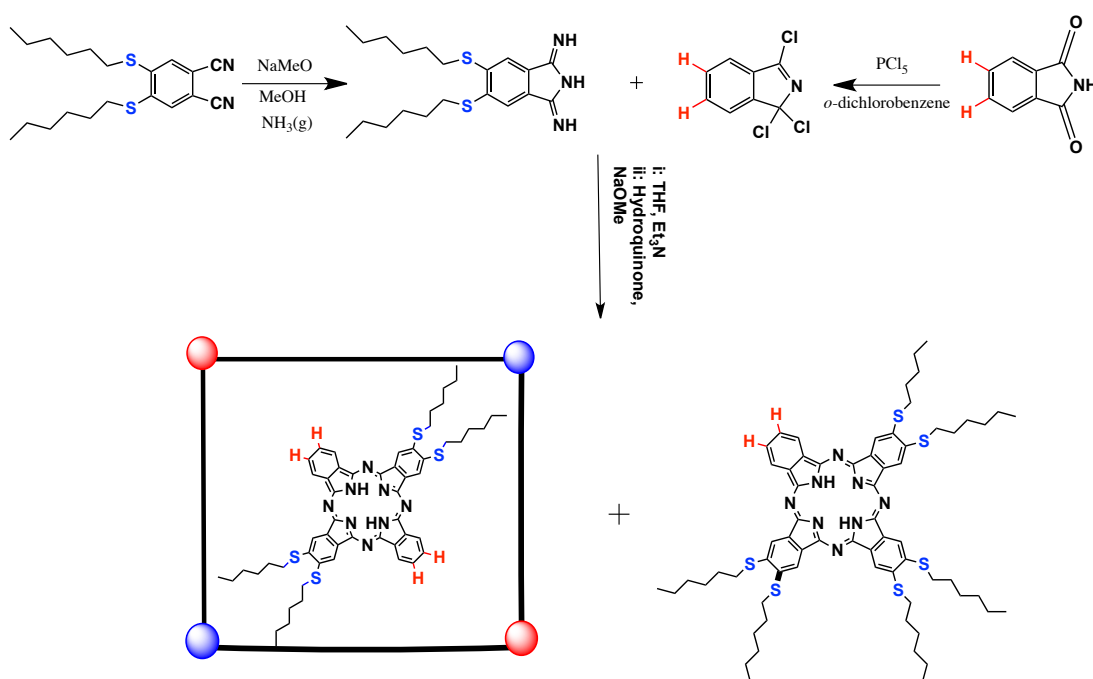


Figure 3.6 Synthetic route of crosswise ABAB type Pc by regioselective approach.

This reaction was repeated to find best reaction conditions and 1,3,3-trichloro isoindoline was used excess in order to obtain the stoichiometric balance of precursors by eliminating of partial hydrolyses of trichloroisoindoline. However,

AB3 type phthalocyanine was obtained repeatedly. It seems that the reason of obtaining AB3 type Pc is not partial hydrolyses of trichloroisindoline as suggested by Hanack and *et. Al* [266]. These results indicate that this method is not enough regioselective to obtain only ABAB type phthalocyanine.

Even though, the yield of this method is not high as Yound and Onyebuagu suggested, it still better than statistical methods and provide easier separation [265]. Detailed synthetic procedures were given in the Experimental Section.

3.1.2.Synthesis of octupolar bis(phthalocyaninato) Ln(III) double-decker complexes (Ln(ABAB)₂ (Lu, Dy, Eu, Y, Nd))

A large number of homoleptic lanthanide sandwich complexes have been prepared with symmetrical bis(phthalocyanines), usually by cyclic tetramerization of the corresponding phthalodinitrile in the presence of a lanthanide salt and an organic base such as 1,8- diazabicyclo[5.4.0]undec-7-ene (DBU) [269,270]. This method cannot be envisaged in our case, as a specific ABAB geometry is required for the two macrocycle.

Controlling the number and location of functional groups on the lanthanide bis(phthalocyanine) complexes requires the synthesis of asymmetrically substituted derivatives, in particular, complexes with ABAB type phthalocyanines. To the best of our knowledge, there have been no homoleptic lanthanide bis(phthalocyanine) complexes containing functionalized ABAB type phthalocyanines reported to date [271-273].

The synthetic procedures available for such compounds are based on the template complexation of a half-sandwich lanthanide compound with lithium phthalocyaninate, which usually give mixtures of products in comparatively low yields that are hard to separate [274].

Alternatively, reactions of Li_2Pc or H_2Pc in the presence of a lanthanide salt and an organic base in a highboiling solvent also lead to the formation of these homoleptic lanthanide sandwich complexes [275]. The use of free phthalocyanines as the starting compounds was shown to be more efficient than the use of the corresponding phthalodinitriles, because the reaction time is shortened substantially, isolation and purification become simpler, and, in most cases, the yield of target products increases [276].

For instance, double decker crown bis(phthalocyanines) by the direct interaction of tetra-15-crown-5-phthalocyanine (H_2Pc) with a $\text{Y}(\text{OAc})_3 \cdot 4\text{H}_2\text{O}$ in the presence of DBU as an organic base in 1-chloronaphthalene under reflux (260 °C) was synthesized with high yield by Gorbunova and et. al. (**Fig.3.7**) [277].

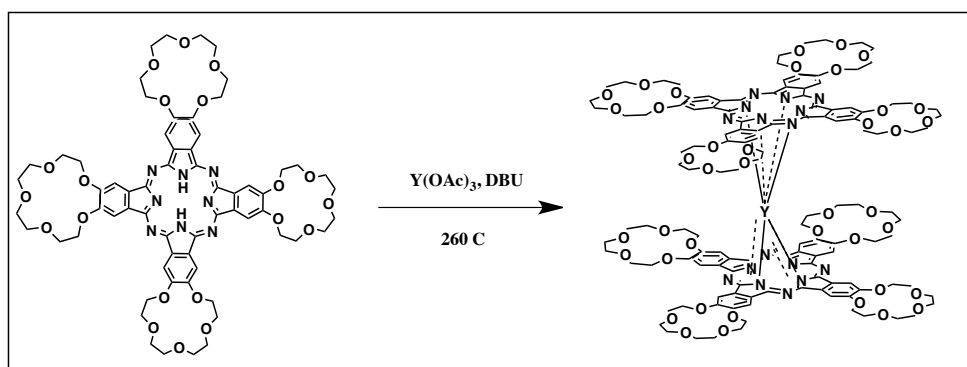


Figure 3.7 Synthesis of bis(phthalocyaninato) Y(III) double-decker complexes

This method offers modularity in terms of ligand choice and forces the two-phthalocyanine units to through space delocalization, both phthalocyanine planes are subjected to severe conformational twisting suitable for conjugation-dependent NLO applications [227]. Moreover, this method is synthetically quite easy and high yielding. Therefore, we initiated our work with this procedure [278].

This synthetic method allowed us to synthesize selectively the double decker bis(phthalocyanine) molecules from free base ABAB type free phthalocyanine (H_2Pc), which represent the cubic octupole as shown in **Figure 3.8**.

Finally, the unsymmetrical bis(phthalocyanine) complexes were obtained in good yield from the **ABAB** type phthalocyanine and lanthanide acetate ($\text{Ln}(\text{OAc})_3$ -Ln: Lu, Eu, Dy, Nd and Y) in refluxing 1-chloronaphthalene using DBU as a base as shown in **Fig. 3.8**[279]. Bis(phthalocyanines) obtained by this approach could lead to noncentrosymmetric and octupolar conformation as shown in **Fig. 3.1 c**.

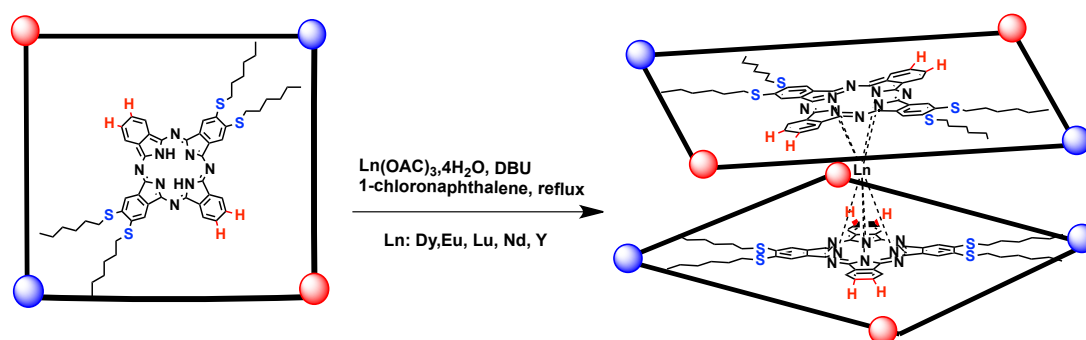


Figure 3.8 The synthesis approach for octupolar $\text{Ln}(\text{Pc})_2$

The reaction yield of lanthanide bis(phthalocyanine) complexes is the order: $\text{Y}(\text{ABAB})_2$: 60%, $\text{Nd}(\text{ABAB})_2$: 60%, $\text{Eu}(\text{ABAB})_2$: 63%, $\text{Dy}(\text{ABAB})_2$: 54%, $\text{Lu}(\text{ABAB})_2$: 60%

Bian and *et. al.* suggested that the reaction yields of lanthanide bis(phthalocyanine) complexes are dependent on the size of the metal centers. For the series of bis(phthalocyaninato) complexes, the yields are lower for those with a larger metal center [280]. However, we didn't observe any relation between the reaction yield and size of metal centers.

$\text{Ln}(\text{Pc})_2$ complexes, which were synthesized during this thesis, were characterized by ^1H NMR, ^{13}C NMR, IR, mass spectrometry, elemental analyses., UV-NIR, X-Ray and second-order NLO properties were investigated by using the HRS techniques.

3.1.3. UV-NIR measurements of neutral form of octupolar bis(phthalocyaninato) Ln(III) double-decker complexes (Ln(ABAB)₂ (Lu, Dy, Eu, Y, Nd))

One of the main parameters for the NLO response of a molecule is the scheme of its electronic energy levels. In accordance with their electronic structure, Pcs present intense π - π bands in the visible (Q band) and UV (B or Soret band) spectral regions [281]. **Fig. 3.9** represents a typical UV-vis spectra and electronic transitions accounting for B and Q bands of unsubstituted Pcs.

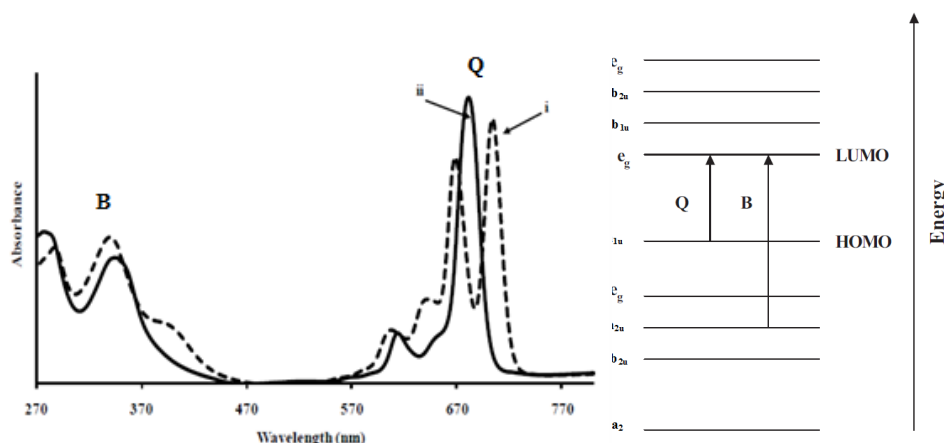


Figure 3.9. Absorption spectra of free phthalocyanine (**i**) and metallo phthalocyanine (**ii**) and Electronic transitions accounting for B and Q bands of phthalocyanines

Fig. 3.10ii shows the absorption spectra of ABAB-H₂Pc (**5**) in solution in chloroform. The Q-band absorption is assigned to a transition from the HOMO of a_{1u} symmetry to the LUMO of e_g symmetry. In H₂Pc the Q-band is split up because of the lower symmetry (D_{2h}) and the consequent loss of degeneracy of the LUMO orbital to produce Q_x and Q_y. ABAB-H₂Pc (**5**) presents the classical spectrum of low symmetry free phthalocyanines with a B-band at 340 (**5**) and intense Q-band split in two with maxima at 682-719 nm (**5**).

The substitution of the Pc ring by electron donating hexyl thio groups provokes a red-shift of the Q band compared to the unsubstituted phthalocyanine

compound [282]. A small bathochromic (red) shift is observed for the most intense absorption peaks Q_x and Q_y of ABAB-H₂Pc (5).

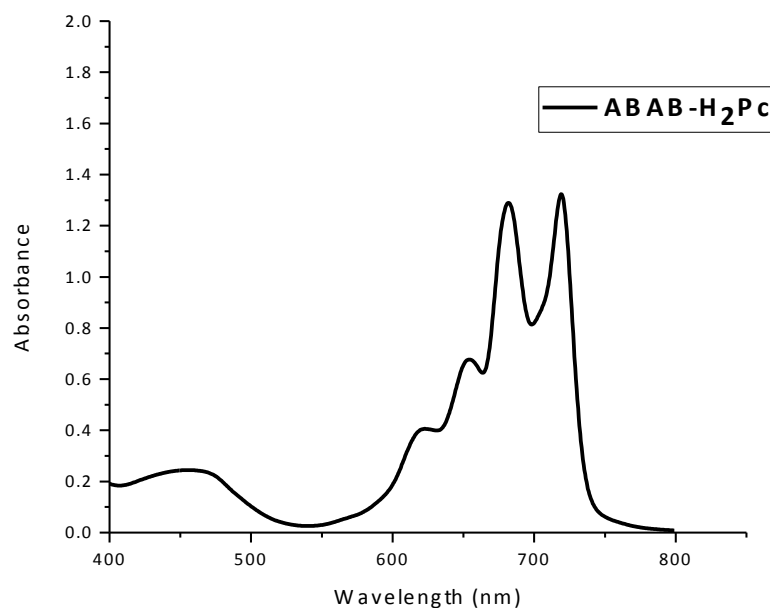


Figure 3.10. UV-Vis Spectrum of ABAB (5) type free phthalocyanine

Fig. 3.10. represents absorption spectrum of typical spectral pattern of metallo phthalocyanine (MPc). The sharp, intense band observed in lowest energy region (674 nm) in a π - π^* transition, referred to as the Q band. The broad band in the 300-400 nm region consists of more than one component, including B₁ and B₂ bands, and referred to as Soret region [283]. Several less intense components observed at the foot of the Q band are considered to be of vibronic origin [284].

The 500-600 nm area of the spectrum is called an optical window, where there is almost no light absorption. When additional bands are observed in the window region, for example due to charge transfer transitions between the central metal ion and the π ring, the colour of the complex changes [285]. The spectral properties of the lanthanide complexes are more complicated than for the metal phthalocyanines with only one Pc-ring. Furthermore, oxidation and reduction of the Pc ring produces π -cationic or π -anionic species, which have both of them characteristic spectroscopic properties [285].

Fig.3.11. shows a UV-NIR spectrum of a neutral $\text{Ln}(\text{Pc})_2$ bisphthalocyanine and schematic representation of the MO levels [286]. The intense Q band in the electronic absorption spectrum of $\text{Ln}(\text{Pc}^{2-})(\text{Pc}^{\bullet-})$ can be considered as the sum of the overlapping Q bands of each species. The band at 469 nm (BV) is attributed to transitions into the SOMO a_{1u} orbital and is specific for the $\text{Pc}^{\bullet-}$ radical. And the band between 1220 and 1600 nm is ascribed to HOMO-LUMO transition and connected to an intramolecular charge transfer (ICT) between two Pc rings: the dianion Pc^{2-} behaves as an electron donor and the $\text{Pc}^{\bullet-}$ radical as an electron acceptor. The weak band at 943 nm (RV) with a vibronic component at 820 nm attributed to SOMO-LUMO transition [286].

The three absorptions at 469 (BV), 943 (RV) and 1500 (ICT) nm are all characteristic $\text{Pc}^{\bullet-}$ related band for bis(phthalocyanine) lanthanide (III) complex [287].

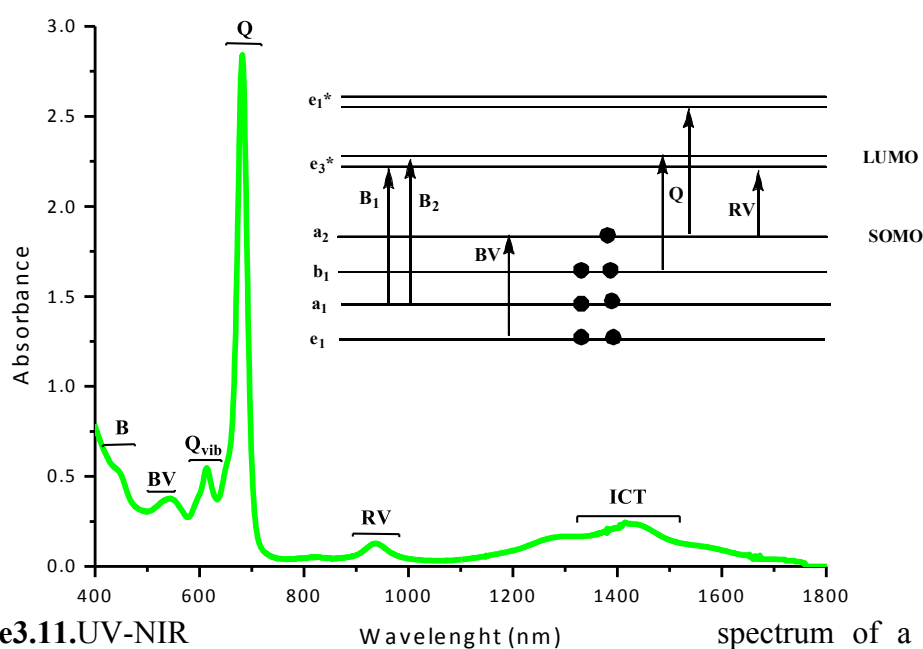


Figure 3.11. UV-NIR spectrum of a neutral $\text{Ln}(\text{Pc})_2$ bisphthalocyanine and schematic representation of the MO levels, Adapted from [287]

The UV-NIR spectrum of neutral $\text{Lu}(\text{ABAB})_2$ Bis(Phthalocyanine) (**9**) is given as example in **Fig. 3.12** shows a relatively intense absorption at 682 nm with a vibronic band at 645 nm is due to the phthalocyanine Q band. The broad band at 400

with a shoulder at 443 nm is attributed to the phthalocyanine Soret band. In addition, the intramolecular charge transfer (ICT) between two Pc rings of neutral Lu(ABAB)₂ bis(phthalocyanine) (**9**) shows broad and intense absorption regions in the infrared region appearing between 1075 and 1705 nm. And the two n-radical anion bands appeared at 550 (BV) and 933 nm (RV).

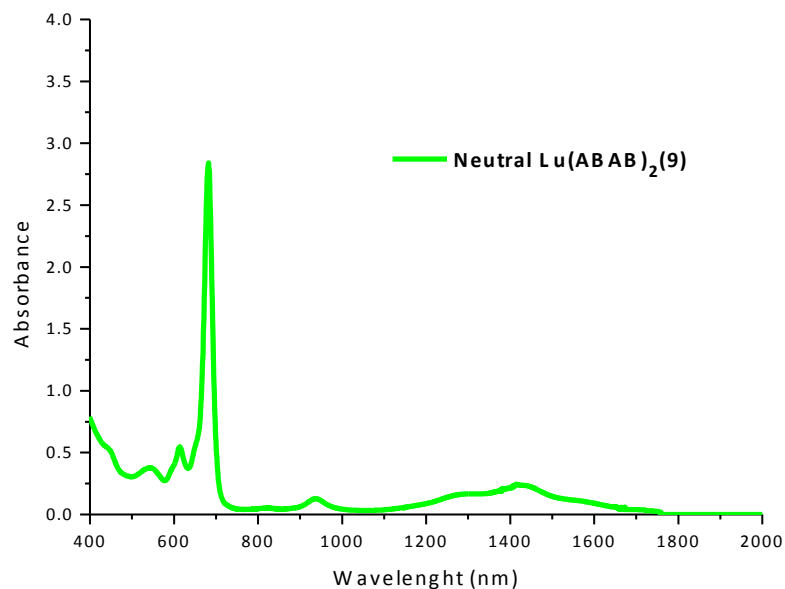


Figure 3.12. UV-NIR spectrum of a neutral Lu(ABAB)₂ bisphthalocyanine in CHCl₃

The electronic absorption spectra of (ABAB)₂Ln (Eu (**7**), Dy (**8**), Nd (**10**) and Y (**11**)) are similar to Lu(ABAB)₂(**9**) and the electronic spectral data summarised in **Table 3.1**.

Table 3.1 UV-NIR spectral data of neutral forms of Ln(Eu, Dy, Lu, Nd, Y)(ABAB)₂ Bis(phthalocyanine) (1 x 10⁻⁵ M)

			λ_{\max} (nm)				
Compound		Form	B	BV	Q	RV	ICT
ABAB (7-11)	Eu(7)	Neutral	322	557	609,686	920	118-1911
	Dy(8)	Neutral	336	554	680	985	1165-1865
	Lu(9)	Neutral	340	533	621,671	925	1075-1705
	Nd(10)	Neutral	328	562	610,694	910	1451-2000
	Y(11)	Neutral	328	550	610,682	946	1205-1733

B: Soret band, BV and RV: radical transition bands, ICT: Intramolecular charge transfer band

The position of the ICT band for the Ln(ABAB)₂ are dependent on the size of

central rare earths [288]. These results indicate that the interaction between the two rings becomes stronger as the ring-to-ring separation decreases along with the lanthanide contraction (**Fig. 3.13**). More accurately, the blue-shifts are due to the decreased distance between the Pc rings.

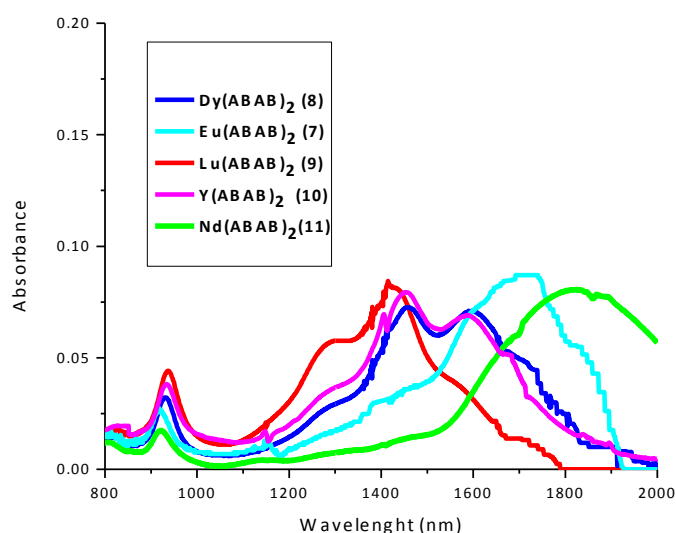


Figure 3.13 The UV-NIR spectrum of neutral Ln(Eu, Dy, Lu, Y, Nd)(Pc(ABAB)₂) in CHCl₃ (1 × 10⁻⁵ M)

The UV-NIR spectra and the ICT bands of (ABAB)₂Ln (Lu, Eu, Dy, Nd and Y) complexes in chloroform are given as example in **Figure 3.13**. The ionic radii of the lanthanides and Y are in the order Lu - 100.8 pm < Y - 104 pm < Dy - 105.2 pm < Eu - 108.7 pm < Nd - 112.3 pm [289].

Consequently, the largest blue-shift is due to the decreased distance between the Pc rings. It can be correlated with the radius of the lanthanide (III): Nd < Eu < Y ≤ Dy < Lu (**Fig. 3.14**). And these results are consistent with the results reported recently showing that for Ln(Por)₂ [290].

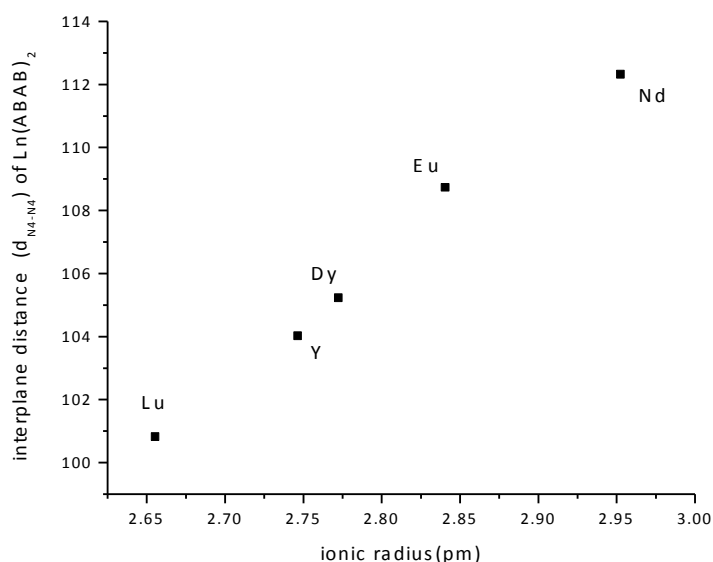


Figure 3.14 Plot of the interplane distances vs lanthanide ionic radius

3.1.4. Single crystal X-Ray measurements of octupolar bis(phthalocyaninato) Ln(III) double-decker complexes (Ln(ABAB)₂ (Lu, Dy, Eu, Y, Nd))

The lanthanide atoms in all complexes are sandwiched between two phthalocyanine rings and are coordinated with eight isoindole nitrogens of the two Pc macrocycles. Since molecular structures of the double decker rare earth Pc complexes are the key point for our real cube octupolar Ln(Pc)₂ expectation, the following structural parameters: the interplanar distance between the two N4 mean planes of tetrapyrrole rings (d_{N4-N4}) and the rotation angle of one tetrapyrrole ring away from eclipsed conformation of the two tetrapyrrole rings (the twist angle, ϕ_T) were investigated and compared for all double decker Pcs series.

All of Ln(ABAB)₂ (Lu, Dy, Eu, Y, Nd) were crystallized from concentrated chloroform solution by slow diffusion of methanol and the crystal structure was resolved by X-ray diffraction. **Fig. 3.15** shows the molecular structure of Lu(ABAB)₂ (**9**) as selected examples to illustrate the structural features of the Ln(ABAB)₂ series of complexes, which are isostructural from each other. The

Crystallographic data, structure refinement parameters and selected distances data of $\text{Ln}(\text{ABAB})_2$ (Lu, Eu, Dy, Y, Nd) and $\text{Eu}(\text{B4})_2$ are listed in ANNEX 2, respectively.

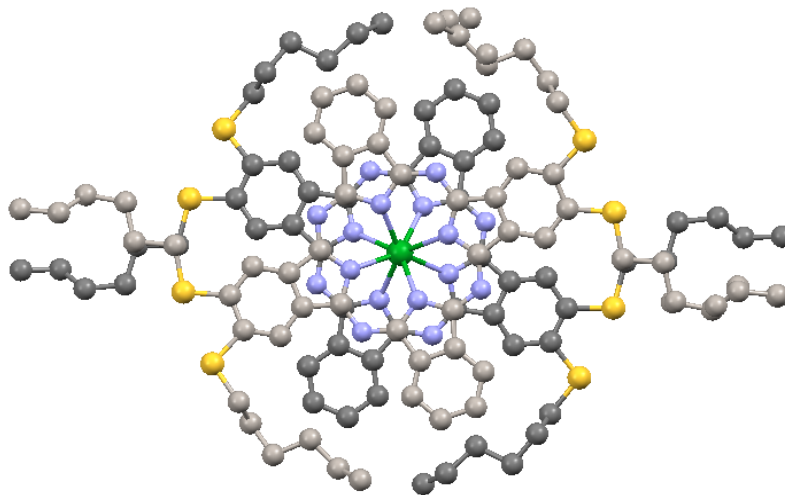
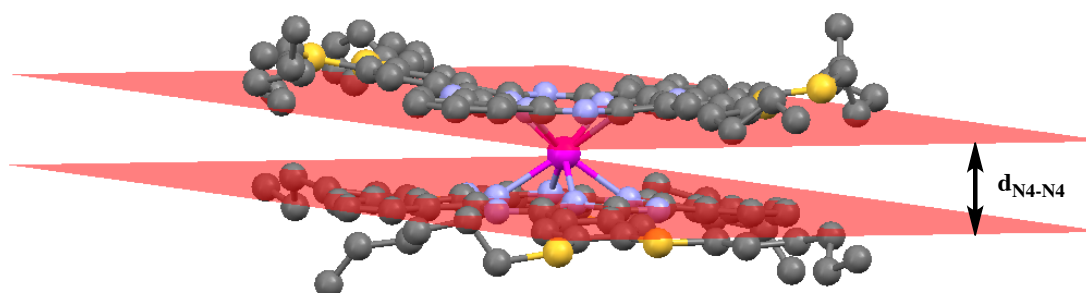


Figure 3.15 The molecular structure of $\text{Lu}(\text{ABAB})_2$ (**9**)

The molecular central core of $\text{Lu}(\text{ABAB})_2$ has a very similar structure to the previously reported unsubstituted (**18**) and hegzadeka-substituted (**21**) bis(phthalocyaninato)lutetium(III) complexes [291,292]. Two phthalocyanine rings are flanking a central Lu^{3+} ion. The Lu^{3+} ion is octacoordinated by eight nitrogen atoms of the isoindole N2 and N6 (Niso) in a slightly distorted square antiprism geometry. The $\text{Lu}-\text{N}_{\text{iso}}$ distances (2.356 and 2.366 Å) are slightly shorter than those reported for similar complexes ($\text{Lu}-\text{N}_{\text{iso}}$ distances between 2.377-2.394 Å for the octakis(hexylthio) analogue and 2.380 Å for Pc_2Lu). The interplane distance ($d_{\text{N4-N4}}$) between the two macrocycle, defined as a distance between the mean planes formed by the four Niso atoms, is also shorter (2.656 Å) than the values reported (2.67-2.70 Å).



	Lu(ABAB)₂	Dy(ABAB)₂	Y(ABAB)₂	Eu(ABAB)₂	Nd(ABAB)₂
d_{N4-N4} (Å)	2.656	2.773	2.747	2.841	2.953

Figure 3.16. The interplane distance (d_{N4-N4}) of Ln(ABAB) (Lu, Eu, Dy, Nd and Y)

Fig. 3.17 shows that the values of the interplane distance (d_{N4-N4}) of Ln(ABAB)₂ decrease from Eu to Lu following the same variations as the ionic radii of the metal cations .

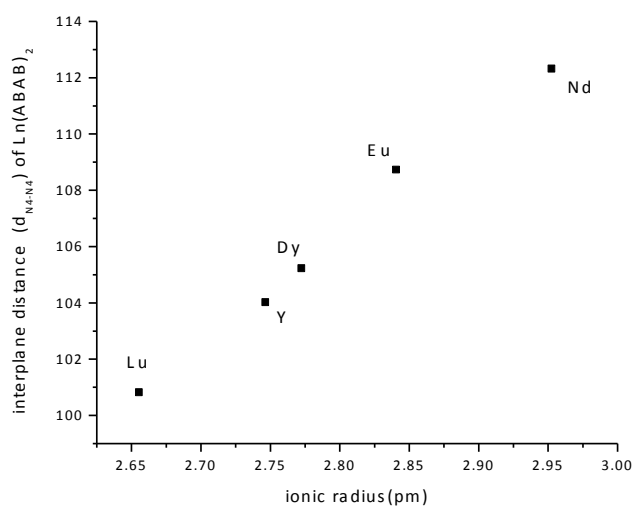
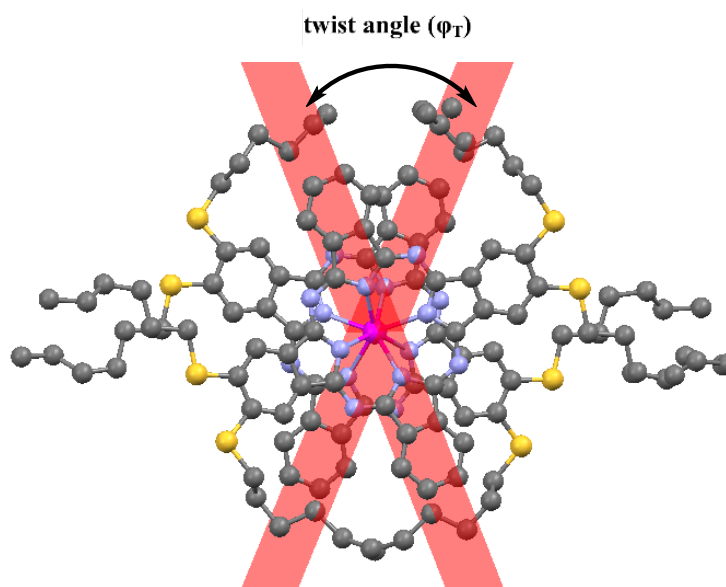


Fig. 3.17The interplane distance (d_{N4-N4}) of Ln(ABAB)₂ vs lanthanide contraction

Moreover, the twist angles of the two macrocycles, φ_T , indicate that the coordination polyhedral of the metals variety from a distorted cube to almost a square antiprism. The twist angle between the two cycles of $\varphi_T : 45.05^\circ$ that creates a chiral non centrosymmetric molecule (**Fig. 3.18**) and also higher than the values reported 45° for unsubstituted (**18**) and 42° for octa-substituted (**19,21**) (**Fig. 3.18**).



	Lu(ABAB)₂	Dy(ABAB)₂	Y(ABAB)₂	Eu(ABAB)₂	Nd(ABAB)₂	Eu(B4)₂
φ_T	45.05°	45.66°	45.08°	45.23°	44.08°	42°

Figure3.18 The twist angles φ_T of Ln(ABAB)_2 (Lu, Eu, Dy, Y, Nd)

According to Koike *et al.* the value of the twist angles φ_T is related to the strength of the π - π interaction between two Pc rings, which is related to interplane distance ($d_{N_4-N_4}$) [293]. However, **Fig 3.17** and **Fig. 3.18** show that though the interplanar distance from Eu to Lu decrease following the same variations as the ionic radii of the metal cations, significant changing on the twist angles wasn't observed. Darovskikh *et al.* suggested that the diversity of twist angles is the result of a fine equilibrium between steric repulsion in the solid state, lattice energy and aromaticity of the Pc macrocycles [294]. And this theory seems more appropriate for our observations.

The four N_{iso} atoms deviate by 0.121 \AA (for Nd), 0.0149 \AA (for Eu), 0.0168 \AA (Y), 0.168 \AA (for Dy) and 0.192 \AA (for Lu) from their respective mean plane so that they are nearly coplanar.

In the neutral radicalic form, $\text{Ln}(\text{Pc})_2$, the unpaired electron is delocalized over both rings and therefore no significant differences are found from both phthalocyanine rings.

3.1.5. Hyper-Rayleigh Scattering (HRS) measurements of neutral form of octupolar bis(phthalocyaninato) Ln(III) double-decker complexes ($\text{Ln}(\text{ABAB})_2$ (Lu, Dy, Eu, Y, Nd))

The first hyperpolarizability β values of the octupoles $\text{Ln}(\text{ABAB})_2$ (7-11) were determined by Hyper-Rayleigh Scattering (HRS) method also named Nonpolarized harmonic light scattering method (HLS). The HRS technique involves the detection of the incoherently scattered second harmonic generated by a solution of the molecule irradiated by a laser of wavelength λ , leading to the measurement of the mean value of the β product.

All HRS measurements were carried out at the Ecole Normale Supérieure de Cachan at the same concentration to avoid concentration effects. It has to be noticed that the neutral form of lanthanide double-decker complexes $\text{Ln}(\text{Pc})_2$ have absorption bands at $\lambda/2$, in order to minimize the interferences of these bands, all measurements were carried out at very low concentration (1×10^{-5} M) and HRS data were corrected for chromophore absorption before determining β_{1907} .

HRS measurements were carried out with a low-energy nonresonant incident radiation of at 1.907 nm, where multi-photon fluorescence (MPF) cannot interfere, thereby avoiding any multiphoton fluorescence contribution to the HRS signal [295]. It must be noted that most classical organic solvents are not transparent at 1.907 nm, which cause interferences with the β values. Chlorinated solvents are an exception, so chloroform was chosen to perform the HRS measurements. And the ethyl violet was used as a reference in order to accurately set up our setup on the determination of β [296].

The error is estimated to be approximately $\pm 15\%$.

The instrumental setup of Hyper-Rayleigh Scattering (HRS), necessary formulas and details of the calculations of β are given in ANNEX 3.

The first hyperpolarizability β obtained for the Ln(ABAB)₂(7-11) in neutral forms are summarized in the Table 3.2.

Table 3.2 The second-order NLO data for the octupole Ln(ABAB)₂(7-11)

Compounds	Form	Absorbance		P _{ETV}	P _S	Corr.P _S	Avg. Corr. $\beta \times 10^{-30}$ esu	
		λ_{1907}	λ_{955}					
ABAB (7-11)	Eu(7)	N.	0.03	0.014	0.067	0.19	0.2073	5429
	Dy(8)	N.	0	0.037	0.0685	0.215	0.2269	5622
	Lu(9)	N.	0	0.05	0.0765	0.251	0.2662	5756
	Nd(10)	N.	0.13	0.032	0.0417	0.033	0.0460	3251
	Y(11)	N.	0	0.055	0.0373	0.034	0.0363	3010

P_{ETV}: Slope of ETV, P_S: Slope of Sample, Corr. P_S: Corrected slope for sample

The first hyperpolarizability of Ln(ABAB)₂ are exceptionally large with a value of 5750×10^{-30} esu for Lu(ABAB)₂ (9), 5622×10^{-30} esu for Dy(ABAB)₂ (8), 5429×10^{-30} esu for Eu(ABAB)₂ (7), 3251×10^{-30} esu for Nd(ABAB)₂ (10) and 3010×10^{-30} esu for Y(ABAB)₂ (11).

To the best of our knowledge these are one of the highest values reported for a non-dipolar compound and compares well with the very best octupolar chromophores described ever reported to date and much larger than the paracyclophane derivative the closest example of the real cube described by Bazan (46×10^{-30} esu) [297]. Moreover, this high NLO activity is roughly 10 times larger than those of octupole phthalocyanine derivatives described in the literature [297, 298].

As already observed for the dipolar and octupolar rare-earth series, the NLO

activity regularly increases from yttrium to lutetium along the f-element row, and called “metal-induced NLO-enhancement”[299,300].

This “metal-induced NLO-enhancement” effect was observed in series Ln (Lu, Eu, Dy, Nd and Y)(ABAB)₂. For instance, although Lu (**9**) and Y (**11**) complexes are isostructural, the β_{1907} value of Lu (**9**) complex is roughly 2 times larger than the one of Y (**11**) complex.

The NLO results of the yttrium complex Y(ABAB)₂ is particularly useful to rationalize the “metal-induced” NLO enhancement effect by comparing it with the dysprosium complex Dy(ABAB)₂. Yttrium presents strong chemical similarities with the lanthanides, and its ionic radius (1.075 Å) is very close to that of dysprosium (1.083 Å). On the other hand, yttrium is not f-block element and therefore has a 4f⁰ electronic configuration. Experimentally, the first hyperpolarizability of yttrium, ($\beta_{1907}:3010 \times 10^{-30}$ esu) is significantly lower than that of dysprosium ($\beta_{1907}:5622 \times 10^{-30}$ esu), even if these two complexes are isostructural and has roughly same ionic radius. It appears that the difference of NLO activity between Y(ABAB)₂ and Dy(ABAB)₂ can be better correlated to the f configuration rather than the ionic radius. Plotting the variation of β_{1907} versus the electronic parameter (f configuration) (**Fig. 3.19 b**), clearly demonstrates the “metal-induced” NLO activity enhancement with the direct contribution of f electrons to the hyperpolarizability and the different in behavior of yttrium.

The order of the experimental hyperpolarizability β are as follow: $\beta_{1907}(\text{Y}) < \beta_{1907}(\text{Nd}) < \beta_{1907}(\text{Eu}) < \beta_{1907}(\text{Dy}) < \beta_{1907}(\text{Lu})$.

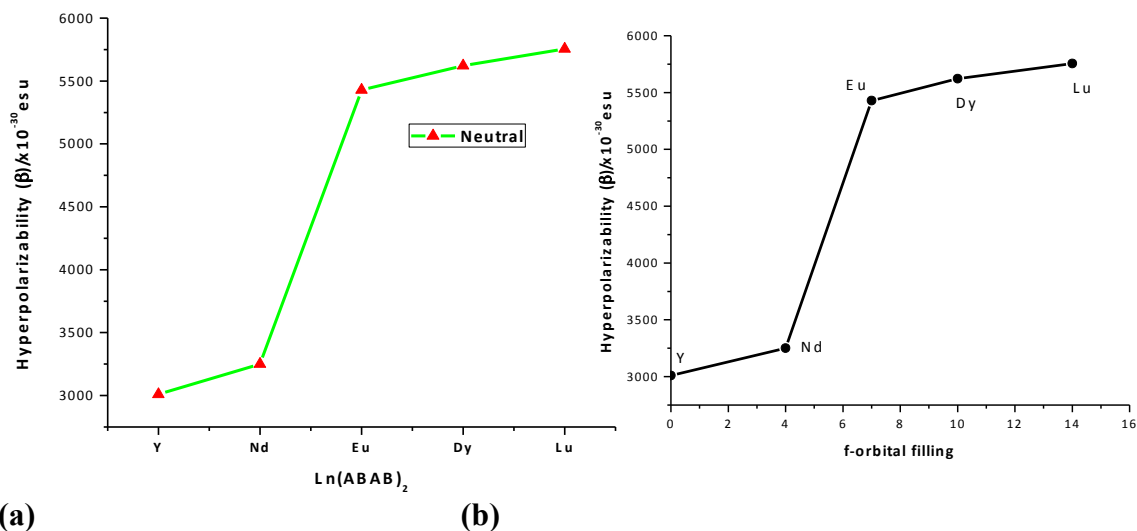


Figure 3.19. Plot of the hyperpolarisability β vs $\text{Ln}(\text{ABAB})_2$ (a) and f-orbital filling (b)

However, the different NLO activities (β_{1907}) between the octupolar lanthanide bis(phthalocyanines) can not be clarified only by the f electrons contribution. The lanthanide contraction is also an important variable and must be taken into account.

Although, all bis(phthalocyanines) octupole are isostructural, they exhibit the unequal absorption spectra. Especially, the position of the intra molecular charge transfer (ICT) band between 1300-1900 nm is highly dependent on the size of central rare earths metal, shifting to higher energy along with lanthanide contraction (see **Fig 3.20 a**) [304].

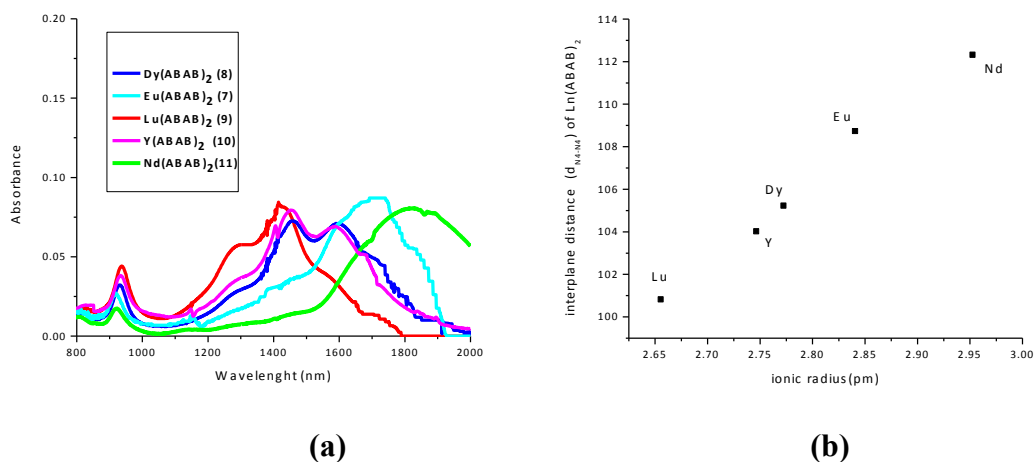


Figure 3.20(a) The UV-NIR spectrum of neutral Ln (Eu, Dy, Lu, Y, Nd)(ABAB)₂ in CHCl_3 ($1 \times 10^{-5} \text{ M}$) **(b)** Plot of the interplane distances vs lanthanide ionic radius

These observations show that the interaction between the two rings becomes stronger as the ring-to-ring separation decreases along with the lanthanide contraction (**Fig 3.20 b**). The short interplanar distance causes better electronic delocalization, which contributes to the hyperpolarizability (β_{1907}). These results clearly indicate that the second-order NLO responses are not only driven by metal-induced NLO-enhancement but also by geometrical parameters, i.e. the lanthanide contraction [224].

Moreover, the position of the intra molecular charge transfer (ICT) band is also important for acquired results. **Fig. 3.20.a** shows that for Ln (**Eu, Dy, Y, Nd**)(ABAB)₂ have absorption at the second harmonic wavelength(1907 nm).

Absorption at the second harmonic wavelength can be problematic for a number of reasons such as resonance enhancement and two-photon absorption induced fluorescence (TPF), which artificially increases the value of β [301,302]. Since many potential industrial applications of NLO materials would involve wavelengths other than 1907 nm, unless resonance enhancement and two-photon absorption induced fluorescence (TPF) are taken into account, β values reported at 1907 nm would exaggerate a potential molecule's usefulness at other wavelengths [303].

However, our results of the values of β show that the intervalence transition has little influence on the quadratic nonlinear response, as was reported previously by Shirk and *et. al.* for third-order nonlinear properties [304].

3.1.6. Analyzes of oxidized and reduced form of octupolar bis(phthalocyaninato) Ln(III) double-decker complexes (Ln(ABAB)₂ (Lu, Dy, Eu, Y, Nd))

In order to better understand the origin of very high β value of neutral form of (Ln(ABAB)₂ (Lu, Dy, Eu, Y, Nd)), the electronic energy levels, which is one of the main parameters for the NLO response of a molecule, were changed by oxidation and reduction. Then HRS measurements of these oxidized and reduced forms were accomplished and compared with previous results.

The oxidation of Ln(ABAB)₂ (Lu, Dy, Eu, Y, Nd) were carried out by adding bromine in CHCl₃ to a solution of Ln(ABAB)₂ (Lu, Dy, Eu, Y, Nd) (10⁻⁵ M). And the reduced form of Ln(ABAB)₂ (Lu, Dy, Eu, Y, Nd) were prepared by adding 3 mg of NaBH₄ to 10 mL of a solution of Ln(ABAB)₂ (Lu, Dy, Eu, Y, Nd) (10⁻⁵ M) in THF/CHCl₃ (1/10).

3.1.6.1. UV-NIR measurements of oxidized and reduced form of octupolar bis(phthalocyaninato) Ln(III) double-decker complexes (Ln(ABAB)₂ (Lu, Dy, Eu, Y, Nd))

Several redox states are known for the Pc₂Ln molecule, but the most important ones for practical purpose are the green neutral molecules Pc₂Ln, the oxidized cation Pc₂Ln⁺, which is orange, and the one-electron reduced anion Pc₂Ln⁻, which is blue (Fig. 3.21)[305,306]:



Figure 3.21 Neutral, oxidized, and reduced forms of Ln(Pc)₂

The spectral changes due to chemical oxidation in the UV-NIR spectrum of Lu(ABAB)₂ Bis(Phthalocyanine) (**9**) is illustrated in **Fig. 3.22** as example. Arrows in spectra indicate the decrease and increase of bands. The oxidation of Lu(ABAB)₂ (**9**) was carried out by adding bromine in CHCl₃ to a solution of Lu(ABAB)₂ (**9**) (10⁻⁵ M).

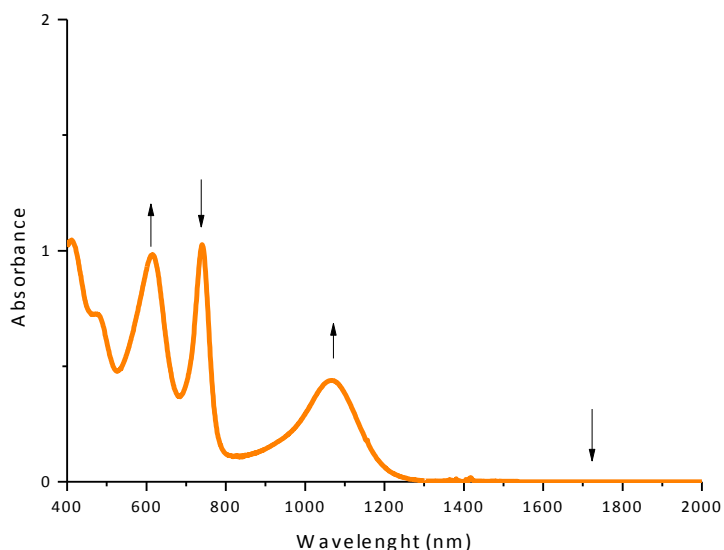


Figure 3.22 UV-NIR spectrum of Lu(ABAB)₂ Bis-phthalocyanine (1 x 10⁻⁵ M) in CHCl₃ + Br₂ (oxidized)

The strongest absorption Q band at 743 nm loses intensity and exhibits red shift. **Fig. 3.22** also shows that intensity of band at 588 nm and 970 nm, corresponding to radical $\pi\text{-}\pi^*$ transition, significantly increase. In addition, because one electron, which causes the intermolecular transition that was prominent in the neutral form complex **9**, is removed from complex, all bands corresponding to those transitions disappeared.

The electronic absorption spectra of oxidized form of (ABAB)₂Ln (Eu (**7**), Dy (**8**), Nd (**10**) and Y (**11**)) are similar to oxidized form of Lu(ABAB)₂(**9**) and the electronic spectral data summarised in **Table 3.3**

Table 3.3 UV-NIR spectra of oxidized forms of Ln(Eu, Dy, Lu, Nd, Y)(ABAB)₂ Bis-

phthalocyanine (1×10^{-5} M)

Compound	Form	λ_{max} (nm)				
		B	BV	Q	RV	ICT
Eu (7)	Oxidized	351	485	614,748	1073	x
Dy (8)	Oxidized	412	477	609,732	1016	x
Lu (9)	Oxidized	417	472	588,726	964	x
Nd(10)	Oxidized	310	496	664,760	x	x
Y (11)	Oxidized	328	466	736,790	1018	x

B: Soret band, BV and RV: radical transition bands, ICT: Intramolecular charge transfer band

The reduced form of Lu(ABAB)₂ Bis(Phthalocyanine) was prepared by adding 3 mg of NaBH₄ to 10 mL of a solution of **9** (10^{-5} M) in THF/CHCl₃ (1/10). The UV-NIR spectrum of reduced form of **9** is given as example in **Fig. 3.23**.

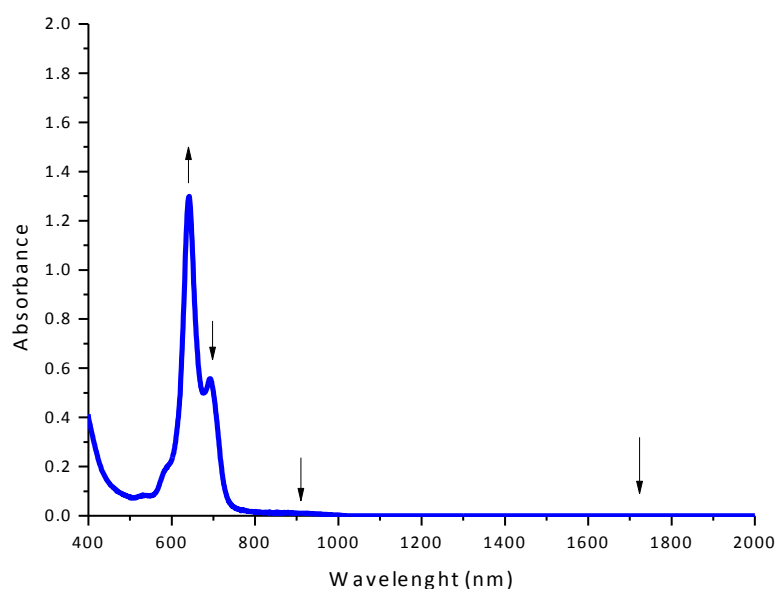


Figure 3.23 UV-NIR spectra of reduced form of Lu(ABAB)₂ Bis-phthalocyanine (1×10^{-5} M) in (1/10 -THF/CHCl₃ + 3 mg NaBH₄)

The anionic complex (Pc₂Lu⁻) displays a splitted Q band absorbing at 631 nm and 711 nm. The intervalence transition is absent due to addition of second

electron by reduction. Moreover the bands at 933 nm and 550 nm, which are linked to the radical part of the complex, also disappeared by reduction of complex **9**.

The electronic absorption spectra of reduced form of (ABAB)₂Ln (Eu (**7**), Dy (**8**), Nd (**10**) and Y (**11**)) are similar to reduced form of Lu(ABAB)₂(**9**) and the electronic spectral data summarised in **Table 3.4**.

Table 3.4 UV-NIR spectra of reduced forms of Ln(Eu, Dy, Lu, Nd, Y)(ABAB)₂ Bis-phthalocyanine (1 x 10⁻⁵ M)

Compound	Form	λ_{\max} (nm)				
		B	BV	Q	RV	ICT
Eu (7)	Reduced	346	580	638,695	x	x
Dy (8)	Reduced	330	584	640,706	x	x
Lu (9)	Reduced	340	572	632,721	x	x
Nd(10)	Reduced	340	589	649,715	x	x
Y (11)	Reduced	328	570	600,692	x	x

B: Soret band, BV and RV: radical transition bands, ICT: Intramolecular charge transfer band

3.1.6.2. Hyper-Rayleigh Scattering (HRS) measurements of oxidized and reduced form of octupolar bis(phthalocyaninato) Ln(III) double-decker complexes (Ln(ABAB)₂ (Lu, Dy, Eu, Y, Nd))

The first hyperpolarizability β obtained for the Ln(ABAB)₂(**7-11**) in oxidized forms are summarized in the **Table 3.5**. The oxidation of Ln(ABAB)₂ was carried out by adding bromine in CHCl₃ to a solution of Ln(ABAB)₂ (10⁻⁵ M).

Table 3.5 The second-order NLO data for the octupole Ln(ABAB)₂ (7-11)

Compounds	Form	Absorbance		P _{ETV}	P _S	Corr.P _S	Avg. Corr. $\beta \times 10^{-30}$ esu	
		λ_{1907}	λ_{955}					
ABAB (7-11)	Eu (7)	Ox.	0	0.087	0.0714	0.140	0.1553	4548
	Dy (8)	Ox.	0	0.18	0.0834	0.155	0.1906	4691
	Lu (9)	Ox.	0	0.32	0.0672	0.136	0.1965	4722
	Nd(10)	Ox.	0	0.097	0.0534	0.040	0.0444	2787
	Y (11)	Ox.	0	0.098	0.0441	0.032	0.0362	2801

P_{ETV}: Slope of ETV, P_S: Slope of Sample, Corr. P_S: Corrected slope for sample

The first hyperpolarizability of the oxidized form of Ln(ABAB)₂ seems more complicated to explain than the one of neutral and reduced forms. The first hyperpolarizability of the oxidized form of Ln(ABAB)₂ are still large with a value of 4722x10⁻³⁰ esu for Lu(ABAB)₂ (9), 4691x10⁻³⁰ esu for Dy(ABAB)₂ (8), 4548x10⁻³⁰ esu for Eu(ABAB)₂ (7), 2787x10⁻³⁰ esu for Nd(ABAB)₂ (10), and 2801x10⁻³⁰ esu for Y(ABAB)₂ (11) (see Fig. 3.24). The first hyperpolarizability of the oxidized form decreased for all Ln(ABAB)₂ (7-11) compare to the neutral form, regardless of the metal center involve in the complex. In comparison, the first hyperpolarisability of the oxidized form are lower than those of neutral form but higher than that of the reduced form values.

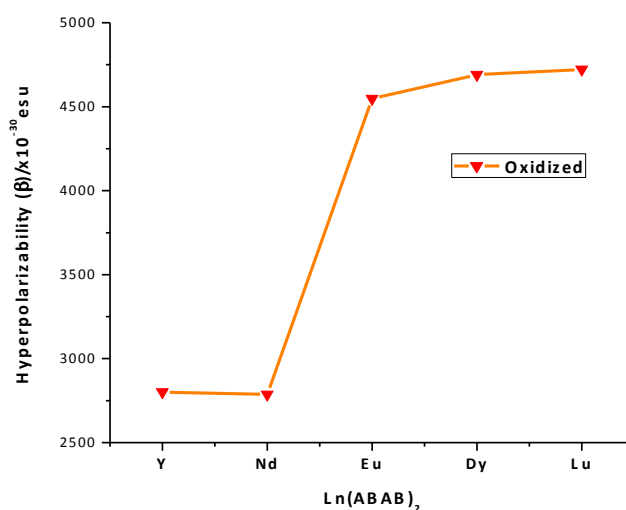


Figure 3.24. Plot of the hyperpolarisability coefficient β vs oxidized form of Ln(ABAB)₂

In the oxidized form, the contribution of the intermolecular charge transfer to the hyperpolarizability vanishes causing lower NLO activity than in the neutral form. While this band disappear, the intensity of the band at 588 and 970 nm, which correspond to the radical $\pi-\pi^*$ transition, significantly increase with cost of optical transparency (see **Fig 3.25**).

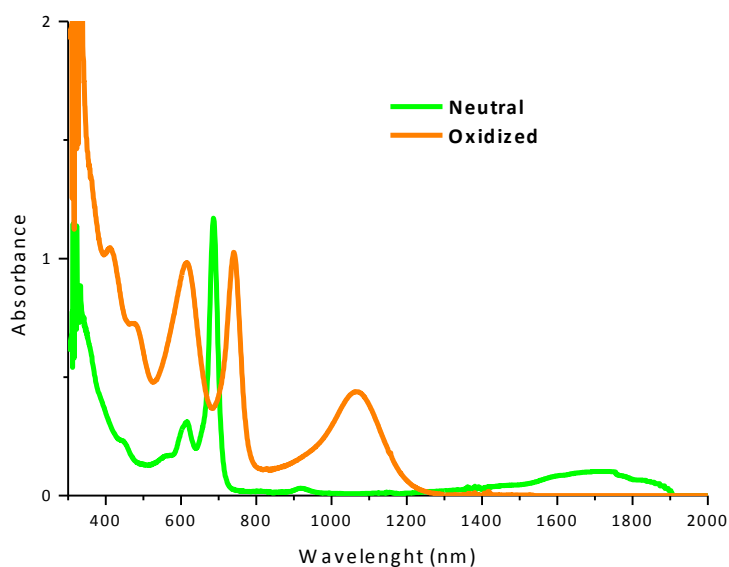


Figure 3.25. UV-NIR spectra of Eu(ABAB)₂ Bis(Phthalocyanine) (7) (1×10^{-5} M)

The intervalence band at 970 nm, partially absorb the scattered light at the second harmonic (953 nm), it might be the reason of the higher NLO activity than the reduced forms, since this new band has substantial ϵ value ($32000 \text{ M}^{-1} \text{ cm}^{-1}$), compare to reduced (0) forms, that might cause disruptive process resonance effects [307].

However, the first hyperpolarizability of the neutral form of octupolar Lu(ABAB)₂ is still higher than the oxidized one, although contribution of disruptive process resonance effects. These results seem to indicate that the resonance effect has small effect on the quadratic nonlinear response compare to ICT band contribution. It must be noted that a resonance-enhanced value does not represent the intrinsic value for a molecule.

The NLO activity of the oxidized form of Ln(ABAB)₂ regularly increases from yttrium to lutetium with the only contribution of the “metal-induced NLO-enhancement”. The oxidized form of Ln(ABAB)₂ has disadvantages, particularly in terms of transparency/nonlinearity tradeoff, because improved neither NLO activity nor optical transparency compare to neutral form of Ln(ABAB)₂.

The first hyperpolarizability β obtained for the Ln(ABAB)₂(7-11) in reduced forms are summarized in the **Table 3.6**. The reduced form of Ln(ABAB)₂ Bis(Phthalocyanine) was prepared by adding 3 mg of NaBH₄ to 10 mL of a solution of complexes (10⁻⁵ M) in THF/CHCl₃ (1/10).

Table 3.6 The second-order NLO data for the octupole Ln(ABAB)₂ (7-11)

Compounds	Form	Absorbance		P _{ETV}	P _S	Corr.P _S	Avg. Corr. $\beta \times 10^{-30}$ esu	
		λ_{1907}	λ_{955}					
ABAB (7-11)	Eu (7)	Red.	0.02	0.01	0.0626	0.125	0.1324	3693
	Dy (8)	Red.	0.02	0.01	0.057	0.147	0.1557	4208
	Lu (9)	Red.	0.02	0.01	0.052	0.160	0.1694	4587
	Nd(10)	Red.	0.01	0.027	0.0447	0.026	0.0278	2426
	Y (11)	Red.	0	0.012	0.543	0.034	0.0350	2454

P_{ETV}: Slope of ETV, P_S: Slope of Sample, Corr. P_S: Corrected slope for sample

In the case of the reduced form of Ln(ABAB)₂, because intermolecular transition is absent, the first hyperpolarizability are still large with a value of 4587x10⁻³⁰ esu for Lu(ABAB)₂ (9), 4208x10⁻³⁰ esu for Dy(ABAB)₂ (8), 3693x10⁻³⁰ esu for Eu(ABAB)₂ (7), 2426x10⁻³⁰ esu for Nd(ABAB)₂ (10), 2454x10⁻³⁰ esu for Y(ABAB)₂ (11) but quite lower than the values of neutral and oxidized form. The hyperpolarizability in function of the type of lanthanide ion is illustrated in **Fig. 3.26**. These results also prove the contribution of the metal-induced NLO-enhancement and the lanthanide contraction to the NLO activity.

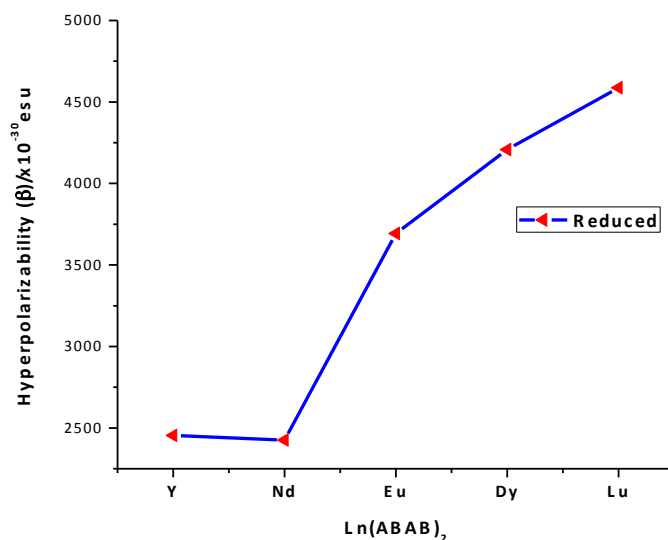


Figure 3.26. Plot of the hyperpolarisability coefficient β vs reduced form of $\text{Ln}(\text{ABAB})_2$

In the case of the reduced form of $\text{Ln}(\text{ABAB})_2$, the addition second electron to the complexes, consequently the intermolecular transition and its corresponding bands that was prominent in the neutral form disappeared (see **Fig. 3.27**). The decrease of the hyperpolarizability values is directly related to the vanishing of this band.

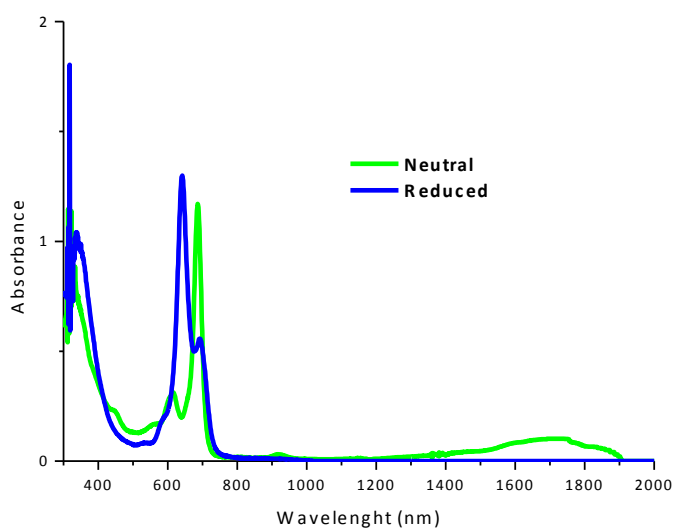


Figure 3.27. UV-NIR spectra of $\text{Eu}(\text{ABAB})_2\text{bis}(\text{Phthalocyanine})$ (**7**) ($1 \times 10^{-5} \text{ M}$)

Although, the reduced form of $\text{Ln}(\text{ABAB})_2$ has lower NLO activity than neutral and oxidized forms, it clearly shows a much better transparency (see **Fig. 3.27**). This transparency of reduced form of $\text{Ln}(\text{ABAB})_2$ provides a unique solution to suppress potential problems associated with the electronic transition at the second harmonic wavelength including the linear absorption of the generated 2ω light and the resonance enhancement that elevates the measured β value which artificially inflates the β value. Simply, the reduced $\text{Ln}(\text{ABAB})_2$ allows us to defeat all potential disruptive processes. One can suggest that, even though β values of the reduced form is lower than that of neutral and oxidized forms, the resulting β values are much more reliable.

3.2. Analyzes of nonoctupolarbis(phthalocyaninato) Ln(III) double-decker complexes $\text{Ln}(\text{AB3})_2$ (12-15), $\text{Ln}(\text{A4})_2$ (16-18), $\text{Ln}(\text{B4})_2$ (19-23), $\text{Ln}(\text{T4})_2$ (24-26)

In order to understand the contribution of octupolar cube structures to the first hyperpolarizability, the nonoctupolar series of lanthanidebis(phthalocyanines) complexes ($\text{Ln}(\text{AB3})_2$ (12-14), $\text{Ln}(\text{A4})_2$ (16-18), $\text{Ln}(\text{B4})_2$ (19-21), $\text{Ln}(\text{T4})_2$ (24-26)) were synthesized and the NLO activity measured.

3.2.1. Synthesis of nonoctupolarbis(phthalocyaninato) Ln(III) double-decker complexes $\text{Ln}(\text{AB3})_2$ (12-15), $\text{Ln}(\text{A4})_2$ (16-18), $\text{Ln}(\text{B4})_2$ (19-23), $\text{Ln}(\text{T4})_2$ (24-26)

The unsubstituted (A_4) and substituted (B_4 , T_4) homoleptic bis(phthalocyaninato)lanthanide (III) complexes can be prepared by cyclic

tetramerization of the corresponding phthalodinitrile with $\text{Ln}(\text{Ac})_3 \cdot n\text{H}_2\text{O}$ either in the solid state or in solution, in the presence of a promoter [308].

In solid state approach, $\text{Ln}(\text{Pc})_2$ are produced by heating (170-190 °C) the powder of unsubstituted or substituted phthalodinitrile with appropriate lanthanide salts (Fig. 3.28). This method is quite simple, however has some important disadvantages. It certainly produces several by products mono-decker, triple-decker derivatives and metal free compounds. Consequently, the yield of corresponding to double decker lanthanide Pc complexes and their purity are low [309].

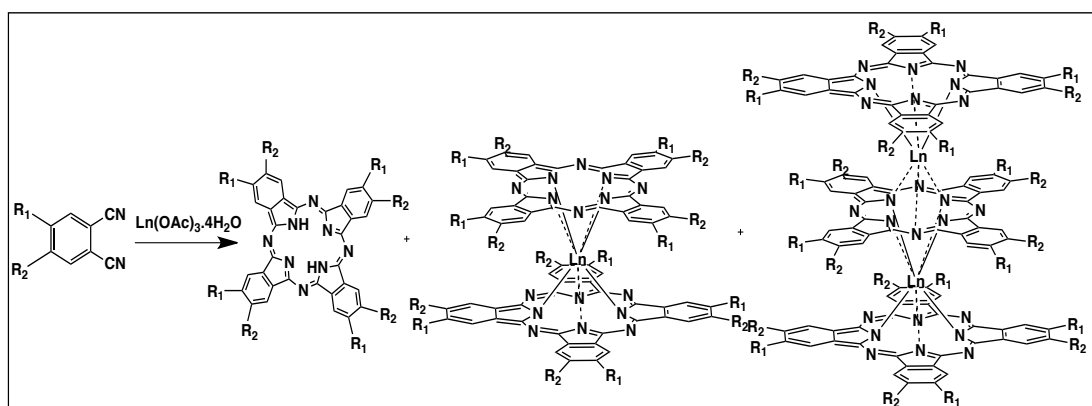


Figure 3.28. Tetramerization solid-state approach for homoleptic bis(Pcs)

In the solution approach, the same reactants as in the mentioned procedure are heated in hexanol in the presence of a promoter DBU (1,8-diazabicyclo (5,5,0)undec-7-ene), a strong organic base which favors the formation of the macrocycle (Fig. 3.29) [310,311]. The yield of $\text{Ln}(\text{Pc})_2$ complexes formed seems to be somehow better than in the former solid-state method.

Therefore, this method was preferred for synthesized aforementioned unsubstituted (A_4) and substituted (B_4 , T_4) symmetric bis(phthalocyaninato)lanthanide (III) complexes. The method also gives small amounts of metal free phthalocyanines as side products that were separated readily from the sandwich complexes by column chromatography.

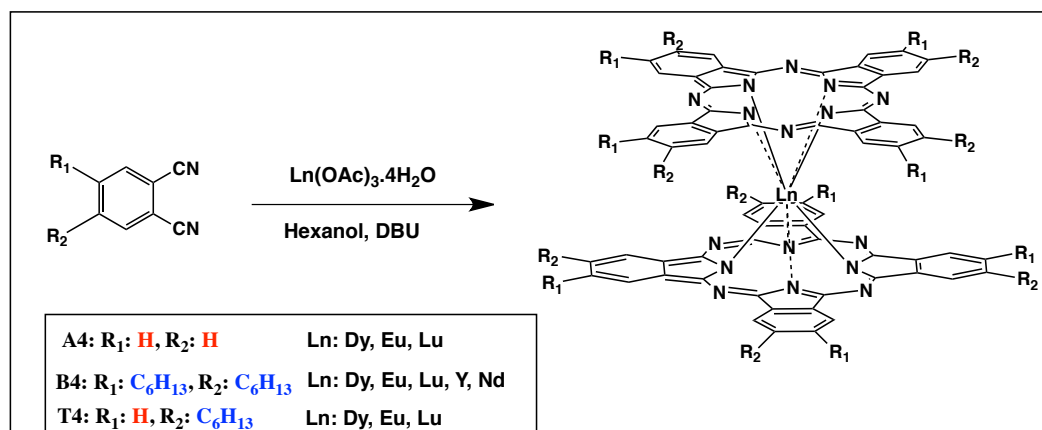


Figure 3.29. The method in solution approach cyclic tetramerization for homoleptic bis-Pcs

The nonoctupolarLn(AB₃)₂ was obtained from AB₃ phthalocyanine with the same method described for octupole Ln(ABAB)₂ (**Fig. 3.30**). Detailed synthetic procedures are given in the Experimental Part.

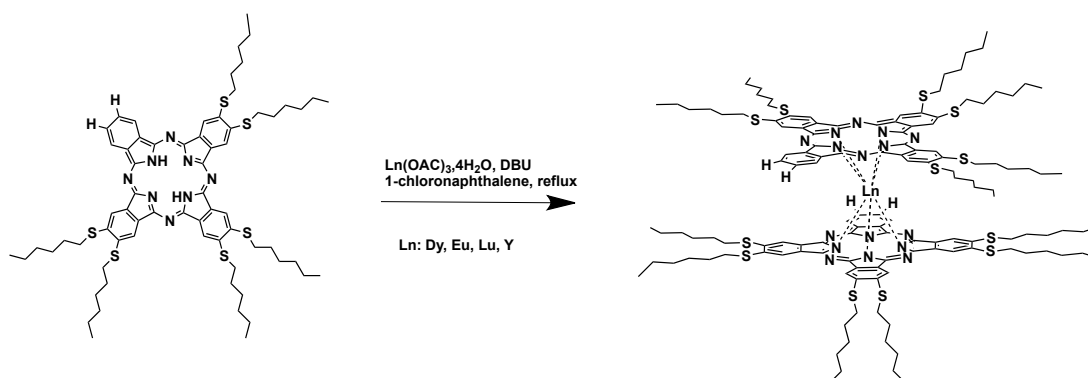


Figure 3.30. The synthesis approach for Ln(AB₃)₂

The non substituted (A₄) and substituted (AB₃, B₄, T₄) homoleptic bis(phthalocyaninato)lanthanide (III) complexes were characterized by ¹HNMR, ¹³C NMR, IR, mass spectrometry, UV-NIR and second-order NLO properties were investigated by using the HRS techniques.

3.2.2. UV-NIR measurements of nonoctupolarbis(phthalocyaninato) Ln(III) double-decker complexes Ln(AB₃)₂ (12-15), Ln(A₄)₂ (16-18), Ln(B₄)₂ (19-23), Ln(T₄)₂ (24-26)

The UV-NIR measurements of non substituted (A₄) and substituted (AB₃, B₄, T₄) homoleptic bis(phthalocyaninato)lanthanide (III) complexes were carried out in chloroform (1x10⁻⁵M).

Fig. 3.31 shows the absorption spectra of AB₃-H₂Pc (6) in solution in chloroform. AB₃-H₂Pc presents the classical spectrum of low symmetry free phthalocyanines with a B-band at 341 (6) and intense Q-band split in two with maxima at 690-723 nm (6). A small bathochromic (red) shift is observed for the most intense absorption peaks Q_x and Q_y of AB₃-H₂Pc (6) compare to ABAB-H₂Pc (5) due to the substitution of the Pc ring by more electron donating thio(hexyl) groups.

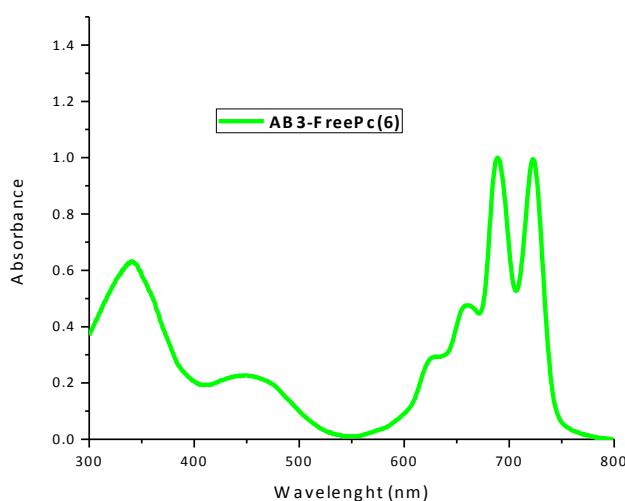


Figure 3.31. UV-Vis Spectra of AB₃ (6) type free phthalocyanine

The characteristics of electronic absorption spectra of Ln(Pc)₂ and effect of nature of the central metal ion were explained for Ln(ABAB)₂ in previous chapter.

The electronic absorption spectra of unsubstituted (A₄) and substituted (AB₃, B₄, T₄) homoleptic bis(phthalocyaninato)lanthanide (III) complexes are similar to

$\text{Ln}(\text{ABAB})_2$. All complexes show three (BV, RV, ICT) absorptions bands which all characteristic Pc^{*-} bands related for bis(phthalocyanine) lanthanide (III) complex. Since, the characteristic $\text{Ln}(\text{Pc})_2$ related bands and effect of nature of the central metal ion were already explained, it wont be repeated for unsubstituted (**A₄**) and substituted (**AB₃**, **B₄**, **T₄**) homoleptic bis(phthalocyaninato)lanthanide (III) complex in this chapter.

The addition of electro-donor substituents to the phthalocyanine core cause a shift of the Q-band and ICT band [317]. All compounds were investigated by UV-NIR in order to investigate how the different numbers of substituted groups and the influence of metal ions to the spectroscopic properties. The UV-NIR spectrum of $\text{Lu}(\text{Pc}(\text{SC}_6)_{n:0-8})_2$ are given as example in **Figure 3.32**

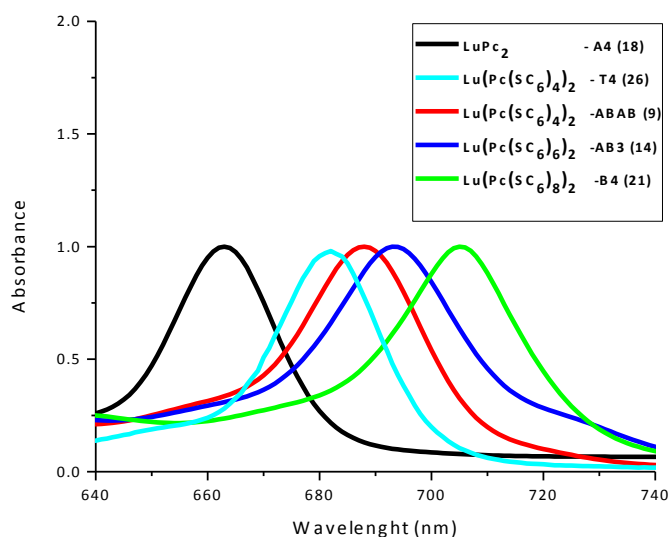


Figure 3.32. The UV-NIR spectra of neutral $\text{Lu}(\text{Pc}(\text{SC}_6)_{n:0-8})_2$ in CHCl_3 (1×10^{-5} M)

The position of the most intense absorption maximum (Q-band) for the bis(thiohexyl substituted phthalocyaninato)Lu(III) complexes depends directly on the electron-donating properties of substituted groups [312]. Due to the better electron-donating property of the alkylthio substituted bis(phthalocyanines) (**9,14,21,27**) all the bands in the electronic absorption spectra of these complexes were found to shift to longer wavelength in comparison substituted $\text{Lu}(\text{Pc})_2$ (**18**). Between our compounds, we observed that the positions of Q_{x,y} bands in the UV-NIR spectra

significantly depend on the number of electron-donating groups for the $\text{Lu}(\text{Pc})_2$. The Q-band was found to shift to the red in the order $\text{Lu}(\text{B}_4)_2$ -705 nm > $\text{Lu}(\text{AB}_3)_2$ -693 nm > $\text{Lu}(\text{ABAB})_2$ -688 nm > $\text{Lu}(\text{T}_4)_2$ -681 nm > $\text{Lu}(\text{A}_4)_2$ -662 nm. The total shift between the sixteen thiohexyl substituted $\text{Lu}(\text{B}_4)_2$ and the unsubstituted $\text{Lu}(\text{A}_4)_2$ phthalocyanines is about 45 nm.

$\text{Lu}(\text{ABAB})_2$ and $\text{Lu}(\text{T}_4)_2$ have the same number of hexyl thio substituted groups on the Pcs core. However the peripherally tetra substituted $\text{Lu}(\text{T}_4)_2$ show slightly different electronic absorption spectra, probably due to the mixture of isomers, compared with the $\text{Lu}(\text{ABAB})_2$. The total shift between the $\text{Lu}(\text{ABAB})_2$ and the $\text{Lu}(\text{T}_4)_2$ phthalocyanines is about 9 nm.

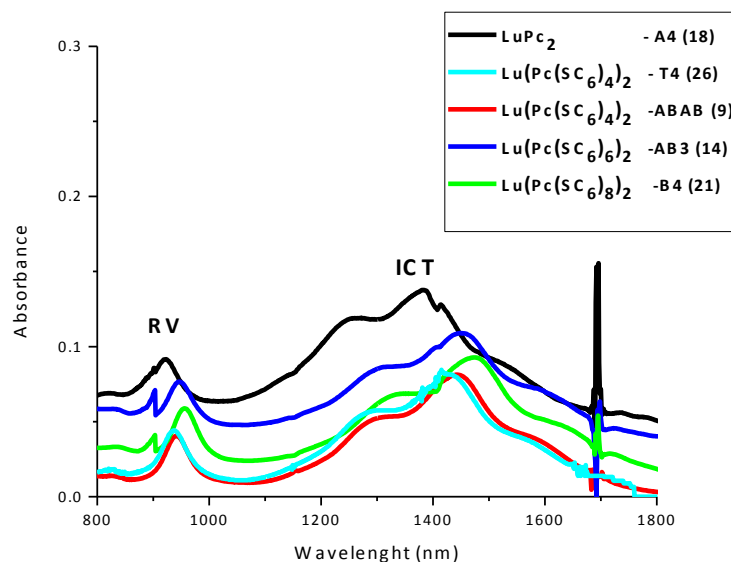


Figure 3.33. The UV-NIR spectrum of neutral $\text{Lu}(\text{Pc}(\text{SC}_6)_{n:0-8})_2$ in CHCl_3 (1×10^{-5} M)

The addition of electron-donating alkylthio substituents to the phthalocyanine core doesn't cause a significant shift of the RV and ICT band (**Fig. 3.33**). The absorption of all $\text{Lu}(\text{III})$ bis(phthalocyanines), regardless of the number of alkylthio substituted, red-shifted about 40 nm compare with unsubstituted $\text{Lu}(\text{A}_4)_2$ phthalocyanines.

The electronic absorption spectra of neutral form of Lu(Pc)₂ are similar to neutral form of nonoctupolar complexes: Ln(AB3)₂ (12-15), Ln(A4)₂ (16-18), Ln(B4)₂ (19-23), Ln(T4)₂ (24-26) and the electronic spectral data summarised in Table 3.7.

Table 3.7 UV-NIR spectral data of neutral forms of Ln(AB3)₂ (12-14), Ln(A4)₂ (16-18), Ln(B4)₂ (19-21), Ln(T4)₂ (24-26) Bis(phthalocyanine) (1 x 10⁻⁵ M)

B: Soret band, BV and RV: radical transition bands, ICT: Intramolecular charge transfer band

		λ_{max} (nm)					
Compound	Form	B	BV	Q	RV	ICT	
AB3 (12-15)	Eu(12)	Neutral	322	566	616,699	942	1373-2000
	Dy(13)	Neutral	321	548	620,696	924	1250-1890
	Lu(14)	Neutral	329	533	616,693	950	1174-1690
	Y(15)	Neutral	328	556	628,694	941	1230-1841
A4 (16-18)	Eu(16)	Neutral	310	477	635,670	910	1407-1883
	Dy(17)	Neutral	318	575	632,64	911	1250-1800
	Lu(18)	Neutral	316	570	626,658	914	1150-1650
B4 (19-23)	Eu(19)	Neutral	329	561	632,710	947	1401-2000
	Dy(20)	Neutral	315	560	640,711	944	1320-1879
	Lu(21)	Neutral	323	544	632,710	931	1235-1710
	Nd(22)	Neutral	322	580	628,718	953	1550-2000
	Y(23)	Neutral	322	562	640,706	953	1325-1847
T4 (24-26)	Eu(24)	Neutral	334	505	632,688	925	1368-2000
	Dy(25)	Neutral	315	483	615,686	939	1264-1859
	Lu(26)	Neutral	315	483	635,686	1006	1158-1711

The spectral changes due to chemical oxidation in the UV-NIR spectrum of Lu(Pc)₂ Bis(Phthalocyanine) (14, 26, 21) is illustrated in Figure 3.34 as example. The oxidation of Lu(Pc)₂(14, 26, 21) were carried out by adding bromine in CHCl₃ to a solution of Lu(Pc)₂ (14, 26, 21) (10⁻⁵ M).

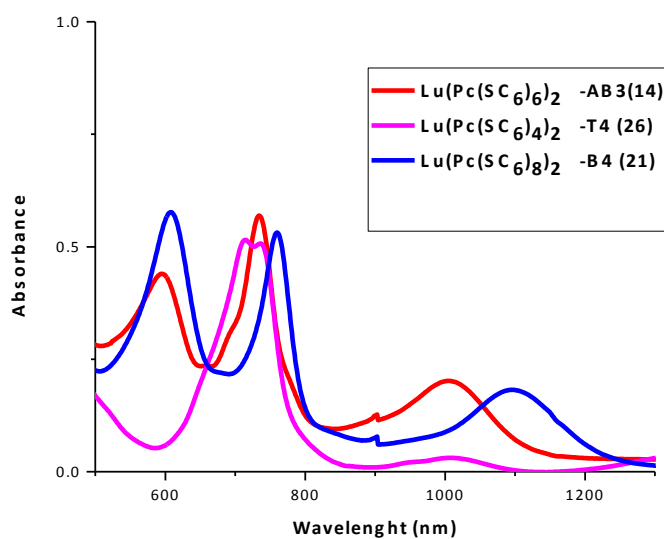


Figure 3.34. UV-NIR spectra of Lu(Pc)₂ Bis(phthalocyanine) (1×10^{-5} M) in CHCl₃ + Br₂ (oxidized)

The strongest absorption Q bands lose intensity and exhibits red shift. Moreover, the intensity of bands (BV and RV) which corresponding to radical π - π^* transition, significantly increase. In addition, because one electron, which causes the intermolecular transition that was prominent in the neutral form complexes, is removed from complex, all bands corresponding to those transitions disappeared.

The position of the Q and RV bands for the Lu(Pc)₂ (**14**, **26**, **21**) complexes depends directly on electron-donating property of substituted groups. Due to the better electron-donating properties of the Lu(B4)₂ (**21**), the Q and RV bands in the electronic absorption spectra were found to shift to longer wavelength in comparison with those of Lu(Pc)₂ (**14**, **26**). **Fig. 3.34** shows that the position of BV bands of complexes is not depend on electron-donating property of substituted groups. However, the intensity of BV bands seems increase with electron donating groups. The intensity of BV band of Lu(B4)₂ (**21**) is much higher than Lu(Pc)₂ (**14**, **26**)

The electronic absorption spectra of oxidized form of Lu(Pc)₂ are similar to oxidized form of nonoctupolar Ln(AB₃)₂ (**12-15**), Ln(A₄)₂ (**16-18**), Ln(B₄)₂ (**19-23**), Ln(T₄)₂ (**24-26**) and the electronic spectral data summarized in **Table 3.8**.

Table 3.8 UV-NIR spectrums of oxidized forms of Ln(AB₃)₂ (12-14), Ln(A₄)₂ (16-18), Ln(B₄)₂ (19-21), Ln(T₄)₂ (24-26) Bis-phthalocyanine (1 x 10⁻⁵ M)

			λ_{max} (nm)				
Compound		Form	B	BV	Q	RV	ICT
AB ₃ (12-15)	Eu(12)	Oxidized	318	x	616,754	1113	x
	Dy(13)	Oxidized	321	x	600,747	1067	x
	Lu(14)	Oxidized	324	594	732	1003	x
	Y(15)	Oxidized	310	405	728	1050	x
A ₄ (16-18)	Eu(16)	Oxidized	310	488	706	955	x
	Dy(17)	Oxidized	318	489	627,704	914	x
	Lu(18)	Oxidized	316	483	696	890	x
B ₄ (19-23)	Eu(19)	Oxidized	329	x	621,765	1157	x
	Dy(20)	Oxidized	315	x	604,757	1092	x
	Lu(21)	Oxidized	323	x	610,760	1091	x
	Nd(22)	Oxidized	322	526	694,820	958	x
	Y(23)	Oxidized	322	x	766	x	x
T ₄ (24-26)	Eu(24)	Oxidized	318	522	721,748	x	x
	Dy(25)	Oxidized	315	518	706,752	x	1230-1730
	Lu(26)	Oxidized	315	477	716	890	1219-1711

B: Soret band, BV and RV: radical transition bands, ICT: Intramolecular charge transfer band

The reduced form of Lu(Pc)₂ bis(Phthalocyanine)(14, 26, 21) were prepared by adding 3 mg of NaBH₄ to 10 mL of a solution of Lu(Pc)₂(14, 26, 21) (10⁻⁵ M) in THF/CHCl₃ (1/10). The UV-NIR spectra of reduced form of Lu(Pc)₂(14, 26, 21) are given as example in Fig. 3.35.

The anionic complex (Pc₂Lu⁻) displays a splitted Q band absorbing at 641 nm and 751 nm. The intervalence transition is absent due to addition of second electron by reduction. Moreover the bands at 933 nm and 550 nm, which are linked to the radical part of the complex, also disappeared by reduction of complex Lu(Pc)₂(14, 26, 21). Moreover, contrast to neutral and oxidized form, the number of electro donating groups don't cause significant red-shift (Fig. 3.35).

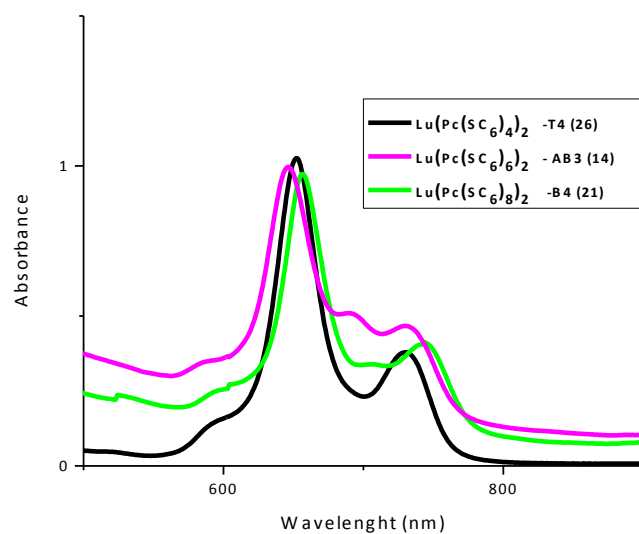


Figure 3.35. UV-NIR spectra of reduced Lu(Pc)₂bis(phthalocyanine) (1×10^{-5} M) in CHCl₃

The electronic absorption spectra of reduced form of Lu(Pc)₂(**14**, **26**, **21**) are similar to reduced form of nonoctupolar Ln(AB₃)₂ (**12-15**), Ln(A₄)₂ (**16-18**), Ln(B₄)₂ (**19-23**), Ln(T₄)₂ (**24-26**) and the electronic spectral data summarized in **Table 3.9**

Table 3.9. UV-NIR spectrums of reduced forms of Ln(AB3)₂ (12-14), Ln(A4)₂ (16-18), Ln(B4)₂ (19-21), Ln(T4)₂ (24-26) Bis-phthalocyanine (1 x 10⁻⁵ M)

		λ_{max} (nm)					
Compound		Form	B	BV	Q	RV	ICT
AB3 (12-15)	Eu(12)	Reduced	373	594	650,710	x	x
	Dy(13)	Reduced	321	574	645,721	x	x
	Lu(14)	Reduced	366	643	693,726	x	x
	Y(15)	Reduced	322	x	658,700	x	x
A4 (16-18)	Eu(16)	Reduced	310	554	609,701	x	x
	Dy(17)	Reduced	310	x	661,668	x	x
	Lu(18)	Reduced	316	x	605,700	x	x
B4 (19-23)	Eu(19)	Reduced	312	599	666,721	x	x
	Dy(20)	Reduced	320	600	665,721	x	x
	Lu(21)	Reduced	312	599	649,737	x	x
	Nd(22)	Reduced	312	602	676,735	x	x
	Y(23)	Reduced	322	610	670,748	x	x
T4 (24-26)	Eu(24)	Reduced	318	472	605,660	710	1310-2000
	Dy(25)	Reduced	366	584	660,721	935	1250-1950
	Lu(26)	Reduced	366	x	650,732	x	x

B: Soret band, BV and RV: radical transition bands, ICT: Intramolecular charge transfer band

3.2.3. Hyper-Rayleigh Scattering (HRS) measurements of nonoctupolar bis(phthalocyaninato) Ln(III) double-decker complexes (Ln(AB3)₂ (12-15), Ln(A4)₂ (16-18), Ln(B4)₂ (19-23), Ln(T4)₂ (24-26))

The first hyperpolarizability β obtained for the Ln(AB3)₂ (12-14), Ln(A4)₂ (16-18), Ln(B4)₂ (19-21), Ln(T4)₂ (24-26) in neutral forms are summarized in the Table 3.10.

Table 3.10 The second-order NLO data for the nonoctupole Ln(AB₃)₂ (12-14), Ln(A₄)₂ (16-18), Ln(B₄)₂ (19-21), Ln(T₄)₂ (24-26)

Compounds		Form	Absorbance		P _{ETV}	P _S	Corr.P _S	Av. Corr. $\beta \times 10^{-30}$ esu
			λ_{1907}	λ_{955}				
AB3 (12-15)	Eu(12)	N.	0.078	0.071	0.087	0.092	0.1196	3622
	Dy(13)	N.	0.021	0.062	0.067	0.097	0.1099	3949
	Lu(14)	N.	0	0.047	0.12	0.252	0.266	4591
A4 (16-18)	Eu(16)	N.	0.037	0.027	0.0968	0.13	0.1462	3790
	Dy(17)	N.	0.012	0.067	0.0648	0.103	0.1048	3923
	Lu(18)	N.	0	0.05	0.108	0.18	0.1906	4116
B4 (19-23)	Eu(19)	N.	0.105	0.052	0.081	0.13	0.1462	3790
	Dy(20)	N.	0.026	0.06	0.076	0.114	0.1298	4037
	Lu(21)	N.	0	0.1	0.095	0.195	0.2187	4680
T4 (24-26)	Eu(24)	N.	0.058	0.019	0.0208	0.028	0.0332	3700
	Dy(25)	N.	0.011	0.035	0.023	0.036	0.0393	3915
	Lu(26)	N.	0	0.061	0.028	0.049	0.0525	4011

P_{ETV}: Slope of ETV, P_S: Slope of Sample, Corr. P_S: Corrected slope for sample

The conclusions, which we came out with these NLO measurements, are that metal-induced NLO-enhancement and lanthanide contraction, also applies for the series of nonoctupolar complexes Ln(AB₃)₂ (12-14), Ln(A₄)₂ (16-18), Ln(B₄)₂ (19-21), Ln(T₄)₂ (24-26) as described previous chapter.

Thereafter only the first hyperpolarizability of nonoctupolar Lutetium complexes Ln(Pc)₂ will be compared. The first hyperpolarizability values 4630×10^{-30} esu for Lu(B₄)₂ (21), 4592×10^{-30} esu for Lu(AB₃)₂ (14), 4116×10^{-30} esu for Lu(A₄)₂ (18), 4011×10^{-30} esu for Lu(T₄)₂ (26) were obtained.

If the first hyperpolarizability versus Lu(Pc)₂ is plotted (See Fig. 3.36), it undoubtedly shows that the octupolar Lu(ABAB)₂ has higher first hyperpolarizability than the corresponding nonoctupolar Lu(Pc)₂ complexes.

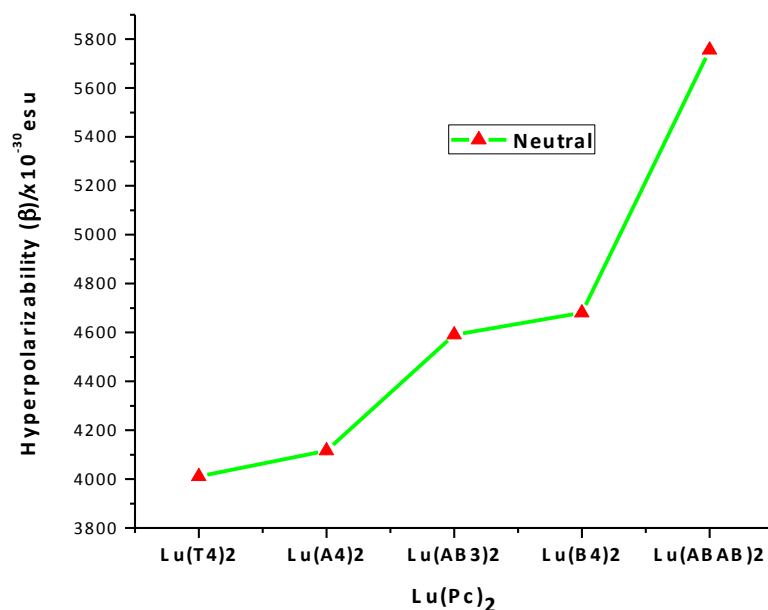


Figure 3.36. Plot of the hyperpolarisability coefficient β vs Lu(Pc)₂

The effect of the contribution of the octupolar structure on the first hyperpolarizability can be highlighted comparing the NLO activity between the octupole Lu(ABAB)₂ (**9**) and the nonoctupole Lu(T₄)₂ (**26**). In both cases, the metal center and the number of thiohexyl substituents are identical, allowing us to eliminate the metal-induced NLO-enhancement, the lanthanide contraction effect and the influence of the number of substituents. Lu(ABAB)₂ and Lu(T₄)₂ have 5756 × 10⁻³⁰ esu and 4011 × 10⁻³⁰ esu β hyperpolarizability values respectively. Only the octupolar structure contribution can explain this huge difference of NLO activity.

If the first hyperpolarizability of the nonoctupole Lutetium complexes Lu(B₄)₂ (**21**), Lu(AB₃)₂ (**14**), Lu(A₄)₂ (**18**), Lu(T₄)₂ (**26**) are confronted, the influence of the number of electron-donating groups on the NLO activity can be observed. The order of β is as follows: Lu(T₄)₂ < Lu(A₄)₂ < Lu(AB₃)₂ < Lu(B₄)₂. Like these complexes have the same metal center but not the same number of thiohexyl substituents, we can deduce that the number of electron-donating groups is the reason of the differences of NLO activity between nonoctupolar compounds.

Considering the UV spectrum of the nonoctupolar Lutetium complexes (see **Fig. 3.37**), the most intense absorption maximum (Q-band) shifts to longer wavelength due to the number of electron-donating groups. This phenomenon is characteristic of the substituted alkylthio substituent.

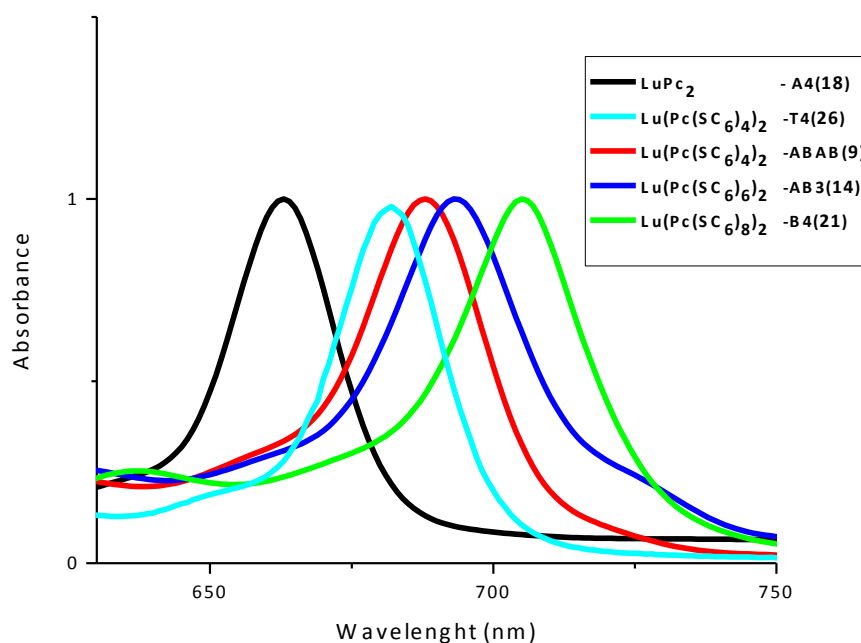


Figure 3.37. The UV-NIR spectrum of neutral $\text{Lu}(\text{Pc}(\text{SC}_6)_{n:0-8})_2$ in CHCl_3 (1×10^{-5} M)

The largest red-shift is the consequence of a smaller HOMO-LUMO gap (the difference between the energies of the HOMO and LUMO). This smaller HOMO-LUMO gap allows a better polarizability, which increases the NLO activity but reduces the optical transparency.

3.2.3.1. Hyperpolarizability of oxidized form nonOctupolar $\text{Ln}(\text{Pc})_2$ ($\text{Ln}(\text{AB3})_2$ (12-14), $\text{Ln}(\text{A4})_2$ (16-18), $\text{Ln}(\text{B4})_2$ (19-21), $\text{Ln}(\text{T4})_2$ (24-26))

The first hyperpolarizability β obtained for the $\text{Ln}(\text{AB3})_2$ (12-14), $\text{Ln}(\text{A4})_2$ (16-18), $\text{Ln}(\text{B4})_2$ (19-21), $\text{Ln}(\text{T4})_2$ (24-26) in oxidized forms are summarized in the **Table 3.11**. The oxidation of $\text{Ln}(\text{Pc})_2$ was carried out by adding bromine in CHCl_3 to a solution of $\text{Ln}(\text{Pc})_2$ (10^{-5} M).

Thereafter only the first hyperpolarizability of nonoctupolar lutetium complexes $\text{Lu}(\text{Pc})_2(\text{Lu}(\text{B4})_2)$ (**21**), $\text{Lu}(\text{AB3})_2$ (**14**), $\text{Lu}(\text{A4})_2$ (**18**), $\text{Lu}(\text{T4})_2$ (**26**) will be compared as example.

Table 3.11 The second-order NLO data for the $\text{Ln}(\text{AB3})_2$ (**12-14**), $\text{Ln}(\text{A4})_2$ (**16-18**), $\text{Ln}(\text{B4})_2$ (**19-21**), $\text{Ln}(\text{T4})_2$ (**24-26**)

Compounds		Form	Absorbance		P_{ETV}	P_{S}	Corr. P_{S}	Av. Corr. $\beta \times 10^{-30} \text{esu}$
			λ_{1907}	λ_{955}				
AB3 (12-14)	Eu(12)	Ox.	0.003	0.097	0.076	0.125	0.1409	4206
	Dy(13)	Ox.	0.043	0.096	0.069	0.103	0.1481	4532
	Lu(14)	Ox.	0	0.15	0.048	0.127	0.1509	5397
A4 (16-18)	Eu(16)	Ox.	0.04	0.09	0.059	0.13	0.1581	5075
	Dy(17)	Ox.	0.006	0.065	0.0547	0.142	0.1556	5216
	Lu(18)	Ox.	0	0.091	0.0548	0.148	0.1643	5349
B4 (19-21)	Eu(19)	Ox.	0.002	0.09	0.084	0.128	0.1435	4015
	Dy(20)	Ox.	0.006	0.111	0.066	0.103	0.1191	4217
	Lu(21)	Ox.	0.059	0.169	0.07	0.132	0.1626	4719
T4 (24-26)	Eu(24)	Ox.	0.043	0	0.0535	0.048	0.0535	2920
	Dy(25)	Ox.	0.008	0.005	0.1242	0.133	0.136	3071
	Lu(26)	Ox.	0	0.039	0.0405	0.059	0.0622	3630

P_{ETV} : Slope of ETV, P_{S} : Slope of Sample, Corr. P_{S} : Corrected slope for sample

It is important to note that, NLO activities of reduced and oxidized $\text{Ln}(\text{A4})_2$ and $\text{Ln}(\text{AB3})_2$ are oddly high and incoherent according to previous results. The origin of this enhancement is unclear. Therefore, we consider that these results come from uncertainty of HLS measurement (15-20 %). We are aware that these experiments will need to be repeating in order to clarify this discrepancy.

As mentioned before, the first hyperpolarizability of octupolar $\text{Ln}(\text{ABAB})_2$ increase in the order reduced < oxidized < neutral form (**Fig. 3.38 (a)**). By contrast, the first hyperpolarizability of nonoctupolar $\text{Ln}(\text{Pc})_2$ increase in the order reduced < neutral < oxidized form (**Fig. 3.38 (b)**). It seems that, in the case of nonoctupole complexes, resonance effects, which is caused by the radical $\pi\text{-}\pi^*$ transition band, contribute to NLO value more than ICT band.

In the oxidized form of nonoctupolar $\text{Lu}(\text{Pc})_2$, the contribution of the intermolecular charge transfer (ICT) to the hyperpolarizability vanishes. While this band disappear, the intensity of the BV and RV bands, which correspond to the radical $\pi\text{-}\pi^*$ transition, significantly increase with cost of optical transparency (see **Fig 3.38**).

The results show that, the first hyperpolarizability of oxidized form nonoctupolar $\text{Ln}(\text{Pc})_2$ is higher than neutral forms, which means in the case of nonoctupole complexes, resonance effects, which is caused by the radical $\pi\text{-}\pi^*$ transition band, contribute to NLO value more than ICT band. Therefore, by contrast octupolar $\text{Ln}(\text{ABAB})_2$, the first hyperpolarizability of nonoctupolar $\text{Ln}(\text{Pc})_2$ increase in the order reduced < neutral < oxidized form (**Fig. 3.38 (b)**)

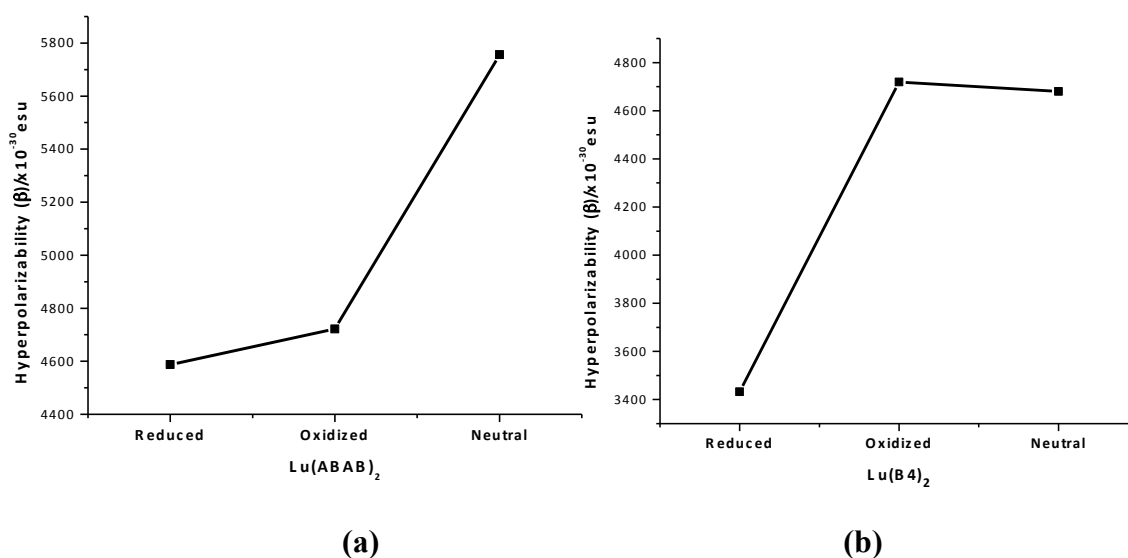


Figure 3.38 Plot of the hyperpolarisability coefficient β vs (a) octupolar $\text{Lu}(\text{ABAB})_2$ (b) nonoctupolar $\text{Lu}(\text{B4})_2$

3.2.3.2. Hyperpolarizability of reduced form nonoctupolar Ln(Pc)₂ (Ln(AB3)₂ (12-14), Ln(A4)₂ (16-18), Ln(B4)₂ (19-21), Ln(T4)₂ (24-26))

The first hyperpolarizability β obtained for the Ln(AB3)₂ (12-14), Ln(A4)₂ (16-18), Ln(B4)₂ (19-21), Ln(T4)₂ (24-26) in reduced forms are summarized in the Table 3.12. The reduced form of Ln(Pc)₂ Bis(Phthalocyanine) were prepared by adding 3 mg of NaBH₄ to 10 mL of a solution of complexes (10⁻⁵ M) in THF/CHCl₃ (1/10).

The first hyperpolarizability of the reduced form of nonoctupolar Ln(Pc)₂ (Ln(AB3)₂ (12-14), Ln(A4)₂ (16-18), Ln(B4)₂ (19-21), Ln(T4)₂ (24-26)) are still large but quite lower than the values of neutral and oxidized form.

Table 3.12 The second-order NLO data for the nonoctupole Ln(AB3)₂ (12-14), Ln(A4)₂ (16-18), Ln(B4)₂ (19-21), Ln(T4)₂ (24-26)

Compounds		Form	Absorbance		P _{ETV}	P _S	Corr.P _S	Av. Corr. $\beta \times 10^{-30}$ esu
			λ_{1907}	λ_{955}				
AB3 (12-14)	Eu(12)	Red.	0	0.02	0.058	0.11	0.1125	3527
	Dy(13)	Red.	0	0.015	0.051	0.098	0.0997	3544
	Lu(14)	Red.	0.019	0.024	0.069	0.226	0.2439	3600
A4 (16-18)	Eu(16)	Red.	0	0	0.0719	0.15	0.15	3692
	Dy(17)	Red.	0	0	0.058	0.133	0.133	3876
	Lu(18)	Red.	0	0.005	0.070	0.168	0.1689	3932
B4 (19-21)	Eu(19)	Red.	0	0.025	0.06	0.096	0.098	3271
	Dy(20)	Red.	0	0.025	0.098	0.159	0.1636	3319
	Lu(21)	Red.	0.026	0.169	0.07	0.17	0.1884	3432
T4 (24-26)	Eu(24)	Red.	0.01	0.017	0.0412	0.036	0.0379	2676
	Dy(25)	Red.	0.005	0.014	0.0415	0.043	0.0442	2875
	Lu(26)	Red.	0.008	0.015	0.0434	0.047	0.0495	2979

P_{ETV}: Slope of ETV, P_S: Slope of Sample, Corr. P_S: Corrected slope for sample

When the nonoctupolar $\text{Ln}(\text{Pc})_2$ is reduced, the intramolecular charge transfer (ICT) band is absent due to addition of second electron. And it seems that the decrease of the hyperpolarizability values is directly related to the vanishing of this band.

As mentioned before, although the reduced form of nonoctupolar $\text{Ln}(\text{Pc})_2$ has lower NLO activity than neutral and oxidized forms, they possess better transparency.

4. EXPERIMENTAL PART

Abbreviations:

Pc= Phthalocyanine, m.p.= melting point, NMR= nuclear magnetic resonance, ppm=parts per million, MW= molecular weight, TMS= tetramethylsilane, FT-IR= Fourier transform infrared, EA= Elemental Analyses, ESI-MS= Electrospray Ionization Mass Spectrometry, MALDI-MS= Matrix-Assisted Laser Desorption/Ionization Mass Spectrometry, TLC=thin layer chromatography, DBU=1,8-diazabicyclo[5.4.0]undec-7-ene, DMSO= dimethylsulfoxide, DCM= dichloromethane, THF= tetrahydrofuran.

4.1. General Remarks

All reactions were performed in standard glassware under an inert atmosphere of argon. Chemicals and reagents for syntheses were purchased from Aldrich, Fluka, E. Merck, Riedel-de Haën or Sigma in puriss. p. a. quality and used without further purification. All solvents used were previously distilled. Dry THF was obtained by distilling over sodium and benzophenone, dry 1-chloronaphthalene by distilling over calcium chloride.

Thin Layer Chromatography (TLC) was performed on glass sheets coated with a mixture of Silica 60G Merck 1.07731 and Merck 60 HF₂₅₄ 1.07739 (2:1) from E. Merck, visualization by irradiation with UV light (366 nm, 254 nm)

Column Chromatography was performed at r.t. under 0.2 atm pressure with silica gel 60 (230-400 mesh, 0.040-0.063 mm), or with silica gel-H (5-40 μ m), purchased from E. Merck and Fluka, respectively.

¹H and ¹³C NMR Spectra were recorded on Bruker AC 200 (500 MHz), spectrometer. All spectra were measured at room temperature. ¹³C NMR spectra were recorded with complete proton decoupling. The chemical shifts (δ) are given in ppm. The coupling constants J are listed in Hz. For proton, the multiplicity of the signals is indicated by s (singlet), d (doublet), t (triplet), q (quartet) and m (multiplet). All spectra were measured using CDCl₃ as solvents.

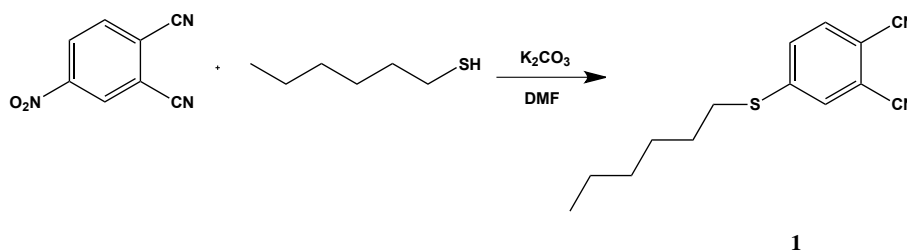
Mass Spectra were recorded by a Bruker Micro TOF-ESI/MS system and a Bruker Microflex LT MALDI-TOF MS with reflectron detection (positive ion mode; matrix: 2,5-dihydroxybenzoic acid)

IR Measurements were carried out on a Bruker Vector 22 spectrophotometer. The spectra were recorded as thin films or as KBr pellets. The absorptions are given in cm^{-1} .

UV-NIR spectra were carried out by SHIMADZU UV-VIS-NIR Spectrophotometer UV-3600. The absorptions are given in nm.

4.2. Syntheses

4.2.1. 4-hexylthio-1,2-dicyanobenzene (1)



A mixture of 4-nitrothalonitrile (2.5 g, 14.45 mmol) and 1-hexanethiol (2.1 g, 14.45 mmol) in DMSO (10 mL) was stirred at room temperature for 10 min. Then, drypotassium carbonate (2 g, 14.5 mmol) was added in small portions during 2 h. The mixture was vigorously stirred under argon atmosphere at room temperature for 16 h. Water (50 mL) was added, and the product was extracted with CH_2Cl_2 (3 x 50 mL). The combined organic phase were washed with water (3 x 50 mL) and dried over sodium sulfate. The solvent was removed under reduced pressure, and the residue was recrystallized from ethanol to give 4-hexylthio-1,2-dicyanobenzene [313].

2.8 g, Yield (80 %)

C₁₄H₁₆N₂S MW: 244.10 g/mol

Mp: 68 °C.

IR (KBr) ν (cm⁻¹): 2970 (s), 2950 (br,w), 2860 (s), 2240 (s), 1560 (s), 1450 (s), 1350 (s), 1280 (s), 1260 (s)

¹H NMR (CDCl₃): δ 7.63 (dd, 1H), 7.55 (d, 1H), 7.49 (dd, 1H), 3.00 (t, *J*: 5.6 Hz, 2H), 1.46 (m, 2H), 1.29 (b, 6H), 0.87 (t, *J*: 6.6 Hz, 3H).

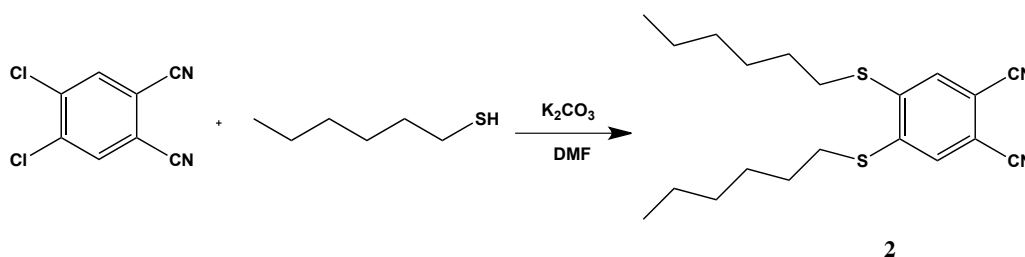
¹³C NMR (CDCl₃): δ 14.05, 22.59, 28.15, 28.77, 31.70, 31.87, 110.57, 115.1, 115.56, 116.19, 129.82, 129.94, 133.12, 147.53.

(ESI-MS) *m/z*: 267.10 [M+Na]

EA: Calculated: C 68.81, H 6.60, N 11.46, S 13.12

Found: C 68.46, H 6.41, N 11.76, S 13.60

4.2.2. 4,5-Bis(hexylthio)-1,2-dicyanobenzene (2)



4,5-Dichloro-1,2-dicyanobenzene (10 g, 50.8 mmol) and pulverized K₂CO₃ (30 g, 21.7 mmol) are stirred in DMF (70 mL), then 1-hexanethiol (14.76 g, 101.6 mmol) was added drop by drop. The reaction mixture was vigorously stirred under argon atmosphere at room temperature overnight. After addition of water, the solution was extracted by DCM. The combined organic phase were washed with water (3 x 50 mL) and dried over sodium sulfate. The solvent was removed under reduced pressure, and the residue was recrystallized from ethanol to give pure 4,5-bis(hexylthio)-1,2-dicyanobenzene (2) [314].

15 g, Yield (82 %)

C₂₀H₂₈N₂S₂, Mw: 360.58 g/mol

Mp: 71 °C.

IR (KBr) $\nu(\text{cm}^{-1})$: 2970 (s), 2950 (br,w), 2860 (s), 2240 (s), 1560 (s), 1450 (s), 1350 (s), 1280 (s), 1260 (s)

$^1\text{H NMR (CDCl}_3)$: δ .7.11 (s, 2H), 4.043 (t, 4H), 1.84 (m, 4H), 1.46 (m, 4H), 1.27 (m, 16H), 0.87 (t, J : 6.5 Hz, 6H).

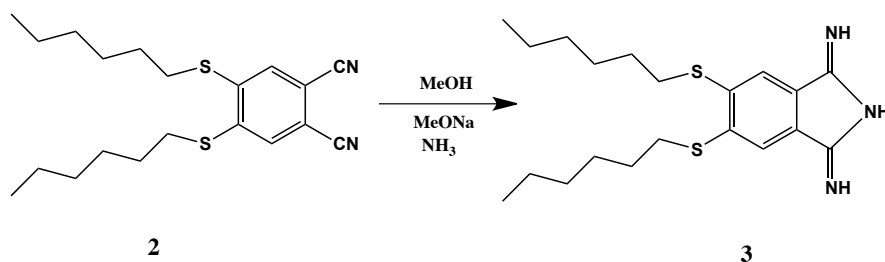
$^{13}\text{C NMR}$: δ 144.83, 134.32, 116, 109.55, 34.21, 31.64, 28.95, 28.50, 22.71, 14.22

ESI-MS m/z : 360 $[\text{M}]^+$

EA: Calculated : C 66.62, H 7.83, N 7.77, S 17.79

Found : C 66.40, H 7.70, N 7.93, S 17.57

4.2.3. 4,5-Bis(hexylthio)-1,3-diiminoisoindolin (3)



100-mL round-bottom flask was filled with fresh solution of sodium methoxide (0.2 g, 8.7 mmol) in 30 mL of dry methanol. 4,5-bis(hexylthio)phthalonitrile (5 g, 13.9 mmol) was added. The solution was stirred at room temperature for 1 h while ammonia was bubbled through. The mixture was then heated to reflux for 5 h with continued bubbling of ammonia. During the bubbling, the product precipitated. After cooling to room temperature, the precipitated product was filtered, washed with methanol and dried under vacuum at 70 °C [314].

4.98 g, Yield (95%)

$\text{C}_{20}\text{H}_{31}\text{N}_3\text{S}_2$ Mw: 377.61

IR (KBr) $\nu(\text{cm}^{-1})$: 3250-3260(d), 2900 (s), 2800 (s), 1560 (s), 1420 (s), 1350 (s), 1260 (s),

$^1\text{H NMR (CDCl}_3)$: δ 7.35 (s, 2H), 4.58 (s, 3H), 3.99 (t, J : 7.9 Hz 4H), 1.19 (m, 16H), 0.79 (t, J : 6.4 Hz, 6H).

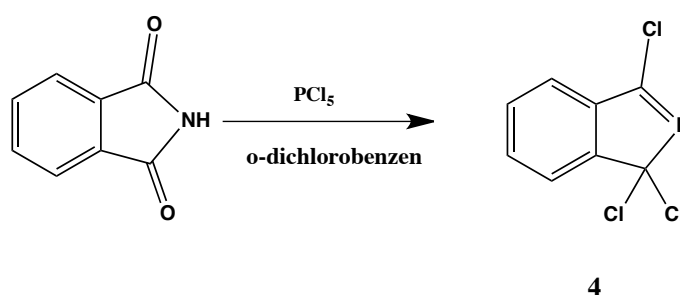
^{13}C NMR (CDCl_3): δ 167.83, 141.32, 131.81, 118.77, 33.36, 28.95, 28.50, 22.71, 14.22

ESI-MS (m/z): 378 $[\text{M}+\text{H}]^+$.

EA: Calculated: C 63.61, H 8.27, N 11.13, S 16.98

Found: C 63.44, H 8.48, N 11.46, S 16.58

4.2.4.1,3,3-Trichloroisindolenine (4)



Phthalimide (30 g, 0,2 mol) and PCl_5 (130 g) were stirred in 1,2-dichlorobenzene (250 mL) at 120 °C during 1 week, then cooled to room temperature. The product was distilled undervacuum (bp 125 °C at 0.05 Torr)[315].
mp: 107 °C, ref. mp: 106 °C

30 g, Yield(80%)

$\text{C}_8\text{H}_4\text{Cl}_3\text{N}$ Mw: 220.48

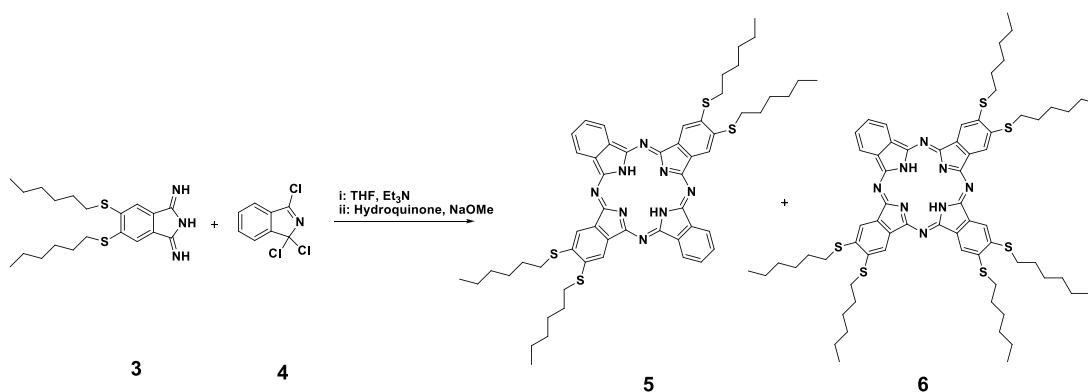
IR (KBr) $\nu(\text{cm}^{-1})$: 3200 (br, w), 3062 (w), 2717 (s) 1744 (s), 1609 (s)

^1H NMR (CDCl_3): Not stable

^{13}C NMR (CDCl_3): Not stable

ESI-MS (m/z): 221 $[\text{M}+\text{H}]^+$

4.2.5. 2,3,16,17-tetra(hexylthio)phthalocyanine (5) and 2,3,9,10,16,17 hexa(hexylthio)phthalocyanine (6)



A mixture of anhydrous triethylamine (0.72 mL, 5.2 mmol, 2 eq) and 1,3,3-trichloroisoindolenine (**4**) (2.9 g, 13 mmol, 5 eq) in anhydrous THF (400 mL) under argon was cooled to approximately 0°C with an ice/salt bath. A solution of 4,5-bis(hexylthio)isoindoline 1,3-diimine (**3**) (1 g, 2.65 mmol, 1 eq) in anhydrous THF (400 mL) was then added over a period of 12 hours. The mixture was reheated slowly to room temperature overnight.

After filtration under argon to remove the triethylammonium chloride, hydroquinone (0.286 g, 2.65 mmol, 1 eq) and sodium methoxide (0.421 g, 7.8 mmol, 3 eq) were added to the filtrate and the resulting mixture was heated at 65°C under argon overnight to obtain a green solution. The solvent was removed under reduced pressure and the crude product extracted in a Soxhlet with ethanol and acetone to take away the organic impurities and the B₄ phthalocyanine, followed by CH₂Cl₂ to obtain a solution containing a mixture of ABAB and AB₃ phthalocyanines. The two compounds were separated by preparative thin layer chromatography on silica eluting with *n*-hexane/dichloromethane (5:2, v/v). Obtained: 65 mg (2 %) of AB₃ (2,3,9,10,16,17 hexa(hexylthio)phthalocyanine) as the first eluting compound and 206 mg (8 %) of the desired ABAB phthalocyanine as the second eluting compound.

ABAB-5:

206mg, Yield (8 %)

C₅₆H₆₆N₈S₄ Mw: 979.44

IR (KBr) $\nu(\text{cm}^{-1})$: 3307 (s), 3070(br, w), 2850-2919 (w), 1603 (s), 1537 (s).

$^1\text{H NMR (CDCl}_3)$: δ . 7.96 (s, 4H), 7.56 (d, 4H), 7.48 (d, 4H), 3.07(t, J : 7 Hz, 8H), 1.96 (m, 8H), 1.72 (m, J_1 : 14 Hz, J_2 : 7.2 Hz, 8H), 1.54 (m, 16H), 1.08 (t, J : 6.3 Hz, 12 H), -5.30 (s, 2H).

$^{13}\text{C NMR (CDCl}_3)$: 138.4, 134.9, 131.04, 128.08, 121.27, 118.20, 33.29, 31.80, 29.20, 28.67, 22.81, 14.27

MALDI-TOF MS: m/z 980 [M+H]⁺.

AB₃-6:

65 mg, Yield(2 %)

C₆₈H₉₀N₈S₆ Mw: 1211.89

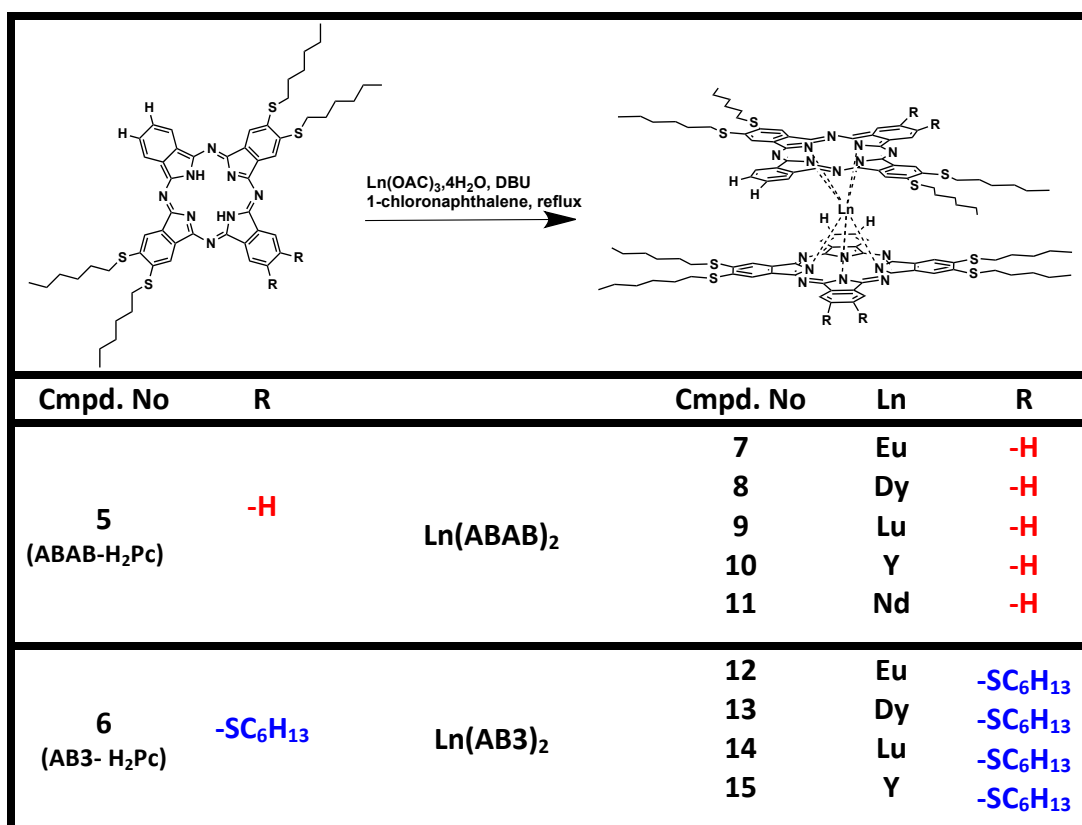
IR (KBr) $\nu(\text{cm}^{-1})$: 3307 (s), 3070(br, w), 2850-2919 (w), 1603 (s), 1537 (s).

$^1\text{H NMR (CDCl}_3)$: δ . 8.36 (s, 2H), 7.77 (m, 6H), 7.63 (d, 2H), 3.13(t, J : 7 Hz, 12H), 1.95 (m, 12H), 1.69 (m, J_1 : 14.8 Hz, J_2 : 7.1 Hz, 12H), 1.44 (m, 24H), 1.00 (t, 18 H), -5.30 (s, 2H).

$^{13}\text{C NMR (CDCl}_3)$: 140.1, 138.9, 138.04, 135.55, 132.27, 131.9, 131.176, 128.48, 121.85, 119.51, 118.8, 117.98, 33.88, 33.66, 33.33, 31.85, 29.31, 29.23, 29.18, 28.66, 22.80

MALDI-TOF MS: m/z 1212 [M]⁺.

4.2.6. General method for the synthesis of ABAB and AB3 homoleptic bis(phthalocyaninato) lanthanide(III) complexes ((Ln(ABAB)₂) (7-11), (Ln(AB3)₂) (12-15))



A mixture of dry Ln(OAc)₃·4H₂O powder (0,1mmol), DBU (1 mL) and a solution of free phthalocyanine (0.21 mmol) in 1-chloronaphthalene (3 mL) was refluxed for 4 h under nitrogen to give dark-green solution. The solution was cooled to room temperature and hexane (100 mL) was slowly added. The precipitated product was filtered off. The filtrate was concentrated and purified by column chromatography on silica gel eluting (Ln(ABAB)₂):(CH₂Cl₂/n-hexane, 2:3 (v/v)[316], Ln(AB3)₂: CH₂Cl₂/n-hexane, 1:1 (v/v) [317]).

4.2.6.1. ABAB bis(phthalocyaninato) europium(III) complex (Eu(ABAB)₂)(7)

Green product was prepared according to the general protocol as described the synthesis method above.

140 mg, Yield (63 %)

C₁₁₂H₁₂₈EuN₁₆S₈ Mw: 2106.81

IR (KBr) $\nu(\text{cm}^{-1})$: 2955 (s), 2923 (s), 2845 (s), 2580 (b, w), 2200 (b, w), 1586 (s), 1496 (s), 1444 (s), 1308 (s).

MALDI-TOF MS: m/z 2108 [M+H]⁺

4.2.6.2. ABAB bis(phthalocyaninato) dysprosium(III) complex (Dy(ABAB)₂)(8)

Green product was prepared according to the general protocol as described the synthesis method above.

130 mg, Yield (54 %)

C₁₁₂H₁₂₈DyN₁₆S₈ Mw: 2117.34

IR (KBr) $\nu(\text{cm}^{-1})$: 2955 (s), 2923 (s), 2845 (s), 2580 (b, w), 2200 (b, w), 1586 (s), 1496 (s), 1444 (s), 1308 (s).

MALDI-TOF MS: m/z 2118 [M+H]⁺

4.2.6.3. ABAB bis(phthalocyaninato) lutetium(III) complex (Lu(ABAB)₂) (9)

Green product was prepared according to the general protocol as described the synthesis method above.

70 mg, Yield (60 %)

C₁₁₂H₁₂₈LuN₁₆S₈ Mw: 2127.01

IR (KBr) $\nu(\text{cm}^{-1})$: 2955 (s), 2923 (s), 2845 (s), 2580 (b, w), 2200 (b, w), 1586 (s), 1496 (s), 1444 (s), 1308 (s).

MALDI-TOF MS: m/z 2128 [M+H]⁺.

4.2.6.4. ABAB bis(phthalocyaninato) yttrium(III) complex (Y(ABAB)₂)(10)

Green product was prepared according to the general protocol as described the synthesis method above.

70 mg, Yield (60 %)

C₁₁₂H₁₂₈YN₁₆S₈ Mw: 2042.05

IR (KBr) $\nu(\text{cm}^{-1})$: 2955 (s), 2923 (s), 2845 (s), 2580 (b, w), 2200 (b, w), 1586 (s), 1496 (s), 1444 (s), 1308 (s).

MALDI-TOF MS: m/z 2043 [M+H]⁺

4.2.6.5. ABAB bis(phthalocyaninato) neodymium(III) complex (Nd(ABAB)₂)(11)

Green product was prepared according to the general protocol as described the synthesis method above.

70 mg, Yield (63 %)

C₁₁₂H₁₂₈NdN₁₆S₈ Mw: 2098.08

IR (KBr) $\nu(\text{cm}^{-1})$: 2955 (s), 2923 (s), 2845 (s), 2580 (b, w), 2200 (b, w), 1586 (s), 1496 (s), 1444 (s), 1308 (s).

MALDI-TOF MS: m/z 2099 [M+H]⁺

4.2.6.6. AB₃bis(phthalocyaninato) europium(III) complex (Eu(AB₃)₂)(12)

Green product was prepared according to the general protocol as described the synthesis method above.

55 mg, Yield (60 %)

C₁₃₆H₁₇₆EuN₁₆S₁₂, Mw: 2570

IR (KBr) $\nu(\text{cm}^{-1})$: 2955 (s), 2923 (s), 2845 (s), 2580 (b, w), 2200 (b, w), 1586 (s), 1496 (s), 1444 (s), 1308 (s).

MALDI-TOF MS: m/z 2571 [M+H]⁺.

4.2.6.7. AB₃bis(phthalocyaninato) dysprosium(III) complex (Dy(AB₃)₂)(13)

Green product was prepared according to the general protocol as described the synthesis method above.

55 mg, Yield (62 %)

C₁₃₆H₁₇₆DyN₁₆S₁₂, Mw: 2581.24

IR (KBr) $\nu(\text{cm}^{-1})$: 2955 (s), 2923 (s), 2845 (s), 2580 (b, w), 2200 (b, w), 1586 (s), 1496 (s), 1444 (s), 1308 (s).

MALDI-TOF MS: m/z 2582 [M+H]⁺

4.2.6.8. AB₃bis(phthalocyaninato) lutetium(III) complex (Lu(AB₃)₂)(14)

Green product was prepared according to the general protocol as described the synthesis method above.

40 mg, Yield (42 %)

C₁₃₆H₁₇₆LuN₁₆S₁₂, Mw: 2592.71

IR (KBr) $\nu(\text{cm}^{-1})$: 2955 (s), 2923 (s), 2845 (s), 2580 (b, w), 2200 (b, w), 1586 (s), 1496 (s), 1444 (s), 1308 (s).

MALDI-TOF MS: m/z 2593 [M+H]⁺

4.2.6.9. AB₃bis(phthalocyaninato) yttrium(III) complex (Y(AB₃)₂)(15)

Green product was prepared according to the general protocol as described the synthesis method above.

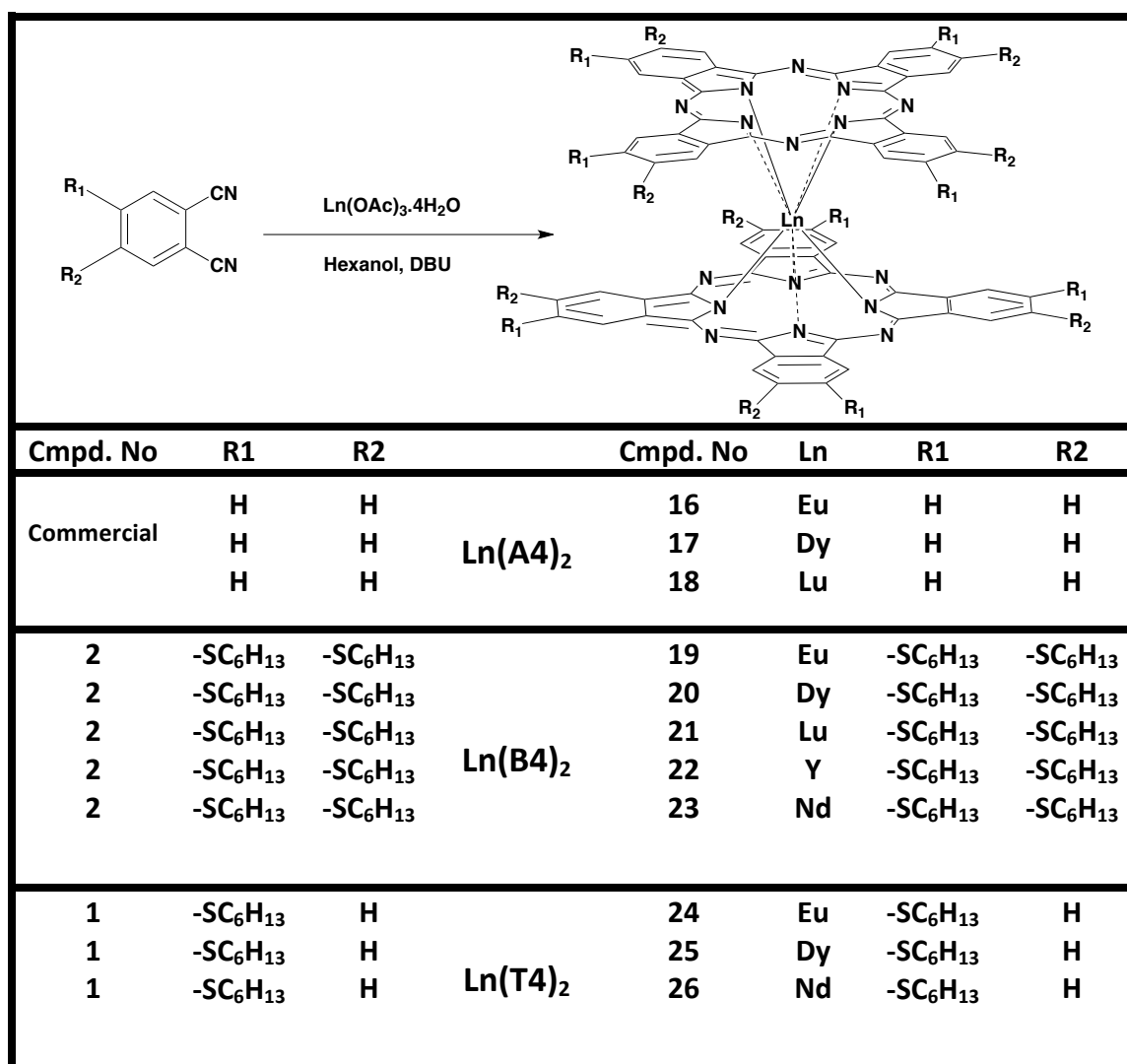
20 mg, Yield (22 %)

C₁₃₆H₁₇₆YN₁₆S₁₂, Mw: 2506.02

IR (KBr) $\nu(\text{cm}^{-1})$: 2955 (s), 2923 (s), 2845 (s), 2580 (b, w), 2200 (b, w), 1586 (s), 1496 (s), 1444 (s), 1308 (s).

MALDI-TOF MS: m/z 2507 [M+H]⁺

4.2.7. General method for the synthesis of homoleptic bis(phthalocyaninato) lanthanide(III) complexes ((Ln(A4)₂) (16-18), (Ln(B4)₂) (19-23), (Ln(T4)₂) (24-26))



A round-bottomed flask fitted with a condenser was degassed and flame-dried under dry argon. The flask was charged under argon with dinitrile derivative (1.56 mmol), anhydrous Ln(OAc)₃.4H₂O (0.195 mmol), DBU (600 μL, 4 mmol), and 16 mL of hexan-1-ol. The mixture was refluxed under argon for 48 h. Evaporation of the hexan-1-ol under reduced pressure left a greenish waxy residue. It was precipitated by hexane, and filtered. The residue was washed with ethanol and acetone several times. Then this compound was solved in dichloromethane and concentrated. The residue was purified by column chromatography on silica gel

eluting (**Ln(A4)₂** : DCM [259], **Ln(B4)₂**: CH₂Cl₂/n-hexane, 1:1 (v/v) [292], **Ln(T4)₂**: CH₂Cl₂/n-hexane, 1:1 (v/v)).

4.2.7.1. The unsubstituted (A4)bis(phthalocyaninato)europium(III) complex(Eu(A₄)₂) (16)

Green product was prepared according to the general protocol as described the synthesis method by using related dinitrile derivative, above.

60 mg, Yield (48 %)

C₆₄H₃₀EuN₁₆ Mw: 1174.99

IR (KBr) $\nu(\text{cm}^{-1})$: 2955 (s), 2923 (s), 2845 (s), 2580 (b, w), 2200 (b, w), 1586 (s), 1496 (s), 1444 (s), 1308 (s).

MALDI-TOF MS: m/z 1177 [M+2H]⁺.

4.2.7.2. The unsubstituted (A4) bis(phthalocyaninato) dysprosium(III) complex (Dy(A₄)₂) (17)

Green product was prepared according to the general protocol as described the synthesis method by using related dinitrile derivative, above.

55 mg, Yield (50 %)

C₆₄H₃₀DyN₁₆ Mw: 1185.53

IR (KBr) $\nu(\text{cm}^{-1})$: 2955 (s), 2923 (s), 2845 (s), 2580 (b, w), 2200 (b, w), 1586 (s), 1496 (s), 1444 (s), 1308 (s).

MALDI-TOF MS: m/z 1189 [M+4H]⁺

4.2.7.3. The unsubstituted (A4) bis(phthalocyaninato) lutetium(III) complex (Lu(A₄)₂) (18)

Green product was prepared according to the general protocol as described the synthesis method by using related dinitrile derivative, above.

55 mg, Yield (56 %)

C₆₄H₃₀LuN₁₆ Mw: 1198.0

IR (KBr) $\nu(\text{cm}^{-1})$: 2955 (s), 2923 (s), 2845 (s), 2580 (b, w), 2200 (b, w), 1586 (s), 1496 (s), 1444 (s), 1308 (s).

MALDI-TOF MS: m/z 1202 [M+4H]⁺.

4.2.7.4. The octahexylthia substituted (B4) bis(phthalocyaninato) europium(III) complex (Eu(B₄)₂)(19)

Green product was prepared according to the general protocol as described the synthesis method by using related dinitrile derivative, above.

110 mg, Yield (10 %)

C₁₆₀H₂₂₄EuN₁₆S₁₆ Mw: 3034.0

IR (KBr) $\nu(\text{cm}^{-1})$: 2955 (s), 2923 (s), 2845 (s), 2580 (b, w), 2200 (b, w), 1586 (s), 1496 (s), 1444 (s), 1308 (s).

MALDI-TOF MS: m/z 3035 [M+H]⁺

4.2.7.5. The octahexylthia substituted (B4) bis(phthalocyaninato) dysproium(III) Complex (Dy(B₄)₂)(20)

Green product was prepared according to the general protocol as described the synthesis method by using related dinitrile derivative, above.

100 mg, Yield (12 %)

C₁₆₀H₂₂₄DyN₁₆S₁₆ Mw: 3046.14

IR (KBr) $\nu(\text{cm}^{-1})$: 2955 (s), 2923 (s), 2845 (s), 2580 (b, w), 2200 (b, w), 1586 (s), 1496 (s), 1444 (s), 1308 (s).

MALDI-TOF MS: m/z 3047 [M+H]⁺

4.2.7.6. The octahexylthia substituted (B4) bis(phthalocyaninato) lutetium(III) complex (Lu(B₄)₂)(21)

Green product was prepared according to the general protocol as described the synthesis method by using related dinitrile derivative, above.

120 mg, Yield (13 %)

C₁₆₀H₂₂₄LuN₁₆S₁₆ Mw: 3058.60

IR (KBr) $\nu(\text{cm}^{-1})$: 2955 (s), 2923 (s), 2845 (s), 2580 (b, w), 2200 (b, w), 1586 (s), 1496 (s), 1444 (s), 1308 (s).

MALDI-TOF MS: m/z 3059 [M+H]⁺

4.2.7.7. The octahexylthia substituted (B4) bis(phthalocyaninato) yttrium(III) complex (Y(B₄)₂)(22)

Green product was prepared according to the general protocol as described the synthesis method by using related dinitrile derivative, above.

100 mg, Yield (12 %)

C₁₆₀H₂₂₄YN₁₆S₁₆ Mw: 2970.04

IR (KBr) $\nu(\text{cm}^{-1})$: 2955 (s), 2923 (s), 2845 (s), 2580 (b, w), 2200 (b, w), 1586 (s), 1496 (s), 1444 (s), 1308 (s).

MALDI-TOF MS: m/z 2971[M+H]⁺

4.2.7.8. The octahexylthia substituted (B4) bis(phthalocyaninato) neodymium(III) complex (Nd(B₄)₂)(23)

Green product was prepared according to the general protocol as described the synthesis method by using related dinitrile derivative, above.

100 mg, Yield (12 %)

$C_{160}H_{224}NdN_{16}S_{16}$ Mw: 3028.88

IR (KBr) $\nu(\text{cm}^{-1})$: 2955 (s), 2923 (s), 2845 (s), 2580 (b, w), 2200 (b, w), 1586 (s), 1496 (s), 1444 (s), 1308 (s).

MALDI-TOF MS: m/z 3030 $[M+H]^+$.

4.2.7.9. The tetrahexylthia substituted (T4)bis(phthalocyaninato) europium(III) complex (Eu(T₄)₂)(24)

Green product was prepared according to the general protocol as described the synthesis method by using related dinitrile derivative, above.

140 mg, Yield (13 %)

$C_{112}H_{128}EuN_{16}S_8$ Mw: 2106.81

IR (KBr) $\nu(\text{cm}^{-1})$: 3020 (s), 2955 (s), 2923 (s), 2845 (s), 2580 (b, w), 2200 (b, w), 1586 (s), 1496 (s), 1444 (s), 1308 (s).

MALDI-TOF MS: m/z 2108 $[M+H]^+$.

4.2.7.10. The tetrahexylthia substituted (T4) bis(phthalocyaninato) dysprosium(III) complex (Dy(B₄)₂)(25)

Green product was prepared according to the general protocol as described the synthesis method by using related dinitrile derivative, above.

125 mg, Yield (12 %)

$C_{112}H_{128}DyN_{16}S_8$ Mw: 2117.34

IR (KBr) $\nu(\text{cm}^{-1})$: 3020 (s), 2955 (s), 2923 (s), 2845 (s), 2580 (b, w), 2200 (b, w), 1586 (s), 1496 (s), 1444 (s), 1308 (s).

MALDI-TOF MS: m/z 2118 $[M+H]^+$

4.2.7.11 The tetrahexylthia substituted (T4) bis(phthalocyaninato) lutetium(III) complex (Lu(T₄)₂) (26)

Green product was prepared according to the general protocol as described the synthesis method by using related dinitrile derivative, above.

110 mg, Yield (10 %)

C₁₁₂H₁₂₈LuN₁₆S₈ Mw: 2126.81

IR (KBr) $\nu(\text{cm}^{-1})$: 3020 (s), 2955 (s), 2923 (s), 2845 (s), 2580 (b, w), 2200 (b, w), 1586 (s), 1496 (s), 1444 (s), 1308 (s).

MALDI-TOF MS: m/z 2128 [M+H]⁺.

5. GENERAL CONCLUSION

Recently, a new class of materials based on octupolar symmetries has been proposed for NLO applications by Zyss and coworkers. Octupolar molecules lack permanent dipole moments and have better chances to adopt noncentrosymmetric packing. Another significant advantage of octupolar systems is that their hyperpolarizability (β) increases steadily as the extent of charge transfer increases, whereas the β of dipolar molecules increases to a maximum value and then decreases as the length of the conjugation increases.

Moreover, it has been shown that the basic template for octupolar molecules is a cube with eight alternated charges at the corner and delocalization of the charges between the higher and lower plans. Despite all the various of 2D and 3D octupolar molecule structures, which were deduced from this basic cubic point charge template by projecting the charges, reported, no molecules actually representing the “real” cube have been achieved so far.

Our initial goal in this thesis was to develop a categorized strategy for the synthesis of cubic octupoles. So, we foreseen that real octupolar cube can be demonstrated by designing a bis(phthalocyaninato)Ln- (III) double-decker complex with a crosswise ABAB phthalocyanine bearing alternating electron-donor and electron-acceptor groups. And these cubic systems are expected to show high nonlinearities and improve nonlinearity/transparency tradeoff.

The crosswise **ABAB** phthalocyanine was synthesized by regioselective approach. Finally, the real octupolar cube bis(phthalocyanine) complexes were obtained in good yield from the **ABAB** phthalocyanine and lanthanide acetate in refluxing 1-chloronaphthalene using DBU as an organic base.

The homoleptic double-decker ABAB bis(Phthalocaynines) are characterized by X-Ray and UV-NIR. And the results show that the homoleptic double-decker ABAB bis(Phthalocaynine) structure provide octupolar structure requirements such as multidirectional charge transfer and noncentrosymmetry.

Then we extended this work in order to understand better of efficiency of octupolar structure, various non-octupolar **AB₃**, **A₄**, **B₄**, **T₄** type double decker

lanthanide homoleptic bisphthalocyanines are synthesized by cyclic tetramerization of the corresponding phthalodinitrile in the presence of a lanthanide salt and DBU.

In summary, a series of octupole and nonoctupole double decker rare-earth bis(Phthalocyanine) complexes have been synthesized, and their linear optical and nonlinear optical properties (first molecular hyperpolarizability β) have been investigated.

The first molecular hyperpolarizability (β) measurement shows that coordination chemistry of lanthanide ions is a powerful instrument for the design of efficient octupole structure and that the molecular quadratic hyperpolarizability (β) values are strongly influenced by the nature of the lanthanide ion. For each series, the NLO activity regularly increases from yttrium to lutetium along the f-element row and this effect is called “metal-induced NLO-enhancement”. Moreover, the Lu(Pc)₂ complexes exhibit the highest hyperpolarizability over the lanthanide series, even if for other ions the 1907 nm laser wavelength comes into resonance with the intervalence band. This seems to indicate that the intervalence transition has small influence on the quadratic nonlinear response. This conclusion is particularly attractive in terms of transparency/nonlinearity tradeoff because NLO activity is significantly improved without any cost of optical transparency.

However, in the case of the reduced form of Ln(Pc)₂, we observed that the NLO activity of Ln(Pc)₂ is intensely influenced not only by the nature of the lanthanide ion but also by the intermolecular charge transfer (ICT). In this case, the contribution of the intermolecular charge transfer (ICT) to the hyperpolarizability vanishes and causes lower NLO activity than in the neutral form. Unfortunately NLO activities of oxidized form of both octupole and nonoctupole bis(Phthalocyanines) are falsely disrupted by resonance effects, which is caused by the radical π - π^* transition band.

The results of β values undoubtedly show that the octupole Ln(ABAB)₂ has higher first hyperpolarizability than the corresponding nonoctupole Ln(Pc)₂ (Ln(AB3)₂, Ln(A4)₂, Ln(B4)₂, Ln(T4)₂) complexes as we expected. The number of electron-donating groups has significant influence on the first hyperpolarizability of

the nonoctupole complexes $\text{Ln}(\text{Pc})_2$ and the order of β is as follow: $\text{Lu}(\text{T}_4)_2 < \text{Lu}(\text{A}_4)_2 < \text{Lu}(\text{AB}_3)_2 < \text{Lu}(\text{B}_4)_2$. While, the electron-donating groups increase NLO activity, clearly cost optical transparency because of red shift.

Finally, we have predicted and achieved the closest structured reported so far for the “true” octupolar cube. And these cubic octupolar bis(phthalocyanines) exhibits the highest quadratic hyperpolarizability ever reported for an octupolar molecule.

BIBLIOGRAPHIC REFERENCES

- [1]. Peter Gunter (ed.), *NLO effects and materials*, Springer-Verlag, **2000**.
- [2]. D.M. Burland, R.D. Miller, C. A. Walsh, *Chem. Rev.* **1994**, 94, 31.
- [3]. D. S. Chemla, J. Zyss, *Nonlinear Optical Properties of Organic Molecules and Crystals*, Academic Press, New York, **1987**, vol. 1-2.
- [4]. P. N. Prasad, B. A. Reinhardt, *Chem. Mater.* **1990**, 2, 660.
- [5]. P. N. Butcher, D. Cotter, *The elements of nonlinear optics.*, New York, Cambridge University Press. **1990**
- [6]. P. Franken, A. Hill, C. Peters, G. Weinreich, *Physical Review Letters* **1961**, 7, 118,
- [7]. F. Agullo-Lopez, J. M Cabrera, F. Agullo-Rueda, *Electrooptics: Phenomena, Materials and Applications*; Academic press: San Diego, CA, **1994**
- [8]. S. Denus, A. Dubik, B. Kaczmarczyk, J. Makowski, J. Marczak, J. Owsik, Z. Patron, M. Szczurek. *Laser and Particle Beams* **1986**, 4: 119-139
- [9]. G.D. Stucky, S. R. Marder, J. E. Sohn, *Materials for Nonlinear Optics: Chemical Perspectives*, ACS, **1991**
- [10]. T. Verbiest, K. Clays, C. Samyn, J. Wolff, D. Reinhoudt, A. Persoons, *J. Am. Chem. Soc.* **1994**, 116, 9320-9323
- [11]. D. J. Williams, *Angew. Chem. Int. Ed. Engl.*, **1984**, 23, 690.
- [12]. S. R. Marder, B. Kippelen, A. K. Y. Jen, N. Peyghambarian, *Nature*, **1997**, 388, 845
- [13]. D. J. Williams, *Angew. Chem. Int. Ed. Engl.*, **1984**, 23, 690.
- [14]. P. W. Smith, *Bell. Syst. Tech. J.* **1982**, 61, 54
- [15]. A. Yariv, *Quantum Electronics*. Wiley, New York **1975**, 327.
- [16]. A. Yariv, *Quantum Electronics*. Wiley, New York **1975**, 407.
- [17]. F. Kajzar, K. S. Lee, A. K. Y. Jen, *Adv. Polym. Sci.* **2003**, 161,1.
- [18]. Y. Shi, C. Zhang, H. Zhang, J. H. Bechtel, L. R. Dalton, B. H. Robinson, W. H. Steier, *Science* **2000**, 288, 199.
- [19]. C. Ruslim, K. Ichimura, *Adv. Mater.* **2001**, 13, 37.
- [20]. A. Abbotto, L. Beverina, R. Bozio, S. Bradamante, C. Ferrante, G. A. Pagani, R. Signorini, *Adv. Mater.*, **2000**, 12, 1963.
- [21]. G. J. Ashwell, D. Bloor, *Optical Materials for Non-linear Optics*, RSC, London **1993**, 42, 291

- [22]. Nalwa, Miyata, *Nonlinear Optics of Organic Molecules and Polymers* CRC Press, **1997**
- [23]. W. Blau, *Phys. Technol.*, **1987**, 18, 250
- [24]. P. A. Franken, A. E. Hill, C. W. Peters, *Phys. Rev. Lett.* **1961**, 7, 118
- [25]. R. C. Miller, D. A. Kleinman, A. Savage, **1963**, 11, 146
- [26]. G. D. Boyd, R. C. Miller, K. Nassau, W. L. Bond, A. Savage, *Appl. Phys. Lett.* **1964**, 5, 234
- [27]. R. C. Miller, G. D. Boyd, A. Savage, *Appl. Phys. Lett.*, **1965**, 6, 77;
- [28]. C. Chen, G. Liu, *Annu. Rev. Mater. Sci.* **1986**, 16, 203.
- [29]. G. F. Lipscomb, A. F. Garrito, R. S. Narang, *J. Chem. Phys.* **1981**, 75, 1509;
- [30]. J. C. Baumert, R. J. Twieg, G. C. Bjorklund, J. A. Logan, C. W. Dirk, *Appl. Phys. Lett.* **1987**, 51, 1484;
- [31]. J. Zyss, *J. Mol. Electron.* **1985**, 1, 24;
- [32]. C. Dehu, F. Meyers, J. L. Bredas, *J. Am. Chem. Soc.* **1993**, 115, 6198.
- [33]. P. N. Prasad, D. R. Ulrich, *Nonlinear Optic and Polymer*, Plenum, New York, **1988**.
- [34]. G. Khananan, *Nonlinear Optical Properties of Organic Molecules SHE*. Bellingham, WA, USA, **1988**, p. 971.
- [35]. S. R. Marder, *Inorganic Materials* Wiley, **1992**, p132
- [36]. J. C. Calahrese, L.-T. Cheng, J. C. Green, S. R. Marder, W. Tam, *JACS*, **1991**, 113, 7227
- [37]. C. C. Frazier, M. A. Harvey, M. P. Cockerham, H. M. Hand, E. A. Chauchard, C. H. Lee, *J. Phys. Chem.*, **1986**, 90, 5703
- [38]. A. Braun, J. Tscherniac, *Ber.* **1907**, 40, 2709.
- [39]. A. G. Dandridge, H. A. E. Drescher, J. Thomas, **GB 322169, 1928**.
- [40]. C. C. Leznoff, *Phthalocyanines, Properties and Applications*, Vols 1-4, VCH Weinheim, **1989**
- [41]. H. Tomoda, S. Saito, S. Ogawa, S. Shiraishi, *Chem. Lett.* , **1980**, 1277
- [42]. S. W. Oliver, T. D. Smith, *J. Chem. Soc. Perkin Trans. 2* , **1987**, 1579
- [43]. S. J. Brach, O. A. Grammatica, L. Ossanna, J. Weinberger, *Heterocyclic Chem.* **1970**, 7, 1403
- [44]. P. A. Barret, C. E. Dent, R. P. Linstead, *J. Chem. Soc.* , 1719, **1936**.
- [45]. P. A. Barret, D. A. Frye, R. P. Linstead, *J. Chem. Soc.* , 1157, **1938**

- [46]. C.C. Leznoff, *Phthalocyanines, Properties and Applications*, Vols 1-4, VCH Weinheim, **1989**
- [47]. C. Piechocki, J. Simon, A. Skoulios, D. Guillon, P. Weber, *J. Am. Chem. Soc.* , 104 , 5245, **1982**.
- [48]. I.S. Kirin, P.N. Moskalev, Y.A. Makashev, *Russ. J. Inorg. Chem.* ,10 , 1065, **1965**
- [49]. C. C. Leznoff, in *Phthalocyanines: Properties and Applications*, Vol. 1, VCH, New York, **1989**
- [50]. H. Tomoda, S. Saito, O. Shojiro, S. Shiraishi, *Chem. Lett.* **1980**, 1277.
- [51]. R. M. Christie, D. D. Deans, *J. Chem. Soc., Perkin Trans. 2* **1989**, 193.
- [52]. K. Janczak, R. Kubiak, *J. Alloy. Compd.* **1992**,190, 121
- [53]. K. Janczak, R. Kubiak, *J. Alloy. Compd.* **1992**,190, 117
- [54]. N.B. McKeown, *Phthalocyanine Materials: Synthesis, Structure, Function*; Cambridge University Press: Cambridge, U.K., **1998**.
- [55]. J. F. Van der Pol, E. Neeleman, J. W. Zwikker, R. J. M. Nolte, W. Drenth, J. Aerts, R. Visser, S. J. Picken, *Liq. Cryst.* 6 ,**1989**, 577.
- [56]. H. Schultz, H. Lehmann, M. Rein, M. Hanack, *Struct. Bond.* **1991**, 74, 41.
- [57]. H. LeC. C. Leznoff, A. B. P. Lever, *Phthalocyanines: Properties and Applications*, VCH: New York, V 1. **1989**
- [58]. C. C. Leznoff, A. B. P. Lever, *Phthalocyanines: Properties and Applications*, VCH: New York, V2. **1993**
- [59]. C. C. Leznoff, A. B. P. Lever, *Phthalocyanines: Properties and Applications*, VCH: New York, V3. **1993**
- [60]. C. C. Leznoff, A. B. P. Lever, *Phthalocyanines: Properties and Applications*, VCH: New York, V4. **1996**
- [61]. F. H. Moser, A. L. Thomas, *Phthalocyanine Compounds*, Reinhold: New York, **1963**.
- [62]. F. H. Moser, A. L. Thomas, *The Phthalocyanines*, CRC: Boca Raton, FL, V 1.**1983**.
- [63]. F. H. Moser, A. L. Thomas, *The Phthalocyanines*, CRC: Boca Raton, FL, V3.**1983**.
- [64]. M. Emmelius, G. Pawlowski, H. W. Vollmann, *Angew. Chem.*,101, 1475. **1989**
- [65]. M. Emmelius, G. Pawlowski, H. W. Vollmann *Angew. Chem. Int. Ed. Engl.*,**1989**, 28, 1445.

- [66]. S. A. Borisenkova, *Pet. Chem.*, **1991**, 31, 379.
- [67]. K.-Y. Law, *Chem. Rev.*, **1993**, 93, 449.
- [68]. G.de la Torre, P. Vazquez, F. Agulló-López, T. Torres, *J. Mater. Chem.*, **1998**, 8, 1671.
- [69]. C. Piechocki, J. Simon, A. Skoulios, D. Guillon, P. Weber, *J. Am. Chem. Soc.*, **1982**, 104, 5245,
- [70]. Z. Ali-Adib, G. J. Clarkson, N. B. McKeown, K. E. Treacher, H. F. Gleeson, A. S. Stennett, *J. Mater. Chem.*, **1998**, 8, 2371,
- [71]. M. J. Cook, M. F. Daniel, K. J. Harrison, N. B. McKeown, A. J. Thomson, *Chem. Commun.*, **1987**, 1148.
- [72]. D. Phillips, *Prog. React. Kinet.*, **1997**, 22, 175.
- [73]. R. Bonnett, *Chem. Soc. Rev.*, **1995**, 24, 19.
- [74]. I. Rosenthal, *Photochem. Photobiol.*, **1991**, 53, 859.
- [75]. J.-J. AndrW, J. Simon, *Molecular Semiconductors*, Springer-Verlag: Berlin, **1985**.
- [76]. T. J. Marks, *Angew. Chem.*, **1990**, 102, 886.
- [77]. N. B. McKeown, *J. Mater. Chem.*, **2000**, 10, 1979.
- [78]. C. W. Tang, *Appl. Phys. Lett.*, **1986**, 48, 183.
- [79]. M. K. Nazeeruddin, R. Humphry-Baker, M. Gratzel, B. A. Murrer, *Chem. Commun.* **1998**, 719.
- [80]. R. J. Mortimer, *Electrochim. Acta*, 44, 2971, **1999**.
- [81]. A. B. P. Lever, M. R. Hempstead, C. C. Leznoff, W. Liu, M. Melnik, W. A. Nevin, P. Seymour, *Pure Appl. Chem.*, **1986**, 58, 1467.
- [82]. J. D. Wright, *Prog. Surf. Sci.*, **1989**, 31, 1.
- [83]. D. Atilla, N. Saydan, M. Durmuş, A.G. Gürek, T. Khan, A. Rück, H. Walt, T. Nyokong, V. Ahsen, *J. Photochem. Photobiol., A: Chemistry*, 186 (2007) 298.
- [84]. S. Tuncel, F. Dumoulin, J. Gailer, M. Sooriyaarachchi, D. Atilla, M. Durmuş, D. Bouchu, H. Savoie, R.W. Boyle, V. Ahsen, *Dalton Trans*, **2011**, 40, 4067.
- [85]. Y. Zorlu, F. Dumoulin, M. Durmuş, V. Ahsen, *Tetrahedron*, **2010**, 66, 3248.
- [86]. F. Dumoulin, M. Durmuş, V. Ahsen, T. Nyokong, *Coordination Chem. Rev.*, **2010**, 2792.

- [87]. T. Nyokong, V. Ahsen (Eds.), *Photosensitizers in Medicine, Environment, and Security*, ISBN: 978-90-481-3872-2, Springer Dordrecht Heidelberg London New York, **2012**.
- [88]. M. Hanack, H. Heckman, R. Polley, In *Methods in Organic Chemistry (Houben-Weyl)*; Schuman, E., Ed.; Georg Thieme Verlag: Stuttgart, **1998**; Vol. E 9d, pp 717-833.
- [89]. G. de laTorre, M. Nicolau, T. Torres, In *Supramolecular Photosensitive and Electroactive Materials*; Nalwa, H. S., Ed.; Academic Press: San Diego, CA, **2001**.
- [90]. H. S. Nalwa, T. Watanabe, S. Miyata, *Adv. Mater.* **1995**, 7, 754.
- [91]. C. Dhenaut, I. Ledoux, D. W. Samuel, J. Zyss, M. Bougandt, H. Le Bozec, *Nature* **1995**, 374, 339.
- [92]. S. Keinan, M. J. Therien, D.N. Beratan, W. Yang, *J. Phys. Chem. A*, **2008**, 112, 12203-12207
- [93]. M.J. Stillman, T.J. Nyokong, *Phtalocyanines, Properties and Applications*, Vol 4, eds. C.C. Leznoff and A.B.P. Lever VCH Weinheim, **1996**.
- [94]. J. S. Shirk, R. G. S. Pong, F. J. Bartoli, A. W. Snow, *Appl. Phys. Lett.* **1993**, 63, 1880
- [95]. R. Bonnett, *Chemical aspects of photodynamic therapy*, Gordon and Breach Science Publishers, Germany, **2000**
- [96]. F. R. Fan, L. R. Faulkner, *J. Am. Chem. Soc.* 101, **1979**, 4779.
- [97]. P. N. Prasad, D. J. Williams, *Introduction to Nonlinear Optical Effects in Molecules and Polymers*, New York, **1991**.
- [98]. B. Zhao, W. Q. Lu, Z. H. Zhou, Y. Wu, *J. Mater. Chem.* **2000**, 10, 1513.
- [99]. G. Alcaraz, L. Eunezat, O. Mongin, C. Katan, I. Ledoux, J. Zyss, M. Blanchard-Desce, M. Vaultier, *Chem. Commun.* **2003**, 2766
- [100]. D. J. Williams, *Angew. Chem., Int. Ed. Engl.*, **1984**, 23, 690
- [101]. F. Meyers, R. Marder, B. S. Pierce, J. L Bredas, *J. Am. Chem. Soc.* **1994**, 116, 10703-10714.
- [102]. G. Bourhill, J.-L. Bredas, L.-T. Cheng, S. R. Marder, F. Meyers, J. W. Perry, B. G. Tiemann, *J. Am. Chem. Soc.* **1994**, 116, 2619-2620.
- [103]. A. F. Garito, K. D. Singer, C. C. Teng, *Appl. Phys. Lett.* **1981**, 39, 1-26.
- [104]. S. J. Lalama, *Appl. Phys. Lett.* **1981**, 39, 940-942.

- [105]. A. E. Stiegman, E. Graham, K. J. Perry, L. R. Khundkar, L.-T. Cheng, J. W. Perry, *J. Am. Chem. Soc.* **1991**, 113, 7658-7666.
- [106]. D. N. Beratan, *In New Materials for Nonlinear Optics*, Washington, D. C., **1991**, pp 89-102.
- [107]. S. R. Marder, D. N. Beratan, L.-T. Cheng, *Science* **1991**, 252, 103-106.
- [108]. S. M. Risser, D. N. Beratan, S. R. Marder, *J. Am. Chem. Soc.* **1993**, 115, 7719-7728.
- [109]. D. J. Williams, *Angew. Chem., Int. Ed. Engl.*, **1984**, 23, 690.
- [110]. J. L. Oudar, D. S. Chemla, *J. Chem. Phys* **1977**, 66, 2664
- [111]. M. Barzoukas, M. Blanchard-Desce, D. Josse, J. M. Lehn, J. Zyss, *Chem. Phys.*, **1989**, 133, 323
- [112]. S. R. Marder, D. N. Beratan, L-T Cheng, *Science*, **1991**, 252, 103
- [113]. S. R. Marder, C. B. Gorman, B. G. Tieman, L-T, Cheng, *J. Am. Chem. Soc.*, **1993**, 115, 3006
- [114]. C. B. Gorman, S. R. Marder, *Proc. Natl. Acad. Sci. USA*, **1993**, 90, 11297
- [115]. S. R. Marder, J. W. Perry, B. G. Tiermann, C. B. Gorman, S. Gilmour, S. L. Biddle, G. Bourhill, *J. Am. Chem. Soc.*, **1993**, 115, 2524
- [116]. G. Bourhill, J.-L. Bredas, L.-T. Cheng, S. R. Marder, F. Meyers, J. W. Perry, B. G. Tiermann, *J. Am. Chem. Soc.*, **1994**, 116, 2619.
- [117]. V. P. Rao, A. K. Y. Jen, K. Y. Wong, K. J. Drost, *Chem. Commun.*, **1993**, 1118
- [118]. S. R. Marder, L.-T. Cheng, B. G. Tiermann, A. C. Frieddli, M. Blanchard-Desce, J. W. Perry, J. Skindhoy, *Science*, **1994**, 263, 511
- [119]. C. R. Moylan, R. D. Miller, R. J. Twieg, V. Y. Lee, I.-H. McComb, S. Ermer, S. M. Lovejoy, D. S. Leung, *Proc. SPIE-Int. Soc. Opt. Eng.*, **1995**, 2527, 150
- [120]. G. A. Lindsay, K. D. Singer, *Polymer for Second-Order Nonlinear Optics*, ACS Symp. Ser. 601, **1995**
- [121]. C. R. Moylan, S. A. Swanson, C. A. Walsh, J. I. Thackara, R. J. Twieg, R. D. Miller, V. Y. Lee, *Proc. SPIE-Int. Soc. Opt. Eng.*, **1993**, 2025, 192
- [122]. D. M. Burland, R. D. Miller, O. Reiser, R. J. Twieg and C. A. Walsh, *J. Appl. Phys.* **1992**, 71, 410
- [123]. D. M. Burland, R. D. Miller and C. A. Walsh, *Chem. Rev.*, **1994**, 94, 31.
- [124]. C. R. Moylan, R. J. Twieg, V. Y. Lee, S. A. Swanson, K. M. Betterson R. D. Miller, *J. Am. Chem. Soc.*, **1993**, 115, 12599

- [125]. V. P. Rao, A. K. Y. Jen and Y. Cai, *Chem. Commun.*, **1996**, 1237
- [126]. R. F. Shi, S. Yamada, M. H. Wu, Y. M. Cai, A. F. Garito, *Appl. Phys. Lett.*, **1993**, 63, 1173
- [127]. N.J. Long, *Angew. Chem., Int. Ed. Engl.*, **1995**, 35, 21.
- [128]. H. S. Nalwa, *Appl. Organomet. Chem.*, **1991**, 5, 349.
- [129]. T. Verbiest, S. Houbrechts, M. Kauranen, K. Clays, A. Persoons, *J. Mater. Chem.*, **1997**, 7(11), 2175-2189.
- [130]. J. A. Mata, E. Peris, I. Asselberghs, R. Van Boxel, A. Persoons, *New J. Chem.*, **2001**, 25, 299.
- [131]. M. L. H. Green, S. R. Marder, M. E. Thompson, J. A. Bandy, D. Bloor, P. V. Kolinsky, R. J. Jones, *Nature*, **1987**, 330, 360–362
- [132]. J. P. Morall, G. T. Dalton, M. G. Humphrey and M. Samoc, *Adv. Organomet. Chem.*, **2008**, 55, 61–136
- [133]. C. Calabrese, L. T. Chen, J. C. Green, S. R. Marder, W. Tam, *J. Am. Chem. Soc.*, **1991**, 113, 7227–7232
- [134]. L. T. Chen, W. Tam, S. H. Stevenson, G. R. Meredith, G. Riken and S. R. Marder, *J. Phys. Chem.*, **1991**, 95, 10631–10643
- [135]. A. Mata, E. Peris, I. Asselberghs, J. A. Mata, E. Peris, I. Asselberghs, R. Van Boxel, A. Persoons, *New J. Chem.*, 2001, 25, 1043–1046
- [136]. T. Verbiest, S. Houbrechts, M. Kauranen, K. Clays, A. Persoons, *J. Mater. Chem.*, **1997**, 7(11), 2175–2189
- [137]. J. C. Calabrese, L. T. Chen, J. C. Green, S. R. Marder and W. Tam, *J. Am. Chem. Soc.*, 113, 7227–7232 (1991).
- [138]. V. Alain, M. Blanchard-Desce, C.-T. Chen, S. R. Marder, A. Fort, M. Barzoukas, *Synth. Met.*, 1996, 81, 133–136
- [139]. B. J. Coe, J. A. Harris, I. Asselberghs, A. Persoons, J. C. Jeffery, L. H. Rees, T. Gelbrich, M. B. Hursthouse, *Dalton Trans.*, **1999**, 3617
- [140]. H. Le Bozec, T. Renouard, *Eur. J. Inorg. Chem.*, **2000**, 229–239
- [141]. E. Cariati, M. Pizzoti, D. Roberto, F. Tessore, R. Hugo, *Coord. Chem. Rev.*, **2006**, 250, 1210–1233
- [142]. D. R. Kanis, P. G. Lacroix, M. A. Ratner, T. J. Marks, *J. Am. Chem. Soc.*, **1994**, 116, 0089–10102
- [143]. D. W. Bruce, A. Thornton, *Mol. Cryst. Liq. Cryst.*, 1993, 231, 253–256

- [144]. M. J. G. Lesley, A. Woodward, N. J. Taylor, T. B. Marder, I. Cazenobe, I. Ledoux, J. Zyss, A. Thornton, D. W. Bruce, A. K. Kakkar, *Chem. Mater.*, **1998**, 10, 1355–1365
- [145]. D. Roberto, R. Ugo, F. Tessore, E. Lucenti, S. Quici, S. Vezza, P. C. Fantucci, I. Invernizzi, S. Bruni, I. Ledoux, J. Zyss, *Organometallics*, **2002**, 21, 161–170
- [146]. D. Roberto, R. Ugo, S. Bruni, E. Cariati, F. Cariati, P. C. Fantucci, I. Invernizzi, S. Quici, I. Ledoux, J. Zyss, *Organometallics*, **2000**, 19, 1775–1788
- [147]. P. G. Lacroix, *Eur. J. Inorg. Chem.*, **2001**, 339–348
- [148]. S. Di Bella, I. Fragala, I. Ledoux, T. J. Marks, *J. Am. Chem. Soc.*, **1995**, 117, 9481–9485
- [149]. S. Di Bella, I. Fragala, T. J. Marks, M. A. Ratner, *J. Am. Chem. Soc.*, **1996**, 118, 12747–12751
- [150]. P. G. Lacroix, S. Di Bella, I. Ledoux, *Chem. Mater.*, **1996**, 8, 541–545
- [151]. D.A. Li, M.A. Ratner, T.J. Marks, *J. Am. Chem. Soc.* **1998**, 110, 1707
- [152]. G. de la Torre, C. G. Claessens, T. Torres, *Eur. J. Org. Chem.* **2000**, 2821.
- [153]. M. S. Rodríguez-Morgade, G. de la Torre, T. Torres, In *Porphyrin and Phthalocyanine Handbook*; Academic Press: Boston, MA, **2003**, Vol 15
- [154]. C. C. Leznoff, A. B. P. Lever, *Phthalocyanine properties and applications*, ed., VCH, Cambridge, **1989, 1993, 1996**, vol. 1-4
- [155]. M. Hanack, H. Heckmann, R. Polley, *Methods of Organic Chemistry*, Stuttgart, **1998**, vol. E. 9d. P. 717.
- [156]. C. C. Leznoff and T.W. Hall, *Tetrahedron Lett.*, **1982**, 23, 3023
- [157]. A.M. McDonagh, M.G. Humphrey, M. Samoc, B. Luther-Davies, S. Houbrechts, T. Wada, H. Sasabe, A. Persoons, *Adv. Mater.* **1999**, 11, 1292
- [158]. B.R. Cho, S.J. Lee, S.H. Lee, K.H. Son, Y.H. Kim, I.-Y. Doo, Lee, Kang G.J., T.I. Lee, M. Y. K. Cho, S.-J. Jeon, *Chem. Mater.* **2001**, 13, 1438
- [159]. M. A. Diaz-Garcia, F. Agollo-Lopez, A. Sastre, B. del Rey, T. Torres, C. Dhenaut, I. Ledoux, J. Zyss, *Nonlinear Opt.*, **1996**, 15, 251
- [160]. A. Sastre, M. A. Diaz-Garcia, B. del Rey, C. Dhenaut, J. Zyss, I. Ledoux, F. Agullo-Lopez, T. Torres, *J. Phys. Chem.*, **1997**, 101, 9773
- [161]. H. Hoshi, T. Yamada, K. Ishikawa, H. Takezoe, A. Fukuda, *Phys. Rev. B: Condens. Matter* **1995**, 52, 12355

- [162]. Y. Liu, Y. Xu, D. Zhu, T. Wada, H. Sasabe, L. Liu, W. Wang, *Thin Solid Films*, **1994**, 244, 943
- [163]. Y. Liu, Y. Xu, D. Zhu, T. Wada, H. Sasabe, X. Zhao, X. Xie, *J. Phys. Chem.*, **1995**, 99, 6957
- [164]. Y. Liu, Y. Xu, D. Zhu, X. Zhao, *Thin Solid Films*, **1996**, 289, 282
- [165]. S. G. Liu, Y. -Q. Liu, Y. Xu, D. -B. Zhu, A. -C. Yu, X. -S. Zhao, *Langmuir*, **1998**, 14, 690
- [166]. Cheng, W. Tam, S. R. Marder, A. E. Stiegman, G. Rikken, C. W. Spangler, *J. Phys. Chem.* **1991**, 95, 10643
- [167]. G. de la Torre, T. Torres, *J. Porphyrins Phthalocyanines* **1997**, 1, 221.
- [168]. T. Torres, G. dela Torre, J. Garcia-Ruiz, *Eur. J. Org. Chem.* **1999**, 2323
- [169]. G. Rojo, G. de la Torre, J. Garcia-Ruiz, I. Ledoux, T. Torres, J. Zyss, F. Agullo-Lopez, *Chem. Phys.* **1999**, 245, 27
- [170]. M. Tian, T. Wada, H. Sasabe, *J. Heterocycl. Chem.* **1997**, 34, 171.
- [171]. M. Tian, T. Wada, H. Kimura-Suda, H. Sasabe, *Mol. Cryst. Liq. Cryst.* **1997**, 294, 271
- [172]. M. Tian, T. Wada, H. Kimura-Suda, H. Sasabe, *J. Mater. Chem.* **1997**, 7 861
- [173]. E. M. Maya, E. M. Garcia-Frutos, P. Vazquez, T. Torres, G. Martin, G. Rojo, F. Agullo-Lopez, R. H. Gonzalez-Jonte, V. R. Ferro, J. M. Garcia de la Vega, I. Ledoux, J. Zyss, *J. Phys. Chem. A*, **2003**, 107, 2110
- [174]. A. Sen, P. C. Ray, P. K. Das, V. Krishnan, *J. Phys. Chem.*, **1996**, 100, 19611.
- [175]. S. M. LeCours, H-W. Guan, S. G. DiMagno, C. H. Wang, M. J. Therien, *J. Am. Chem. Soc.*, **1996**, 118, 1497.
- [176]. S. Priyadarshy, T. M. J. Therien, D. N. Beratan, *J. Am. Chem. Soc.*, **1996**, 118. 1504
- [177]. I. D. L. Albert, T. J. Marks, M. A. Ratner, *Chem. Mater.*, **1998**, 10, 753
- [178]. K. S. Suslick, C. T. Chen, G. R. Meredith, L. T. Cheng, *J. Am. Chem. Soc.* **1992**, 114, 6928
- [179]. S. M. LeCours, H.-W. Guan, S. G. DiMagno, C. H. Wang and M. J. Therien, *J. Am. Chem. Soc.*, 1996, 118, 1497–1503
- [180]. M. Yeung, A. C. H. Ng, M. G. B. Drew, E. Vorpagel, E. M. Breitung, R. J. McMahon, D. K. P. Ng, *J. Org. Chem.*, **1998**, 63, 7143–7150
- [181]. G. Martin, M. V. Martinez-Diaz, G. de la Torre, I. Ledoux, T. Torres, F. Agullo-Lopez, J. Zyss, *Synth. Met.* **2003**, 139, 95–98

- [182]. L. R. Dalton, W. H. Steier, B. H. Robinson, C. Zhang, A. Ren, S. Garner, A. Chen, T. Londergan, L. Irwin, B. Carlson, L. Fifield, G. Phelan, C. Kincaid, J. Amend, A. Jen, *J. Mater. Chem.*, **1999**, 9, 1905.
- [183]. G. Knöpfle, R. Schlessler, R. Ducret and P. Gunter, *Nonlinear Opt.*, **1995**, 9, 143.
- [184]. H. M. Kim, B. R. Cho, *J. Mater. Chem.*, **2009**, 19, 7402-7409.
- [185]. G. P. Bartholomew, I. Ledoux, S. Mukamel, G. C. Bazan, J. Zyss, *J. Am. Chem. Soc.* **2002**, 124, 13480-13485.
- [186]. D. M. Burland, *Chem. Rev.* **1994**, 94, 1-278.
- [187]. I. Ledoux, J. Zyss, J. S. Siegel, J. Brienne, J. M. Lehn, *Chem. Phys. Lett.* **1990**, 172, 440-444.
- [188]. J. Zyss, *Octupolar Organic Systems in Quadratic Nonlinear Optics: Molecules and Materials. Nonlinear Opt.* **1991**, 1, 3-18.
- [189]. C. Lambert, G. Nöll, E. Schamlzlin, K. Meerholz and C. Brauchle, *Chem. Eur. J.*, **1998**, 4, 512.
- [190]. J. Zyss, I. Ledoux, *Chem. Rev.* **1994**, 94, 77.
- [191]. J. L. Bredas, F. Meyers, B. Pierce, J. Zyss, *J. Am. Chem. Soc.* **1992**, 114, 4928-4931.
- [192]. M. Joffre, D. Yaron, R. Silbey, J. Zyss, *J. Chem. Phys.* **1992**, 97, 5607-5615
- [193]. Y.-K. Lee, S.-J. Jeon, M. Cho, *J. Am. Chem. Soc.*, **1998**, 120, 10921
- [194]. W.-H. Lee, H. Lee, J.-A. Kim, J.-H. Choi, M. Cho, S.-J. Jeon and B. R. Cho, *J. Am. Chem. Soc.*, **2001**, 123, 10658.
- [195]. M. Cho, S.-Y. An, H. Lee, I. Ledoux and J. Zyss, *J. Chem. Phys.*, **2002**, 116, 9165.
- [196]. V. R. Thalladi, S. Brasselet, H.-C. Weiss, D. Blaser, A. K. Katz, H. L. Carrell, R. Boese, J. Zyss, A. Nangia, G. R. Desiraju, *J. Am. Chem. Soc.*, **1998**, 120, 2563
- [197]. V. Le Floch, S. Brasselet, J.-F. Roch, J. Zyss, B. T. Cho, S. H. Lee, S.-J. Jeon, M. Cho, K. S. Min and M. P. Suh, *Adv. Mater.*, **2005**, 17, 196.
- [198]. J. Brunel, O. Mongin, A. Jutand, I. Ledoux, J. Zyss, M. Blanchard-Desce, *Chem. Mater.*, **2003**, 15, 4139
- [199]. G. Alcaraz, L. Euzenat, O. Mongin, C. Katan, I. Ledoux, J. Zyss, M. Blanchard-Desce, M. Vaultier, *Chem. Commun.*, **2003**, 2766. 5

- [200]. B. R. Cho, S. J. Lee, S. H. Lee, K. H. Son, Y. H. Kim, J.-Y. Doo, G. J. Lee, T. I. Kang, Y. K. Lee, M. Cho, S.-J. Jeon, *Chem. Mater.*, **2001**, 13, 1438;
- [201]. B. R. Cho, S. B. Park, S. J. Lee, K. H. Son, S. H. Lee, M.-J. Lee, J. Yoo, Y. K. Lee, G. J. Lee, T. I. Kang, M. Cho, S.-J. Jeon, *J. Am. Chem. Soc.*, **2001**, 123, 6421
- [202]. B. R. Cho, M. J. Piao, K. H. Son, S. H. Lee, S. J. Yoon, S.-J. Jeon, M. Cho, *Chem. Eur. J.*, **2002**, 8, 3907
- [203]. B. R. Cho, K. Chajara, H. J. Oh, K. H. Son, S.-J. Jeon, *Org. Lett.*, **2002**, 4, 1703
- [204]. M. J. Lee, M. Piao, S. H. Lee, M.-Y. Jeong, K. M. Kang and S.-J. Jeon, *J. Mater. Chem.*, **2003**, 13, 1030
- [205]. H. C. Jeong, M. J. Piao, S. H. Lee, M.-Y. Jeong, K. M. Kang, G. Park, S.-J. Jeon and B. R. Cho, *Adv. Func. Mater.*, **2004**, 14, 64
- [206]. J. L. Oudar, D. S. Chemla, *J. Chem. Phys.*, **1977**, 66, 2664
- [207]. M. Barzoukas, M. Blanchard-Desce, D. Josse, J. M. Lehn, J. Zyss, *Chem. Phys.*, **1989**, 133, 323
- [208]. I. Ledoux, J. Zyss, J.S. Siegel, J. Brienne, J.-M. Lehn, *Chem Phys. Lett.*, **1990**, 172, 440.
- [209]. B.R. Cho, S. J. Lee, S. H. Lee, K. H. Son, Y. H. Kim, J. Y. Don, G. J. Lee, T. I. Kang, Y. K. Lee, M. Cho, S. J. Jeon, *Chem. Mater.*, **2001**, 13, 1438-1440.
- [210]. B.R. Cho, S. B. Park, S. J. Lee, K. H. Son, S. H. Lee, M. J. Lee, J. Yoo, Y. K. Lee, K. J. Lee, T. I. Kang, M. Cho, S. J. Jeon, *J. Am. Chem. Soc.* **2001**, 123, 6421-6422.
- [211]. P. C. Ray, P. K. Das, *Chem. Phys. Lett.*, **1995**, 244, 153-156
- [212]. C. Lambert, G. Noll, E. Schmalzlin, K. Meerholz, C. Brauchle, *Chem. Eur. J.*, **1998**, 4, 2129;
- [213]. C. Lambert, W. Gaschler, E. Schmalzlin, K. Meerholz, C. Brauchle, *J. Chem. Soc. Perkin Trans.*, **1999**, 2, 577;
- [214]. J. Brunel, O. Mongin, A. Jutand, I. Ledoux, J. Zyss, M. Blanchard-Desce, *Chem. Mater.*, **2003**, 15, 4139
- [215]. Y.-K. Lee, S.-J. Jeon, M. Cho, *J. Am. Chem. Soc.*, **1998**, 120, 10921;
- [216]. B. R. Cho, K. Chajara, H. J. Oh, K. H. Son, S.-J. Jeon, *Org. Lett.*, **2002**, 4, 1703;

- [217]. B. R. Cho, S. J. Lee, S. H. Lee, K. H. Son, Y. H. Kim, J.-Y. Doo, G. J. Lee, T. I. Kang, Y. K. Lee, M. Cho, S.-J. Jeon, *Chem.Mater.*, **2001**, 13, 1438;
- [218]. H. Le Bozec, T. Renouard, *Eur. J. Inorg.Chem.*, **2000**, 229.
- [219]. C. Dhenaut, I. Ledoux, I. D. W. Samuel, J. Zyss, M. Bourgault, H. Le Bozec, *Nature*, **1995**, 374, 339.
- [220]. T. Weyland, I. Ledoux, S. Brasselet, J. Zyss, C. Lapinte, *Organometallics*, **2000**, 19, 5235.
- [221]. A. M. McDonagh, M. G. Humphrey, M. Samoc, B. Luther-Davies, S. Houbrechts, T. W. Hiroyuki and S. A. Persoons, *J. Am. Chem. Soc.*, **1999**, 121, 1405.
- [222]. K. Se'ne'chal, L. Toupet, I. Ledoux, J. Zyss, H. Le Bozec and O. Maury, *Chem Commun.*, **2004**, 2180–2181
- [223]. N. Tancrez, C. Feuvrie, I. Ledoux, J. Zyss, L. Toupet, H. Le Bozec, O. Maury, *J. Am. Chem. Soc.* **2005**, 127, 13474–13475.
- [224]. K. Se'ne'chal-David, A. Hemeryck, N. Tancrez, L. Toupet, J. A. G. Williams, I. Ledoux, J. Zyss, A. Boucekkine, J.-P. Gue'gan, H. Le Bozec and O. Maury, *J. Am. Chem. Soc.*, 2006, 128, 12243–12255
- [225]. A. Sarkar, J. J. Pak, G. W. Rayfield, M. M. Haley, *J. Mater. Chem.* **2001**, 11, 2943
- [226]. M. Quintiliani, E. M. Garcia-Frutos, A. Gouloumis, P. Va'zquez, I. Ledoux, J. Zyss, C. G. Claessens, T. Torres, *Eur. J. Org. Chem.* **2005**, 3911.
- [227]. G. Rojo, G. Martin, F. Agulló-López, T. Torres, H. Heckman, M. Hanack, *J. Phys. Chem. B*, **2000**, 104, 7066
- [228]. C.G. Claessens, D. González-Rodríguez, T. Torres, *Chem. Rev.* **2002**, 102, 835
- [229]. A. Sastre, T. Torres, M.A. Díaz-García, F. Agulló-López, C. Dhenaut, S. Brasselet, I. Ledoux, J. Zyss, *J. Am. Chem. Soc.* **1996**, 118(11), 2746
- [230]. J. Zyss, I. Ledoux, S. Volkov, V. Chernyak, S. Mukamel, G. P. Bartholomew, G. C. Bazan, *J. Am. Chem. Soc.* **2000**, 122, 11956 -11962
- [231]. M. Blanchard-Desce, J.-B. Baudin, O. Ruel, L. Jullien, S. Brasselet, J. Zyss, *Optic. Mat.* **1998**, 9, 216.
- [232]. G. P. Bartholomew, G. C. Bazan, *J. Am. Chem. Soc.* **2002**, 125, 5183.
- [233]. G. P. Bartholomew, I. Ledoux, S. Mukamel, G.C. Bazan, J. Zyss *J. Am. Chem. Soc.* **2002**, 124, 13480-13485

- [234]. J. Zyss, C. Dhenaut, T. Chau Van, I. Ledoux, *Chem. Phys. Lett.* **1993**, 206, 409
- [235]. O. Maury, L. Viau, Katell Senechal, B. Corre, J.-P. Guegan, T. Renouard, I. Ledoux, J. Zyss, H. Le Bozec, *Chem. Eur. J.* **2004**, 10, 4454 – 4466
- [236]. G. Bottari, T. Torres, *Chem. Commun.* **2005**, 2668
- [237]. G. de la Torre, A. Gouloumis, P. Vázquez, T. Torres, *Angew. Chem. Int. Ed.* **2001**, 40(15), 2895
- [238]. M. Quintiliani, J. Pe´rez-Moreno, I. Asselberghs, P. Vazquez, K. Clays, T. Torres, *J. Phys. Chem. B*, **2010**, 114, 6309–6315
- [239]. R. L. Sutherland, *Handbook of Nonlinear Optics*, Marcel Dekker, New York, USA **2003**.
- [240]. S. K. Kurtz, T. J. Perry, *J. Phys.* **1968**, 39, 3768.
- [241]. S. D. Bella, *Chem. Soc. Rev.*, **2001**, 30, 355-366.
- [242]. T. Verbiest, S. Houbrechts, M. Kauranen, K. Clays, A. Persoons, *J. Mater. Chem.* **1997**, 7, 2175.
- [243]. K. D. Singer, A. F. Garito, *J. Chem. Phys.* **1981**, 75, 3572.
- [244]. J. L. Oudar, H. L. Person, *Opt. Comm.*, **1975**, 15, 258.
- [245]. M. O. Senge, M. Fazekas, E. G. A. Notares, W. J. Blau, M. Zawadzka, O. B. Locos, E. M. N. Mhuirheartaigh, *Adv. Mater.* **2007**, 19, 2737-2774.
- [246]. R. W. Terhune, P. D. Maker, C. M. Savage, *Phys. Rev. Lett.*, **1965**, 14, 681.
- [247]. K. Clays, A. Persoons. *Phys. Rev. Lett.*, **1991**, 66, 2980.
- [248]. T. Verbiest, K. Clays, A. Persoons, F. Meyers, J. L. Bredas, *Opt. Lett.*, **1993**, 18, 225.
- [249]. J. Zyss, *Nonlinear Optics*, **1991**, 1, 3.
- [250]. J. Zyss, *J. Chem. Phys.*, **1993**, 98, 6583.
- [251]. J. Zyss, I. Ledoux, *Chem. Rev.*, **1994**, 94, 77.
- [252]. P. C. Ray, P. K. Das, *Chem. Phys. Lett.* **1992**, 44, 153.
- [253]. P. C. Ray, P. K. Das, *J. Phys. Chem.* **1995**, 99, 17891.
- [254]. P. C. Ray, P. K. Das, *Curr. Sci.* **1995**, 68, 526.
- [255]. P. C. Ray, P. K. Das, *J. Phys. Chem.* **1995**, 99, 14414.
- [256]. S. Stadler, G. Bourhill, C. Brauchle, *J. Phys. Chem.* **1996**, 100, 6927.
- [257]. C. C. Teng, A. F. Garito, *Phys. Rev. B*, **1983**, 28, 6766.
- [258]. F. L. Huysken, P. L. Huysken, A. Persoons, *J. Chem. Phys.* **1998**, 108, 8161.
- [259]. J. Zyss, T. Chauvan, C. Dhenaut, I. Ledoux, *Chem. Phys.*, **1993**, 177, 281.

- [260]. A. G. Gürek, T. Basova, D. Luneau, C. Lebrun, E. Koltsov, A. K. Hassan, V. Ahsen, *Inorg. Chem.* **2006**, *45*, 1667.
- [261]. T. E. Youssef, S. O'Flaherty, W. Blau, M. Hanack, *Eur. J. Org. Chem.* **2004**, 101,108.
- [262]. N.B. Subbotin, V. N. Nemykin, V. Z. Voloshin, *Mendeleev Commun.*, **1993**, 3, 12.
- [263]. N. Kobayashi, T. Ashida, K. Hiroya, T. Osa, *Chem. Lett.*, **1992**, 8, 1567.
- [264]. E. V. Kudrik, I. Yu. Nikolaev, G. P. Shaposhnikov, *Russ. Chem. Bull., Int. Ed.*, **2000**, *49*, 12.
- [265]. J. G. Young, W. Onyebuagu, *J. Org. Chem.*, **1990**, Vol. 55, 7,
- [266]. P. Stihler, B. Hauschel, M. Hanack, *Chem. Ber.* **1997**, 130, 801-806
- [267]. M. Back, B. Hauschel, M. Hanack, *Chem. Ber.* **1996**, 129, 237-242
- [268]. *Farbenfabriken Bayer*, US Patent 2,701,255, **1955**.
- [269]. J. Jiang, J. Xie, M. T. M. Choi, Y. Yan, S. Sun, D. K. P. Ng, *J. Porphyrins Phthalocyanines*, **1999**, 3, 322–328.
- [270]. W. Liu, J. Jiang, D. Du, D. P. Arnold, *Aust. J. Chem.* **2000**, 53, 131–135
- [271]. N. Ishikawa, Y. Kaizu, *Chem. Lett.* **1998**, 27, 183–184;
- [272]. D. Pernin, K. Haberoth, J. Simon, *J. Chem. Soc. Perkin Trans.*, **1997**, 1265–1266
- [273]. N. Sheng, R. Li, C.-F. Choi, W. Su, D. K. P. Ng, X. Cui, K. Yoshida, N. Kobayashi, J. Jiang, *Inorg. Chem.* **2006**, 45, 3794.
- [274]. S. Kyatskaya, J. R. G. Mascaros, L. Bogani, F. Hennrich, M. Kappes, W. Wernsdorfer, M. Ruben, *J. Am. Chem. Soc.* **2009**, 131, 15143.
- [275]. J. Jiang, R. C. W. Liu, T. C. W. Mak, T. W. D. Chan, D. K. P. Ng, *Polyhedron*, **1997**, 16, 515.
- [276]. V. E. Pushkarev, A. V. Ivanov, I. V. Zhukov, E. V. Shulishov, Yu. V. Tomilov, *Russ. Chem. Bull., Int. Ed.*, **2004**, *3*, 554.
- [277]. Y. G. Gorbunova, L. A. Lapkina, S. V. Golubeva, V. E. Larchenko, A. Yu. Tsivadze, *Mendeleev Commun.* **2001**, 11(6), 214.
- [278]. L.A. Lapkina, Y. G. Gorbunova, S. E. Nefedov, A. Y. Tsivadze, *Rus. Chem. Bul.* **2003**, 52, 7 1633.
- [279]. J. G. Young, W. Onyebuagu, *J. Org. Chem.*, **1990**, 55(7), 2155
- [280]. Y. Bian, R. Wang, D. Wang, P. Zhu, R. Li, J. Dou, W. Liu, C.-F. Choi, H.-S. Chan, C. Ma, D. K. P. Ng, J. Jiang, *Helv. Chim. Acta* **2004**, 87, 2581.

- [281]. K. M. Kadish, M. K. Smith, R. Guillard, *Handbook of Porphyrin Science*, **2011**, V.14.
- [282]. R. Weiss, J. Fischer, *Lanthanide Phthalocyanine Complexes. In The Porphyrin Handbook*, **1999**; Vol. 16, pp 171.
- [283]. T. Nyokong, Z. Gasyna, M. Stillman, *J. Inorg. Chem.* **1987**, 26, 1087-1095
- [284]. A. B. P. Lever, *Adv. Inorg. Radiochem.* **1965**, 7, 27-114.
- [285]. M.J. Stillman, T.J. Nyokong, *Phthalocyanines, Properties and Applications*, **1996**, Vol 4.
- [286]. K. M. Kadish, M. K. Smith, R. Guillard, *The Porphyrin Handbook*, **2003**, V.14.
- [287]. E. Orti, J. L. Bredas, C. Clarisse, *J. Chem. Phys.*, **1990**, 92, 1228.
- [288]. F. Lu, *Polyhedron*, **2007**, 26, 3939.
- [289]. S. Cotton, *Lanthanide and actinide chemistry*, Wiley, **2006**.
- [290]. J. W. Buchler, P. Hammerschmitt, I. Kaufeld, J. Lattler, *Chem. Ber.* **1991**, 124, 2151.
- [291]. A. De Cian, M. Moussavi, J. Fisher, R. Weiss, *Inorg. Chem.* **1985**, 24 (20), 3162.
- [292]. A. G. Gürek, V. Ahsen, D. Luneau, J. Pecaut, *Inorg. Chem.* **2001**, 40 (18), 4793.
- [293]. N. Koike, H. Uekusa, Y. Ohashi, C. Harnood, F. Kitamura, T. Ohsaka, K. Tokuda, *Inorg. Chem.* **1996**, 35, 5798.
- [294]. A. N. Darovskikh, A. K. Tsytsenko, O. V. Frank-Kamenetskaya, V. S. Fundamenski, P. N. Moskalev, *Kristallografiya*, **1984**, 29, 455-461
- [295]. M. A. Pauleya, C. H. Wang, *Review of Scien. Instru.* **1999**, 70, 2
- [296]. J. Zyss, T. Chauvan, C. Dhenaut, I. Ledoux, *Chem. Phys.*, **1993**, 177, 281.
- [297]. G. P. Bartholomew, I. Ledoux, S. Mukamel, G. C. Bazan, J. Zyss, *J. Am. Chem. Soc.* **2002**, 124, 13480.
- [298]. T. Ishizuka, L. E. Sinks, K. Song, S.-T. Hung, A. Nayak, K. Clays, M. J. Therien, *J. Am. Chem. Soc.* **2011**, 133 (9), 2884.
- [299]. K. Senechal, L. Toupet, J. Zyss, I. Ledoux, H.; Le Bozec, O. Maury, *Chem. Commun.* **2004**, 2180-2181.
- [300]. N. Tancrez, C. Feuvrie, I. Ledoux, J. Zyss, Loic Toupet, H. Le Bozec, O. Maury, *J. Am. Chem. Soc.* **2005**, 127, 13474-1347
- [301]. J.L. Oudar, *J. Chem. Phys.* **1977**, 67, 446.

- [302]. A. Fischer, C. Cremer, E.H.K. Stelzer, *Appl. Opt.* **1995**, 34
- [303]. M.A. Pauley, C.H. Wang, *Chemical Physics Letters* **1997**, 280, 544–550
- [304]. J. S. Shirk, J. R. Lindle, F. J. Bartoli, M. E. Boyle, *J. Phys. Chem.* **1992**, 96, 5847-5852
- [305]. P. N. Moskalev, I. S. Kirin, *Opt. Spectrosc.* **1970**, 220.
- [306]. F. Castaneda, C. Piechocki, V. Plichon, J. Simon, J. Vaxiviere, *Electrochim. Acta*, **1986**, 31, 131.
- [307]. K. M. Kadish, M. K. Smith, R. Guillard, *The Porphyrin Handbook*, **2003**, V.16
- [308]. Y. Liu, K. Shigehara, A. Yamada, *Thin Solid Films* **1989**, 179, 303.
- [309]. J. Janczak, R. Kubiak, *Acta Cryst. C*, **1995**, 2039.
- [310]. M. Bouvet, P. Bassoul, J. Simon, *Mol. Cryst. Liq. Cryst.* **1994**, 252, 31.
- [311]. C. Clarisse, M. T. Riou, *Inorg. Chim. Acta.* 1981, 53, L241-L243.
- [312]. J. Jiang, R. C. W. Liu, T. C. W. Mak, T. W. D. Chan, D. K. P Ng, *Polyhedron* **1997**, 16, 3, 515.
- [313]. Y. Arslanoğlu, A. M. Sevim, E. Hamuryudan, A. Gül, *Dyes and Pigments*, **2006**, 68, 129.
- [314]. A. G. Gürek, Ö. Bekaroğlu, *J. Chem. Soc., Dalton Trans.* **1994**, 1419.
- [315]. *Farbenfabriken Bayer*, US Patent 2,701,255, **1955**.
- [316]. L.A. Lapkina, E.a Niskanene, H. Rönkkömaki, V. E. Larchenco, K. I. Popov, A. Yu. Tsivadze. *J. Porphyrins and Phthalocyanines*, **2000**, 4, 588.
- [317]. V. E. Pushkarev, A.Yu. Tolbin, N. E. Borisova, S. A. Trashin, L. G. Tomilova. *Eur. J. Inorg. Chem.* **2010**, 5254.
- [318]. C. Clarisse, M. T. Riou, *Inorg. Chim. Acta*, **1987**, 130, 139.

ANNEX-1

The UV-NIR spectra of all complexes were carried out by SHIMADZU UV-VIS-NIR Spectrophotometer UV-3600.

Since, most classical organic solvents are not transparent at near-IR, chloroform was used as solvent for the UV-NIR measurements. The measurements were carried out in same concentration (1×10^{-5} M) to avoid concentration effects.

While, the oxidized forms were carried out by adding bromine in CHCl_3 to 10 mL of a CHCl_3 solution of complexes, the reduced forms were prepared by adding 3 mg of NaBH_4 to 10 mL of a solution of complexes in THF/ CHCl_3 (1/10).

UV-NIR Spectra of $\text{Ln}(\text{Pc})_2$

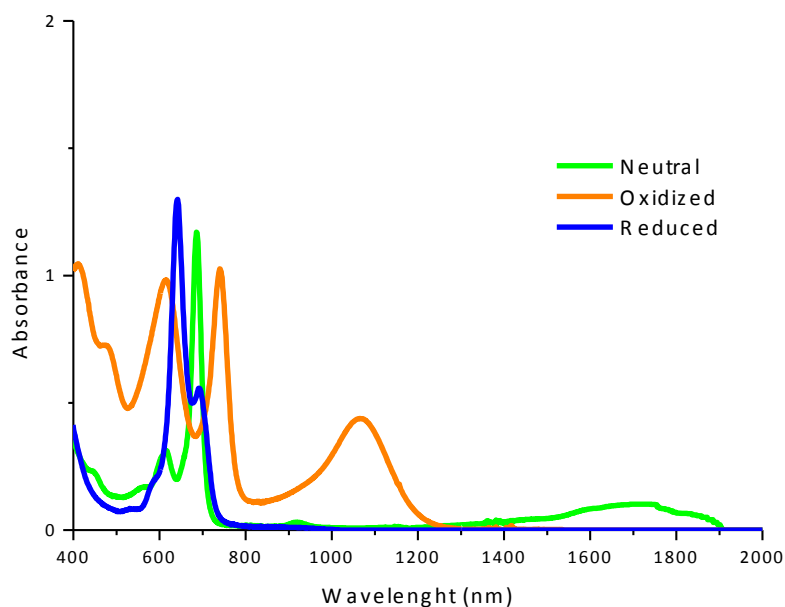


Figure ANNEX1.1. UV-NIR spectra of ABAB bis(phthalocyaninato) europium(III) complex ($\text{Eu}(\text{ABAB})_2(7)$) (1×10^{-5} M)

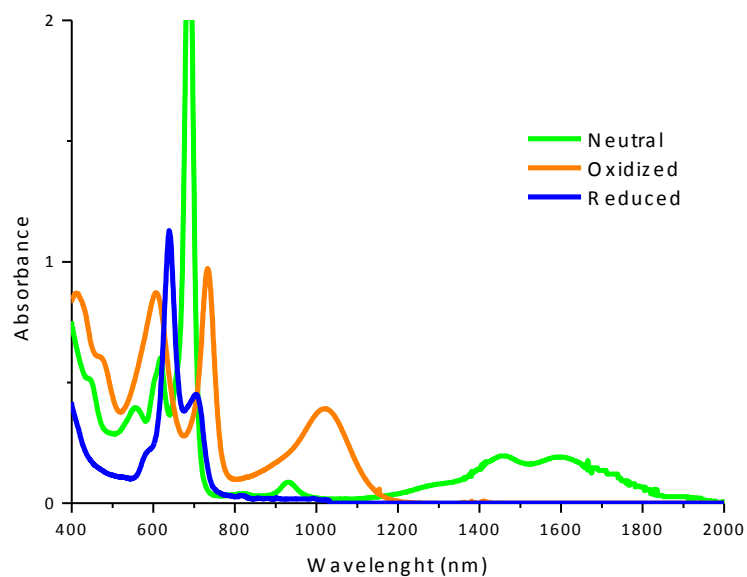


Figure ANNEX1.2. UV-NIR spectra of ABAB bis(phthalocyaninato) dysprosium(III) complex (Dy(ABAB)₂)(8) (1×10^{-5} M)

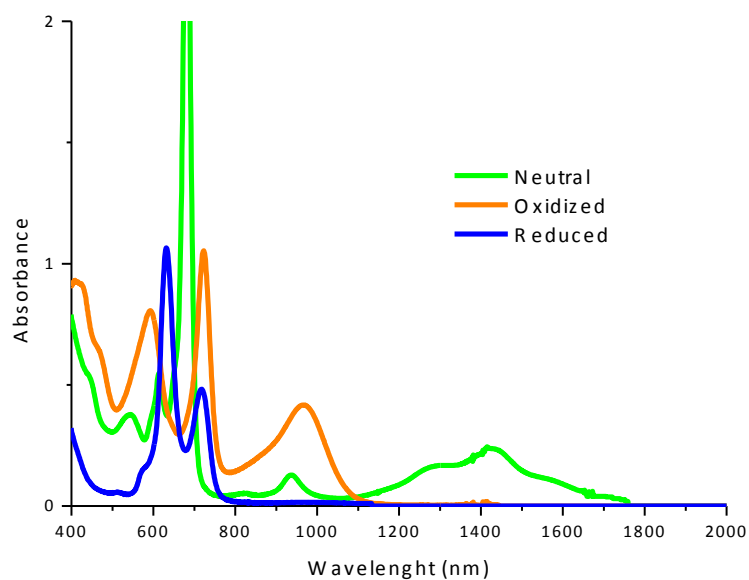


Figure ANNEX1.3. UV-NIR spectra of ABAB bis(phthalocyaninato) lutetium(III) complex (Lu(ABAB)₂)(9) (1×10^{-5} M)

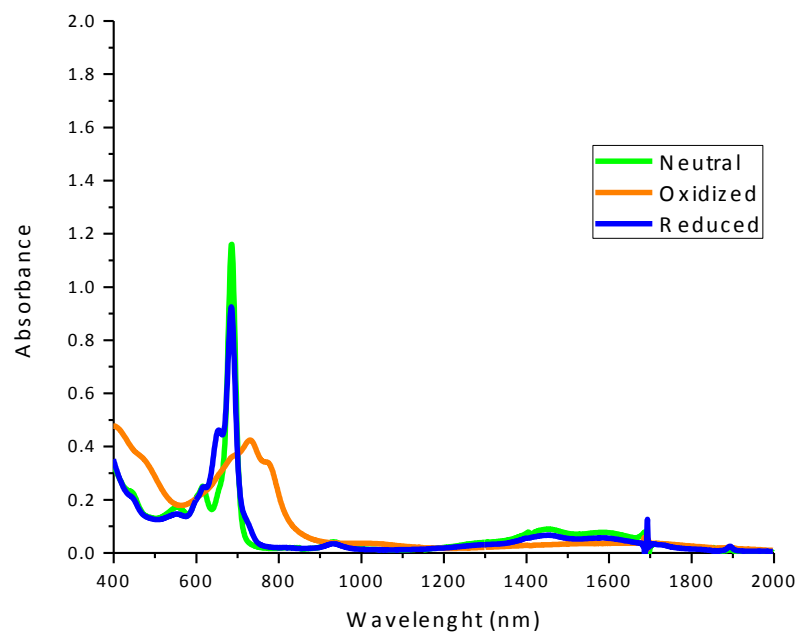


Figure ANNEX1.4. UV-NIR spectra of ABAB bis(phthalocyaninato) yttrium(III) complex ($\text{Y}(\text{ABAB})_2(\mathbf{10})$) ($1 \times 10^{-5} \text{ M}$)

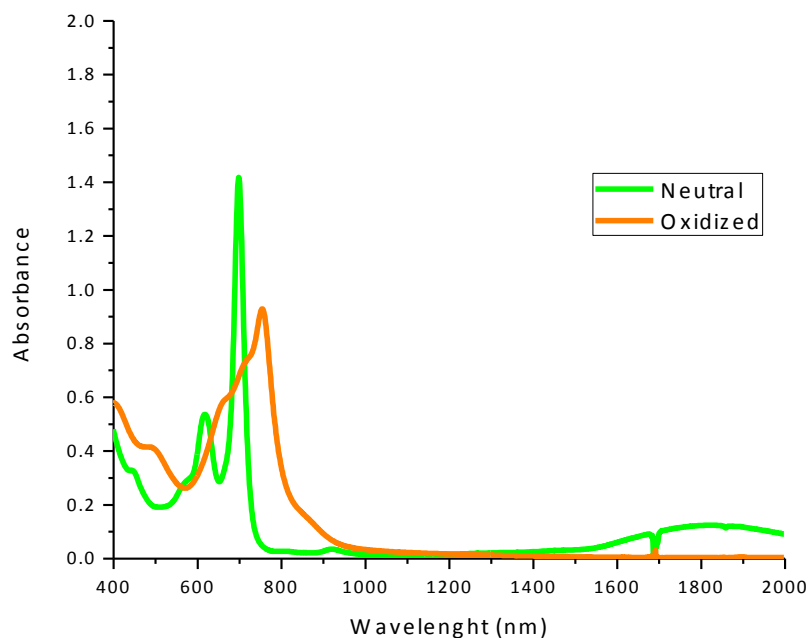


Figure ANNEX1.5. UV-NIR spectra of ABAB bis(phthalocyaninato) neodymium(III) complex ($\text{Nd}(\text{ABAB})_2(\mathbf{11})$) ($1 \times 10^{-5} \text{ M}$)

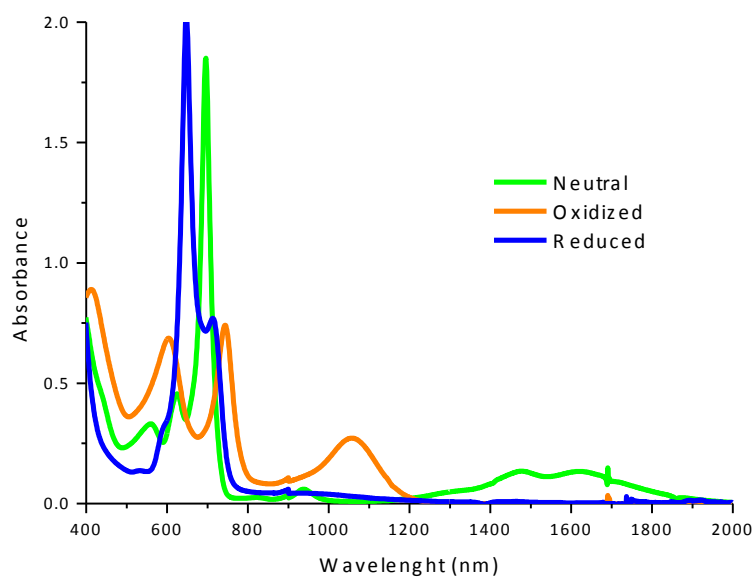


Figure ANNEX1.6. UV-NIR spectra of AB3 bis(phthalocyaninato) europium(III) complex ($\text{Eu}(\text{AB}3)_2$)(**12**) ($1 \times 10^{-5} \text{ M}$)

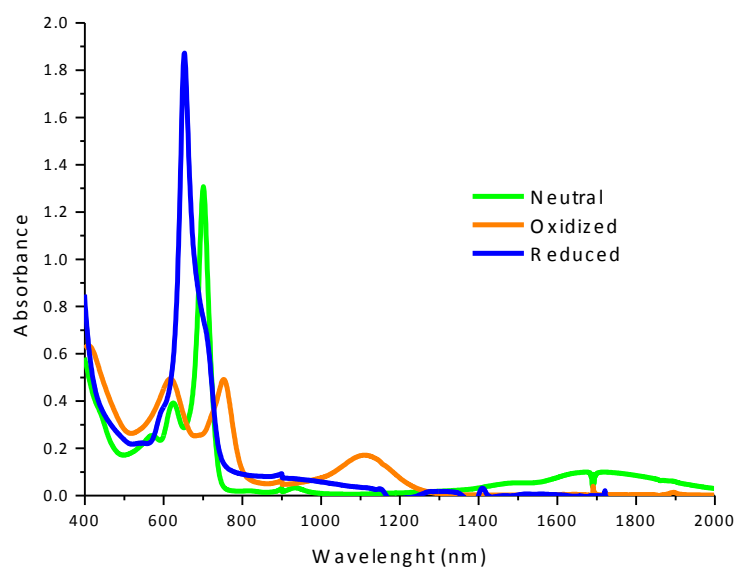


Figure ANNEX1.7. UV-NIR spectra of AB3 bis(phthalocyaninato) dysprosium(III) complex ($\text{Dy}(\text{AB}3)_2$)(**13**) ($1 \times 10^{-5} \text{ M}$)

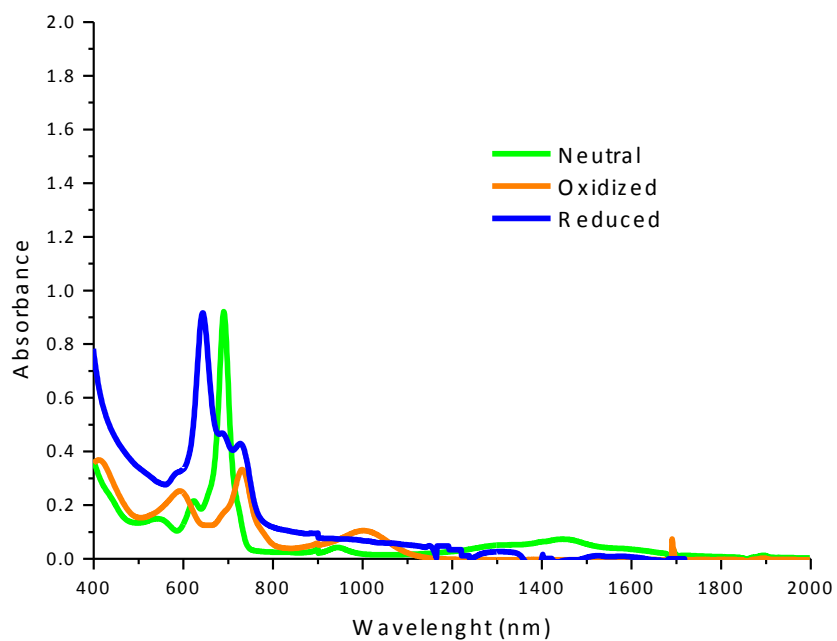


Figure ANNEX1.8. UV-NIR spectra of AB3 bis(phthalocyaninato) lutetium(III) complex (Lu(AB3)₂)(14) (1×10^{-5} M)

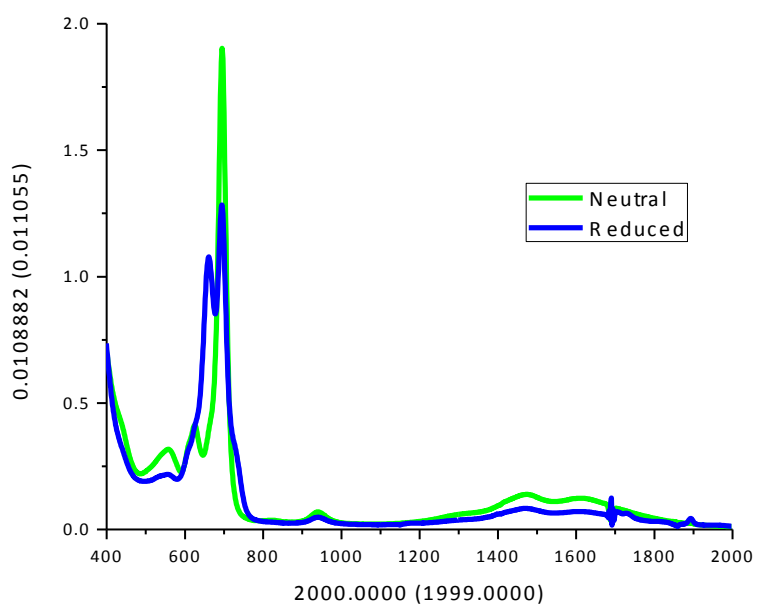


Figure ANNEX1.9. UV-NIR spectrum of AB3 bis(phthalocyaninato) yttrium(III) complex (Y(AB3)₂)(15) (1×10^{-5} M)

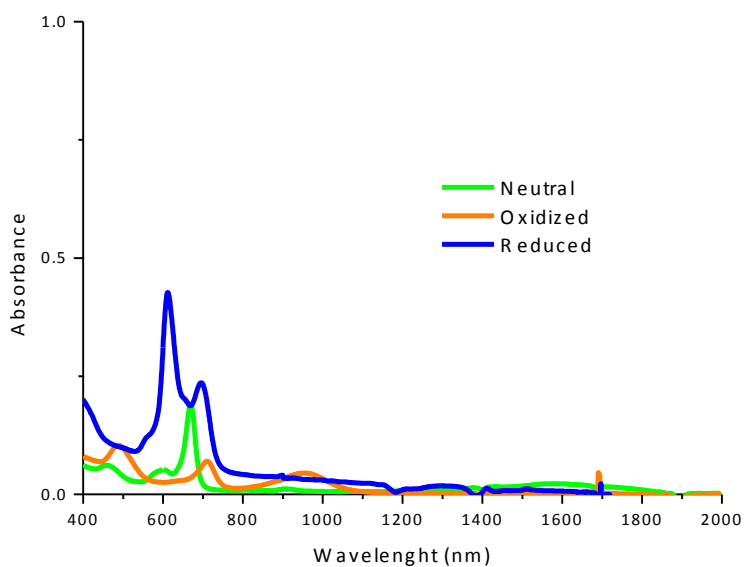


Figure ANNEX1.10. UV-NIR spectra of unsubstituted (A4) bis(phthalocyaninato) europium(III) complex (Eu(A₄)₂) (**16**)(1 x 10⁻⁵ M)

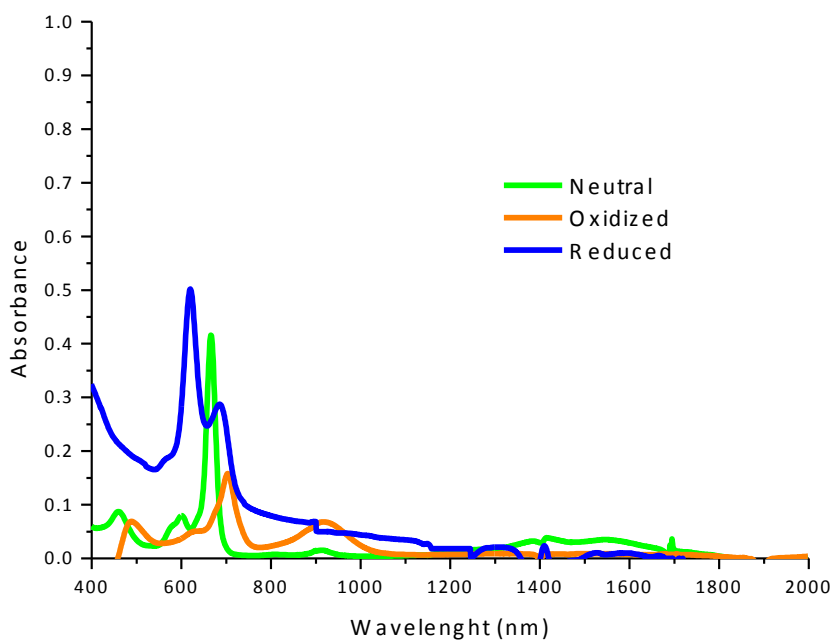


Figure ANNEX1.11. UV-NIR spectra of unsubstituted (A4) bis(phthalocyaninato) dysprosium(III) complex (Dy(A₄)₂)(**17**) (1 x 10⁻⁵ M)

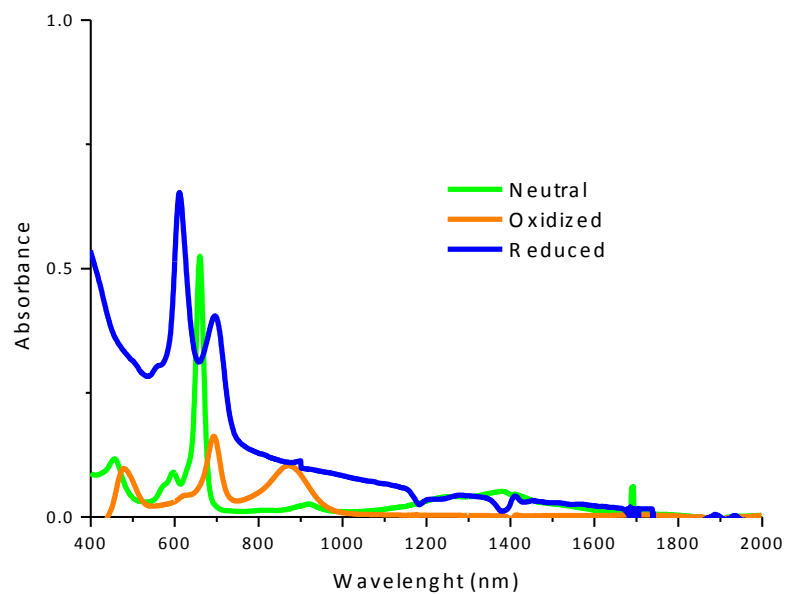


Figure ANNEX1.12. UV-NIR spectra of unsubstituted (A4) bis(phthalocyaninato) lutetium(III) complex (Lu(A₄)₂)(**18**) (1×10^{-5} M)

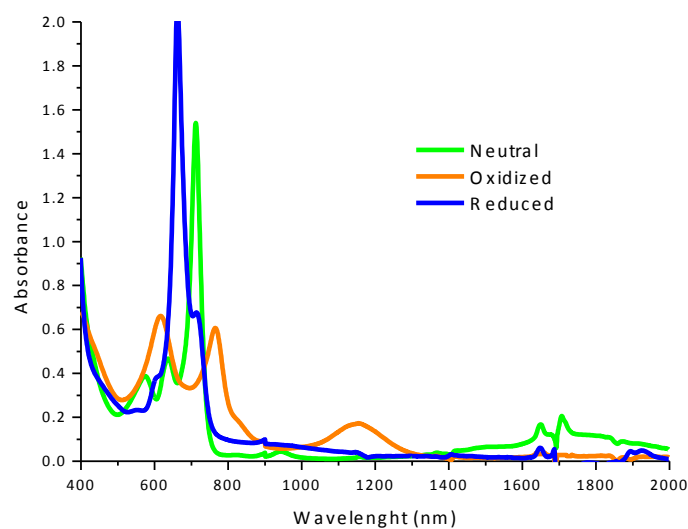


Figure ANNEX1.13. UV-NIR spectra of octahexylthia substituted (B4) bis(phthalocyaninato) europium(III) complex (Eu(B₄)₂)(**19**) (1×10^{-5} M)

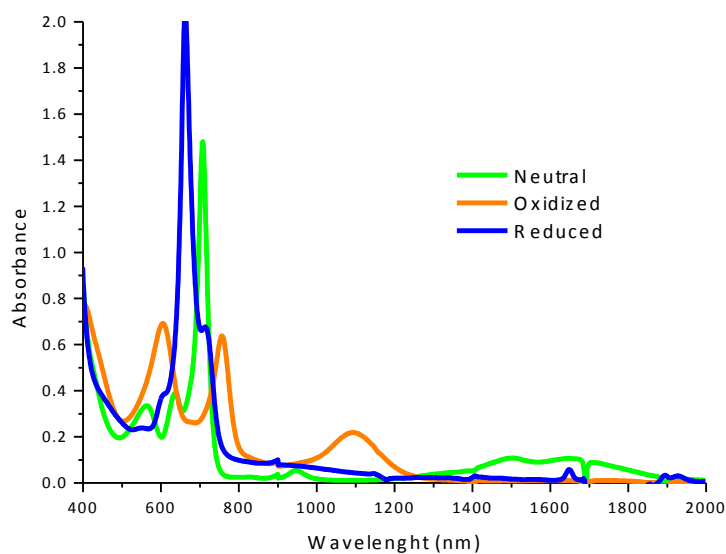


Figure ANNEX1.14. UV-NIR spectra of octahexylthia substituted (B4) bis(phthalocyaninato) dysprosium(III) complex ($\text{Dy}(\text{B}_4)_2(\mathbf{20})$) ($1 \times 10^{-5} \text{ M}$)

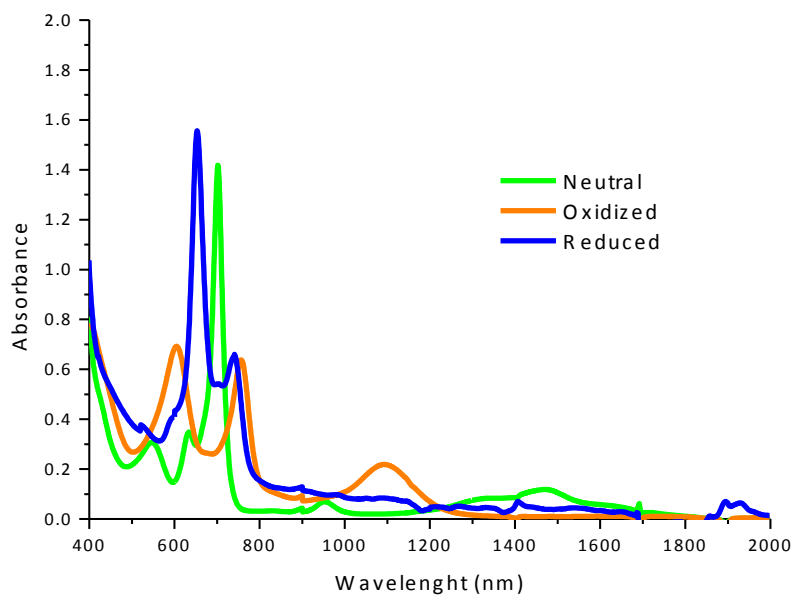


Figure ANNEX1.15. UV-NIR spectrum of octahexylthia substituted (B4) bis(phthalocyaninato) lutetium(III) complex ($\text{Lu}(\text{B}_4)_2(\mathbf{21})$) ($1 \times 10^{-5} \text{ M}$)

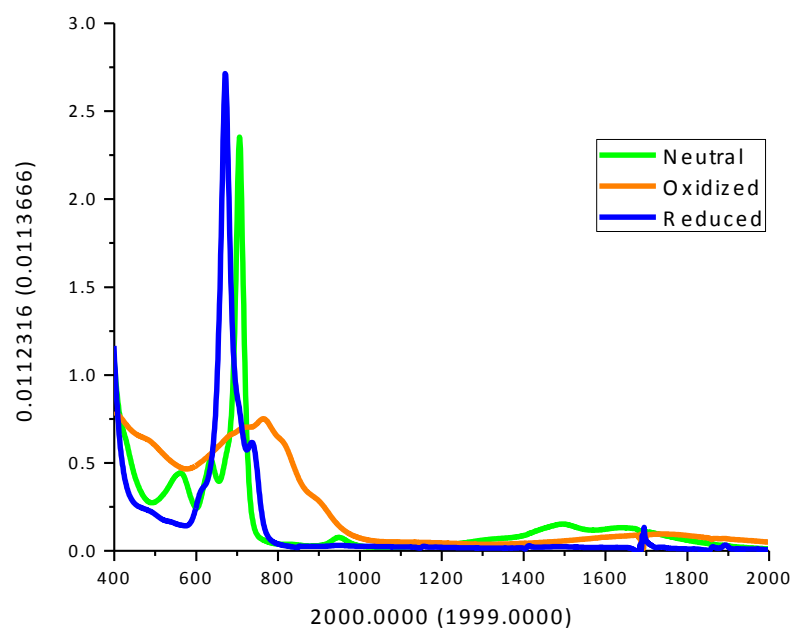


Figure ANNEX1.16. UV-NIR spectrum of octahexylthia substituted (B4) bis(phthalocyaninato) yttrium(III) complex (Y(B₄)₂)(**22**) (1×10^{-5} M)

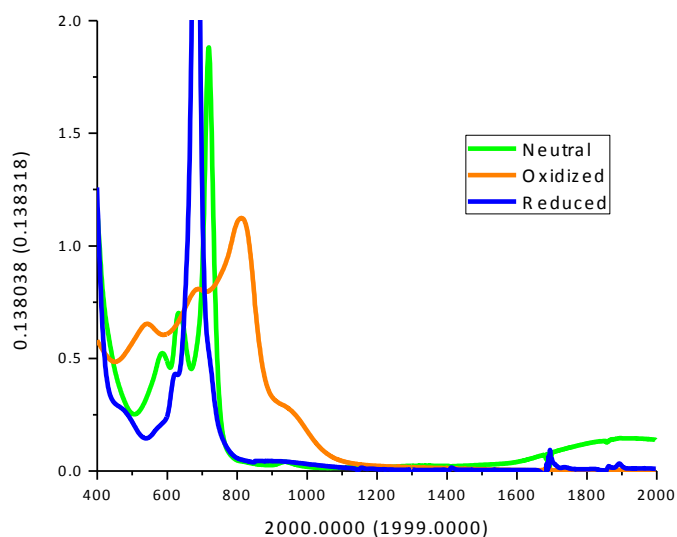


Figure ANNEX1.17. UV-NIR spectra of octahexylthia substituted (B4) bis(phthalocyaninato) neodymium(III) complex (Nd(B₄)₂)(**23**) (1×10^{-5} M)

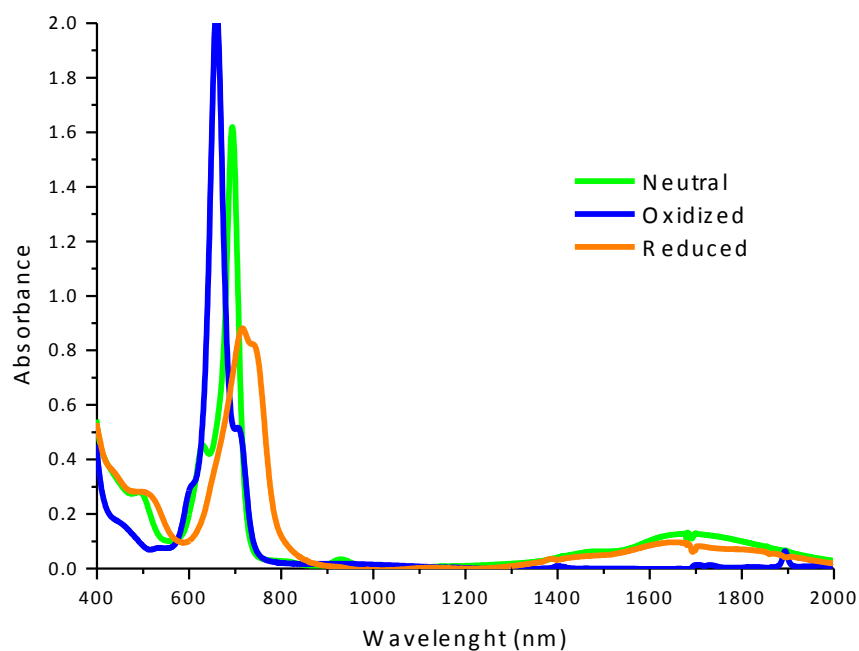


Figure ANNEX1.18. UV-NIR spectra of tetrahexylthia substituted (T4) bis(phthalocyaninato) europium(III) complex ($\text{Eu}(\text{T}_4)_2$)(**24**) ($1 \times 10^{-5} \text{ M}$)

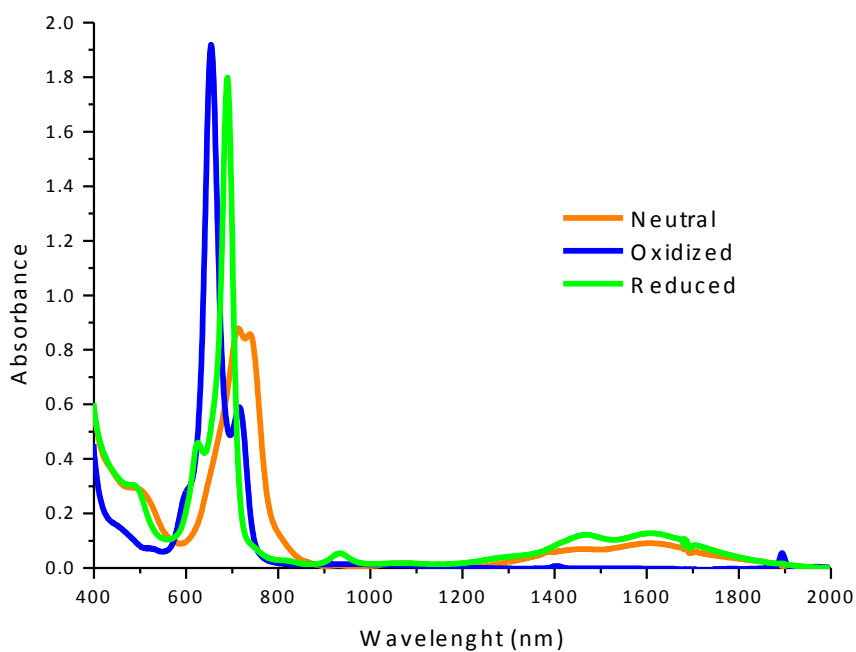


Figure ANNEX1.19. UV-NIR spectra of tetrahexylthia substituted (T4) bis(phthalocyaninato) dysprosium(III) complex ($\text{Dy}(\text{T}_4)_2$)(**25**) ($1 \times 10^{-5} \text{ M}$)

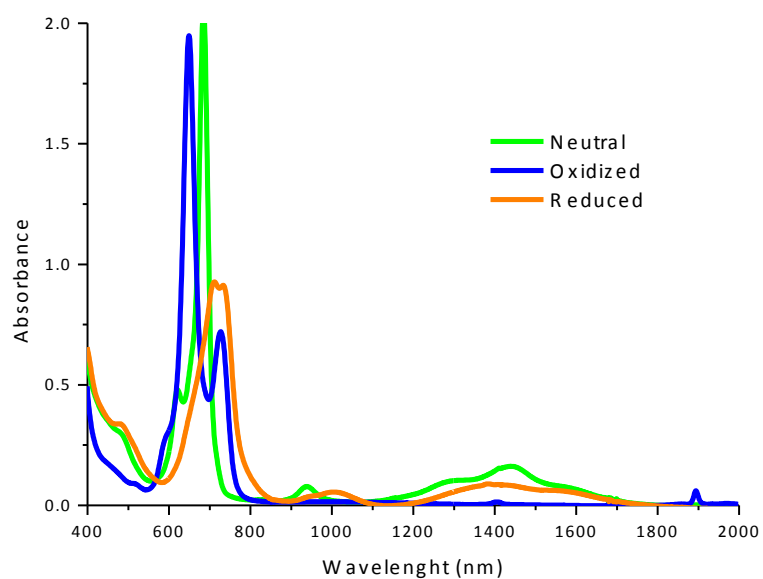


Figure ANNEX1.20. UV-NIR spectra of tetrahexylthia substituted (T4) bis(phthalocyaninato) lutetium(III) complex (Lu(T₄)₂)(**26**) (1×10^{-5} M)

ANNEX 2

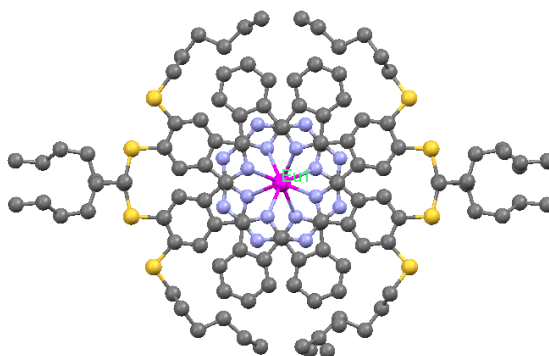
Single-crystal X-ray structure determination

A Suitable crystal was selected and mounted on a Gemini kappa-geometry diffractometer (Agilent Technologies UK Ltd) equipped with an Atlas CCD detector and using Mo radiation ($\lambda = 0.71073 \text{ \AA}$).

Intensities were collected at 100 K by means of the CrysAlisPro software [1]. Reflection indexing, unit-cell parameters refinement, Lorentz-polarization correction, peak integration and background determination were carried out with the CrysAlisPro software [1]. An analytical absorption correction was applied using the modeled faces of the crystal [2]. The structures were solved by direct methods with SIR97 and the least-square refinement on F^2 was achieved with the CRYSTALS software [3,4].

All non-hydrogen atoms were refined anisotropically. The hydrogen atoms were all located in a difference map, but those attached to carbon atoms were repositioned geometrically. The H atoms were initially refined with soft restraints on the bond lengths and angles to regularize their geometry (C---H in the range 0.93--0.98 \AA) and $U_{\text{iso}}(\text{H})$ (in the range 1.2-1.5 times U_{eq} of the parent atom), after which the positions were refined with riding constraints.

Table ANNEX2.1. Crystallographic data and structure refinement parameters for Eu(ABAB)₂ Bis(Phthalocyanine) (7)

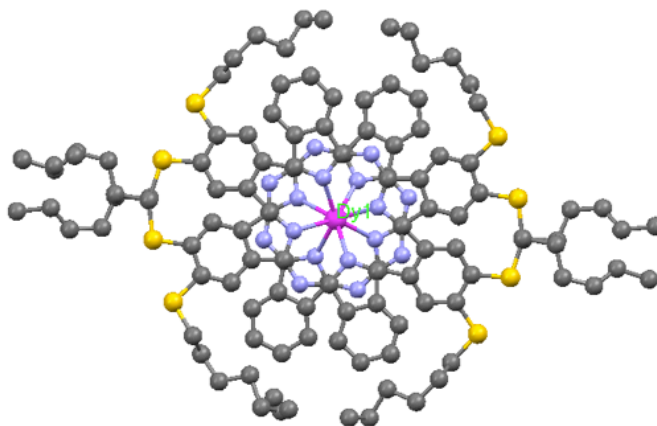


Formula	C₁₁₂H₁₂₈EuN₁₆S₈2(CHCl₃)
M.w. (g.mol⁻¹)	2106.81
Crystal System	Orthorhombic
Space group	Fddd
a(Å)	23.288 (1)
b(Å)	29.342 (2)
c(Å)	31.977 (1)
V(Å³)	21850(3)
Z	8
T(K)	110
λ(MoKα)(Å)	0.7107
Dx(Mg.m⁻³)	1.419
μ (mm⁻¹)	0.93
R[F₂ > 2σ(F₂)]	0.07
wR(F₂)	0.185

Table ANNEX2.2. Selected Distances (Å) and Angles (°) for Eu(ABAB)₂.

Eu–N2	2.424(4)
Eu–N6	2.446(4)
N2ⁱⁱ–Eu–N6	143.68(12)
N2–Eu–N2ⁱⁱ	144.26(17)
N6ⁱⁱ–Eu–N2	143.68(12)
N6ⁱ–Eu–N6ⁱⁱ	108.05(18)
Symmetry code:(i) 7/4-x, y, 3/4-z; (ii) x, 3/4-y, 3/4-z.	

**Table ANNEX2.3. Crystallographic data and structure refinement parameters
Dy(ABAB)₂ Bis(Phthalocyanine)(8)**



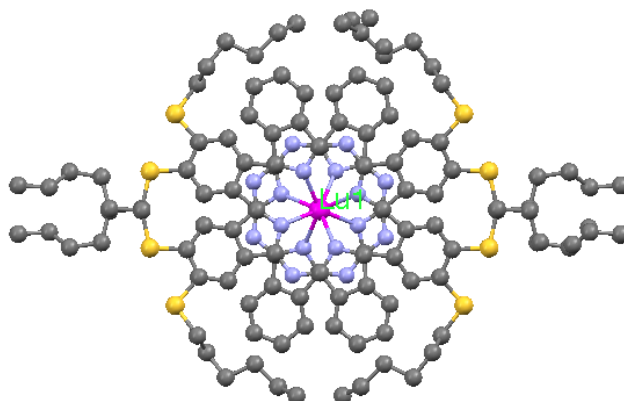
Formula	C ₁₁₂ H ₁₂₈ DyN ₁₆ S ₈ 2(CHCl ₃)
M.w. (g.mol ⁻¹)	2117.34
Crystal System	Orthorhombic
Space group	Fddd
a(Å)	23.144 (2)
b(Å)	29.482 (3)
c(Å)	32.219 (2)
V(Å ³)	21984(3)
Z	8
T(K)	100
λ(MoKα)(Å)	0.7107
D _x (Mg.m ⁻³)	1.421
μ (mm ⁻¹)	1.03
R[F ² > 2σ(F ²)]	0.058
wR(F ²)	0.163

Table ANNEX2.4. Selected Distances (Å) and Angles (°) for Dy(ABAB)₂ .

Dy–N2	2.410(3)
Dy–N6	2.410(3)
N2 ⁱⁱ –Dy–N6	143.37(11)
N2–Dy–N2 ⁱⁱ	82.99(16)
N6 ⁱⁱ –Dy–N2	143.37(11)
N6 ⁱ –Dy–N6 ⁱⁱ	110.38(16)

Symmetry code:(i) 7/4-x, y, 3/4-z; (ii) x, 3/4-y, 3/4-z.

**Table ANNEX2.5. Crystallographic data and structure refinement parameters
Lu(ABAB)₂ Bis(Phthalocyanine)(9)**



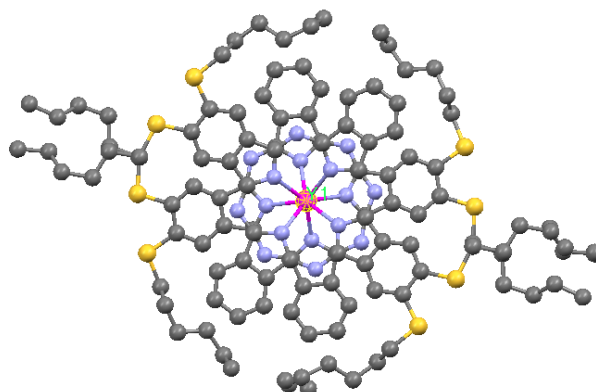
Formula	C₁₁₂H₁₂₈LuN₁₆S₈2(CHCl₃)
M.w. (g.mol⁻¹)	2129.81
Crystal System	Orthorhombic
Space group	Fddd
a(Å)	23.206 (5)
b(Å)	29.902 (5)
c(Å)	31.760 (5)
V(Å³)	21523(5)
Z	8
T(K)	100
λ(MoKα)(Å)	0.7107
D_x(Mg.m⁻³)	1.451
μ (mm⁻¹)	1.28
R[F₂ > 2σ(F₂)]	0.059
wR(F₂)	0.17

Table ANNEX2.6. Selected Distances (Å) and Angles (°) for Lu(ABAB)₂.

Lu–N2	2.366(4)
Lu–N6	2.356(4)
N2ⁱⁱ–Lu–N6	71.22(12)
N2–Lu–N2ⁱⁱ	11.29(17)
N6ⁱⁱ–Lu–N2	71.22(12)
N6ⁱ–Lu–N6ⁱⁱ	79.89(12)

Symmetry code:(i) 7/4-x, y, 3/4-z; (ii) x, 3/4-y, 3/4-z.

**Table ANNEX2.7. Crystallographic data and structure refinement parameters
Y(ABAB)₂ Bis(Phthalocyanine)(10)**



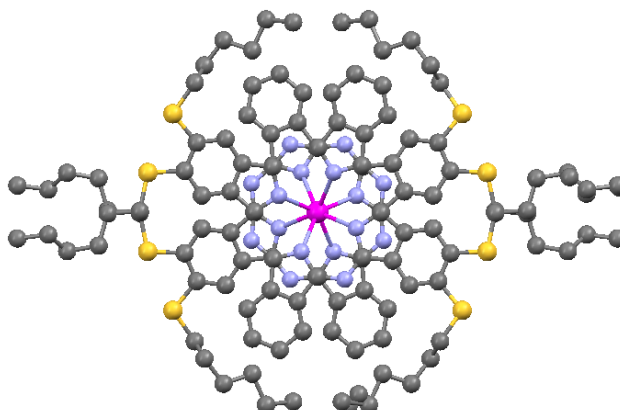
Formula	C₁₁₂H₁₂₈YN₁₆S₈2(CHCl₃)
M.w. (g.mol⁻¹)	2043.75
Crystal System	Orthorhombic
Space group	Fddd
a(Å)	23.206 (5)
b(Å)	29.902 (5)
c(Å)	31.760 (5)
V(Å³)	21523(5)
Z	8
T(K)	100
λ(MoKα)(Å)	0.7107
D_x(Mg.m⁻³)	1.451
μ (mm⁻¹)	1.28
R[F₂ > 2σ(F₂)]	0.059
wR(F₂)	0.17

Table ANNEX2.8. Selected Distances (Å) and Angles (°) for Y(ABAB)₂.

Y–N2	2.400(3)
Y–N6	2.400(3)
N2ⁱⁱ–Y–N6	71.47(10)
N2–Y–N2ⁱⁱ	110.78(13)
N6ⁱⁱ–Y–N2	71.47(10)
N6ⁱ–Y–N6ⁱⁱ	142.95(13)

Symmetry code:(i) 7/4-x, y, 3/4-z; (ii) x, 3/4-y, 3/4-z.

**Table ANNEX2.9. Crystallographic data and structure refinement parameters
Nd(ABAB)₂ Bis(Phthalocyanine)(11)**



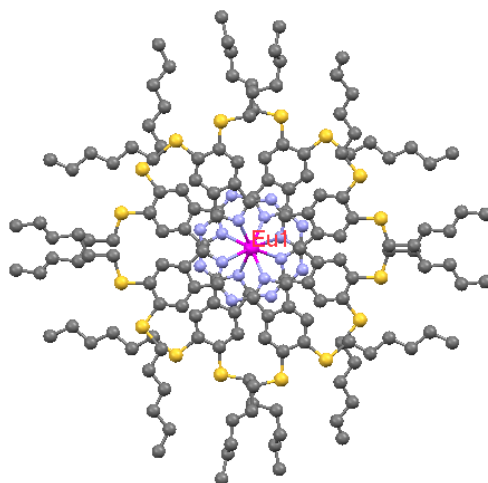
Formula	C₁₁₂H₁₂₈NdN₁₆S₈2(CHCl₃)
M.w. (g.mol⁻¹)	2099
Crystal System	Orthorhombic
Space group	Fddd
a(Å)	23.275 (5)
b(Å)	29.404 (5)
c(Å)	31.015 (5)
V(Å³)	21226(5)
Z	8
T(K)	100
λ(MoKα)(Å)	0.71069
D_x(Mg.m⁻³)	1.456
μ (mm⁻¹)	0.86
R[F₂ > 2σ(F₂)]	0.089
wR(F₂)	0.191

Table ANNEX2.10. Selected Distances (Å) and Angles (°) for Nd(ABAB)₂.

Nd–N2	2.421(4)
Nd –N6	2.470(4)
N2ⁱⁱ– Nd –N6	144.35(13)
N2– Nd –N2ⁱⁱ	144.14(18)
N6ⁱⁱ– Nd –N2	144.35(13)
N6ⁱ– Nd –N6ⁱⁱ	145.07(16)

Symmetry code:(i) 7/4-x, y, 3/4-z; (ii) x, 3/4-y, 3/4-z.

**Table ANNEX2.11. Crystallographic data and structure refinement parameters
Eu(B4)₂ Bis(Phthalocyanine)(19)**



Formula	C₁₆₀H₂₂₄EuN₁₆S₁₆2(CHCl₃)
M.w. (g.mol⁻¹)	3036.60
Crystal System	Monoclinic
Space group	C2/c
a(Å)	30.417 (2)
b(Å)	32.877 (2)
c(Å)	20.2030 (14)
V(Å³)	16301.3(18)
Z	4
T(K)	293
λ(MoKα)(Å)	0.71073
D_x(Mg.m⁻³)	1.237
μ (mm⁻¹)	0.64
R[F₂ > 2σ(F₂)]	0.047
wR(F₂)	0.131

Table ANNEX2.12. Selected Distances (Å) and Angles (°) for Eu(B4)₂.

Eu–N3	2.433(2)
Eu –N7	2.437(2)
N3– Eu –N7	107.90(8)
N3– Eu –N3ⁱ	143.72(10)
N7ⁱ– Eu –N3	84.66(8)
N7– Eu –N7ⁱ	141.85(10)

Symmetry code:(i) –x,y,-z+1/2

References.

- [1] CrysAlisPro, Agilent Technologies, Version 1.171.34.49 (release 20-01-2011 CrysAlis171 .NET) (compiled Jan 20 2011,15:58:25)
- [2] Clark, R. C. & Reid, J. S. (1995). *Acta Cryst.* A51, 887-897.
- [3] Altomare, A.; Burla, M.C.; Camalli, M.; Cascarano, G. L.; Giacovazzo, C.; Guagliardi, A.; Grazia, A.; Moliterni, G.; Polidori, G.; Spagna, R. *J. App. Cryst.* 1999, 32, 115-119.
- [4] Betteridge, P.W.; Carruthers, J. R.; Cooper, R. I.; Prout, K.; Watkin, D. J. *J. Appl. Cryst.* 2003, 36, 1487.

ANNEX 3

Hyper-Rayleigh Scattering (HRS) Instrumental Setup:

The experimental HRS apparatus that we used to measure the quadratic hyperpolarizabilities presented in **Fig. ANNEX3.1** were performed in collaboration with the Laboratory of Quantum and Molecular Photonics where is a joint research unit of CNRS dependent INSIS and Ecole Normale Supérieure de Cachan under the supervision of Prof. Dr. Isabelle Ledoux-Rak and Prof. Dr. Joseph Zyss.

The HRS experiments have been performed at 1910 nm, using a commercial (SAGA from Thales Laser) Q-switched Nd³⁺: YAG nanosecond laser operating at $\lambda = 1064$ nm, 10 Hz repetition rate and pulsed duration is 9 ns. The 1064 nm laser beam then enter into the 50 cm long hydrogen Raman cell of high pressure (H₂ at 55 atm.) which shifts the fundamental beam to $\lambda = 1910$ nm (only the back scattered 1910 nm Raman emission was collected at a 45° incidence angle by use of a dichroic mirror in order to eliminate most of the residual 1064 nm pump photons. A Schott RG 1000 filter was used to filter out any remaining visible light from the laser flash lamp. The intensity of the incoming fundamental beam was varied using a half-wave plate rotated between two crossed polarizers. HRS photons at 955 nm are focused onto a photomultiplier using two collecting lenses. The detected signal was then sampled and averaged using a Stanford research system boxcar integrator and processed by a computer as shown in **Figure ANNEX3.1**.

A low intensity reference beam was extracted from the main beam at a 45° incidence angle by a glass plate and focused onto a highly nonlinear NPP (*N*-4-nitrophenyl-prolinol) powder used as a frequency doubler. The variation of the second harmonic intensity scattered from the solution is recorded on the computer as a function of the reference second harmonic signal provided by the NPP powder which scales like the square of the incoming fundamental intensity.

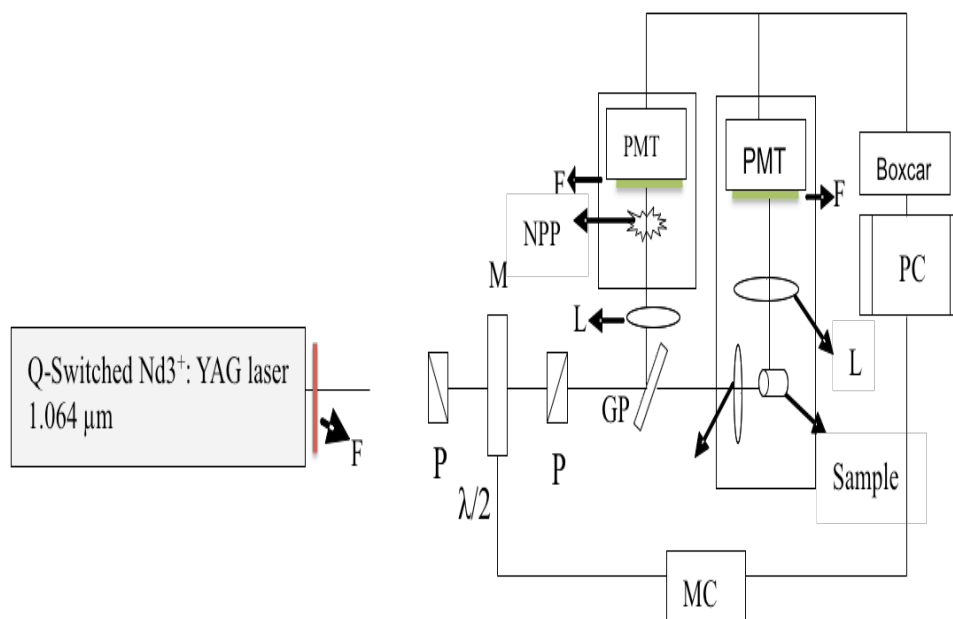


Figure ANNEX3.1. Schematic representation of HLS at 1.907 μm . **F**: Filter; **M**: Mirrors; **A**: Attenuator; **GP**: Glassplate; **L**: Lens; **P**: Polarizer; $\lambda/2$: Half wave plate; **PMT**: Photomultiplier tube; **NPP**: Reference material; **PC**: Personal computer, **MC**: Micro controller.

The intensity of the second-harmonic (I^{2w}) light is proportional to the number of scattering centers (N), the square of the first hyperpolarizability (β^2) and the square of the intensity of harmonic light (I_w^2). For a solvent (s) and chromophore (c) combination the following relation has been derived: $I_{2w} = g (N_s \beta_s^2 + N_c \beta_c^2) I_w^2$ with g being a geometry factor indicating the amount of signals captured by the experimental geometry, For a simple two component system,

$$\hat{a}^2 = N_{\text{solvent}} \hat{a}_{\text{solvent}} + N_{\text{chromophore}} \hat{a}_{\text{chromophore}}$$

Where,

N_s and N_c is the number of solvent and chromophore molecules per unit volume, β_s and β_c are the molecular hyperpolarizability of the solvent and chromophore molecule.

To obtain the β values, it was necessary to work in three steps. First, the second-order intensity of the octupolar ethyl violet as reference only was measured. The same experiment was then carried out with the solution of the complex and measurement of reference was repeated in order to have more acquired results. In these two cases, I^{2w} (intensity of the second-harmonic) versus I^w (the square of the intensity of harmonic light) was plotted (Fig. ANNEX3.2).

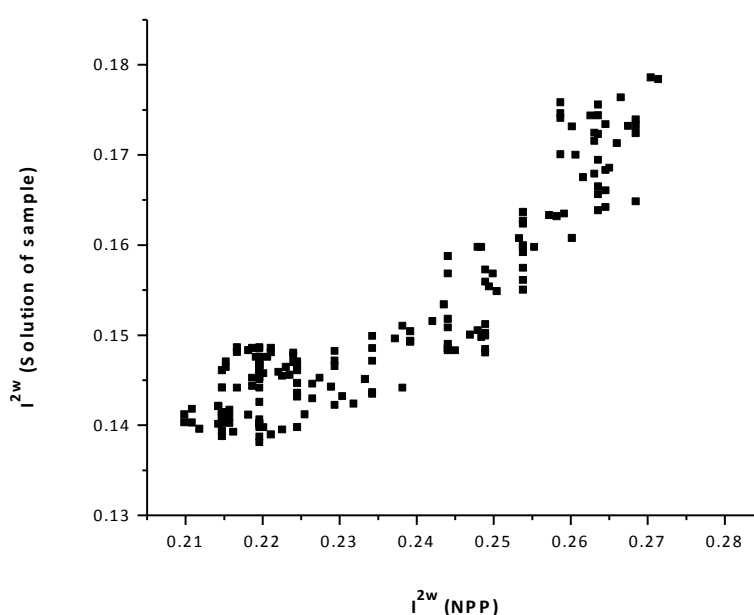


Figure ANNEX3.2. Plot the intensity of the second-harmonic (I^{2w}) of sample vs reference material NPP = (frequency doubler N-4-nitrophenyle-L-prolinol).

Knowing the β_{ref} value, β was determined by calculating the ratio of the two slopes. To obtain the most precise results as possible, around 3 slopes for both reference and solution of complex were plotted for each compound. And then, average of these slopes were used for calculation of the β values.

Formula to correct the value when compound absorbs:

$$P_{\text{slope corrected}} = P_{\text{slope observed}} \times 10^{\text{Absorption}(w)} \times 10^{\frac{\text{Absorption}(2w)}{2}}$$

e.g. : Calculation $P_{\text{slope corrected}}$ for neutral Lu(ABAB)₂:

$$\begin{aligned} P_{\text{slope corrected}} &= 0.2513 \times 10^0 \times 10^{\frac{0.05}{2}} \\ &= 0.2513 \times 1 \times 1.0592 \\ &P_{\text{slope corrected}} \end{aligned}$$

Here,

$$\beta_{HLS} = \sqrt{\langle \beta_s^2 \rangle} = \beta_{ETV} \sqrt{\frac{N_{ETV}}{N_s} \times \frac{P_s}{P_{ETV}}}$$

Where,

N_{ETV} : Concentration of ETV (3.29x10⁻³M for oxidized and neutral form and 2.24x10⁻³M for reduced measurements)

N_s : Concentration of Sample(1x10⁻⁵M)

P_{ETV} : Slope of ETV, P_s : Slope of Sample, β_{ETV} : 170x10⁻³⁰esu

e.g.: calculation β for neutral Lu(ABAB)₂(9),

$$\begin{aligned} \beta_{HLS} &= \sqrt{\langle \beta_s^2 \rangle} = 170 \times 10^{-30} \text{esu} \sqrt{\frac{3.29 \times 10^{-3} \text{M}}{1 \times 10^{-5} \text{M}} \times \frac{0.2662}{0.0765}} \\ \beta_{HLS} &= \sqrt{\langle \beta_s^2 \rangle} = 5756 \end{aligned}$$

ANNEX 4

^1H -, ^{13}C - NMR and Mass Analyzes

^1H - and ^{13}C - NMR measurements were carried out in CDCl_3 by Varian INOVA 500MHz NMR. Mass measurements were carried out by Matrix Assisted Laser Desorption Ionization Time of Flight mass spectrometer (MALDI-TOF) with 2,5-dihydroxybenzoic acid (DHB) as matrix.

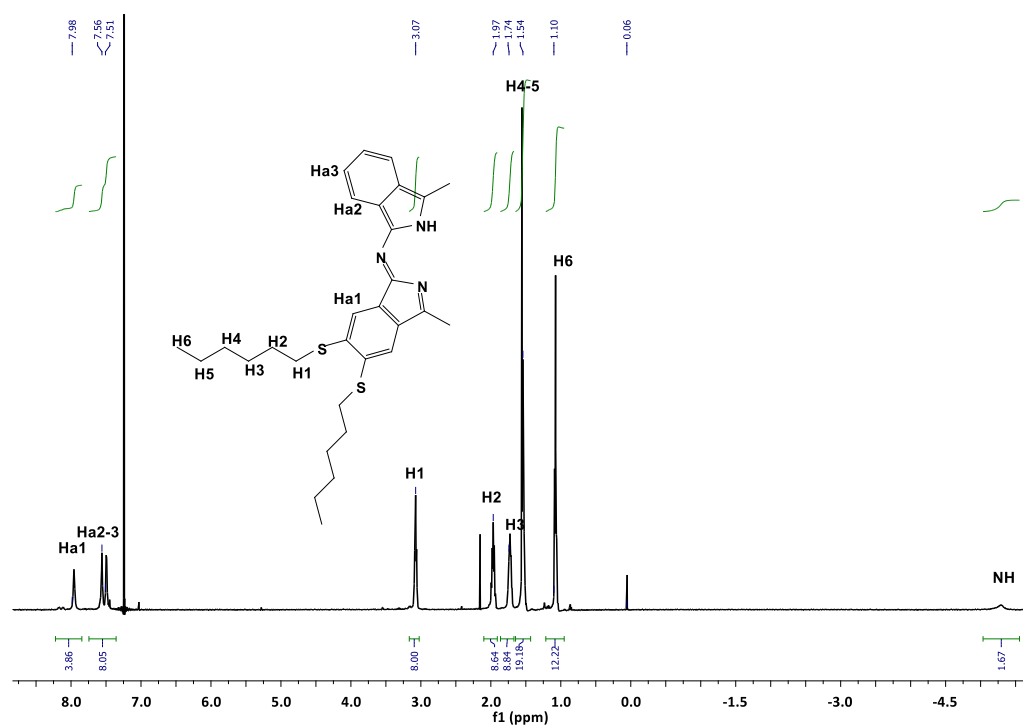


Figure ANNEX4.1 ^1H - NMR spectrum of 2,3,16,17-tetra(hexylthio)phthalocyanine (ABAB)(5)

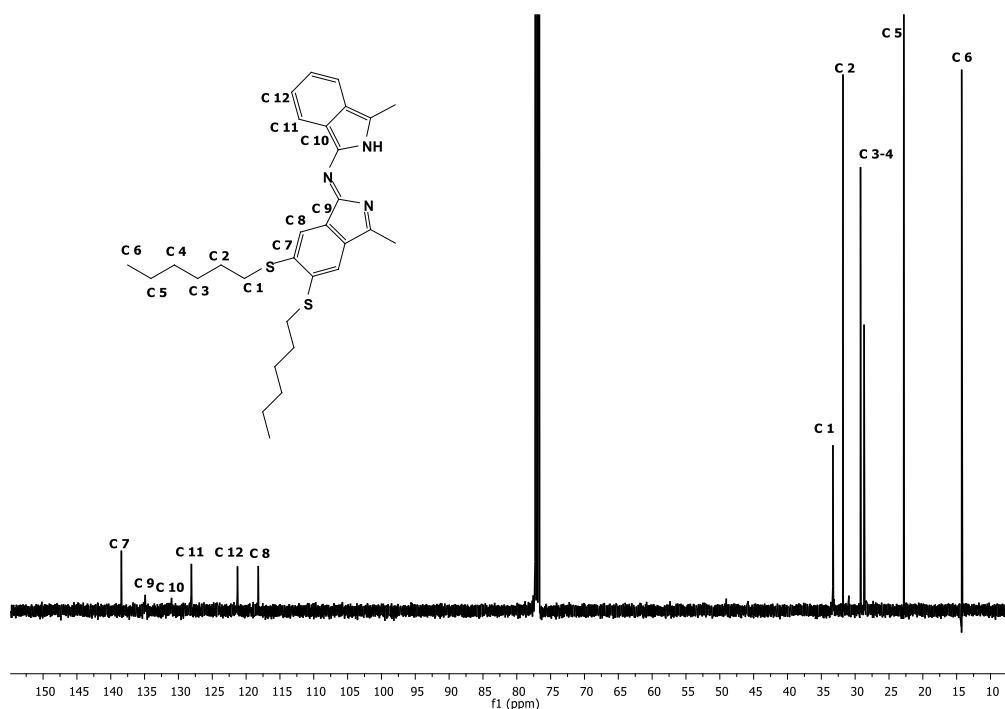


Figure ANNEX4.2 ^{13}C - NMR spectrum of 2,3,16,17-tetra(hexylthio)phthalocyanine (ABAB)(5)

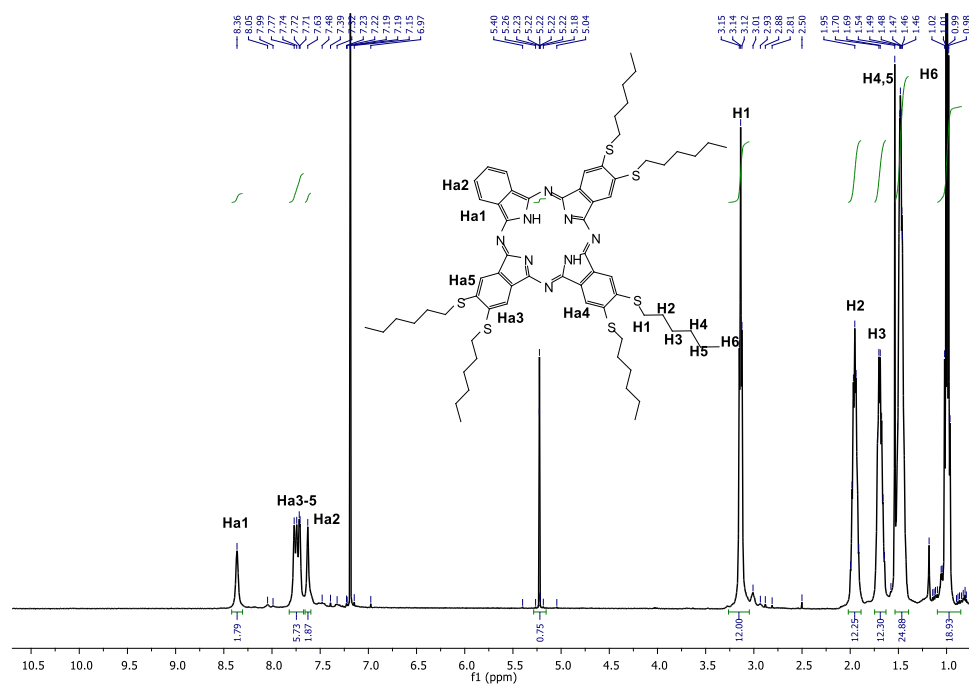
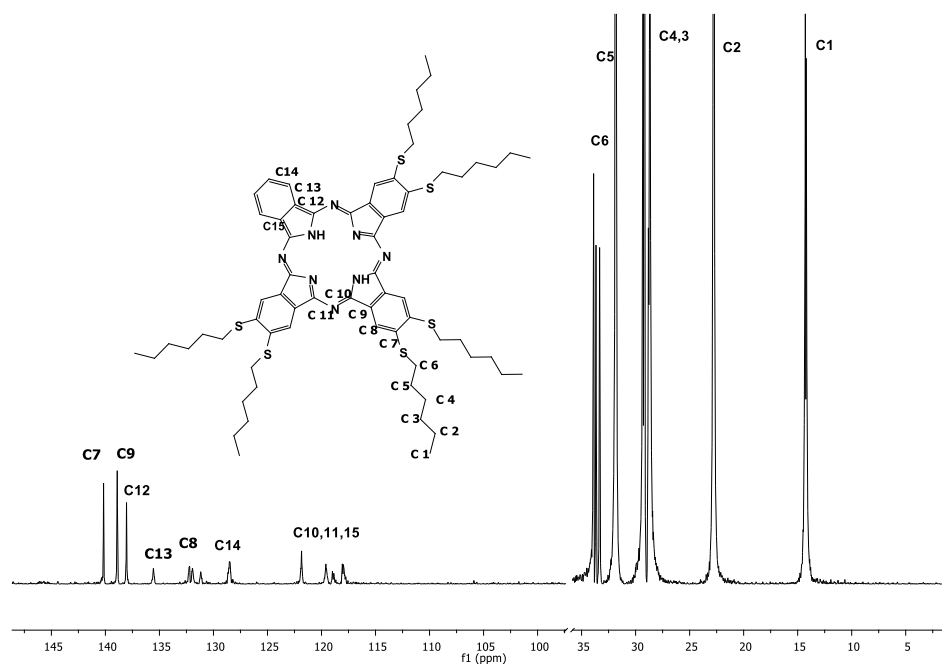
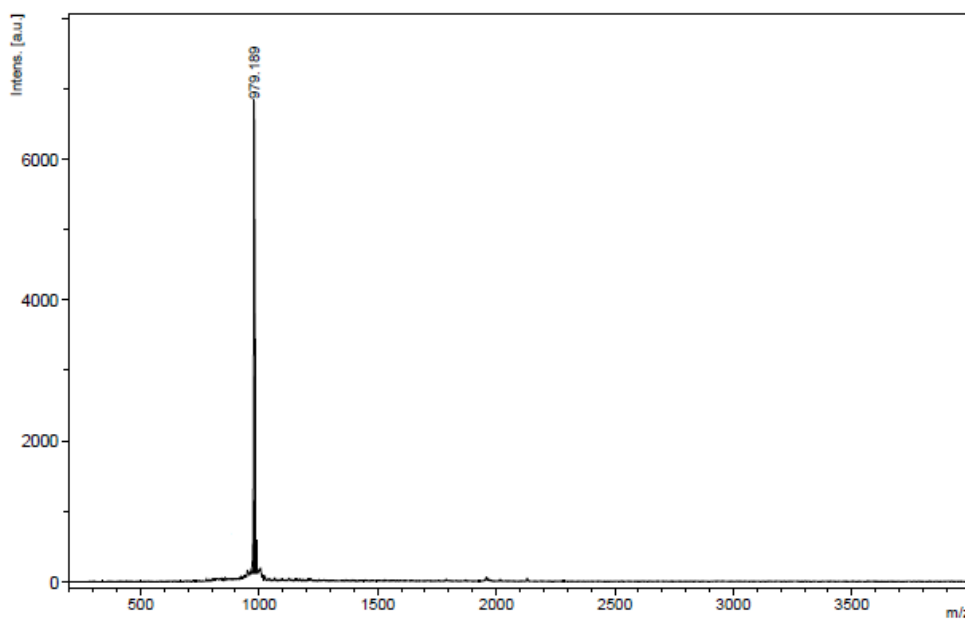


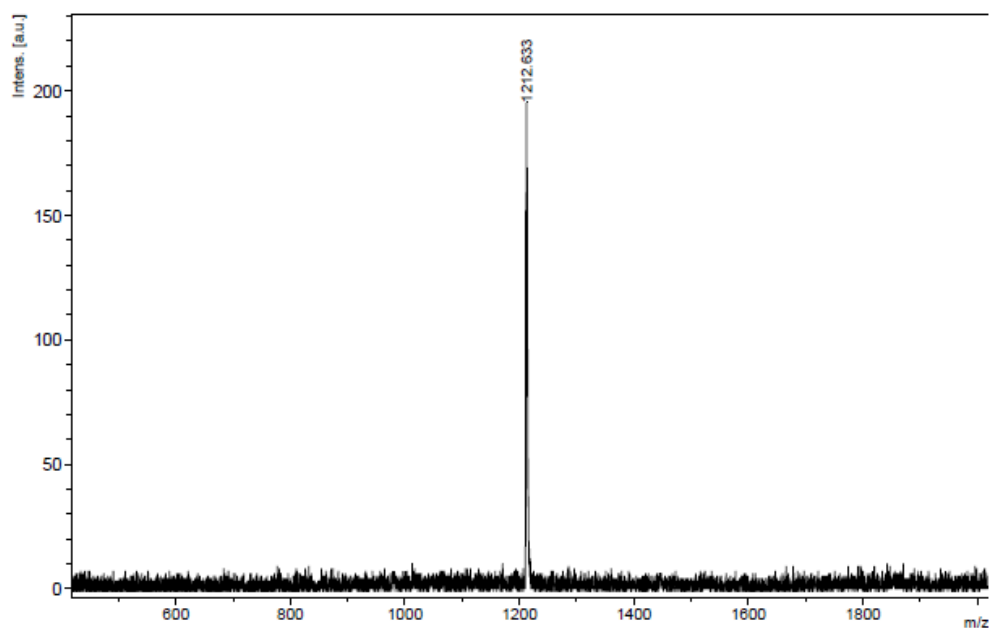
Figure ANNEX4.3 ^1H - NMR spectrum of 2,3,9,10,16,17 hexa(hexylthio)phthalocyanine (AB3) (6)



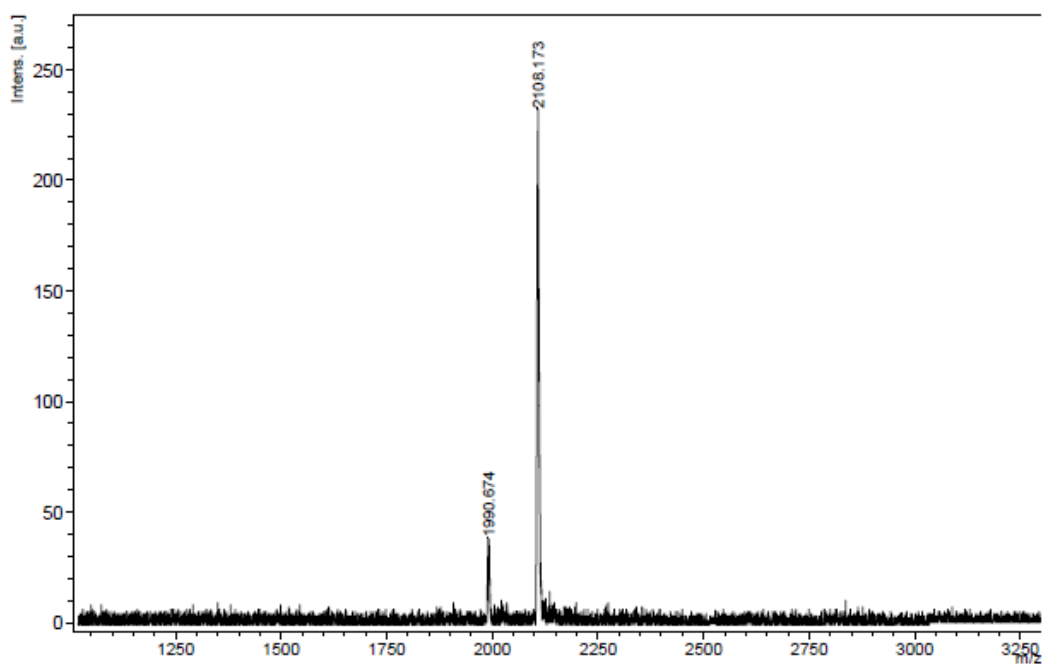
FigureANNEX4.4 ^{13}C - NMR spectrum of 2,3,9,10,16,17 hexa(hexylthio)phthalocyanine (AB3) (6)



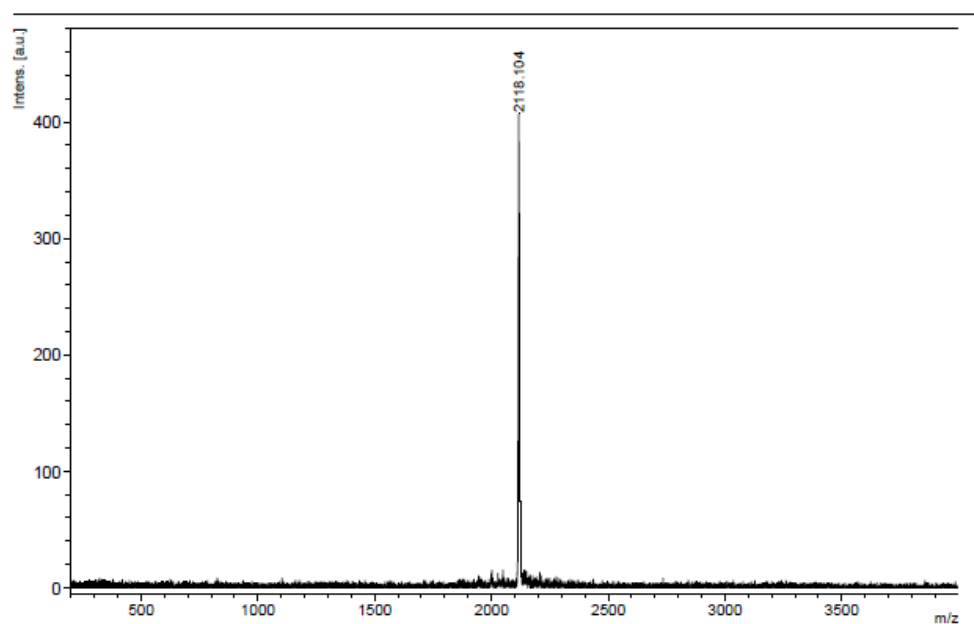
FigureANNEX4.5. Maldi-TOF spectrum of 2,3,16,17-tetra(hexylthio)phthalocyanine (ABAB)(5) [M^+ : 980]



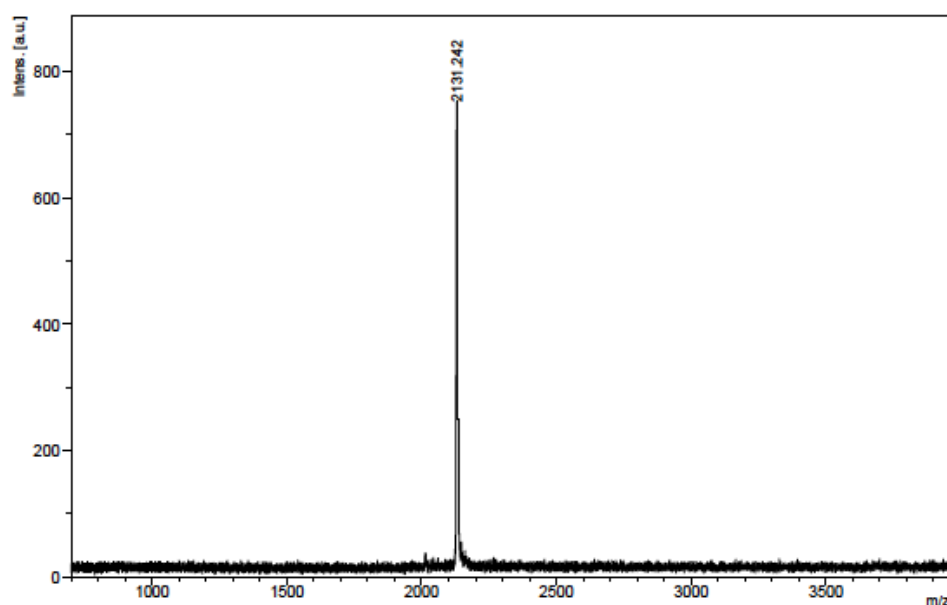
FigureANNEX4.6. Maldi-TOF spectrum of 2,3,9,10,16,17 hexa(hexylthio)phthalocyanine(AB3) (**6**) [M^+ : 1212]



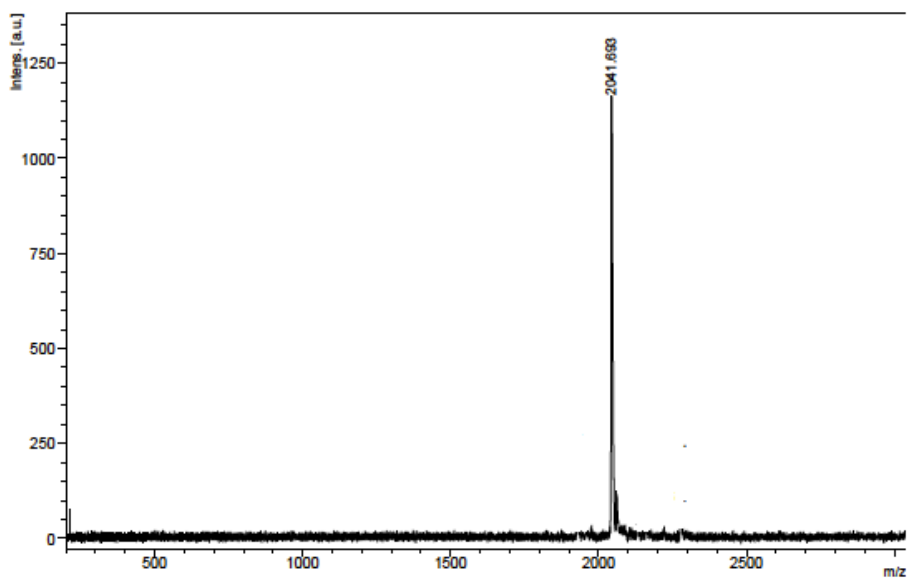
FigureANNEX4.7 Maldi-TOF spectrum of ABAB Bis(phthalocyaninato)Europium(III) Complex ($\text{Eu}(\text{ABAB})_2$) (**7**) [$(M+H)^+$: 2108]



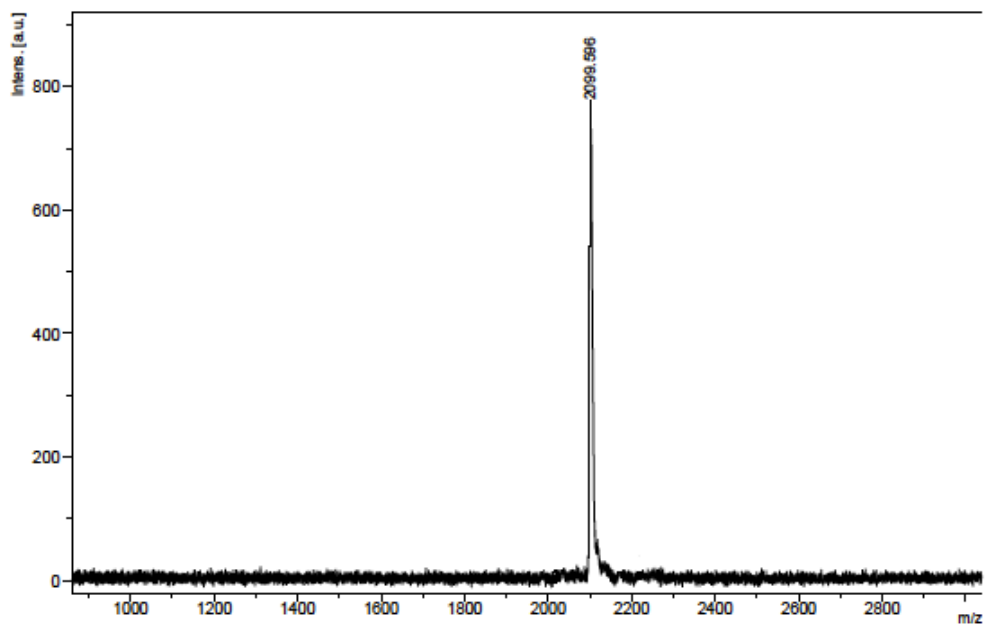
FigureANNEX4.8Maldi-TOFspectrum of ABAB bis(phthalocyaninato) dysprosium(III) complex ($\text{Dy}(\text{ABAB})_2(\mathbf{8})$) [$(\text{M}+\text{H})^+$: 2118]



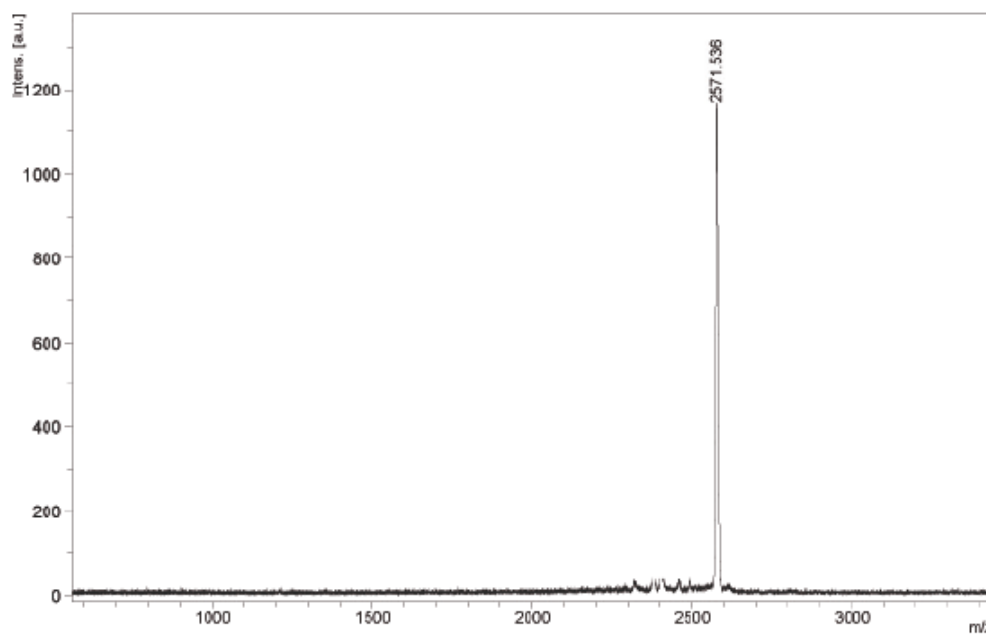
FigureANNEX4.9Maldi-TOFspectrum of ABAB bis(phthalocyaninato) lutetium(III) complex($\text{Lu}(\text{ABAB})_2(\mathbf{9})$) [$(\text{M}+2\text{H})$: 2131]



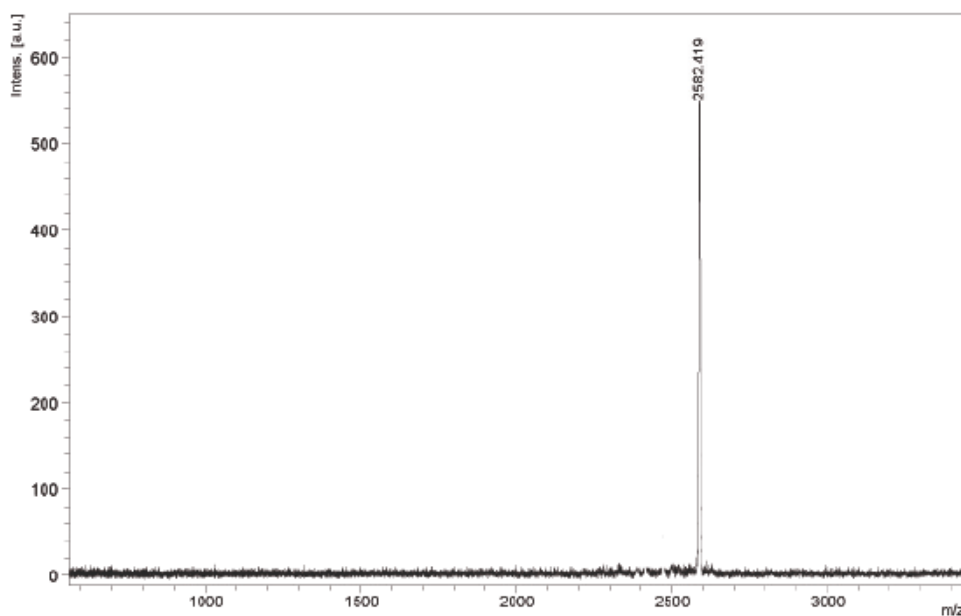
FigureANNEX4.10 Maldi-TOF spectrum of ABAB bis(phthalocyaninato) yttrium(III) complex (Y(ABAB)₂)(**10**) [M^+ : 2041]



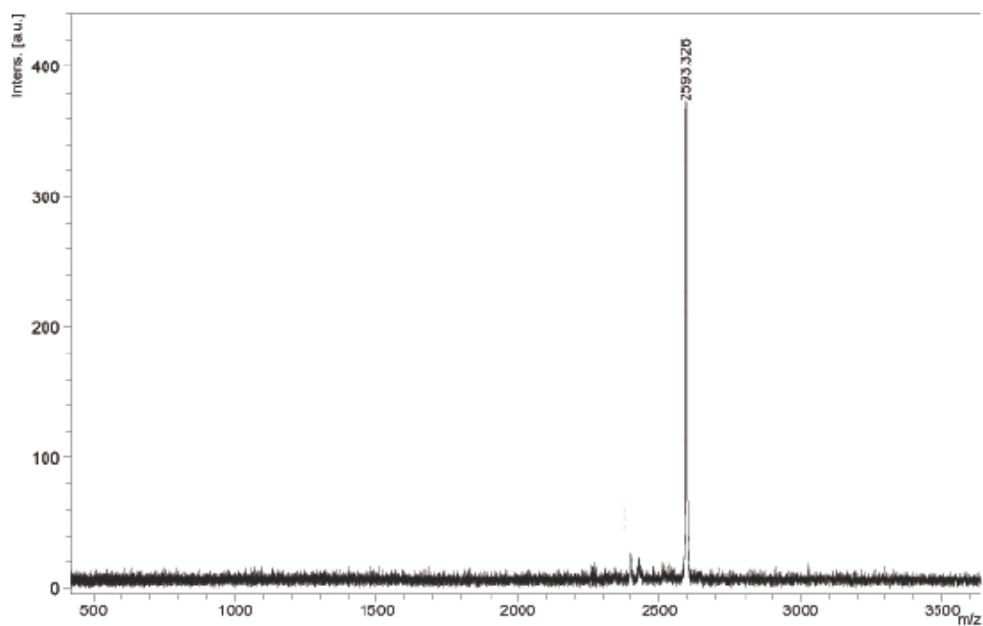
FigureANNEX4.11 Maldi-TOF spectrum of ABAB bis(phthalocyaninato) neodymium(III) complex (Nd(ABAB)₂)(**11**) [M^+ : 2099]



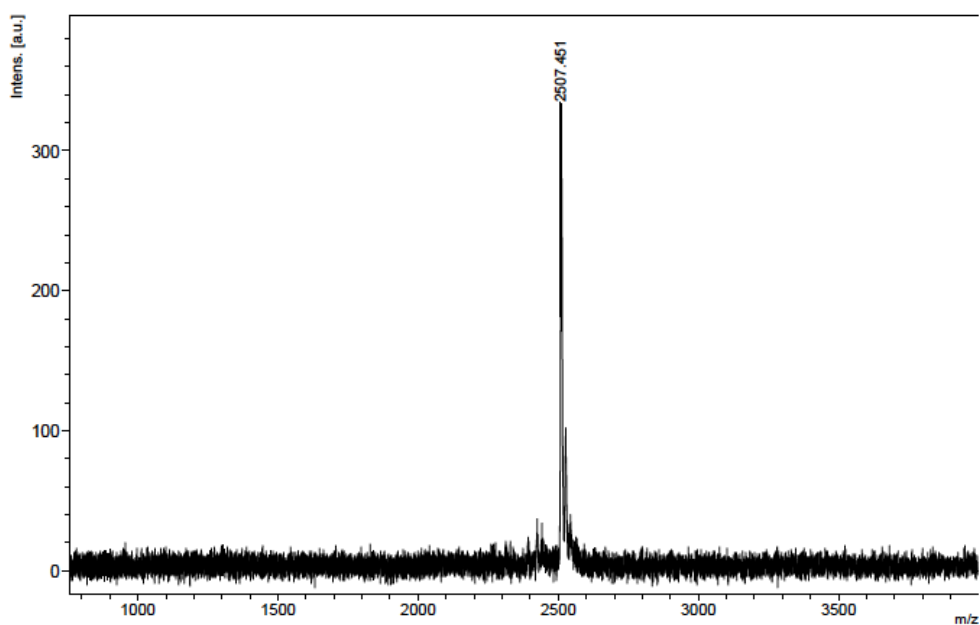
FigureANNEX4.12 Maldi-TOF spectrum of AB3 bis(phthalocyaninato) europium(III) complex (Eu(AB3)₂)(**12**) [M^+ : 2571]



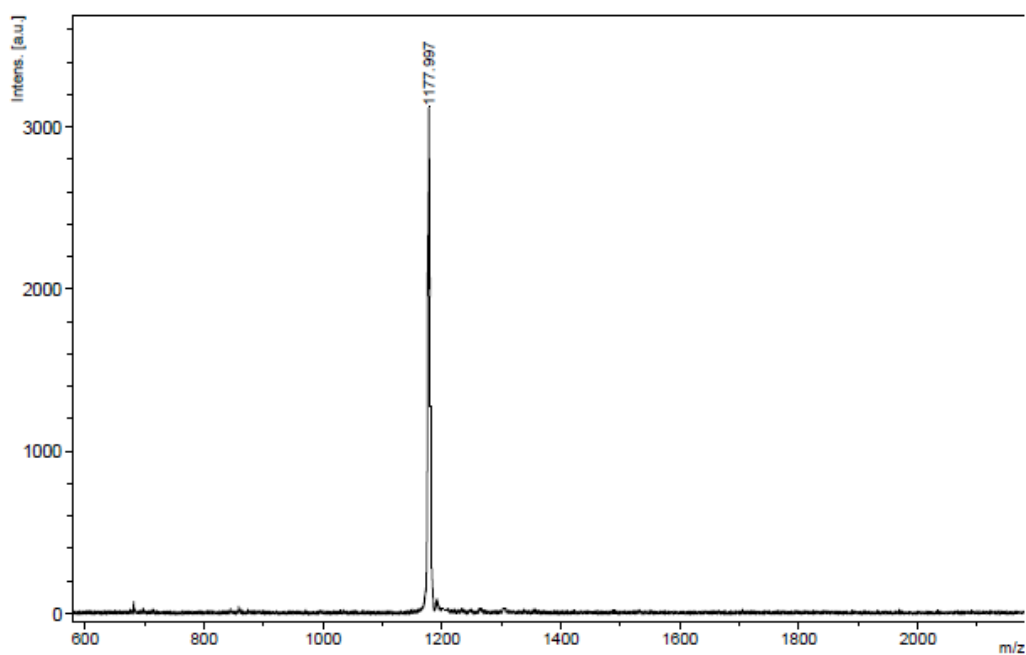
FigureANNEX4.12 Maldi-TOF spectrum of AB3 bis(phthalocyaninato) dysprosium(III) complex (Dy(AB3)₂)(**13**) [M^+ : 2582]



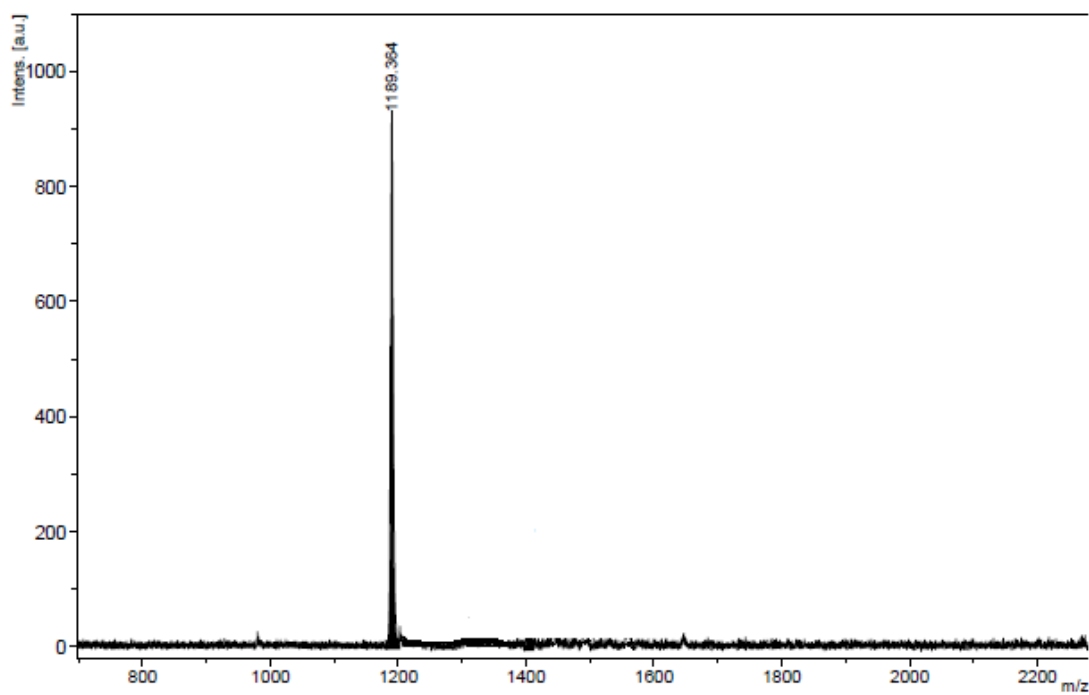
FigureANNEX4.14Maldi-TOFspectrum of AB3 bis(phthalocyaninato) lutetium(III) complex (Lu(AB3)₂)(**14**) [M⁺: 2593]



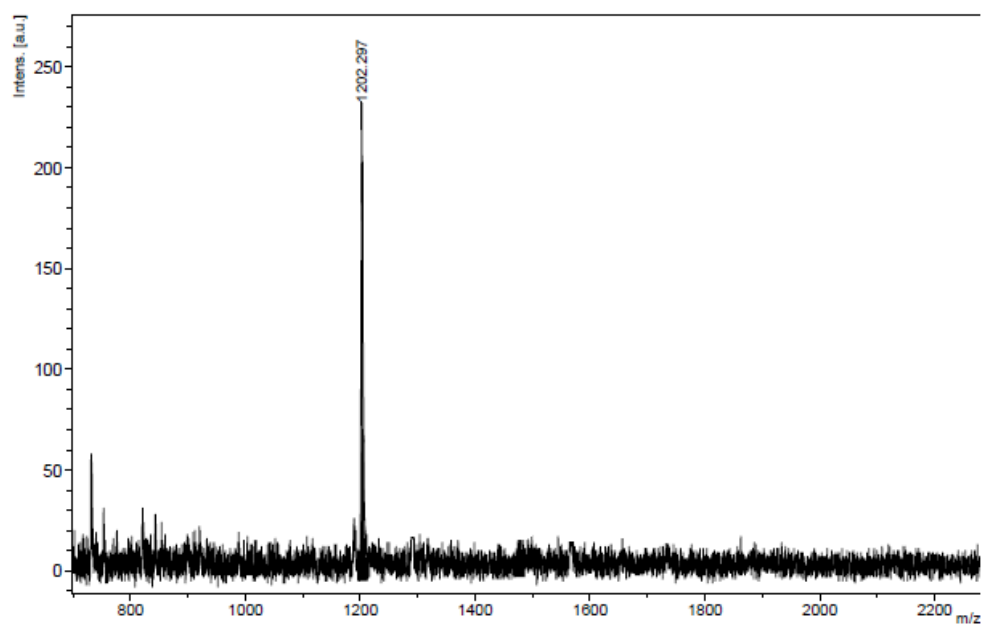
FigureANNEX4.15Maldi-TOFspectrum of AB3 bis(phthalocyaninato) yttrium(III) complex (Y(AB3)₂)(**15**) [M⁺: 2507]



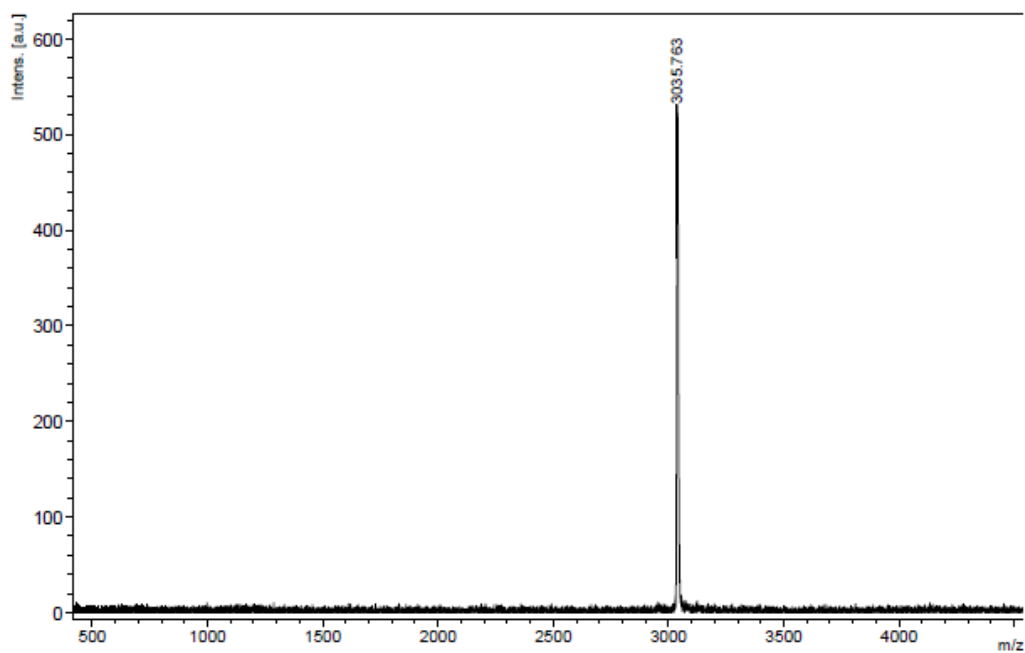
FigureANNEX4.16Maldi-TOFspectrum of unsubstituted (A4) bis(phthalocyaninato) europium(III) complex (Eu(A₄)₂) (**16**)[M⁺: 1177]



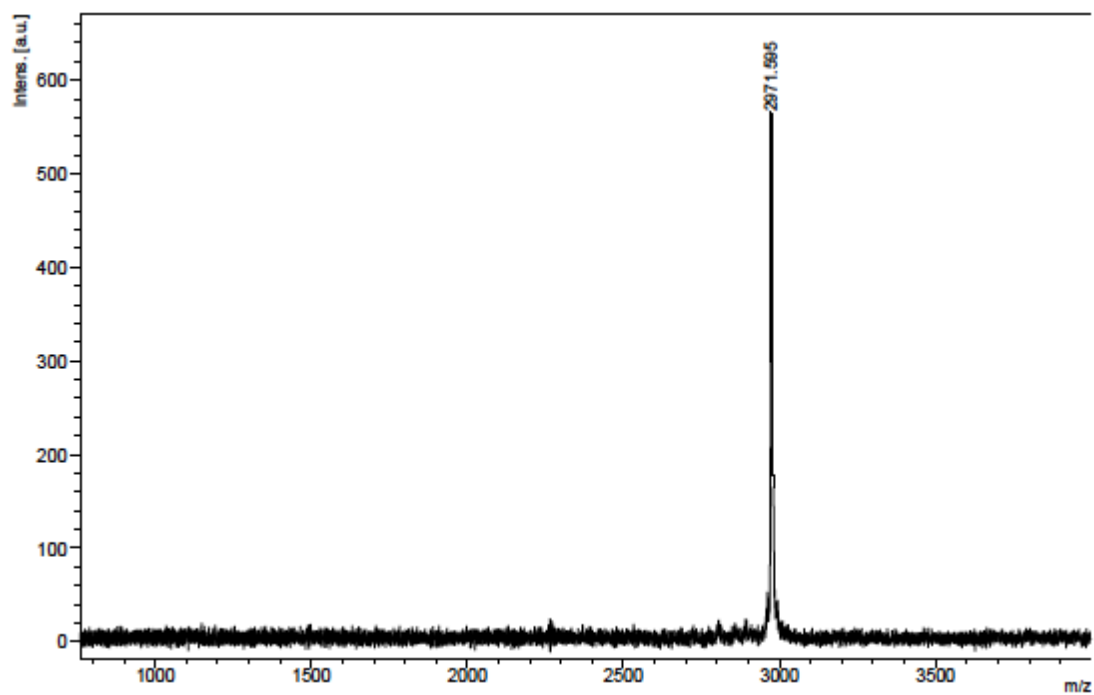
FigureANNEX4.17Maldi-TOFspectrum of unsubstituted (A4) bis(phthalocyaninato) dysprosium(III) complex (Dy(A₄)₂)(**17**) [M⁺: 1189]



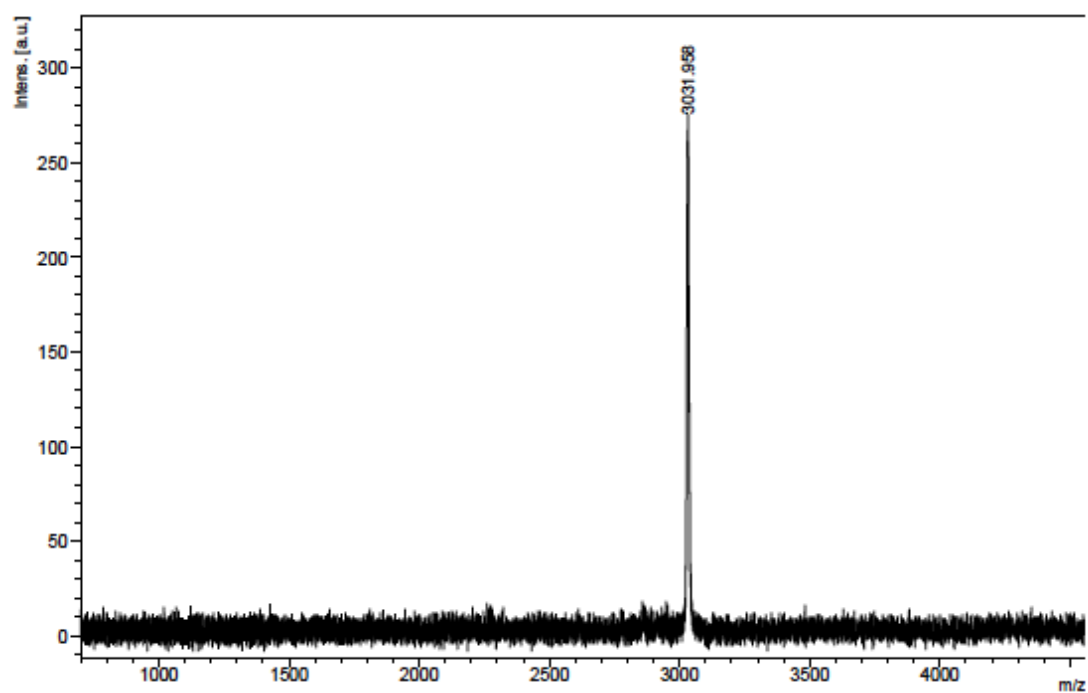
FigureANNEX4.18. Maldi-TOFspectrum of unsubstituted (A4) bis(phthalocyaninato) lutetium(III) complex (Lu(A₄)₂)(**18**) [M⁺: 1202]



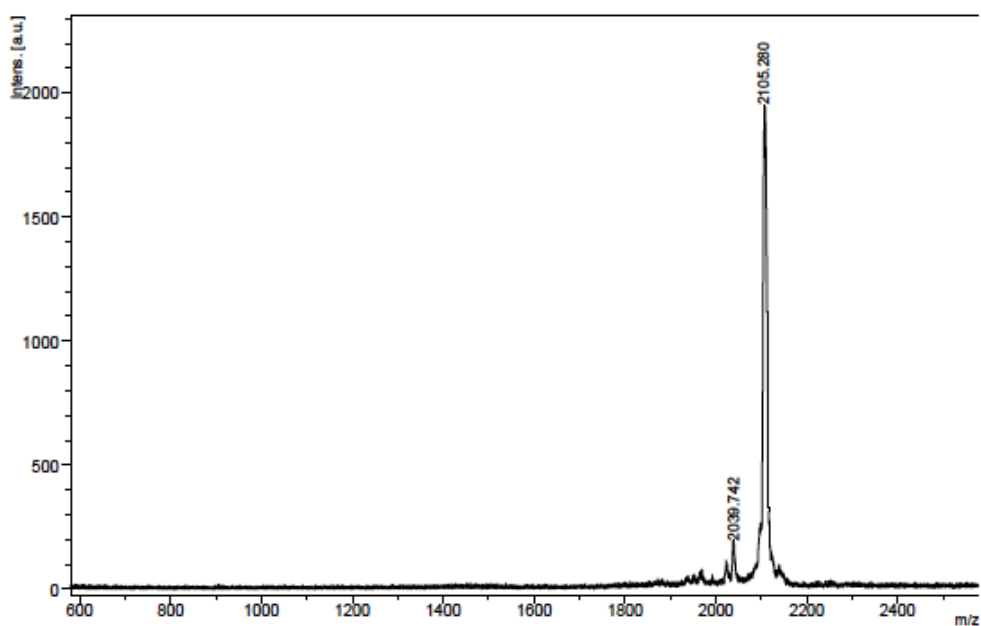
FigureANNEX4.19Maldi-TOFspectrum of octahexylthia substituted (B4) bis(phthalocyaninato) europium(III) complex (Eu(B₄)₂) (**19**) [M⁺: 3035]



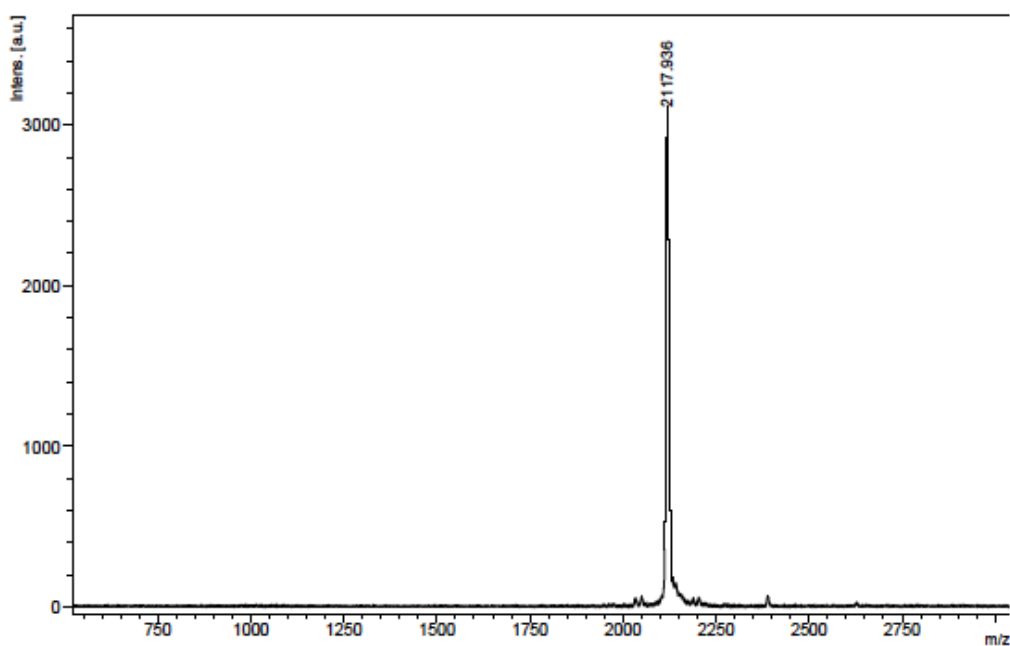
FigureANNEX4.20Maldi-TOFspectrum of octahexylthia substituted (B4) bis(phthalocyaninato) yttrium(III) complex (Y(B₄)₂)(**22**) [M⁺: 2970]



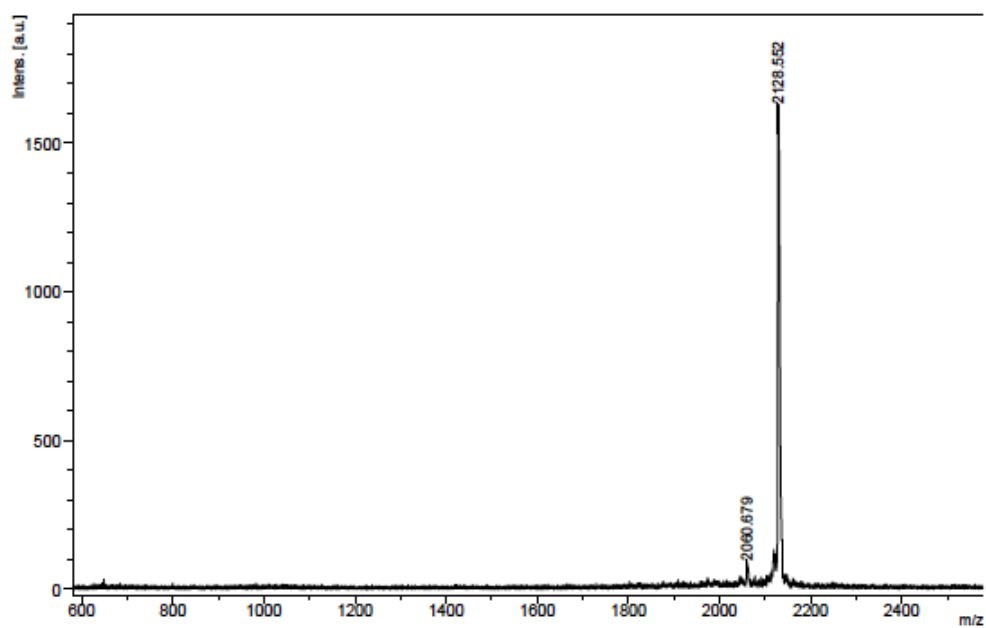
FigureANNEX4.21Maldi-TOFspectrum of octahexylthia substituted (B4) bis(phthalocyaninato) neodymium(III) complex (Nd(B₄)₂)(**23**) [M⁺: 3030]



FigureANNEX4.22Maldi-TOFspectrum of tetrahexylthia substituted (T4) bis(phthalocyaninato) europium(III) complex ($\text{Eu}(\text{T}_4)_2$)(**24**) [M^+ : 2105]



FigureANNEX4.23Maldi-TOFspectrum of tetrahexylthia substituted (T4) bis(phthalocyaninato) dysprosium(III) complex ($\text{Dy}(\text{T}_4)_2$)(**25**) [M^+ : 2117]

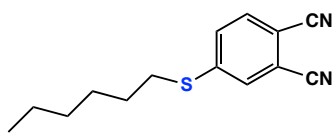


FigureANNEX4.24Maldi-TOFspectrum of tetrahexylthia substituted (T4) bis(phthalocyaninato) lutetium(III) complex (Lu(T₄)₂)(**26**) [M⁺: 2128]

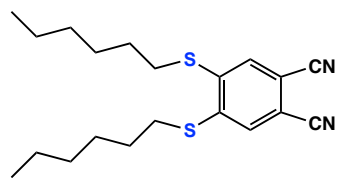
CURRICULUM VITAE

Mehmet Menaf AYHAN was born in 1981 in Batman, Turkey. He obtained his B.S. degree in Chemistry from University of Akdeniz in 2003. He then moved to Gebze Institute of Technology(GIT), to begin his graduate study under the supervision of Professor. Ayşe Gül GÜREK. Then he obtained his master degree in 2006 and he has worked as Research Assistant in the Chemistry Department of GIT since 2006. His current research interests include design, synthesis, and nonlinear optical properties of phthalocyanine derivatives.

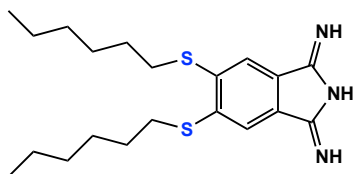
List and number of the molecules described in the manuscript



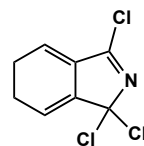
(1)



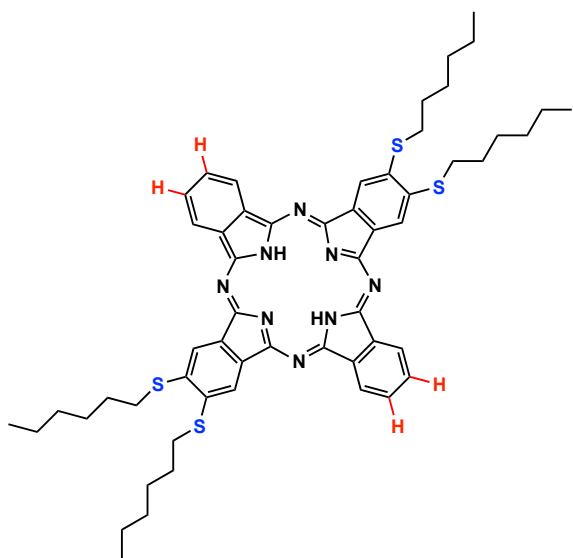
(2)



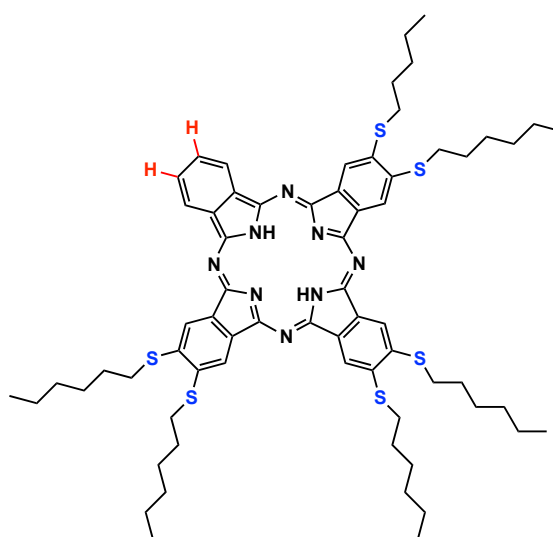
(3)



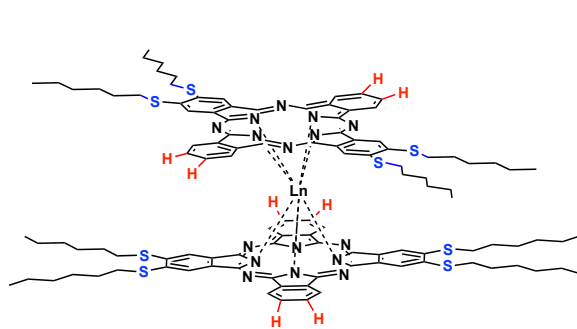
(4)



ABAB (5)

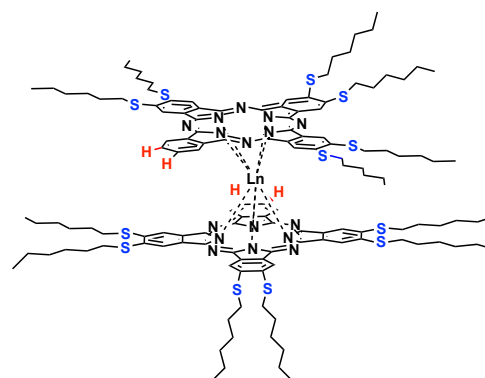


AB3 (6)



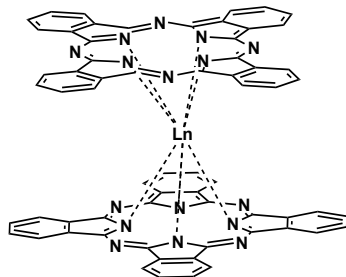
Octupolar-Ln(ABAB)₂

Ln: Eu (7), Dy(8), Lu (9), Y(10), Nd(11)



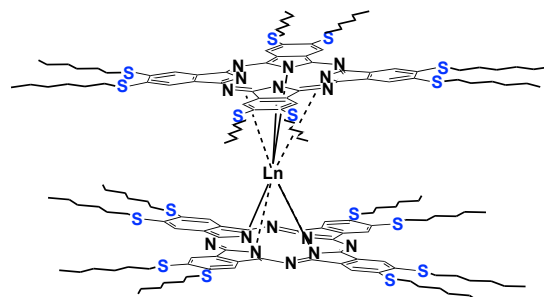
Ln(AB3)₂

Ln: Eu (12), Dy(13), Lu (14), Y(15)



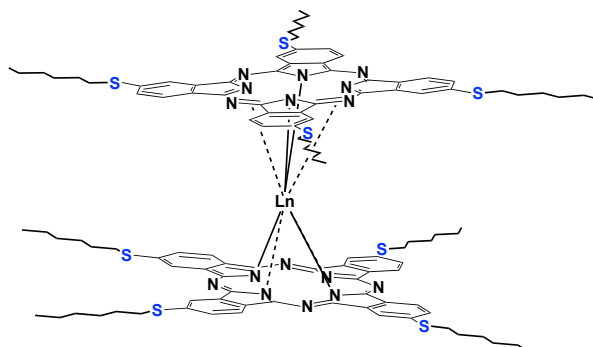
Ln(A4)₂

Ln: Eu (16), Dy(17), Lu (18)



Ln(B4)₂

Ln: Eu (19), Dy(20), Lu (21), Y(22), Nd(23)



Ln(T4)₂

Ln: Eu (24), Dy(25), Lu (26)

